NTNU
Norwegian University of
Science and Technology

Development of Hybrid Aluminum Carbon Fiber Composite Wheels for a Formula Style Race Car

Christer Kobbevik Oldeide

Master of Science in Mechanical Engineering
Submission date: November 2017
Supervisor: Jan Torgersen, MTP

Norwegian University of Science and Technology
Department of Mechanical and Industrial Engineering

Thesis supervisor: Jan Torgersen Christer Kobbevik Oldeide

Development of Hybrid Aluminum Carbon Fiber Composite Wheels for a Formula Style Race Car

Abstract

Modern short product life cycles and the necessity to rapidly manufacture components with minimal production needs poses stringent requirements on both time and sophistication of modern product design. Light weight components are more and more in demand, which drives industry to utilize advanced materials like Carbon Fiber Reinforced Polymer (CFRP). The ever-increasing demands of conventional design methods often fail to fulfill the necessary requirements for complex, high performing components. For example, conventional design methods for composites are done manually and often based on experience which is time consuming and can result in non-optimal designs. Using simulation based design (SBD) approaches, this thesis presents FE optimization models that can lead to next generation CFRP designs. A two module wheel is presented consisting of a topology optimized aluminum center for easy machinability and a CFRP rim, for which the layup was optimized in a self-developed evolution based material optimization algorithm. The design considerations and developed algorithm are presented in this thesis as well as the results on optimization with the weight target of 700 g and maximization of the total global stiffness which yielded a deflection of maximum 2.27 mm in cornering at 110 km/h. The optimization was based on two quasi static load scenarios gathered from vehicle dynamic simulations performed by collaborators. The optimized rim shell has an increased specific stiffness of around 45 % and a decreased rotational inertia of nearly 70 %, compared to an aluminum rim shell. The combination of the optimized design and a high quality production resulted in high performing rims that worked well throughout the competitions and during tuning of the car. Mechanical tests on the wheel showed the perfect agreement between the simulation and the experimental results. The largest discrepancy was found in large static loads up to 200 kg, where the discrepancy of the total deformation was 15.6 %. To the best of the author's knowledge, this work presents the first complete and successful approach towards the parametric material optimization of a CFRP component linked to an entire product development process from the initial design consideration all the way to mechanical testing and application. It is likely helpful to many researchers and developers of next-generation composite designs.

Utvikling av Hybrid Aluminum Karbonfiberforsterket Polymer Felger for en Formula type racerbil

Sammendrag

Moderne produkters korte livssykluser og krav om rask produksjon og minimerte produksjonsbehov stiller høye krav til et sofistikert design av produktet. Etterspørselen etter lette produkter presser næringslivet til å anvende avanserte materialer, slik som karbonfiberforsterkede polymerere (CFRP). Konvensjonelle designmetoder evner derimot ikke å oppfylle de nødvendige kravene stilt til komplekse komponenter, som skal yte på høyt nivå. For eksempel er design for kompositter ofte gjort manuelt og basert på erfaring, hvilket er tidskrevende og ikke nødvendigvis gir det beste designet. Denne avhandlingen kommer til å presentere FE-optimaliseringsmodeller ved bruk av simuleringsbasert design (SBD), som kan føre til neste generasjons komposittdesign. Designet som er presentert, er et todelt hjul bestående av et topologioptimalisert aluminiumssenter, som også er optimalisert for maskinering, og en CFRP-felg, som er optimert med en egenutviklet og evolusjonsbasert materialoptimaliseringsalgoritme. Designkravene og den utviklede algoritmen er her presentert sammen med resultatene fra optimaliseringen. Optimaliseringen hadde et vektkrav på 700 g, samtidig som den globale stivheten skulle maksimeres. Det resulterte i en maksimal defleksjon på 2.27 mm når belastet med kreftene fra sving ved 110 km/t. Optimeringen ble basert på to kvasistatiske lastscenarioer gitt av analyser av bilens kjøredynamikk, utført av samarbeidspartnere. Den optimerte felgbanen har omtrent 45% høyere spesifikk stivhet og nesten 70 % lavere treghetsmoment enn en felgbane av aluminium. Optimalisert design sammen med høy-kvalitets produksjon førte til et sluttprodukt av høy kvalitet, som fungerte bra både under konkurransene og testingen. Mekaniske tester av det fullstendige designet viste perfekt overensstemmelse med simuleringene. Det største avviket var på 15.6 % og inntraff ved store statiske laster opp til 200 kg. Så vidt forfatteren vet er dette arbeidet det første som kan vise til et fullstendig og vellykket design ved parametrisk materialoptimalisering av en CFRP-komponent, som også er en del av en fullstendig produktutviklingsprosess fra konseptualisering til mekanisk testing og faktisk anvendelse av ferdig produkt. Sannsynligvis vil det være hjelpsomt for utviklere av neste generasjons komposittdesign.

Acknowledgments

I would like to direct special thanks to my supervisor Jan Torgersen who has been helpful, inspiring and my biggest motivation through the work of this thesis.

For a person who has been active in Revolve NTNU and Formula Student over the last five years, and is generally interested in motorsport, this is a dream come true to be able to write about your favorite topic. As an car enthusiast and a person that dreams about working in the car industry, getting the chance to write for an organization like Revolve NTNU, is possibly the best opportunity to get involved with the car manufacturing and the motorsport, as Formula Student collaborattes closely with the car industry and the motorsport society.

I would like to give thanks to Revolve NTNU for giving me this unique chance and to the sponsors, Mjøs Metallvarefabrikk AS, Dassault Systèmes Simulia Corp., Molstad modell and Kongsberg Gruppen for helping me bring this work to life. A special thanks goes to Jon Martin Haaland for helping me getting a better knowledge of vehicle dynamics and also Jørgen Eliassen, Jacob Vigerust, Jens Mildestveit and Simen Ekornåsvåg for general engineering advise. I would also thank my mom and dad, Oddrun and Øystein for encouraging. Without their support I would not have the opportunity to take this degree.

Last but not least, I would thank Maria Bjelland and Maria Dyrseth for the endless hours they spent helping in the production of the carbon fiber reinforced rim shell.

I would like to dedicate my thesis to Revolve NTNU

- my biggest passion over the last five years

Contents

Listing of figures

Listing of tables

Abbreviations

α	Ratio between m_{out} & m_{in}
ε	Micro Strain
ω	Rotational velocity of rim
E	Elastic Modulus
E_t	Total energy stored in the rim
f_x	Reaction force on tire - Longitudinal direction
f_y	Reaction force on tire - Lateral direction
f_z	Reaction force on tire - Vertical direction
G	Shear Modulus
I	Rotational inertia of rim
m	Total mass of rim
m_e	Equivalent mass
m_{in}	Mass of rim center
m_{out}	Mass of rim shell
N_i	Cycles of stress causing failure at each stress amplitude
n_i	Cycles of reversed stress amplitude
ν	Poisson Ratio
5HS	5 Harness Satin

CAD Computer Aided Design

CAM Computer Aided Manufacturing

CF Carbon Fiber

CFRP Carbon Fiber Reinforced Polymer

CM Center Mount

CMM Coordinate Measuring Machine

CNC Computer Numerical Control

CS Center Shell

DA Drapability Analysis

ETRTO European Tyre and Rim Technical Organisation

FEA Finite Element Analysis

FEM Finite Element Model

FS Formula Student

IB Inner Bead

ID Inner Drop

IF Inner Flange

MO Material Optimization

OB Outer Bead

OD Outer Drop

OF Outer Flange

SBD Simulation Based Design

TO Topology Optimization

UD Unidirectional

There are two really innovative forms of motorsport left: Formula One and Formula Student.

Ross Brawn

1 Introduction

The motorsport industry is constantly working to improve the performance of their cars by looking into advanced materials and manufacturing methods. Key factors to improved performance of a race car are to reduce mass and compliance. The wheel is one of the most important components where mass and stiffness affect the performance of a race car the most. The effect of unsprung and rotational mass is well known as well as how the compliance affects the handling predictability.

In terms of tackling the above challenges with appropriate material choice, there is no material that can compete with carbon fiber-reinforced polymers (CFRP) when it comes to reducing weight in the automotive industry. CFRP has excellent qualities when it comes to strength, weight, and formability. Carbon Fiber composites have been used for a long time in Formula 1 and other extreme sports as their unique stiffness and tunability to specific load cases allows to limit material use and hence to reduce mass. The mechanical property advantage is paired with low investment requirements for production and ease to shape these materials routinely into complex aerodynamic shapes. Due to the polymeric nature, CFRPs are superior for corrosion and energy uptake in high-speed crashes. The main advantage of utilizing fiber composites is the possibility to produce a tailor-made material with the desired geometry for a specified application. It is not a surprise that the unsprung and rotational mass problem in race cars is a ideal scenario for the use of CFRPs. In 2013, Koenigsegg made the world's first hollow, one piece, super light carbon fiber wheel, using their proprietary method named Aircore™ Technology[1]. This wheel is about 40 % lighter and 60 % stiffer than a commercial aluminium alloy race rim.

1.1 Performance of a Wheel

The performance of a wheel is crucial for a race car. The interaction between suspension, rim, tire, and road can be what makes your team win or lose. The weight and stiffness of the rim is very important for the performance of the suspension and the overall vehicle dynamics. In this section, there will be a short introduction on how weight and stiffness are influencing the vehicle performance, the key motivational backrground of this thesis.

1.1.1 Unsprung Mass

By using a quarter model of the car to simulate a bump, it can be illustrated easily how the unsprung mass impacts the air time of the wheel and the suspension travel. Parameters used for the quarter model ((Figure 1.1.1) is found in table 1.1.1). A bump is modeled as an extreme case, when the wheel leaves the bump with a characteristics initial velocity of 3 m/s, while the chassis is staying still. The simulation shows that doubling the unsprung mass, doubles the air time of the wheel and increases the suspension travel by 85.7 % .

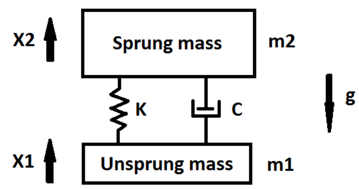

Figure 1.1.1: Simplified quarter model

Table 1.1.1: Parameters for Quarter Model

Case	m1 [kg]	m2 [kg]	k [N/mm]	g[m/s^2]
1	6.8	60	35	9.81
2	13.6	60	35	9.81

1.1.2 Concept of Equivalent Mass

The effect of rotational inertia affects the car during braking, acceleration and overall handling properties. One way to compare the effect of rotational inertia is to introduce the concept of equivalent mass. The total energy stored in the rim is a combination of its translational kinetic energy and its rotational kinetic energy, $E_t = \frac{1}{2}mv^2 + \frac{1}{2}I\omega^2$. Expressing the total energy as the non-rotating energy of some equivalent mass m_e, the equivalent mass can be simplified to[2]:

$$m_e = m + I\omega^2 \tag{1.1}$$

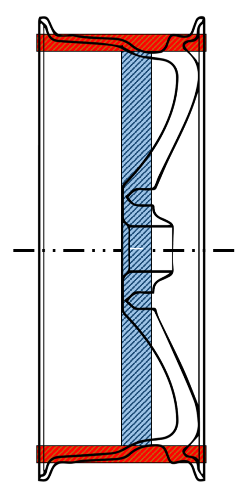

Figure 1.1.2: Simplified rim

Simplifying the rim to a solid disk and a cylindrical shell (Fig: 1.1.2) and defining α as the ratio between outer mass and the inner mass, m_{out} and m_{in}:

$$\alpha = \frac{m_{out}}{m_{out} + m_{in}} \tag{1.2}$$

Then the relation between equivalent mass and sprung-mass is:

$$m_e = m(1 + \frac{\alpha + 1}{2}) \tag{1.3}$$

Reducing rotational mass is 1.5 - 2.0 times more effective than reducing the same amount of "static mass" (fig: 1.1.3).

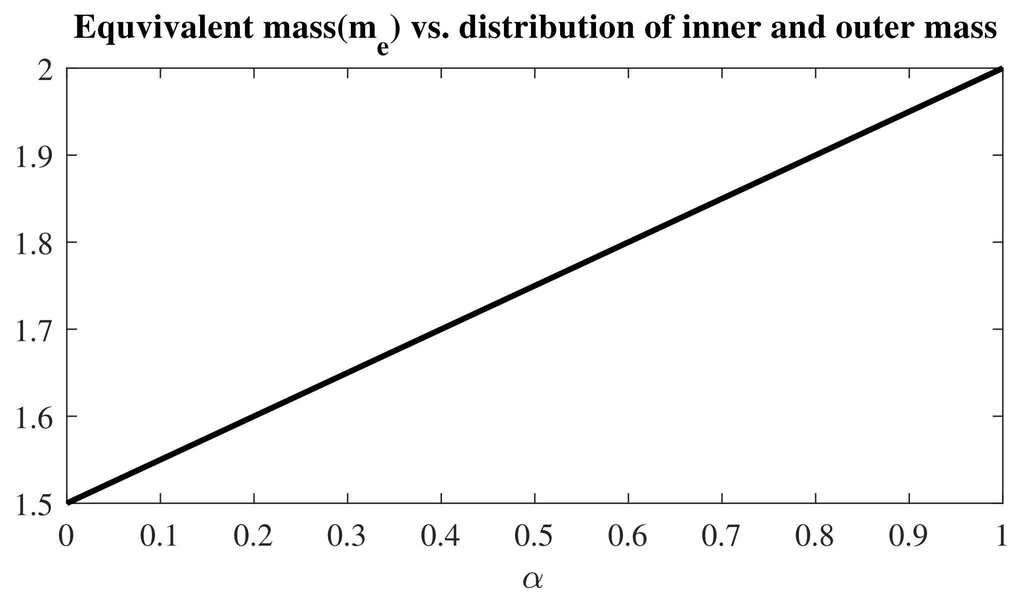

Figure 1.1.3: Plot of how the distribution between inner and outer mass effect equivalent mass

1.1.3 Stiffness

Rim stiffness influences the vehicle dynamics, both in terms of possible camber gain and delay of load transfer. The stiffness versus mass can be looked at as a compromise where the performance of the wheel is directly affected by both parameters. By looking at the camber sensitivity in Figure 1.1.4 it is possible to understand how the stiffness of the rim affects the vehicle performance. Following the curves from Figure 1.1.4 we see that the tires actually increase the lateral capacity with camber going in the right direction. This means that if the tire leans in the turn, (negative camber on outer and positive camber on inner tire) camber thrust will give positive effects. The car is turning both right and left, and the most important criteria is that the outer wheel, which have the greatest load, cannot have positive camber, which a flexible rim could contribute to. A stiffer rim could give a quicker load transfer between tire and suspension, which will make transients faster.

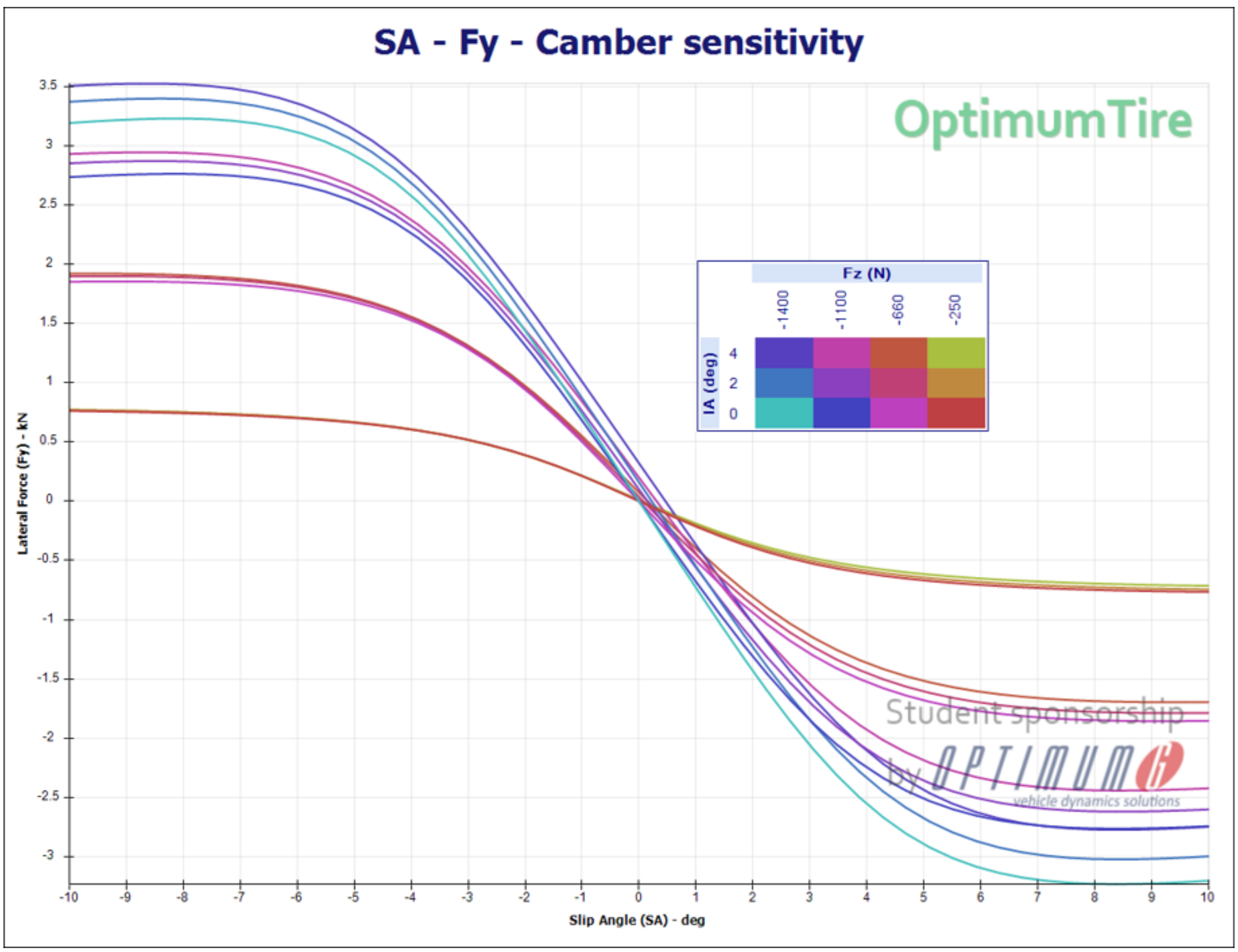

Figure 1.1.4: Continental C16 7J-13 rim 80kPa - Camber sensitivity estimated by Jon Martin Haaland[3]

With this motivational background, this thesis reports the development of a unique CFRP race rim for the 2017 Revolve student race car ELD.

1.2 Revolve NTNU and Team Role

Revolve NTNU is an independent student organization at the Norwegian University of Science and Technology. In one year, the team completes a full product development process in order to produce a fully functional race car to compete in one of the largest engineering competitions for students in the world, the Formula Student (FS). I was part of the suspension group, where my main task was to develop and produce the wheels for the 2017 car.

This thesis will introduce the reader to the entire product development process of this rim, from the initial design considerations and the reasoning of the multi-material choices, to the developed algorithm for the CFRP layup, the material optimization with weight target procedure as well as the production, the use in the race car competition and the mechanical testing in static and dynamic load case scenarios. This thesis is hence an elaborate work involving overlaps between product design, development of simulation tools and production challenges. In the ambit of the extend of the work, the writer wants to keep the information restricted to the novelties developed within this thesis without spending too much time on revisiting the basic concepts and theory this work is based on. Hence the writer requires the reader to have a basic understanding on:

- Finite Element Method (FEM)
- Topology Optimization (TO)
- Computer Aided Design (CAD)
- Application of FEA in Abaqus for both isotropic and anisotropic materials.
- Carbon Fiber Reinforced Polymer (CFRP)
- Basic Racecar Vehicle Dynamic

1.3 Rim Concepts

1.3.1 2-piece CFRP shell with alloy center

The multi-piece rim consists of two separate carbon fiber reinforced plastic wheel shells, which hold the tire and are joined by an alloy metal center connecting the wheel assembly. One of the advantages of having a multi-piece rim is that the tire could be mounted while assembling the rim. This eliminates the use of conventional tire mounting machines that pull the sidewalls of the tires over the flanges on the rims. Sometimes this requires a lot of force which could shatter or permanently damage the brittle CFRP rims, as seen in the competitions.

Figure 1.3.1: 2-piece concept, Revolve NTNU 2014 [4]

1.3.2 1-piece CFRP shell with alloy center

The 1-piece or single-piece shell solution is quite similar to the latter solution. The production is potentially more difficult but can result in a lighter solution as less carbon is needed. Fewer discontinuities in the layup could benefit in a stiffer rim. However, it would not be possible to mount the tire without a tire changing machine. Furthermore, if the drop center is not designed properly, the flange could be susceptible to cracking or might experience high damage making the rim unsafe to run. To prevent this, a possible solution is to add more fibers around the flanges and dimension the rim for the loads related to mounting, resulting in a heavier solution. For this reason, the drop center should be carefully designed.

Figure 1.3.2: 1-piece concept, GreenTeam 2013[5]

1.3.3 Monoblock CFRP wheel

The monoblock CFRP rim is the lightest and stiffest solution. It can be produced using CFRP only , or by introducing the use of a core, resulting in a sandwich type structure. In 2013 Koenigsegg made the world's first hollow, one-piece and super light carbon fiber wheel, using a proprietary method developed named Aircore™ Technology[1]. Another way to produce a hollow, or a complete CFRP wheel, is to experiment with an air bladder or a 3D-printed core subsequently melted or dissolved and drained out through shear-pin holes or valve steam holes. Again, this solution would have the same issues related to the tire mounting as the previous solution. It is also the most complex and expensive solution discussed here with respect to production.

Figure 1.3.3: Monoblock CFRP rim, The Koenigsegg Carbon Fiber Wheel[6]

1.3.4 2-piece full CFRP wheel

The 2-piece full CFRP solution is quite similar to the monoblock solution, but it consists of two separate parts. The 2 pieces can be joined through bolts or adhesives. If bolted, the same mounting situation as in the 2-piece shell arises. Weight and stiffness advantages close to the monoblock design, however, arise especially if glued. This solution is almost as complex as the monoblock CFRP, but is simplified by splitting up the layup, since the rim produced in two pieces, making it faster to produce.

Figure 1.3.4: 2-piece full CFRP concept, Revolve NTNU 2016

Table 1.3.1: Pro and cons of concepts CFRP concepts

		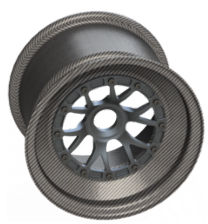			
		2-piece CFRP shell with alloy center	**2-piece full CFRP wheel**	**1-piece CFRP shell with alloy center**	**Monoblock CFRP wheel**
Must	Quality assurance	++	-	++	-
	Production, time, & cost	++	-	++	-
	Ability to hold pressure	-	-	++	++
Should	Assembly of rim	-	-	+	++
	Stiffness	-	+	+	++
	Weight	-	++	+	++

++ Superior + Good - Poor

1.4 CFRP LAYUP

Carbon Fiber is usually arranged to a filament before it is woven into a fabric or into a branch of unidirectional (UD)fibers. A satin weave or more specific a 5 Harness satin weave (5HS) which is found to the left in the Figure 1.4.1, usually has a weft with the same amount fibers in both principal directions resulting in the same properties in both principle directions. An UD weave illustrated right in the Figure 1.4.1, has most of its fiber in the first principle direction, this gives the UD more strength in one direction (typical $E_1 \simeq 25 \cdot E_2$). Using UD in strategical places can save weight by making use of the nonisotropic strength properties. However, UD layups are not as flexible as a weave, since they have most of the fibers in one direction, which more or less limits their use to curved surfaces in the the principal direction only.

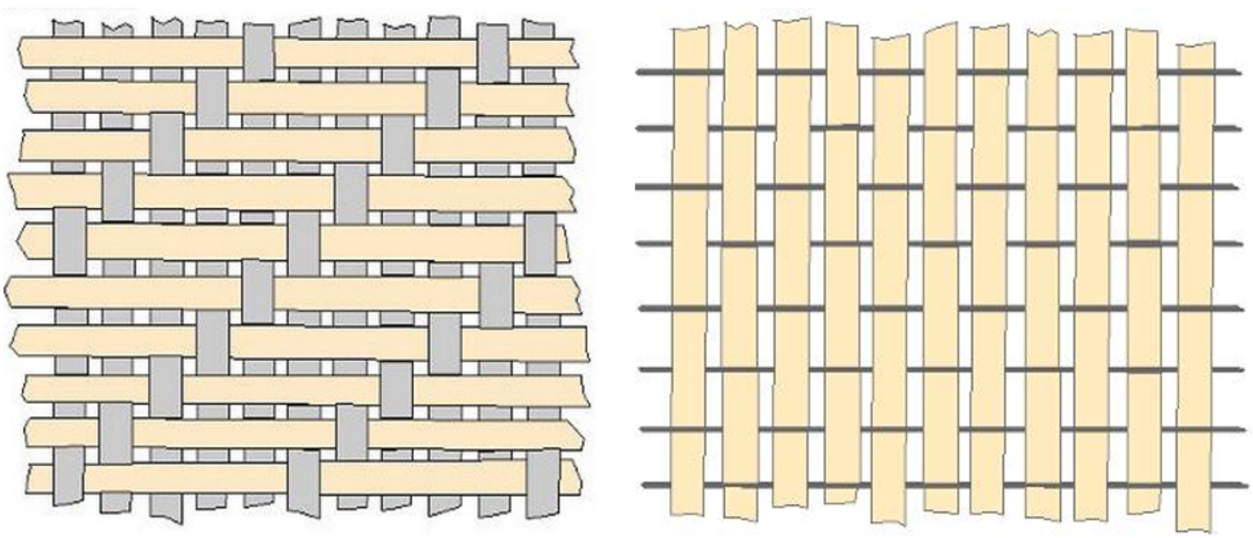

Figure 1.4.1: Weave types: left 5 harness sating weave , right Unidirectional-fibers [7]

1.4.1 MODELING OF CFRP LAMINATES

A laminate consists of two or more lamina/plies bonded together in one single structural element. Modeling of composite laminates are often conducted utilizing the Classic Laminate Theory (CLT). The basic assumptions of CLT are based on Kirchhoff Hypothesis [8]:

1. straight lines normal to the mid-surface remain straight after deformation
2. straight lines normal to the mid-surface remain normal to the mid-surface after deformation
3. the thickness of the plate does not change during a deformation

CLT also assumes perfect bonded layers with infinitesimally thin non-deformable bonding agents. Any out-of-plane stresses would subject a lamina to unnatural stresses, as the lamina can only resist significant stresses in the fibre direction. This modeling technique is not accurate for composites if the laminate is thick or the transverse shear modulus G_{23} of one or more lamina are small, in which case the shear deformation may be underestimated [9]. For thin composite shells with materials of high shear modulus, it will give an accurate representation.

1.5 Structural Optimization & Simulation Driven Design

Topology optimization (TO) is getting more and more attention especially in engineering problems, where low mass and high stiffness is essential for high performance. TO is a mathematical method with the goal to maximize the performance of a system by optimizing the material distribution within a given design space. The material distribution is optimized with respect to given loads, boundary conditions and constraints. The performance is usually the boundary condition/constraint in TO, e.g minimizing compliance and reducing the mass. TO of isotropic materials is purely geometrical. Here we are looking at composites, i.e. CFRP, which has anisotropic properties. The aim is to use similar approahes, yet not for optimizing the outer dimensions of the component but its internal composition and layup; the routine hence becomes a material optimization (MO). As the reader will go through this thesis, it will become evident that this approach opens new roads towards simulation based composite and likely other multimaterial based optimization.

1.6 Previous Work and Motivation

Based on the previous work done in my project work fall semester 2016/2017[10], where different wheel concepts were explored, a Hybrid Aluminum Carbon Fiber Composite Wheel has been chosen as the overall best concept (See Table 1.3.1). The hybrid rim is divided into two pieces, consisting of an aluminum center and a CFRP rim shell. A machinable aluminum center reduces the CFRP production time and manufacturing risk considerably. The CFRP shell, in contrast, reduces the mass where it has most impact on performance. This allows the production of a CFRP with reduced complexity. The goal of the thesis is to develop, implement and apply a simulation-driven material optimization approach to develop a fully working race wheel where boundary conditions are set such that maximum number of iterations and hence a wide solution space is possible without constraining the algorithm to known design solution from previous engineering experience. Where the biggest challenge will be to develop a method for implementing Simulation-driven Design approach for Material Optimization.

Manufacturing is more than just putting parts together. It's coming up with ideas, testing principles and perfecting the engineering, as well as final assembly.

James Dyson

2

Methods and Procedure

2.1 Load Scenarios

The load distribution on the rim was estimated from the reaction forces acting on the tire. Reaction forces from the tires were obtained from tire data considering load transfer and power limit calculated by Jon Martin Haaland, responsible for vehicle dynamics in the team. Together with Jon Martin Haaland and the suspension group, a common load case was decided, where the dynamic loads of the tire were divided into 6 quasi static load cases illustrated in Table 2.1.1 [3]. From this, a correlation between reaction forces and load distribution on the tire rim interaction was established. The load distribution on a rim consist of mainly 4 different cases; static tire pressure, lateral loads, vertical loads and torque due to acceleration/braking. Inflation pressure works laterally on the rim flanges and prevents the tire from slipping and causing debeading. The reactions forces are assumed to have a linear distribution and work equally on each side. The vertical loading was simplified by using a cosine function. This simplification is valid and can be traced back to Hertz in 1882 [11]. For the cornering, brake and acceleration loads, a model was established that is based on the work of Jesuette and Thives [12]. All the load distributions are derived in Appendix A.1

Table 2.1.1: Quasi static load scenarios for warm tires [3]

	Cornering (110 kph) Inside Wh.	Cornering (110 kph) Outside Wh.	Acceleration	Brake (110 kph)	3g Bump	2g Bump + Cornering (110 kph)	2g Bump + Brake (110 kph)
Front Wheels							
F_x	0 N	0 N	462 N	2797 N	0 N	0 N	2797 N
F_y	574 N	2907 N	0 N	0 N	0 N	2907 N	0 N
F_z	241 N	1959 N	482 N	1762 N	1688 N	3084 N	2887 N
Rear Wheels							
F_x	0 N	0 N	2420 N	1275 N	0 N	0 N	1275 N
F_y	832 N	2968 N	0 N	0 N	0 N	2968 N	0 N
F_z	358 N	2122 N	1302 N	578 N	1903 N	3390 N	1846 N

Reaction forces: F_x - longitunal dir. , F_y - lateral dir. , F_z - vertical dir.

2.2 Rim Center

This section will present the methods utilized for design and production of the rim center. Details on the software used will not be presented here. Detailed procedures and setup, the reader is referred to the Appendix A.4. For the design of the rim center, the following software were used, SolidWorks, Abaqus and Tosca Structures. The procedure was be divided into four steps:

- 3D-Modeling of the design space in Solidworks
- Building the Finite Element Model in Abaqus
- Setup the topology optimization in Tosca Structures
- Regeneration(3D modeling) of the topology optimized center in SolidWorks

2.2.1 Modeling of Design Space

The design space for the rim center was only restricted by caliper position and the shell size. Geometry and the dimensions of the design space are found in Figure 2.2.1 and were defined by the design constraint found in table 2.2.1. A manufacturing constraint was introduced since the center should be machineable.

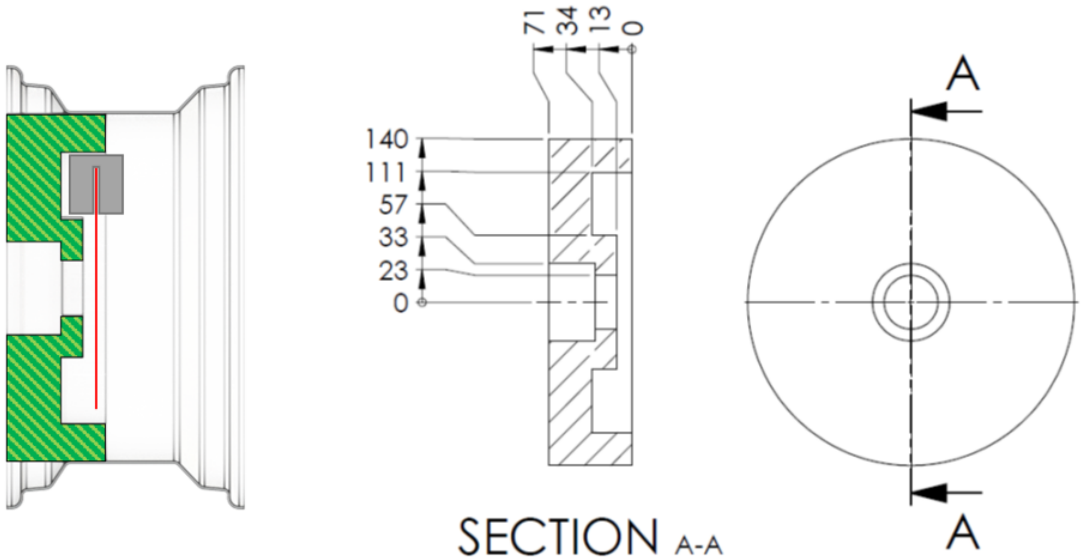

Figure 2.2.1: Illustration of design space for Rim Center

Table 2.2.1: Design constrains for the center

#	Description	Value
1.	Outer diameter	Ø 280
2.	Center hole diameter for axle	46 mm
3.	Chamfer in center compatible with retaining nut	Must
4.	6 x 6 mm modular bolt circle for aligning studs on hub	Ø 61
5.	Positive offset, center depth from outer shell contact surface	36 mm
6.	Material type	AL 7075-T651
7.	Production method	Machining
8.	Max mass per center	1 kg
9.	Clearance for internal components	<2mm

2.2.2 FE-Model

The FE-model for the topology optimization was simplified by modeling the design space for one spoke of the rim center.

Mesh

The finite element mesh was constructed out of 8-node linear brick elements with reduced integration and hourglass control (C3D8R-elements). A structured mesh control was selected with a target approximate global mesh size of 2 mm. The material was modeled as a linear elastic material with two constants E-moduli and poison ratios, respectively. It was applied to a geometry with a homogeneous section. Material constants for the applied material (AL 7075-T651) are found in the Appendix D.2.

Loads and interactions

The loads were simplified and assumed to act equally on each spoke. Loads were applied on a dummy shell with simplified tie interaction between the shell and the design space. All boundary conditions were applied to the the center lock with a kinematic coupling to the contact surfaces, where the hub and the center nut interact. The loads were defined by 2 independent quasi-static load scenarios defined with linear perturbation steps.

2.2.3 Topology Optimization

The topology optimization set-up is presented in Table 2.2.2. The optimization task was to minimize the strain energy of the design space under a weight target. The design space is partitioned into both non-design elements and design elements. The non-design elements are located in the center lock region. These elements are not modified during TO and hence called frozen elements in Tosca. Tosca structure does not contain machining as a implemented production constraint. This was approximated, applying the 3-axis milling constraint via a forging constraint acting from both sides in axial direction combined with rotational symmetry.

The weight constraint was set to below 1 kg. The information on finite elements, i.e. the raw data generated by the TO was modified using TOSCA.SMOOTH to smooth the surface. This created an iso-surface of elements, where intermediate densities are equal or greater than 0.3 (default).

Table 2.2.2: Topology Optimization Set-up

Material	Aluminium (7075-T651)
Element Type	Structured hexahedral
Abaqus Load Definition	Brake/acceleration & Cornering
Design Response	Strain energy (all steps),Weight
Objective Function	Minimize Strain Energy
Constraint	Weight Target
Geometric Constriants	Frozen sections, Forging
Design Cycles	50

2.2.4 Computer Numerical Control Machining

The manufacturing of the rim center was done with Computer Numerical Control (CNC) machining. This process was outsourced to Mjøs Metallvarefabrikk located in Lonevåg near Bergen. The machining was done on specifications which are found in the Appendix B.1. This CNC machining process consisted of tree main steps:

- Programming the machine paths in Computer Aided Manufacturing (CAM) software
- Setup and machining
- Validation of geometric tolerances, done with a Coordinate-measuring machine (CMM)

2.3 Rim Shell

This section presents the methods utilized for design and production of the rim shell. The main focus is on the method developed for the Material Optimization. Details on the application and software used, will not be presented here. Detailed procedure and set-up can be found in the Appendix A.3. For the material CFRP layup optimization, the following software were used: Isight, Matlab and Abaqus. The work-flow is illustrated in Figure 2.3.1. Isight was used for the optimization strategy linking the different software packages together -> Matlab generated ply text-files in a format suitable to Abaqus based on variables from Isight -> Abaqus performed the FEA simulation of the rim, and uses a pre. python-script to read the layup files from Matlab and then a post. python-script to read the result values, which consisted of the total strain energy for each load case.

2.3.1 3D-modeling of Rim Shell

The Shell geometry was limited geometrically by the suspension geometry, brake system (Table 2.3.1) and standards recommended by the tire manufacture Continental. The standard is defined by ETRTO – The European Tyre and Rim Technical Organisation. The ETRTO standard for drop center and hump design is found in the Appendix C.4.

Table 2.3.1: Design requirements for the shells

#	**Description**	**Value**
1.	Compatible with Continental FormulaStudent C16 7J-13	Must
2.	Min. internal diameter (caliper, suspension and upright clearance)	Ø 280 mm
3.	Max shell weight	0.8 kg
4.	Drop center and bead designed acording to ETRTO standard	Must
5.	Material choice	Hexcel 6376; UD & 5H

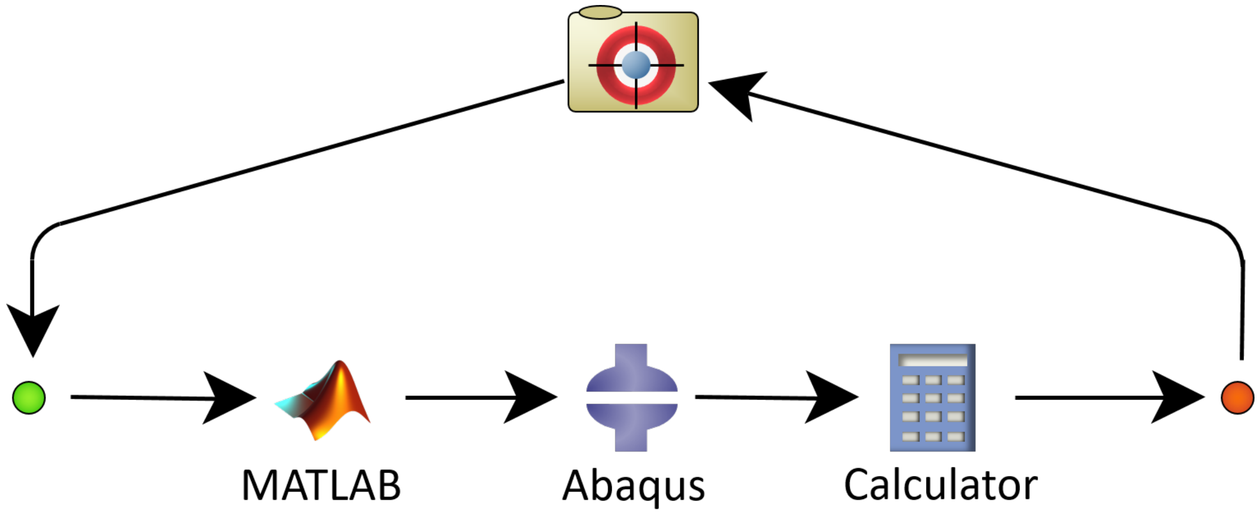

Figure 2.3.1: Work flow - Material Optimization

2.3.2 FE-Model

The composite shell was modeled with conventional shell elements with linear elastic properties. The properties of a single lamina was defined by 6 independent lamina constants: $E_1, E_2, \nu_{12}, G_{12}, G_{13}, G_{23}$. Material properties are found in the Appendix. Full composite layup properties were found by stacking every individual ply together and assigning their respective angles. This was done with the composite module in Abaqus.

Mesh

The finite element mesh was constructed out of 4-node doubly curved thin linear shell elements with reduced integration, hourglass control and finite membrane strains (S4R-elements). A structured mesh control was selected with a target approximate global mesh size of 5 mm.

Loads and Interactions

Loads were applied to the shell with surface traction following the pressure distribution derived in Appendix A.1 All boundary conditions were applied to the the center lock with a kinematic coupling to the contact surfaces where the hub and the center nut interact. The loads were defined by 2 independent quasi-static load scenarios defined with linear perturbation steps.

2.3.3 Material optimization

The optimization procedure was based on two load cases; cornering and braking. The optimization constraint is the total mass of the shell, and is set as the optimization target. The weight target was set according such that the total weight would be around 10 % lighter than the wheel assembly (rim and tire) of the 2016 car of Revolve NTNU. The optimization contains one objective, which is minimizing strain energy for each load case. Minimizing strain energy is the same as maximizing stiffness. Due to a limited amount of available UD-fibers from the sponsors, a second constraint was added, which was a limit of maximum UD-fiber in square meter per rim shell.

Segmentation and Parameters

Segmentation of the rim shell was based on anisotropic loads and drapeability properties. The shell was exposed to higher loads on the inner part of the rim and near the interaction points of the rim center. Double curved surfaces were separated form single curved due to the difference in drapeability properties of the layups. The design variable was based on dividing the rim into 8 sections (see Figure 2.3.2). Each section has a range of different design variables, orientations and number of layers. For the sections IB, CM, CS and OB the optimization procedure included a material selection, where a 5 harness satin weave (5HS) CFRP and a unidirectional (UD) CFRP available. All variables and parameters used for the MO is found in Appendix A.3 Table A.3.2.

Optimization Algorithm

The optimization is based on an evolutionary optimization algorithm. It is well-suited for non-linear and discontinuous design spaces. Another important factor is that it also works well for long running simulations, which is the case for this problem. Evol is an evolution strategy based on the works of Rechenberg and Schwefel[13], which mutates designs by adding a normally distributed random value to each design variable. The mutation strength (standard deviation of the normal distribution) is self-adaptive and changes during the optimization process. The evolution optimization has three stop criteria; converged, reached ultimate iteration or more than n failed iterations.

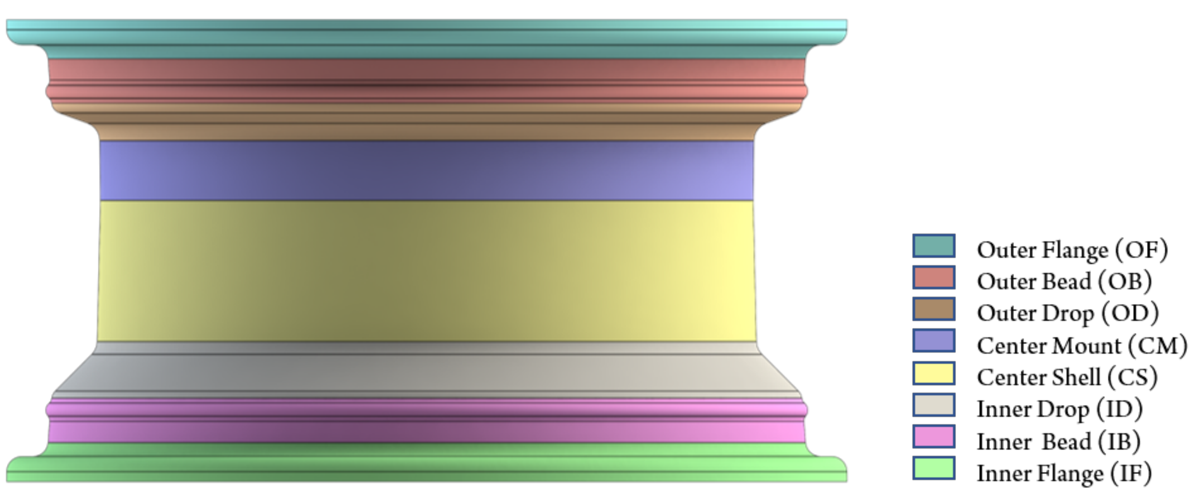

Figure 2.3.2: Segmentation of the Rim Shell

2.3.4 Carbon Fiber Reinforced Polymer Laminate Production

The production of the shells was accomplished with the use of carbon fiber with pre-impregnated active resin (CF-prepreg). The production was divided into tree phases:

- Pre-production of the Shell
  - Drapeability analysis (DA) and ply segmentation
  - CNC cutting of each plies based on DA
- Production of the Shell
- Post-production of the shell
  - Trimming and CNC machining of mounting holes

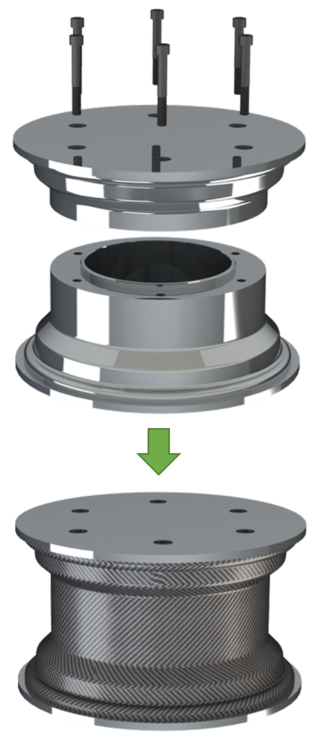

Figure 2.3.3: 2-piece positive mold design

Shells were manufactured by hand, by the author himself. This was done a with 2-piece aluminum moulds that were bolted together (Figure 2.3.3). The moulds were treated with a release agent before manufacturing the layup. After finishing the layup, the mould was bagged, set under vacuum, and then cured in an autoclave(Figure 2.3.4) subjected to heat and pressure. A high quality part with high surface finish, low resin content and excellent structural performance was obtained. Detailed pictures from the production are found in Appendix A.8.

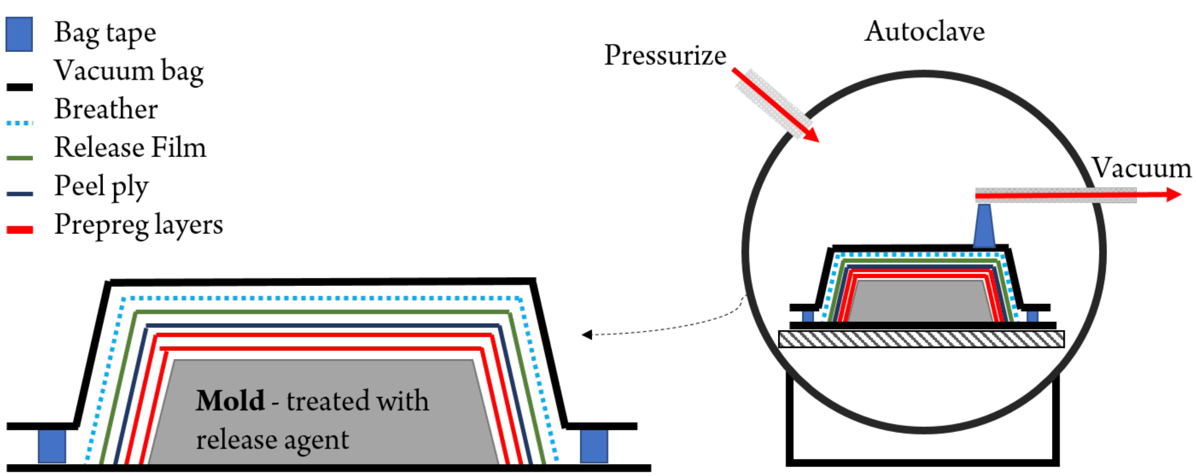

Figure 2.3.4: Illustration of Autoclave prepreg Casting process

Ply Segmentation and CNC-Cutting

Form and segmentation of each ply were designed according to a drapeability analysis. For the drapeability analysis, Simens NX and Fibersim were used. The focus on the segmentation for the first layer was to have the biggest and most continuous layer possible. On the rest of the layers, the aim was to minimize angle deviation due to double curvature and to avoid joints on same spots and rather have overlapping joints, see Figure 2.3.6. Based on the drapeability analysis, production manuals(see Figure 2.3.5) were compiled. They contain ply-number, sequence, orientation, placement and material. Each ply was CNC-cut according to the simulated shape in FiberSim. All plies were marked and sorted after ply-number and sequence for each rim. The unidirectional fiber is very brittle and was handled extra carefully by placing on stiff cardboard.

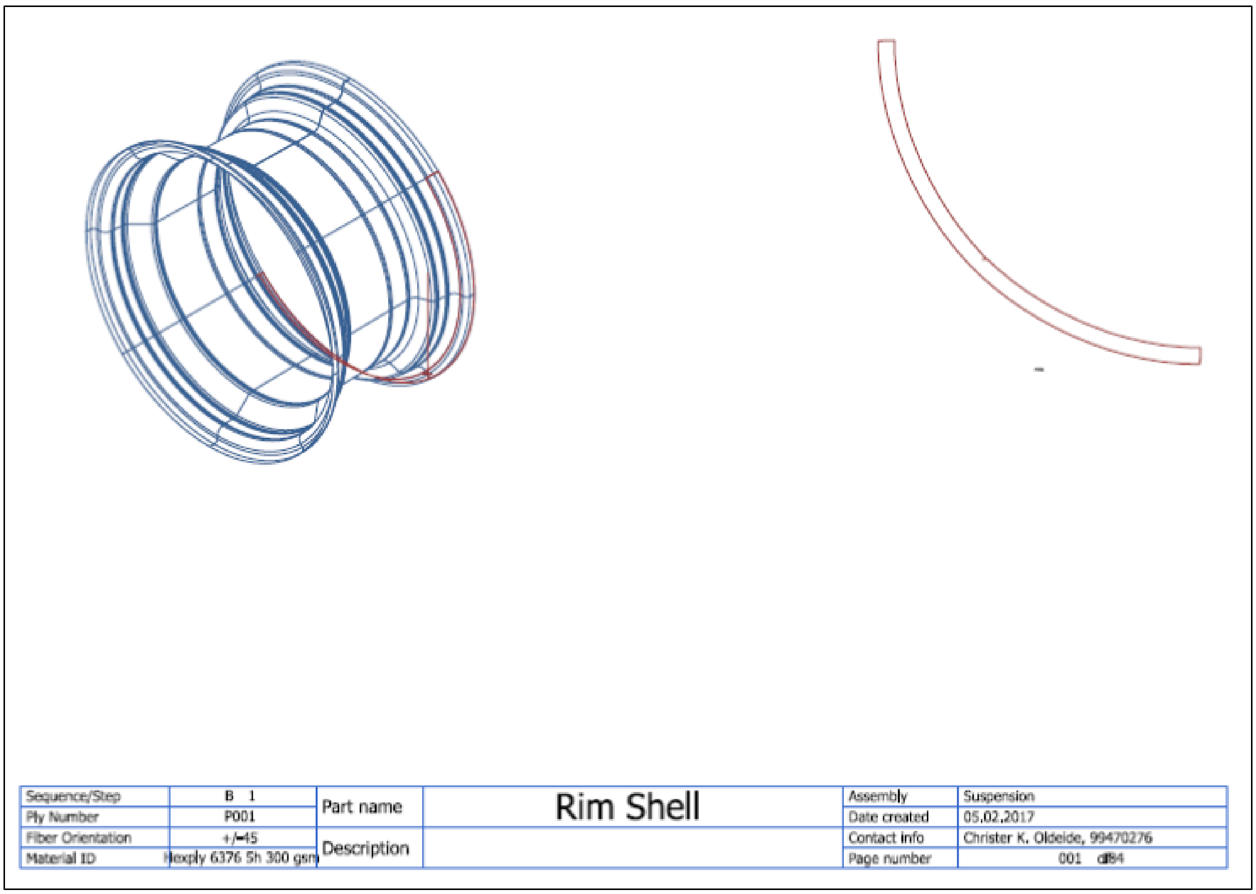

Figure 2.3.5: Production documentation for Rim Shell

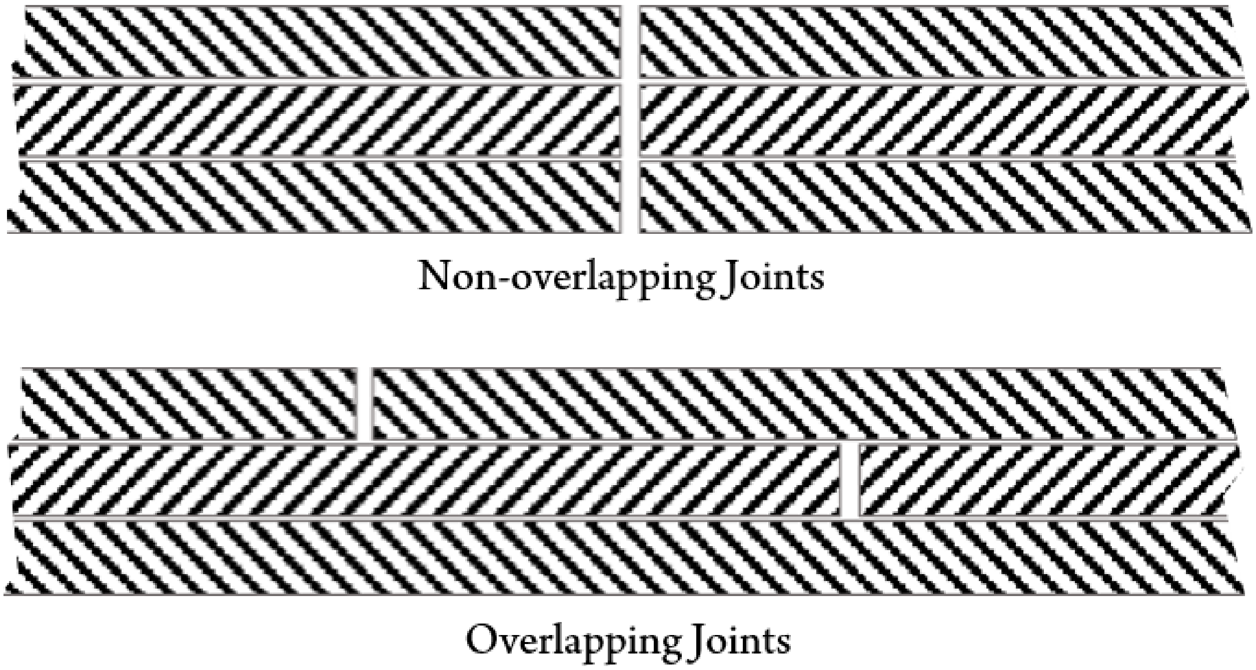

Figure 2.3.6: Joint designs for CFRP layup

Mould Design

Positive mould design was chosen due to high curing temperature, which led to high thermal expansion. The contribution of thermal expansion was assumed to be linear and uniform. The moulds were CNC machined at Molstad Modellfabrikk according to the specifications found in Appendix B.2. After machining, the moulds were wet-sanded, starting with p400 and performing final sanding with p2000. After wet-sanding, the moulds were polished and cleaned with acetone. The moulds were then treated with two layers of sealer to fill remaining pores. They were then coated with 5 layers of release agent. The process was repeated for every cast. The application of sealer and release agents was done according to the datasheet found in Appendix D.6-D.7

Layup

The layup was done manually by hand according to the documentation made in Fibersim. Firstly, the inner backing on the ply was removed, the outer backing was kept during forming of the ply to minimize distortion. On the first layer a heat gun was used to make the epoxy stick better to the mould (Application of initial ply is seen in Figure 2.3.7 a)). Each layer was shifted 15^o to ensure overlapping joints. Two different prepregs were used, a 5HS weave and a UD-fiber. Applying the UD-fiber (Figure 2.3.7 b)) was done extra carefully as this material is sensible for tears and requires an exact placement according to draping analysis to minimize tears and bridges. Between every first and second layer, a debulking (Figure 2.3.7 c)) step of 20 min was executed to minimize bridging and to ensure proper bonding between each layers. After the last layer was debulked, a layer of peel ply (Orange fabric in Figure 2.3.7 d)) was added. The peel ply removes excessive epoxy and is usually used to make an even surface finish with high surface roughness suited for bonding. For the rim shell, the peel ply was applied to save weight and improve the sealing properties between the tire and rim shell.

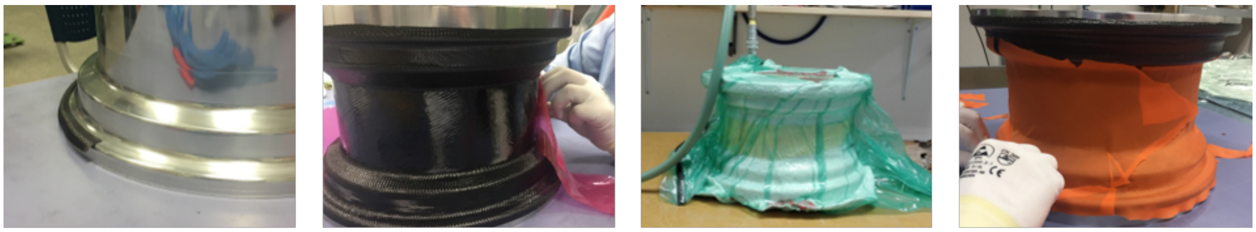

a) b) c) d)

Figure 2.3.7: a) Initial ply, b) Application of UD-ply, c) Debulking of Rim Shell, d) Application of peel ply

Bagging

After the peel ply was applied, a release film was added as seen in Figure 2.3.8. In this application, the release film has two functions; isolate the laminate from foreign bodies and prevent the breather from absorbing epoxy. After the release film, a layer of breather was applied around the whole mould, extra layers was added to every sharp edge to reduce the risk of bag burst during curing. The heat rate allowed during curing was determined by the temperature of the mould. To control the heat rate during a curing, a temperature sensor was placed between the laminate and the mould. A high temperature tube bag was chosen only requiring a seal on each end reducing the risk of leakage and bag failure during curing. The bag was sealed with a high temperature proof Vacuum Bag Sealant Tape. Two vacuum ports were placed on top of the mould, one for ensuring vacuum during curing and one for monitoring. Before curing, all bags were evacuated and checked for leakages leading to a pressure drop of more than 0.05 bar in 5 minutes.

a) b) c)

Figure 2.3.8: a) Finished application of release film, b) Bagging of Rim Shell, c) Vacuum test of bag

Autoclave Curing

The control program for curing the rim shell was set-up according to recommended curing procedure found in Appendix D.3 and is illustrated in Figure 2.3.9. To compensate for the reduced heat rate caused by the high heat capacity of the aluminum mould the temperature set point in the Autoclave was set to 190 C^o (maximum allowed for Hexcel 6376).

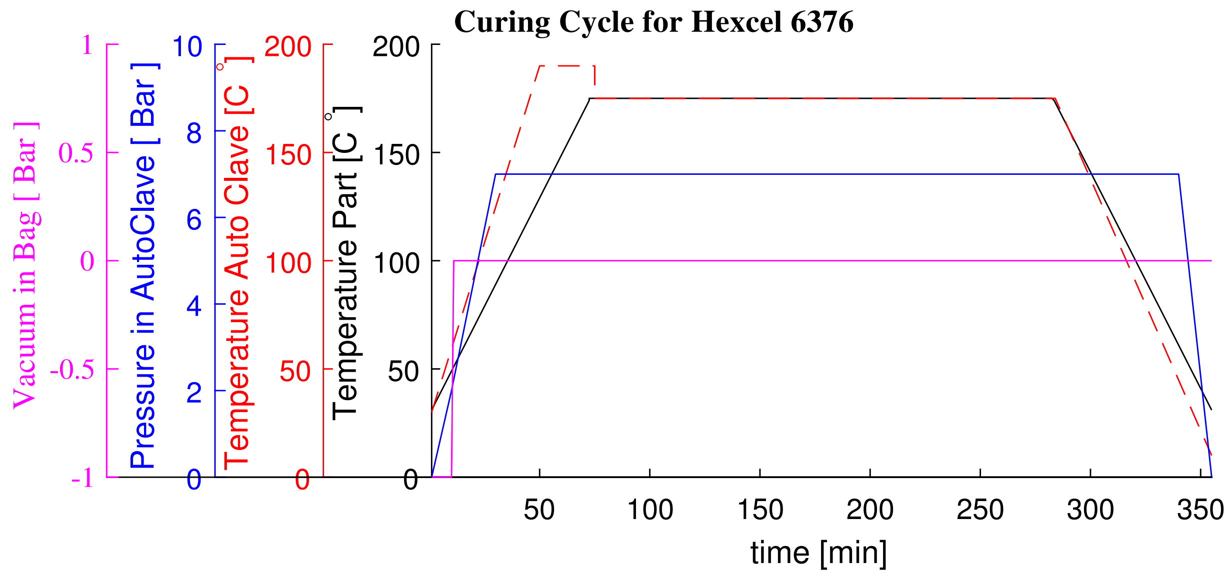

Figure 2.3.9: Curing cycle for Hexcel 6376 prepreg

Demoulding & CNC-Machining

After curing the used bag, release film and peel ply were removed from the cured rim shell before demoulding (Figure 2.3.10). The rim shell was then machined by Kongsberg Gruppen (KOG) at the Kongsberg Defence Systems (KDS) department in accordance with specifications found in Appendix B.3.

a) b) c)

Figure 2.3.10: a) Removing of vacuum bag and breather after curing, b) Removing of release film after curing, c) Removing of peel ply after curing

2.4 Validation

To validate the assembled wheel design (Rim shell and Rim center), an FE-model including non-linear effects was constructed. This section will not go into details concerning applications and software. Complete software set-up and applications used in Abaqus can be found in Appendix A.2.

2.4.1 FEM validation

Modeling of the rim center and rim shell was based on FE-models described in Section 2.2.2 & 2.3.2. Interactions and loads were changed to give a more accurate representation of the physical model. To include the non-linear effects from the pre-tension in bolts and center-lock, the linear perturbation step was changed to a static general step.

Mesh

The same mesh procedure as in the previous model was used but with a mesh refinement near the contact regions.

Loads and Interactions

In addition to load scenarios defined in Appendix A.1, the interaction between the rim center and rim shell was modeled with contacts and bolts, the adhesive used to seal the rim was neglected. To include the pretension on the center lock, a dummy hub was modeled. This dummy hub was also applied to all boundary conditions.

2.5 Mechanical Testing

This section will explain mechanical set-up, fixtures, and measurements needed for verifying laminate modeling and loads for the FE-model in Abaqus.

a) b) c)

Figure 2.5.1: Mechanical testing: a) set-up of fixture in hydraulic load applicator, b) Placement of inductive displacement sensor for outer bead, c) Placement of inductive displacement sensor for inner bead.

2.5.1 Measurement

The measuring of the strains and displacements was done digitally and logged according to the applied load. To measure the applied load, a load cell with a range up to 2 tonne was used.

Strain

3-axis strain gauges were used to measure the strains along the axis illustrated in Figure 2.5.2. Five strain gauges were placed along the profile of the rim (the type of strain gauges can be found in Appendix D.1). They were placed according to the five red lines in Figure 2.5.3 following the coordinate system in the Figure.

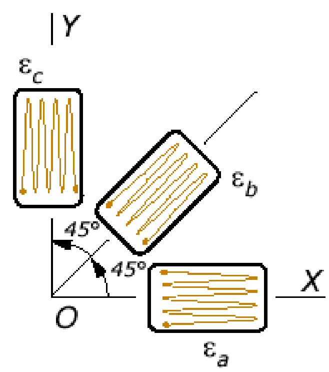

Figure 2.5.2: Illustration of a 3-axis strain gauge rosette [14]

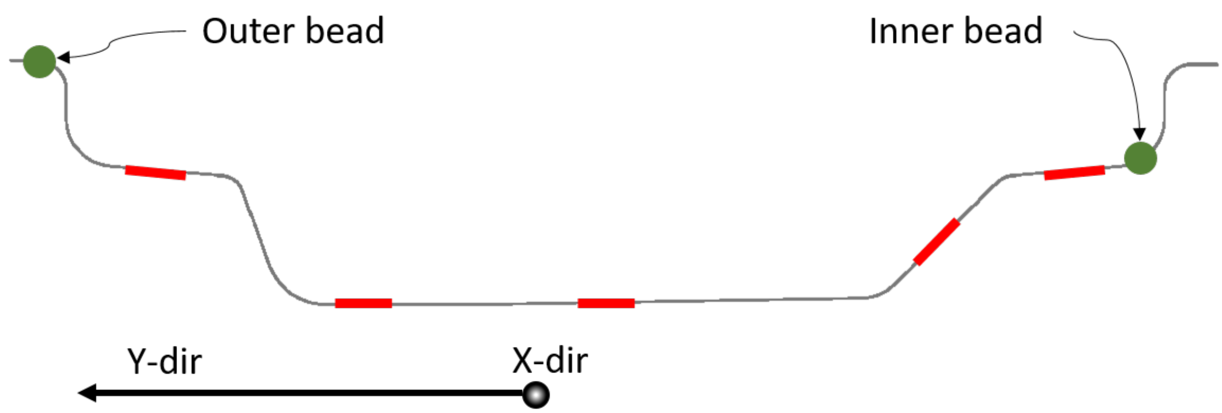

Figure 2.5.3: Illustration of strain gauge positions and placement of displacement sensors

The surface, where strain gauges were mounted, was sanded with a sand paper and cleaned with acetone before the gauge was glued with an adhesive specialized for this application. In Figure 2.5.4 picture a), a strain gauge is glued to the rim, picture b) shows the strain gauge after it is glued in place, picture c) shows all the strain gauges mounted in place.

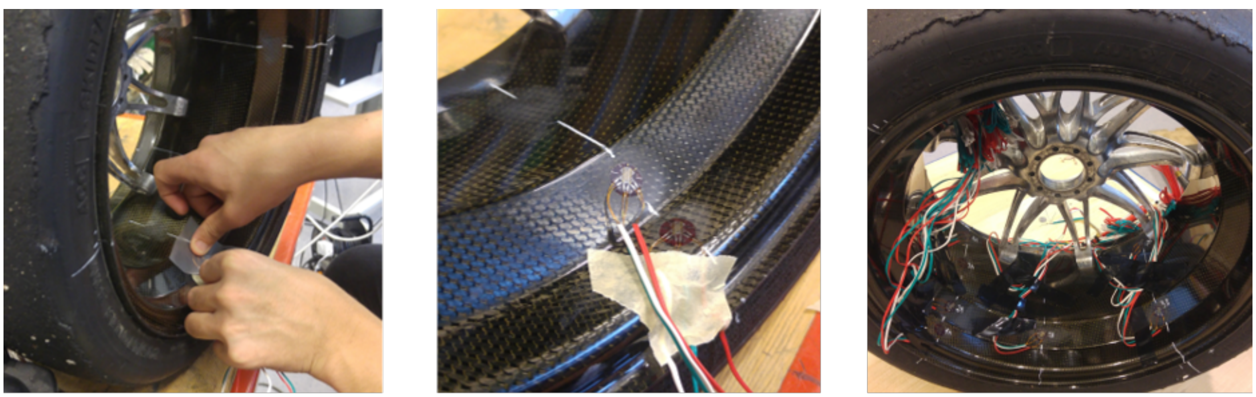

a) b) c)

Figure 2.5.4: a) Gluing of strain gauge, b) Strain gauge mounted in place, c) Strain gauges mounted and organized

Displacement

Both, the displacement on the inner and outer bead was measured as illustrated in Figure 2.5.3 by the green circles. The sensor was mounted with a magnetic holder as showed picture b) and c) in Figure 2.5.1. To reduce the measuring error coming from compliance of the rig, the magnetic holders were mounted as near the center lock as possible.

2.5.2 Test Procedure

The mechanical testing of the rim was divided in 3 load cases, inflation pressure, vertical load and dynamical load. Inflation pressure is the simplest load case to replicate in Abaqus and was therefore used to benchmark the laminate modeling of the rim shell. The vertical load case was done to benchmark the modeling of the vertical load case and the modeling of the interaction between the rim center and the rim shell. The dynamical load case was executed to see whether the quasi-static load scenarios were in apropriately chosen.

Inflation Pressure

The inflation pressure load was calibrated to zero at the values of the strain gauges obtained at 0 bar over-pressure in the wheel. The pressure was then increased to 2 bar and the strain gauge was measured for 60 seconds. The pressure was than decreased to 1.5 bar and measured again for 60 seconds. The same procedure was repeated for 1.0, 0.75, 0.5 and 0.25 bar. This test was then repeated 3 times for acquiring an appropriate amount of data for comparing.

Vertical Load

For the vertical load case, the vertical load was set to 3g bump, which is a vertical load of around 2000 N. Both strains and displacement of inner and outer bead were of interest during this test. The vertical load was applied according to Figure 2.5.5 and repeated 3 times. This procedure was done with the rim oriented around the axial direction at three different angles. First, such that the strain gauge was oriented at top and then shifted to 90^o and 180^o, respectively. This was done to acquire a better understanding of the load distribution around the wheel.

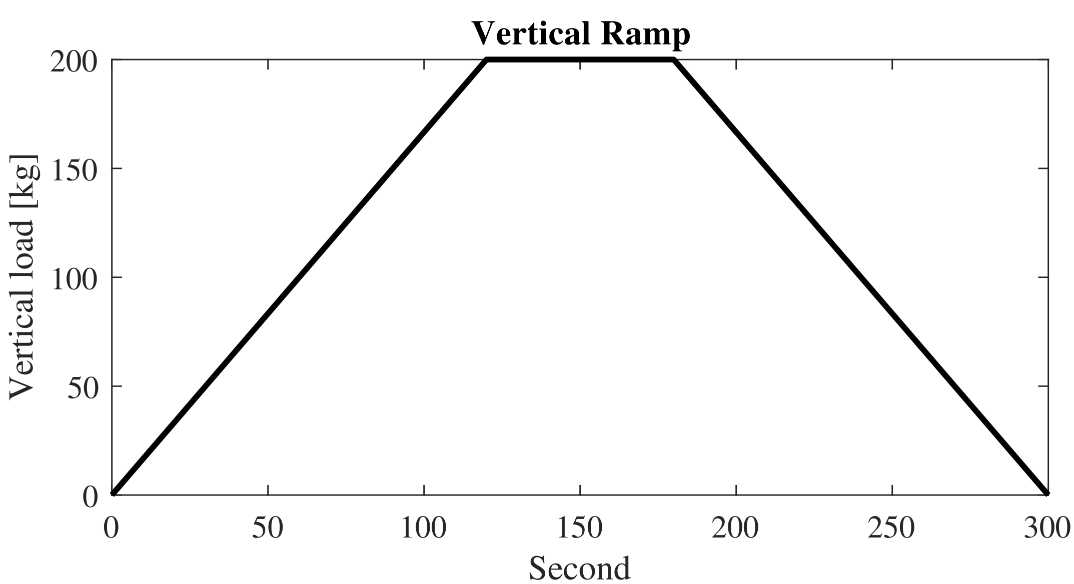

Figure 2.5.5: Ramp for Vertical Load during quasi static testing of Rim

Dynamical Loads

For the dynamical loads, the vertical load was applied with a square wave function ranging from 180-200 kg. The dynamical load was applied with different frequencies ranging from 0.5-8 Hz. Displacements and strains were logged for each load case.

2.5.3 Mechanical Set-up

A fixture jig made of steel was designed to keep the wheel in place during mechanical testing. To mount the wheel, a simplified hub with the same center locking mechanism as on the race car was created. The rig was designed to have a stiffness giving a displacement at the hub of less than 1% of the estimated displacement of the rim . Machine drawings of fixture jig is found in Appendix B.4.

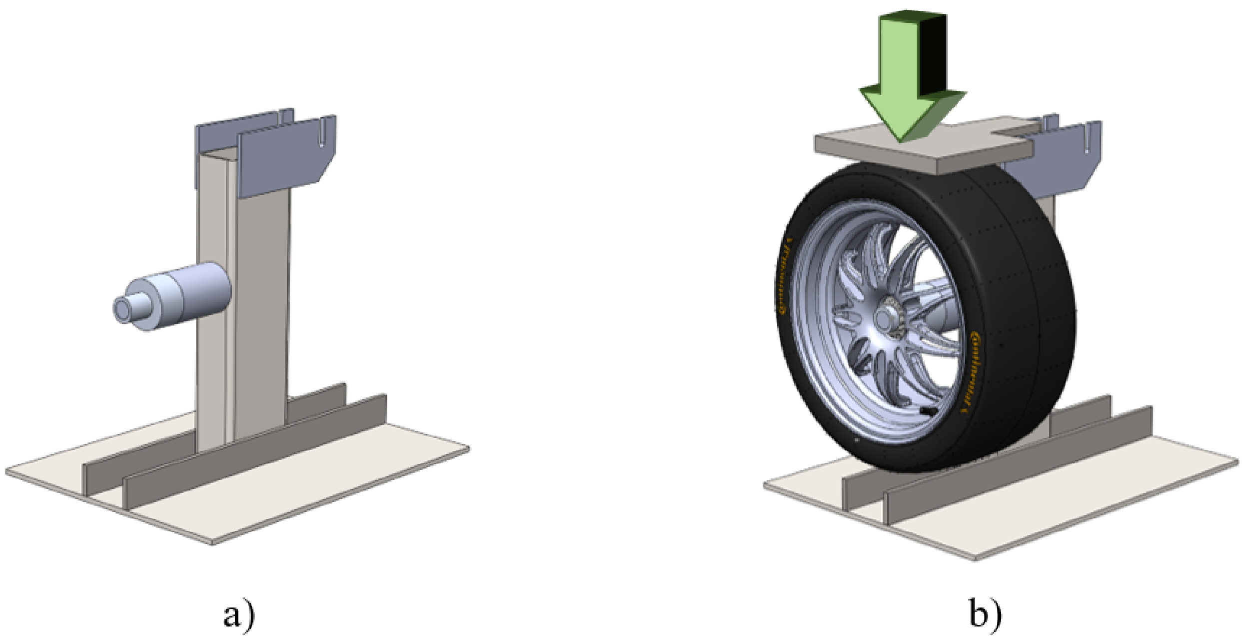

Figure 2.5.6: Fixture jig for applying vertical loads during mechanical testing: a) Illustration of test jig b) Illustration of wheel mounted in test jig, green arrow illustrate vertical load

Failure is central to engineering. Every single calculation that an engineer makes is a failure calculation. Successful engineering is all about understanding how things break or fail.

Henry Petroski

3

Results & Discussion

3.1 Rim Center Design

3.1.1 Topology Optimization

The resulting raw geometry from the topology optimization carried out in Tosca is found in Figure 3.1.4. After 38 iterations, the optimization converged and the mass and strain energy is plotted in Figure 3.1.3. The raw geometry is presented in figure 3.1.2, one can see that the forging production constraint gives a good starting point for a machinable design. The cross-section in Figure 3.1.1 a) shows that all the available design space (Figure 3.1.1 b)) in x-y plane is used near the center-lock, definition of design space is found in Chapter 2 Section 2.2.1. This is not that odd since the cornering load case is one of the biggest. This is in line with many commercial racing center lock rims.

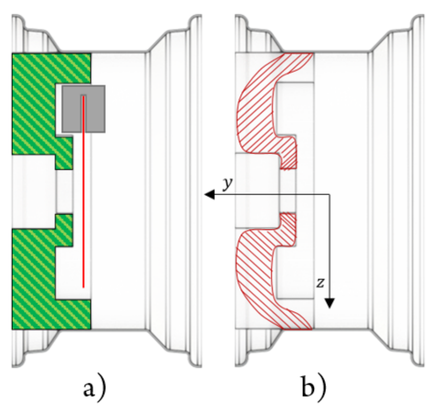

Figure 3.1.1: a) Design space for rim center b) Cross-section of Topology Rim Center

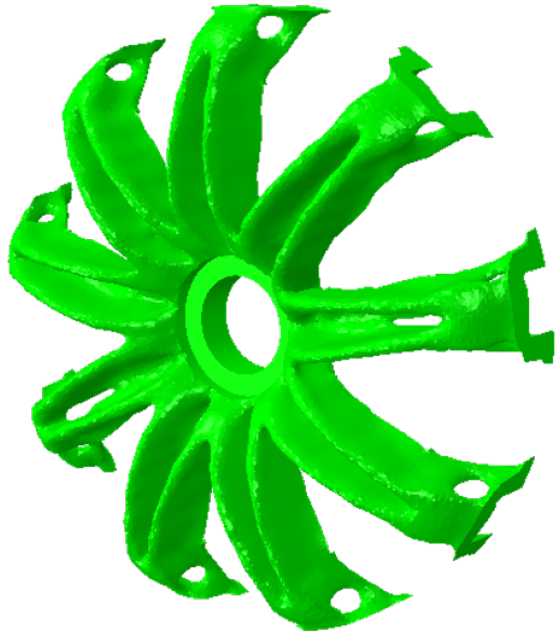

Figure 3.1.2: Raw data from Topology Optimization performed in Tosca

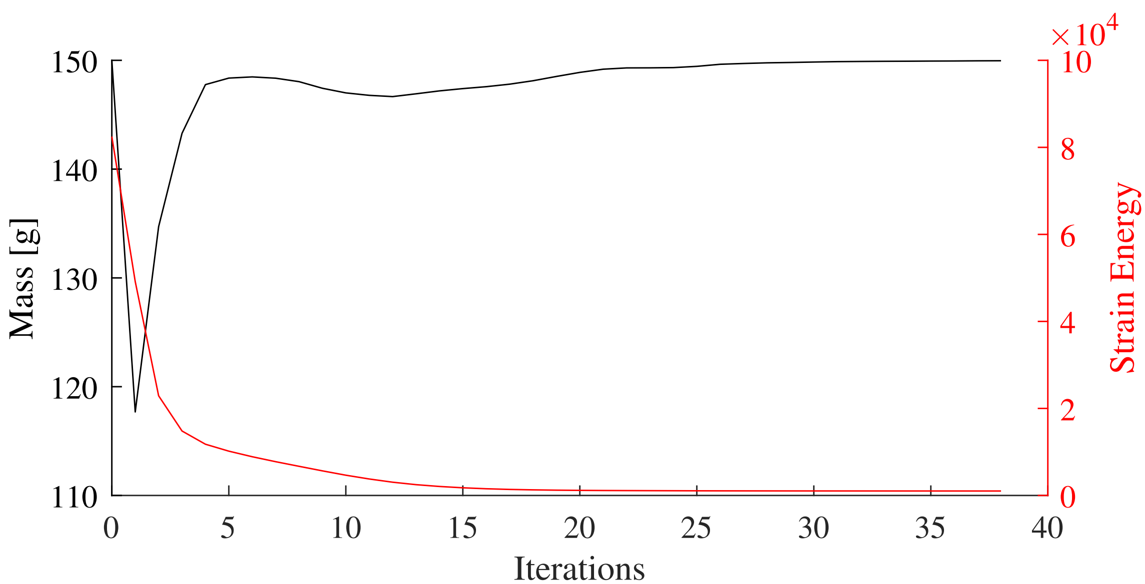

Figure 3.1.3: Iterations from Tosca Structure of the 9 spoke rim center

3.1.2 Regeneration

A draft analysis, (Figure 3.1.4 a)) shows all positive (green) and negative (red) draft angles. The negative draft is undesirable for a 3-axis machinable design. Two regenerated machinable designs are presented in figure 3.1.4, see Chapter 2 Section 2.2.3 for machining constraints. Both of the designs use the same cross-section as the TO, figure 3.1.1. The data in Table 3.1.1 is the relative specific stiffness of the regenerated designs with respect to the raw data obtained from TO. The 5-axis design has a specific stiffness of 18 % higher than the TO design and 44.9 % higher than the 3-axis design. The 3-axis design has a lower relative specific stiffness mainly due to a through hole bolted connection which results in a less optimal geometry near the interference to the shell. The 5-axis design has higher relative specific stiffness, this is because it has a greater design freedom than the TO and the 3-axis design.

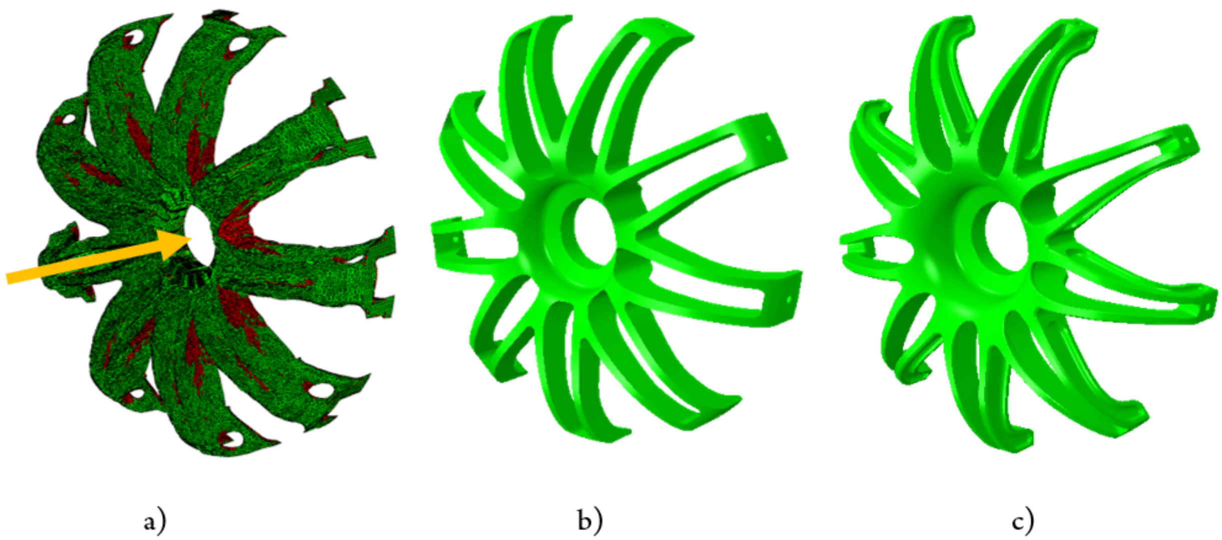

Figure 3.1.4: a) Draft analysis of TO design. Regenerated designs: b) subject to 3-axis and c) subject to 5-axis machining constraint

Table 3.1.1: Specific stiffness for the 2 different center designs,normalized respect to topology optimized design

Design	3-axis	5-axis	Difference
Mass[g]	1021	910	12.2 %
Lateral deflection [mm]	0.93	0.73	27.4 %
Specific stiffness	81.4	118	44.9 %

100 = specific stiffness of TO

3.2 Rim Shell

The CFRP Layup optimization result is presented in figure 3.2.1. The figure shows the mass to strain energy for all optimization iterations. Iteration 1-500 result in a mean mass of 818.0 g with a standard deviation of 110.7 g, iteration 500-1500 provide a mean mass of 781.2 g and a standard deviation of 80.1 g, and the last iterations yield a mean mass of 717.1 g and a standard deviation of 43.3 g. In the beginning of the optimization, the mass had a large deviation and is random. The deviation of the mass is getting lower for each data set, and the mean mass tends to converge around the target mass of 700 g, see Chapter 2 Section 2.3.3 for weight target. The evolution-based layup optimization converged after 3699 iterations, with a resulting mass of 710 g. In figure 3.2.2 the layup iterations are sorted with strain energy in ascending order. Looking at mass plotted in black, one can see that there is a clear trend at the lower bound between mass and strain energy. No extreme values at the lower bound is a good indication of convergence.

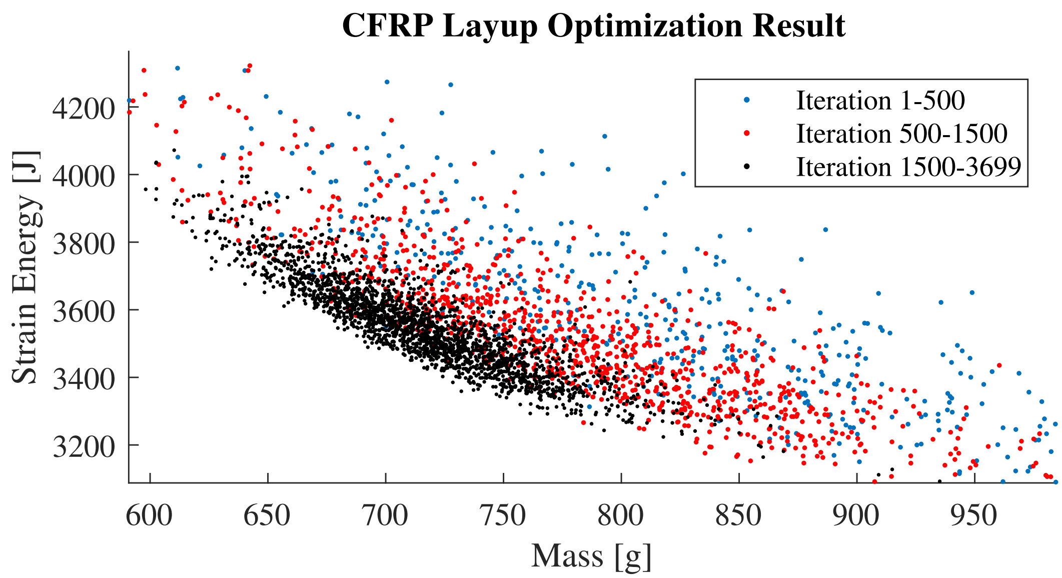

Figure 3.2.1: All CFRP Layup Optimization iterations presented in a mass vs. strain energy plot

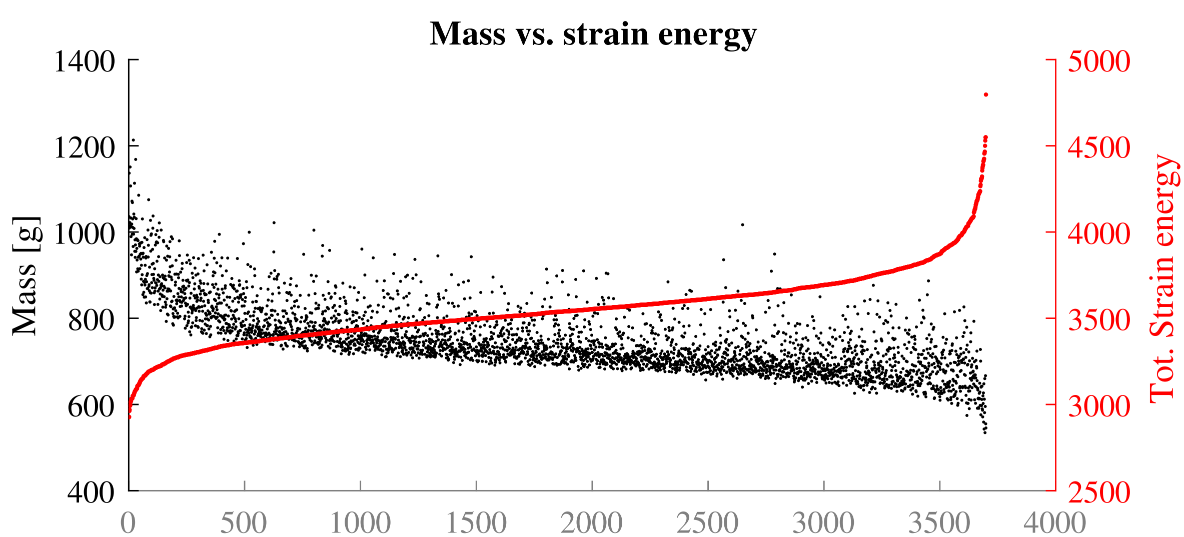

Figure 3.2.2: Sorted layup iterations with strain energy in ascending order

The resulting layup is presented in Table 3.2.1. Notation of segmentation is illustrated in Chapter 2 Section 2.3.3 Figure 2.3.2. Each row in the table represents one layer on the laminate. The layup stacking is not typical in engineering practice, there is no symmetry in the thickness. However, there seems to appear a pattern where the UD-Fiber are arranged in complementing pairs, similar to a balanced laminate. The optimization has prioritized more plies, close to where the center is mounted to the rim shell, i.e. on the center mount (CM) section see Chapter 2, Section 2.3.3. This priority can be explained by the unsymmetrical loads the rim shell is subjected to and that interaction between the Rim center will lead to some form of stress concentrations.

Table 3.2.1: Layup Result from Material Optimization

Ply.	OF	OB	OD	CM	CS	ID	IB	IF
1	S 45	S 45	S45	S 45	S 45	S 45	S 45	S 45
2	S 45	S 0	S 0	S 0	S 0	S 45	U -75	S 0
3	S 0	U -30	S 0	U 30	U 30	S 0	S 0	S 45
4	S 0	U 0	S 45	U -30	U -30	S 0	S 45	S 0
5	S 0	U 30	S 0	U -60	U -60	S 0	U 0	S 0
6	S 45	S 45	S 45	U 0	U 0	S 0	U 75	S 0
7	-	S 0	S 0	U 60	U 60	S 0	U 0	S 45
8	-	-	-	U 0	S 0	S 0	S 0	S 0
9	-	-	-	S 45	-	S 45	-	-
10	-	-	-	S 0	-	-	-	-
11	-	-	-	S 45	-	-	-	-

S - Satin weave U - Unidirecitonal

3.2.1 Performance of Optimized Layup

In Table 3.2.2 the performance of the layup is compared to an aluminum shell and a shell with the layup developed for the CFRP rim for the 2014 Revolve NTNU car. The aluminum shell has a thickness of 3.18 mm, which is the same thickness as formula student aluminum rim sold by K2W Precision Inc.[15]. All shells have the same shell geometry. The layup of the 2014 shell is found in Appendix A.9.

Table 3.2.2: Performance of optimized layup compared to a aluminum shell and the 2014 layup

Design	Mass [g]	Lateral Deflection [mm] (cornering@110km/h)	Specific Stiffness	Rotationa Inertia [gmm^2]
Shell with Optimized layup	700	1.476	100.0	$1.7 \cdot 10^7$
Aluminum Shell	2150	0.856	56.1	$5.3 \cdot 10^7$
Shell with 2014 layup	600	1.901	90.6	$1.5 \cdot 10^7$

Specific Stiffness Normalized to Optimal layup

The optimized layup has a specific stiffness of around 45 % higher than the aluminum shell with a decreased rotational inertia of nearly 70 %. Compared to the 2014 layup, the optimized layup has an increased specific stiffness of almost 10% and 23% lower lateral deflection with only 10 % higher rotational inertia.

3.3 Validation

In Table 3.3.1 max stress, deflection and safety factors for all load cases are presented. This validation model includes non-linear effects like contact and pre-tension on bolts and the center lock. The connection of the rim center to the rim shell was done as described in Chapter 2 Section 2.4.1. In Figure 3.3.1, the FEA results for the cornering load case is presented, together with a detail view of pretension effects. The Von-Mises stresses in cornering on the center is lower than 50 MPa for most of the center and 115 MPa on a small region for the heaviest loaded spokes. The maximum shell stress in cornering is 51.8 MPa and has 0.187 according to Tsai-Wu failure criterion where 1 is failure. The lowest safety factor for the centerpiece is 3.43 against yield, and 0.235 for the shell according to Tsai-Wu failure criterion. The overall low stresses indicate that the overall stiffness is high. FEM results for all load cases are found in Appendix A.5.

Table 3.3.1: Validation result including non-linear effects

Load case	f_x [N]	f_y [N]	f_z [N]	Max shell stress[MPa]	Max center Mises [MPa]	Deflection mag. [mm]	Shell Tsai-Wu Failure Criterion	Center Safety Factor Yield
Turn	-	2968	2122	51.8	115	2.27	0.187	4.78
Brake	2876	-	1895	57.3	133	0.96	0.132	4.11
3g bump	-	-	1903	58.1	64.2	0.811	0.118	8.56
2g bump +turn	-	2968	3390	66.9	137.93	2.82	0.235	3.99
2g bump +brake	2876	-	3020	54.6	160.35	1.39	0.196	3.43

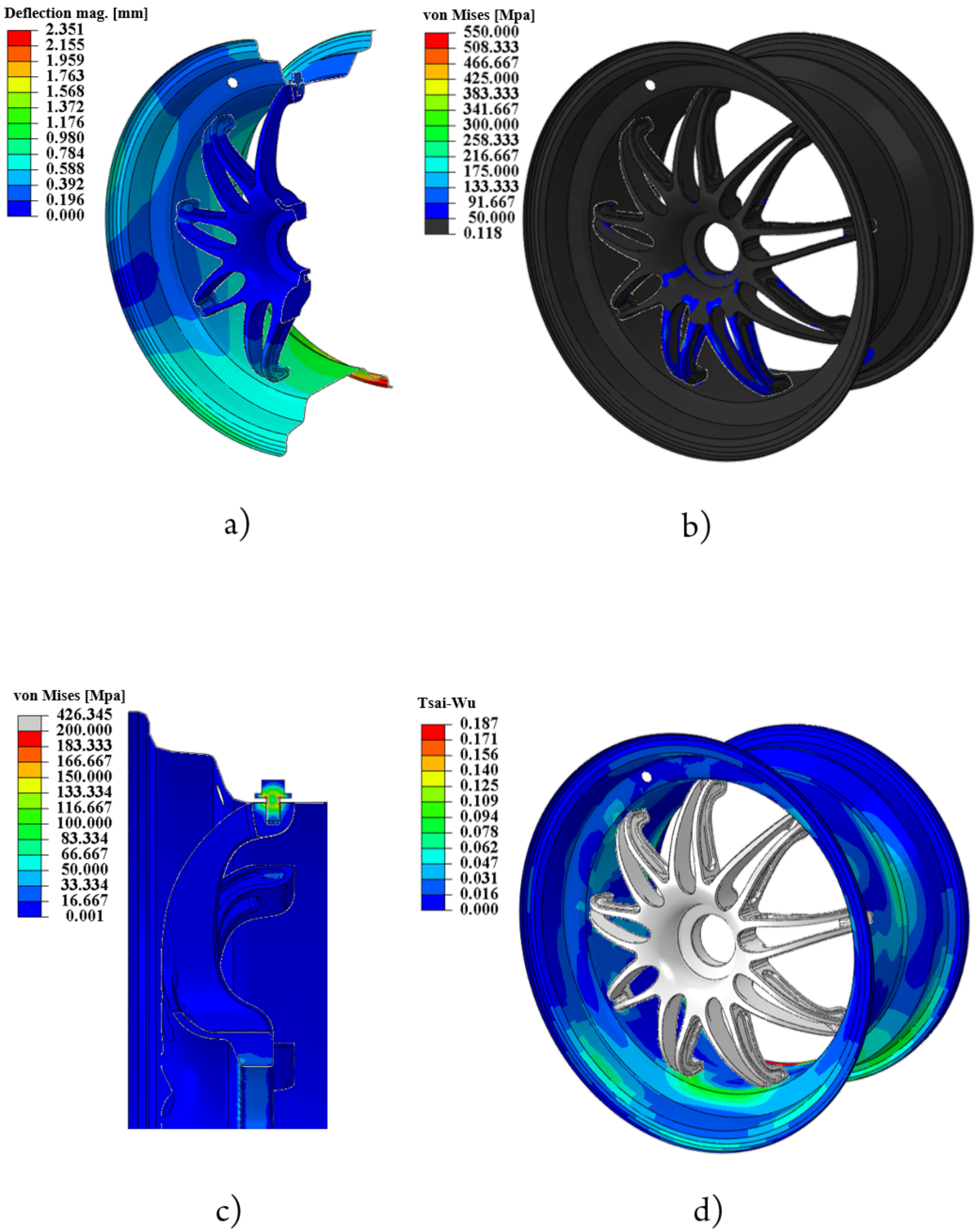

Figure 3.3.1: Validation results from Abaqus: a)Deflection magnitude in cornering @110km/h. b) Von-mises stress on center in cornering @110km/h. c) Pretension on center lock and bolts. d) Tsai-Wu failure criterion on shell in cornering @110km/h

3.3.1 Fatigue properties Rim Center

The stress spectrum for the most stressed section of the rim is presented in Figure 3.3.3, the most stressed section is found in Figure 3.3.2. This is the stress spectrum based on half endurance (11 km), where the loads are coming from actual log-data (Appendix A.7). The stress spectrum is estimated from FEA in Abaqus and a linear regression performed in MatLab.

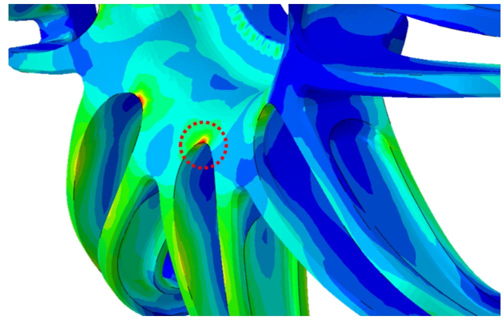

Figure 3.3.2: Most stressed section of rim center

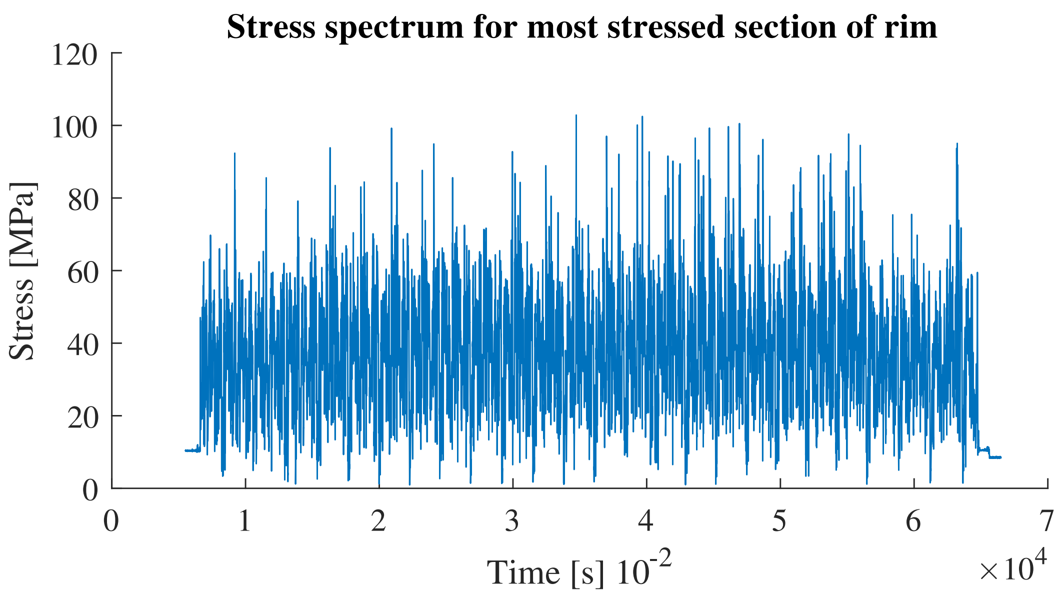

Figure 3.3.3: Stress spectrum for most stressed section of the Rim Center

In Figure 3.3.4, the whole stress cycles based on Standardized 'Rainflow' algorithm (ASTM E1049 [16]) is presented. Based on these stress cycles and the SN-curve found in the Appendix D.2, the fatigue properties of the rear and the front rim center are presented in Table 3.3.2. The Palmgren-Miner linear damage rule, or damage index predicts fatigue failure of the component when the summation of the cycles of reversed stress amplitude, n_i, to the cycles of stress causing failure at each stress amplitude, N_i, equals unity, i.e., $\sum_i n_i/N_i = 1$[17]. Number of endurance run before failure is estimated by the inverse of the damage index for one endurance.

Table 3.3.2: Fatigue properties of Rim Center

#	Rear Rim Center	Front Rim Center
Damage Index (Minor damage rule for one endurance)	0.006	0.009
Number of endurance before failure	166	110

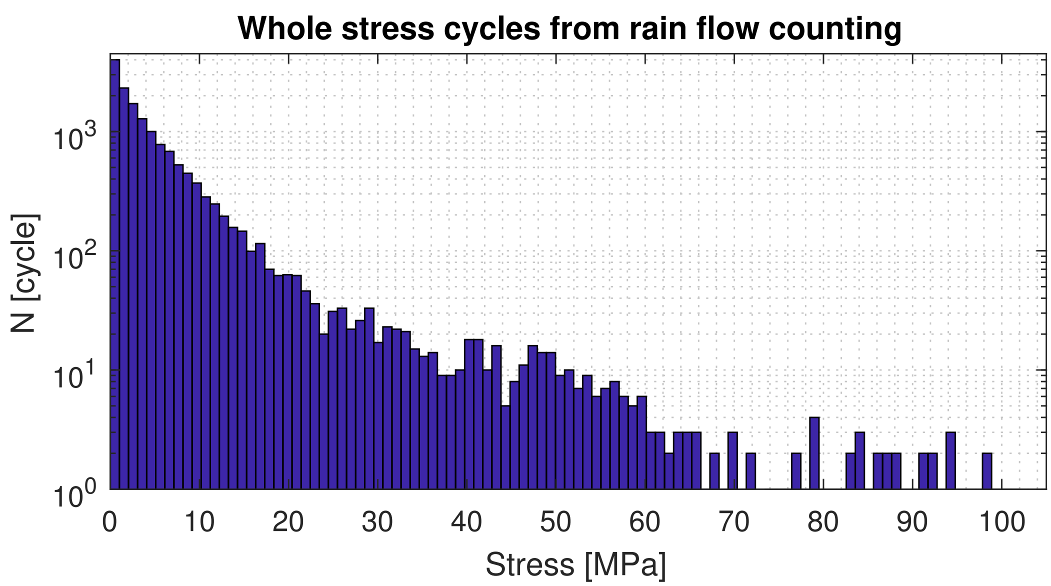

Figure 3.3.4: Whole stress cycles for half endurance counted with Rainflow counting

Looking at the fatigue data, one can see that fatigue is not an issue for the wheel center. This is a good indication that the optimization has worked since a design optimized for stiffness should indicate in general overall low stress. The front rim, which has the lowest fatigue life, is estimated to last 110 endurances, which is equivalent to around 2400 km racing distance, which is way over the requirement for a Formula Student race car.

3.4 Production

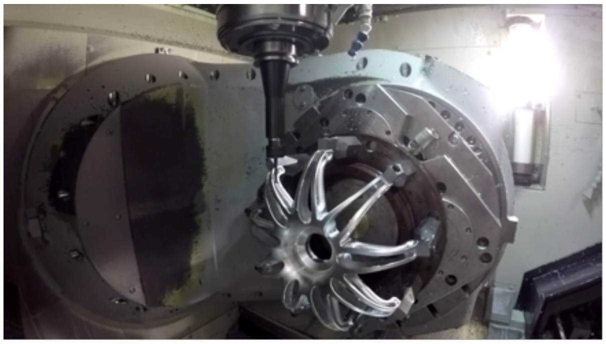

a)

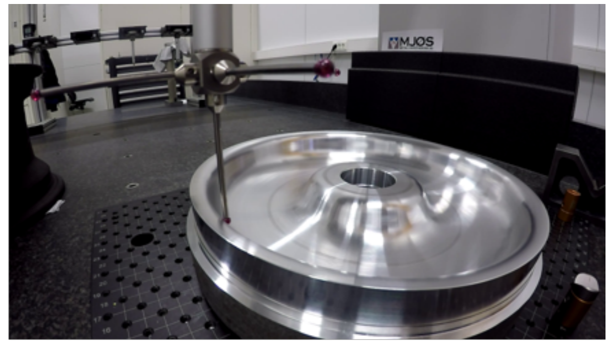

b)

c)

d)

Figure 3.4.1: a) 5-axis milling of Rim Center, b) Control of specified tolerances on rim center on coordinate measuring machine(CMM) during production c) Rim Shell before Autoclave curing, d) Rim Shell at weight after curing and demolding

In Figure 3.4.1, the manufacturing of the rim center and the rim shell is presented. Picture: a) shows the rim center during the last machining step, where the pockets are milled. Picture: b) shows the probing of the rim center after the last lathe operation. Picture: c) shows the rim shell ready for autoclave curing. Picture: d) shows the finished rim shell after demoulding with a resulting weight of 710 g. The final assembled wheel is presented in Figure 3.4.2. Measuring reports for both rim center and rim shell are found in Appendix C.1. The rim shell was measured to have a roundness of 50μm at the rim center interference. The final assembled rim was measured to have a run out of 50 μm. Overall, the production went well and resulted in high quality parts proving that the manufacturing design specifications applied in the optimization step were successful.

Figure 3.4.2: Final assembled wheel

3.5 Mechanical Testing and Verification

Axial strain and hoop strain for inflation pressure of 2 bar are presented in Figure 3.5.1 & 3.5.2. The experimental strain data from the strain gauge is plotted with respect to the strain calculated in Abaqus. Modeling of the inflation pressure is the simplest and most documented load scenario. There is a clear relationship between the physical data and the simulation in FEA. This indicates that the modeled laminate represents the physical laminate well.

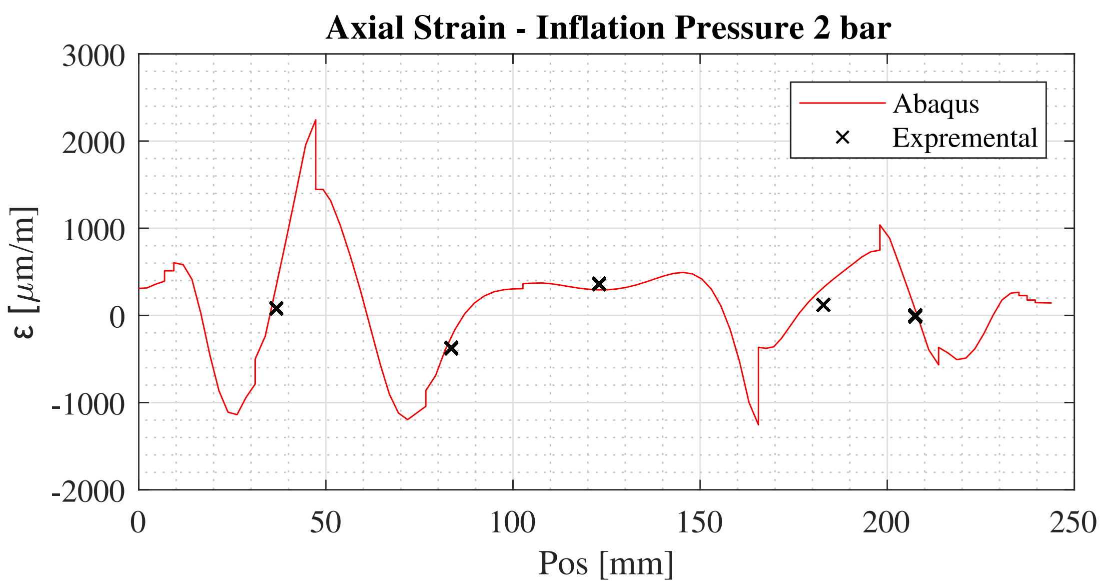

Figure 3.5.1: Comparison of axial strain between FEA and mechanical testing of rim shell

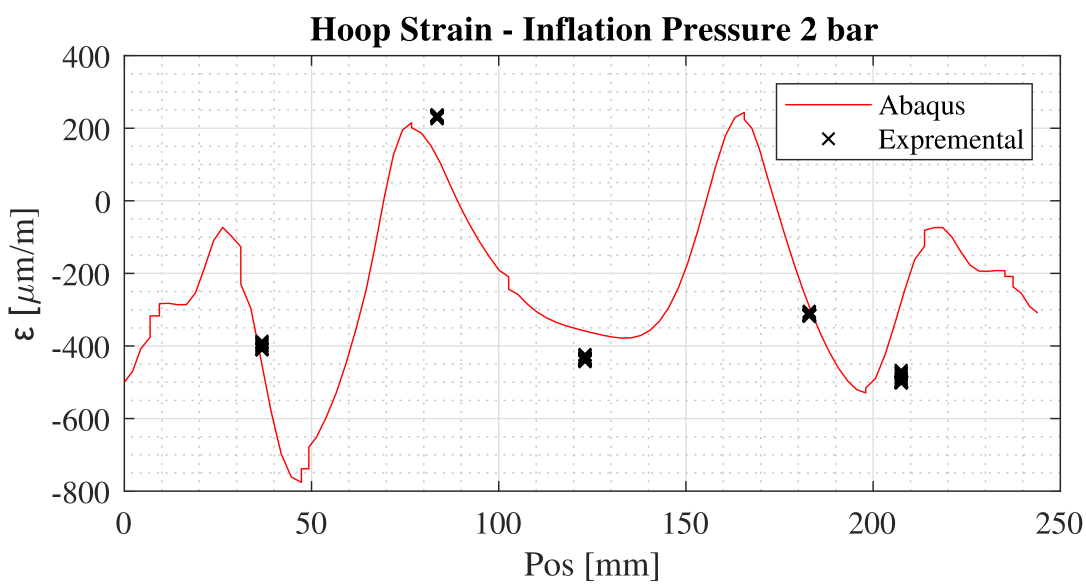

Figure 3.5.2: Comparison of hoop strain between FEA and mechanical testing of rim shell

In figure 3.5.3 & 3.5.4, the displacement of the inner and outer bead during vertical loading is presented. The modeled displacement resembles the physical one with a difference of maximum 15.6 %. The deflection slope changes around 1100 N. The slope has a negative change in the outer bead and a positive change in the inner bead. This non-linearity could be caused by tire behavior or deformation and misalignment of the fixture.

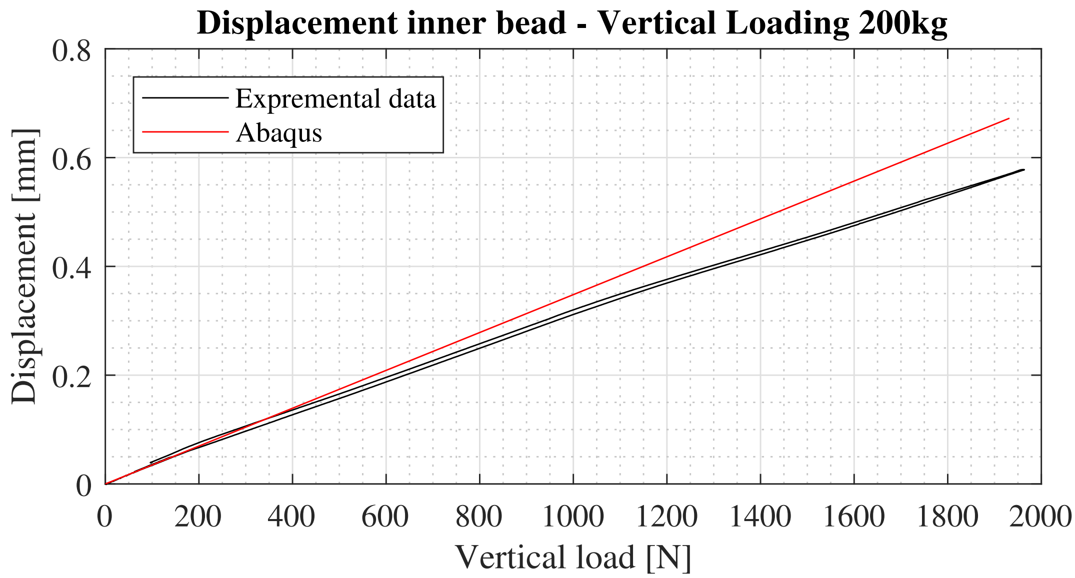

Figure 3.5.3: Comparison of displacement at inner bead between FEA and mechanical testing with a vertical loading of 200 kg

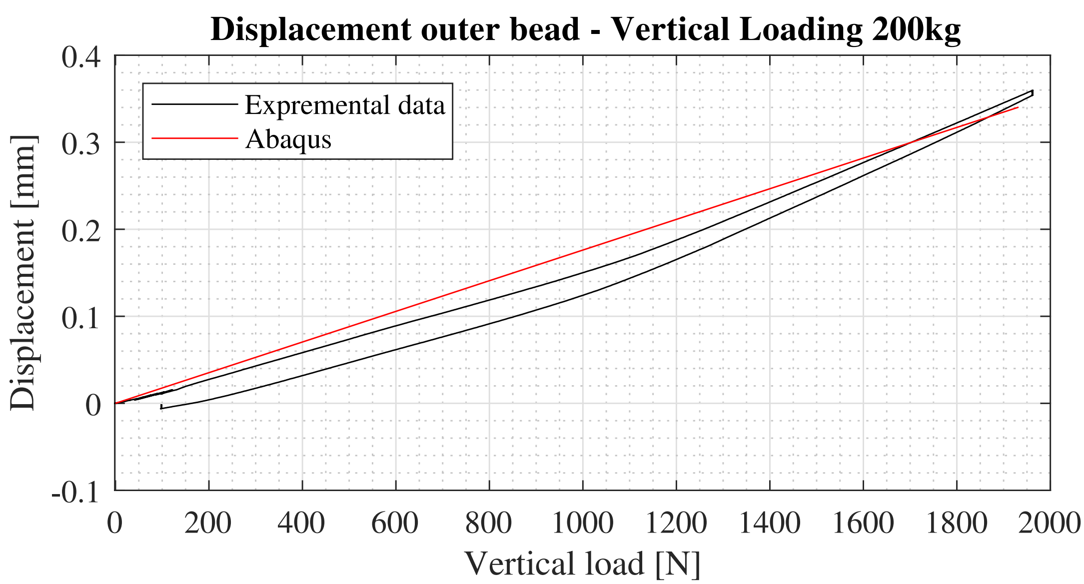

Figure 3.5.4: Comparison of displacement at outer bead between FEA and mechanical testing with a vertical loading of 200 kg

Axial and hoop strain for vertical loading is presented in Figure 3.5.5 & 3.5.6. The strain from the experimental testing matches the model well. Axial strain near the interference with the tire is significantly lower on the physical test, nearly a factor of 11. The tire load is modeled as a surface traction on FEM, which does not take into account the extra stiffness the physical tire will give to the bead. The vertical load model seems to represent well the overall physical load but tends to overestimate the axial load near the interaction with the tire.

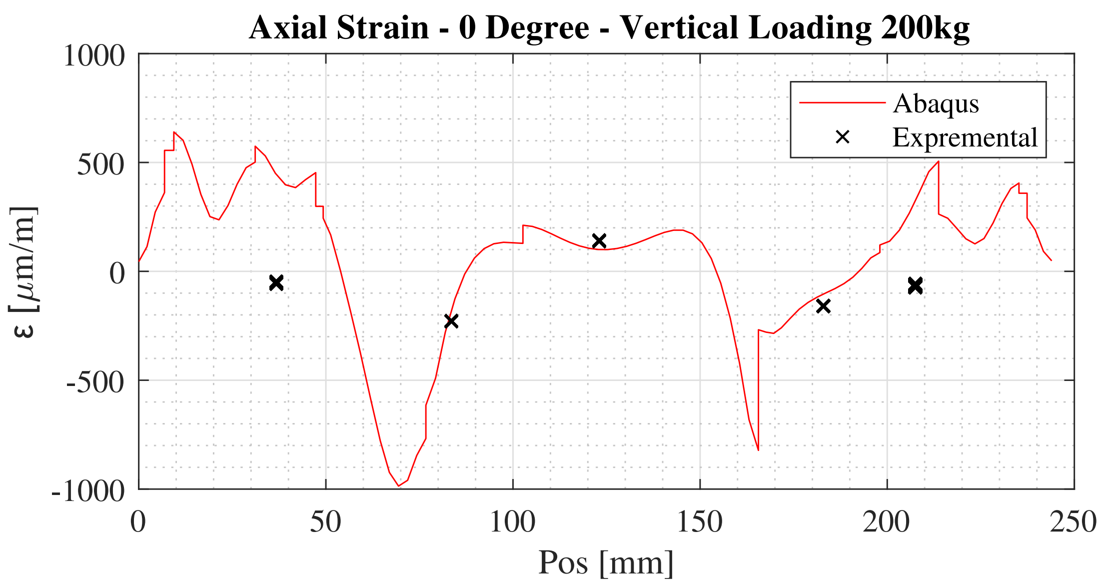

Figure 3.5.5: Comparison of axial strain between FEA and mechanical testing of rim shell subjected to a vertical load of 200 kg

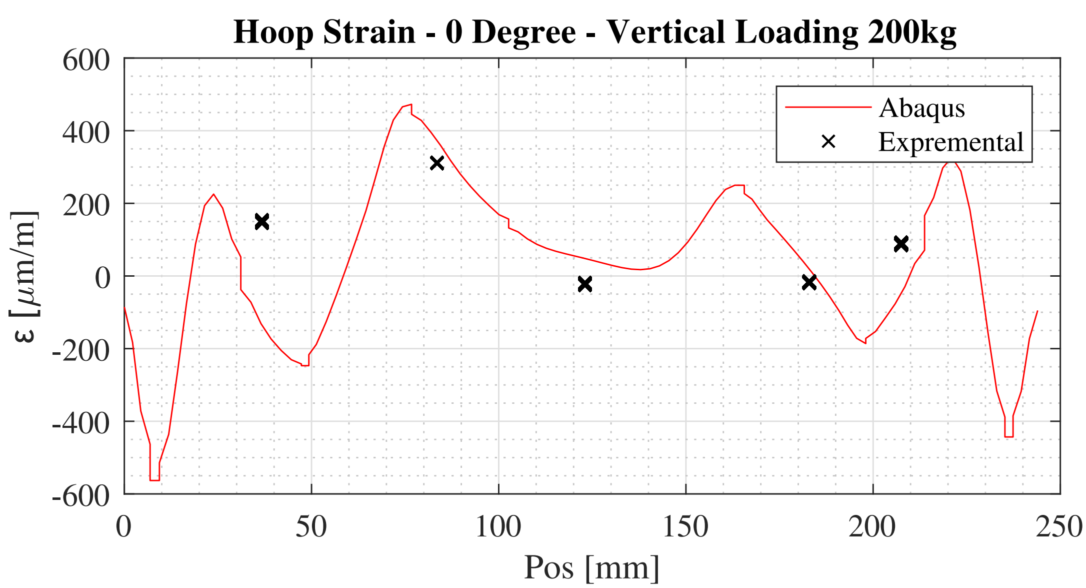

Figure 3.5.6: Comparison of hoop strain between FEA and mechanical testing of rim shell subjected to a vertical load of 200 kg

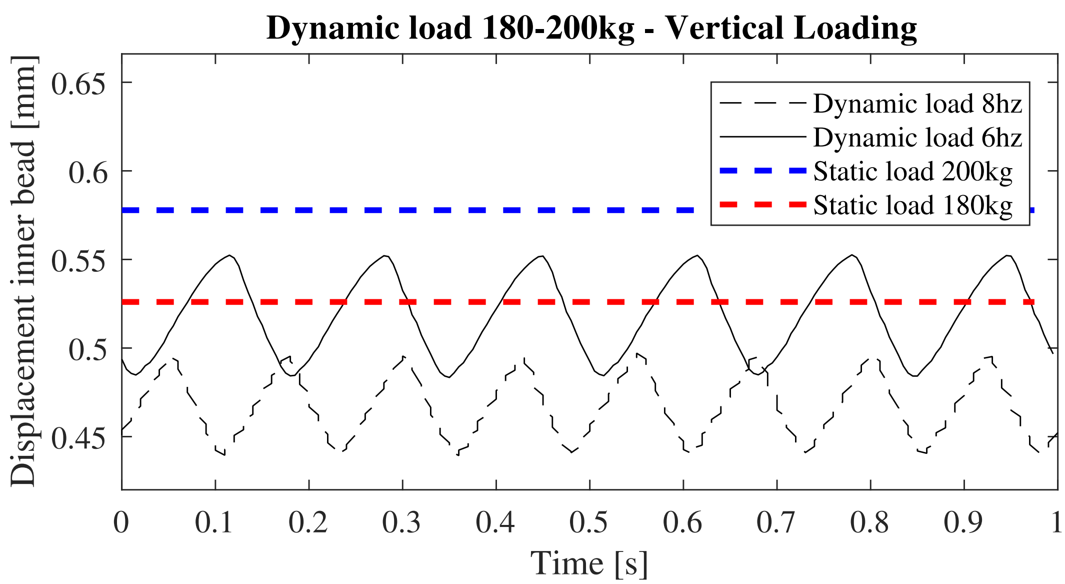

Figure 3.5.7: Dynamical loading of wheel with a vertical loading of 180-200 kg

In Figure 3.5.7 data from the dynamic testing is presented. Displacement for the static loading is higher than for the dynamic loading. The displacement is lowest for the dynamic loading with the highest frequency. The tire has damping properties, which lower the displacement for dynamic loads. For quasi-static loads scenarios, this damping effect can be neglected. This indicates that modeling loads as quasi-static for dimensioning and design of the rim are conservative and applicable. All test results are found in Appendix A.6.

Table 3.5.1: Error contribution in Mechanical Testing

Source of Error	Magnitude of Error	Correctability
Jig Complince	Small	Easy
Inaccuracy of Jig	Medium	Moderate
Load path in Tire	Unknown	Hard
Positioning of Strain Gauge	Small	Easy
Missalignment of Strain Gauge axis	Medium	Moderate
Inaccuracy of measurements from Strain Gauge	Neglectable	Easy
Positioning of Displacement Sensor	Medium	Moderate
Inaccuracy of measurements from Displacement Sensor	Small	Easy
Inaccuracy of measurements from Load Cell	Small	Moderate

In Table 3.5.1 some possible contributions to errors for the mechanical testing are listed. Various of tire inflation pressures were tested. Displacement at inner and outer bead varied for the tests done at 0.5, 0.75, and 1.0 bar. Tests done at 1.0 bar and above gave same displacement. This could be explained by the deformation of the tire that is greater for lower pressure, which could result in an uneven load distribution as the load applicator could touch the sidewalls of the tire. Some tests were done by adjusting the angle of the load applicator, a change of 0.2 degree shifted 0.05 mm between the inner and the outer bead displacement at the vertical load of 200 kg. This indicates that the angle of loading has a big impact on the load path in the tire. The sources of error during testing are not fully understood, and should be investigated further.

3.5.1 Field Testing

All 3 sets of the rims worked and performed well during testing and the 2 Formula Student(FS) competitions; Formula Student Germany and Formula Student Spain. In Figure 3.5.8 ELD is in Germany at the Karlsruhe Institute of Technology FS teams' test facilities. The wheels did not leak air, which is one the most common problems for FS-wheels. Normally, tire changes are time-consuming due to the need for a sealant between the tire and the rim. The rough surface finish coming from the peel ply used in the casting process for rim shell had excellent sealing properties to the tire. This eliminated the need for a sealant, saving both weight and time. In total 8 sets of tires were used, all tire changes were performed on a tire changing machine. In Figure 3.5.9, a picture of a tire change is presented. None of the rims experienced any issues during this process and were not subjected to any cracks or delamination. Delamination and cracks on tire flanges are one of most common failure of one-piece rim shells during the competition.

Figure 3.5.8: Eld at testing in Karlsruhe ,Germany

Figure 3.5.9: Tire changing performed with a tire changing machine

Scientists investigate that which already is;
Engineers create that which has never been.

Albert Einstein

4 Conclusion

Formula student is a perfect environment to test and explore new ways of high performance product design and manufacturing. The access to an excellent network of industrial partners, software solutions and university labs and competences puts one on the forefront of engineering practice development. This report presents the first entire process development of a segmented Formula student wheel with Topology optimized aluminum center and optimized CFRP rim shell. The design considerations are outlined allowing an ideal balance between manufacturability (center), inertia and stiffness (rim). for the rim, an evolution based algorithm was developed and presented in this work that allows to iterate through millions of different layups to find the optimum with minimum compliance under a certain weight target. The weight target of 710 g was met giving a deflection of maximum 2.27 mm in two quasi static critical load scenarios. The entire wheel was validated under 6 quasi static load conditions including bolt forces, center lock connection and full contact as well as fatigue properties. The report further described the production process, where the rim was fabricated by the author himself exactly meeting dimensions and weight target. The manufactured wheels performed well in race conditions; tire changes worked seamlessly as no additional sealing was required due to the manufactured CFRP surfaces that were air tight. Mechanical tests on the wheel showed the perfect agreement between the simulation and the experimental results with the local strain discrepancies ranging from 4.7 % to 21.3 % in load cases of inflation pressure (2 bar). The largest discrepancy was found in large static loads up to 200 kg, where the discrepancy for the total deformation was 15.6 %. The impacts of dynamic loads were negligible due to the damping behavior of the tire. This shows that simulation based design is a feasible approach to infuse innovation into next generation high performing products and presents, to the best of the author's knowledge, the first evolution based composite layup optimization inked to an entire product development process all the way to testing and application. This could be beneficial in a wide range of composite material applications, where key aspects of this procedure could be further improved.

4.1 Future Work

A novel simulation Driven Design approach has been developed and used to design and manufacture fully working and high performing set of wheels for a formula style race car. A design approach with minimal influence by an engineer is not better than the task given to the computer. Yet, the design success is subject to defining proper inputs than in a conventional design process. This implementation of a simulation Driven Design approach for composite material optimization shows promising results, regarding the possibility to design a high-performance composite layup by only defining geometry, loads and boundary conditions. To the best of my knowledge, I have not seen any successful composite designs with a similar design approach. The method works well as it is now, but there is a great potential for the improvement of this process avoiding steps, where the Evolution based algorithm may not be appropriate for the task. A suggestion would be to use the evolution based algorithm for the first iterations and then switching over to a gradient based algorithm. Another improvement that should be investigated is segmentation of the layup, this is done manually and by experience for now. Implementing a segmentation optimization could improve the performance of the design considerably. This could also be combined with a production constraint like drapability, which could give the design a variable segmentation for each layer. This could improve both design performance and manufacturability.

References

[1] E.Astrén. Koenigsegg reinvents the wheel, 2013.
http://koenigsegg.com/koenigsegg-reinvents-wheel/, accessed: 2016-12-10.

[2] S.Mason. Rotational Inertia of a Rim, 2016.
http://stephenmason.com/cars/rotationalinertia.html, accessed:2016-11-29.

[3] J.M.Haaland. Vehicle Dynamics Simulation for setting up a Four-Wheel Independent Drive Electric Race Car. Master's thesis, The Norwegian University of Science and Technology, 2017.

[4] H.Sølvberg. Carbon Fiber Composite Wheels for Formula Student. Master's thesis, The Norwegian University of Science and Technology, 2014.

[5] Greenteam Uni Stuttgart. E0711-4 (2012/2013), 2017.
https://www.greenteam-stuttgart.de/en/e0711-4-20122013/, accessed: 2017-18-01.

[6] Carbon Fiber Gear, a dpitMedia Company. The Koenigsegg Carbon Fiber Wheel is So Light You Can Throw It Around, 2017.
https://blog.carbonfibergear.com/the-koenigsegg-carbon-fiber-wheel-is-so-light-you-can-throw-it-around, accessed: 2017-29-11.

[7] Fibermax Composites. Weaving Styles, © Copyright 2002 - 2014.
https://www.fibermaxcomposites.com/shop/index_files/weavingstylesandpatterns.php, accessed: 2017-07-04.

[8] T.D.Barry. Study of a Post Structure in Composite Material for Rail Line Electrification Assembly, 2011.
http://bibing.us.es/proyectos/abreproy/70301/fichero/5_Laminate+Theory.pdf, accessed: 2017-10-11.

[9] E.J.Barbero. *Finite Element Analysis of Composite Materials Using Abaqus*. CRC Press, 2013.

[10] C.K.Oldeide. Design and analysis of CFRP wheels for a formula student race car. Project work, 2016.

[11] H.Hertz. *The Contact of Elastic Solids*. Macmillan, 1896.

[12] J.P.Jesuette and M.Theves. Finite Element Analysis of Tire/Tire Interface Forces Under Braking and Cornering Loads[2]. *Tire Science and Technology*, Vol.20(2):83–105., April-June 1992.

[13] Dassault Systèmes. *Isight documentation*. ©Dassault Systèmes, 2006.

[14] eFunda. Strain Rosette for Strain Measurement.
http://www.efunda.com/formulae/solid_mechanics/mat_mechanics/strain_gage_rosette.cfm, accessed: 2017-10-11.

[15] K2W Precision Inc. FormulaSAERacing Wheels, Geometrical specification:, 2017.
http://keizerwheels.com/wp-content/uploads/2015/03/Kosmo-Series.zip, accessed: 2017-14-11.

[16] ASTM International. Standard Practices for Cycle Counting in Fatigue Analysis.
https://www.astm.org/Standards/E1049.htm, accessed: 2017-8-11.

[17] J.J.Kauzlarich. The Palmgren-Miner rule derived. *Tribological Design of Machine Elements, Proceedings of the 15th Leeds-Lyon Symposium on Tribology held at Bodington Hall, The University of Leeds*, 14:175–179, 1989.

[18] J.C.Stearns. *An investigation of stress and displacement distribution in a aliminum alloy automobile rim*. PhD thesis, The University of Akron, 2000.

[19] J.Montgomery. Boundary Condition Influences on Shank Stress in 3D Solid Bolt Simulation . *2008 Abaqus Users' Conference*, page 18, may 2002.

[20] Dassault Sys-temes. Isight & the SIMULIA Execution Engine, Process automation and design exploration., 2016.
http://www.3ds.com/products-services/simulia/products/isight-simulia-execution-engine/, accessed: 2016-12-04.

[21] Dassault Systèmes. *Abaqus 6.14 Documentation: Abaqus/CAE User's Manual, 9.5.5 Creating and running a macro*. ©Dassault Systèmes, 2014.

Appendices

A
Modeling, Set-Up, Procedures & Results

A.1 Load Scenarios

Tire Pressure

Inflation pressure works laterally on the rim flanges and prevents the tire from slipping and causing debeading. The reactions forces (grey arrows in fig:(a)) which balancing the pressure that acts on the tire's sidewall (red arrows in fig:(a)) are assumed to have a linear distribution and that they work equally on each side, then the resultant force F_{flange} working on each side are given:

$$F_{flange} = \frac{\pi((r_t - t_t)^2 - r^2)P}{2} \tag{A.1}$$

On the rest of the rim there is a even distributed pressure illustrated in Figure (b).

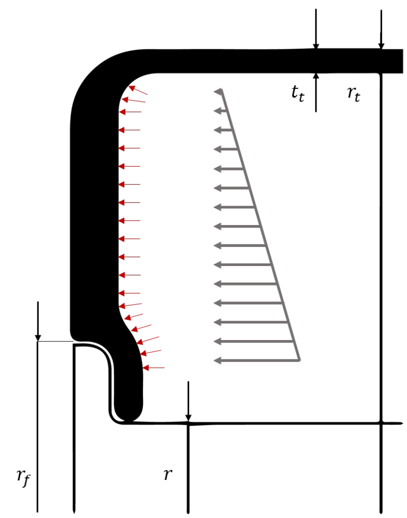

(a) Simplefied pressure distribution inside wheel

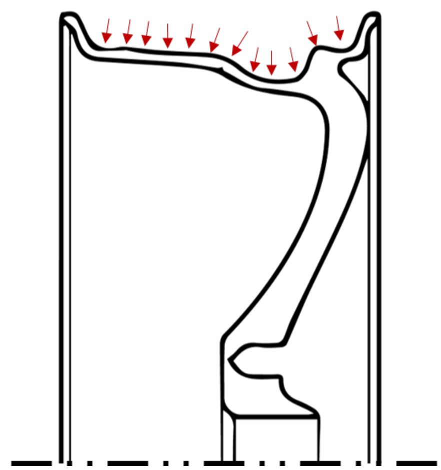

(b) Load distribution due to tire pressure

Bump Load

There are known methodologies for modeling the load on the rim due to the weight of the vehicle. Both the eye bar link and the cosine function are accepted models and have been studied by a range of tire companies. The simplifying of the load using a cosine function can be traced back to Hertz in 1882 [11]. John C. Stearns [18] did a study were he investigated different load methodologies in FEA and compared them to a experiment of the real rim under going the same load condition. He investigated the cosine, eye bar and a Fourier series expansion of the contact patch loading. The cosine function was found to predict the experimental data best, this methodology will be used in further analysis. The cosine methodology

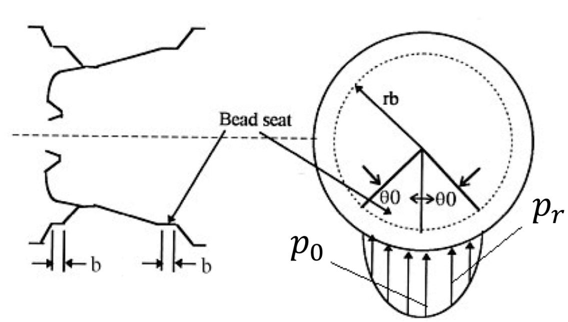

Figure A.1.2: Radial Loading Schematic [18] is done by assuming that the bead pressure have a cosine function distribution mode within a central angle of 40° in a circumferential direction as shown in Figure A.1.2 Then the distributed pressure, p_r , is given as:

$$p_r = p_0 \cdot \cos\left(\frac{\pi}{2} \cdot \frac{\theta}{\theta_0}\right) \tag{A.2}$$

Setting up a integral of (A.2) the total radal load, f_z, can be found:

$$f_z = b\int_{-\theta_0}^{\theta_0} p_0 \cdot r_b d\theta \tag{A.3}$$

Substituting (A.2) into (A.3),

$$f_z = b\int_{-\theta_0}^{\theta_0} p_0 \cdot r_b \cdot \cos\left(\frac{\pi}{2\theta_0} \cdot \theta\right) \tag{A.4}$$

Integration and solving for W_0 leads to:

$$p_0 = \frac{f_z \cdot \pi}{b \cdot r_b \cdot 4 \cdot \theta_0} \tag{A.5}$$

Braking and acceleration

The loads during braking and acceleration is quite similar. Braking will usually be the most critical load for most vehicles. Braking is limited by tire capacity and acceleration is usually limited by motor power. The max load working on the tires can be calculated from tire capacity and power limit. Acceleration/deceleration of the wheels involves tangential shear forces between the tire/rim-interface. Jesuette & Thive did a study where they investigated the interface forces under braking and cornering loads by FEA. The distribution profile of the shear stresses along the rim flange was extracted from the result found by Jesuette & Thive [12].

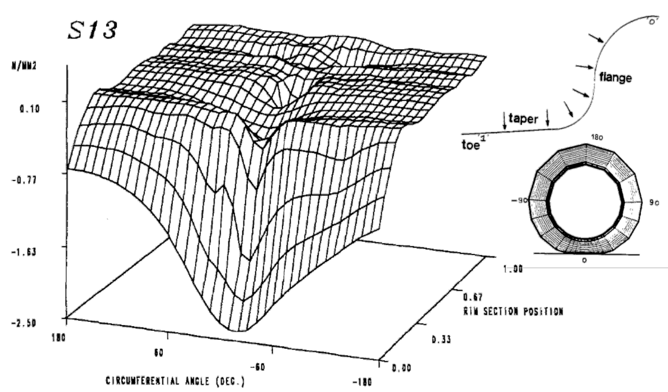

Figure A.1.3: Distribution of the tire/rim contact pressures under braking[12]

This was then used to do a sin-regression of the extracted data and by normalizing the curve:

$$y = 0.71 + 0.31 \cdot \sin(0.017x + 1.9) \tag{A.6}$$

Assuming that the pressure p for a race car rim follow the same curve multiplied with a constant p_0, then:

$$p = p_0 \cdot (0.71 + 0.31 \cdot \sin(0.017\theta + 1.9)) \tag{A.7}$$

The constant p_o can be found by including the force working on the tires while braking f_x:

$$f_x = p_o \cdot b \cdot \pi \cdot 2r_b \int_{-\theta_o}^{\theta_o} 0.71 + 0.31 \cdot \sin(0.017\theta + 1.9) d\theta \tag{A.8}$$

Integrating and solving for p_o:

$$p_o = \frac{f_x}{2\pi r_b b \cdot (1.42\theta_o + 6.8878 \sin(0.017\theta_o))} \tag{A.9}$$

Cornering Loads

Lateral load during cornering is maybe the most important load case regarding vehicle performance, and also one of the load case involving most energy. Lateral loads impose camber gain which in a extreme case could lead into a positive camber (Figure A.1.4) making all of the suspension geometry work useless. A rim without sufficient stiffness could result in a loss of work efficiency of the tire regarding loss in adhesion between the tire and the ground. The lateral distribution was found by using the same regression procedure as in brake loads, by extracting the pressure distribution from Figure A.1.4, with the assumtion that the pressure will follow the cosine distribution illustrated in Figure A.1.7, then p is:

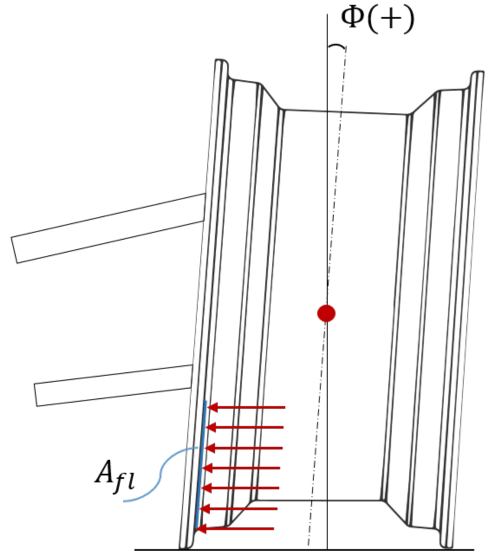

Figure A.1.4: Positive camber gain

$$p = p_o \cdot \cos\left(\frac{\pi\theta}{140}\right) \tag{A.10}$$

The lateral force, f_y, and the areal of the flange were the lateral force is working, A_{fl},is then used to find p_o:

$$f_y = p_o A_{fl} \int_{-\theta}^{\theta} \cos\left(\frac{\pi\theta}{140}\right) d\theta \tag{A.11}$$

Integrating and solving for p_o:

$$p_o = \frac{f_y \cdot \pi}{280 p_o A_{fl} \cdot \cos\left(\frac{\pi\theta}{140}\right)} \tag{A.12}$$

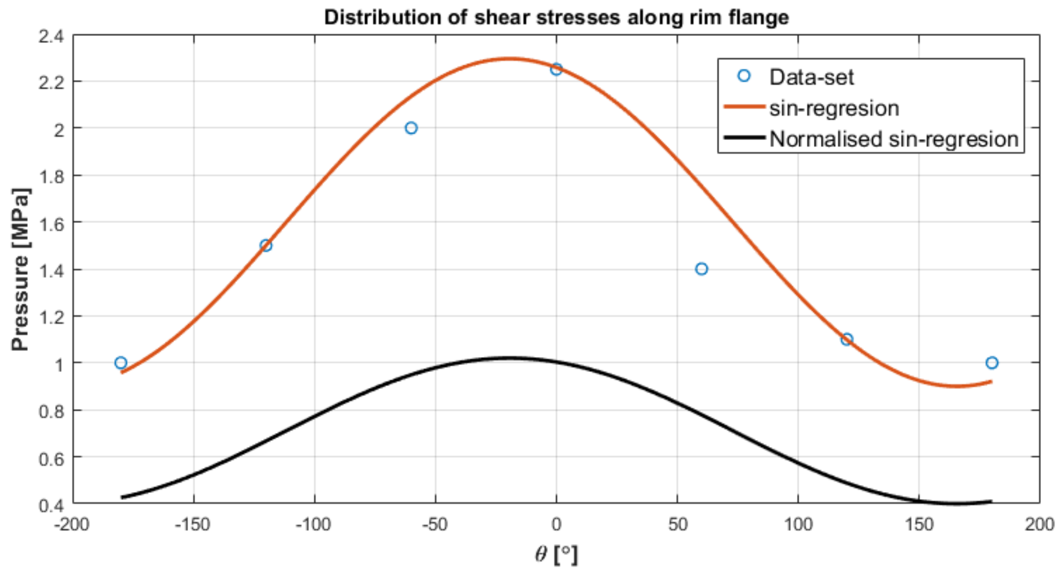

Figure A.1.5: Regression of extracted brake data from Jesuette & Thive [12]

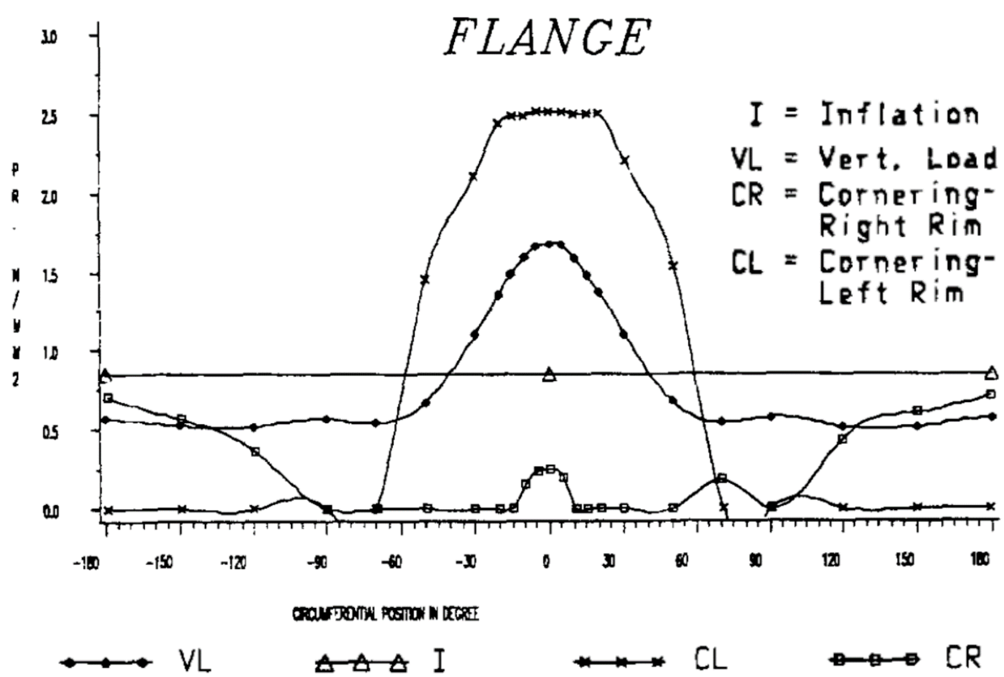

Figure A.1.6: Peak pressure distribution during cornering loads [12]

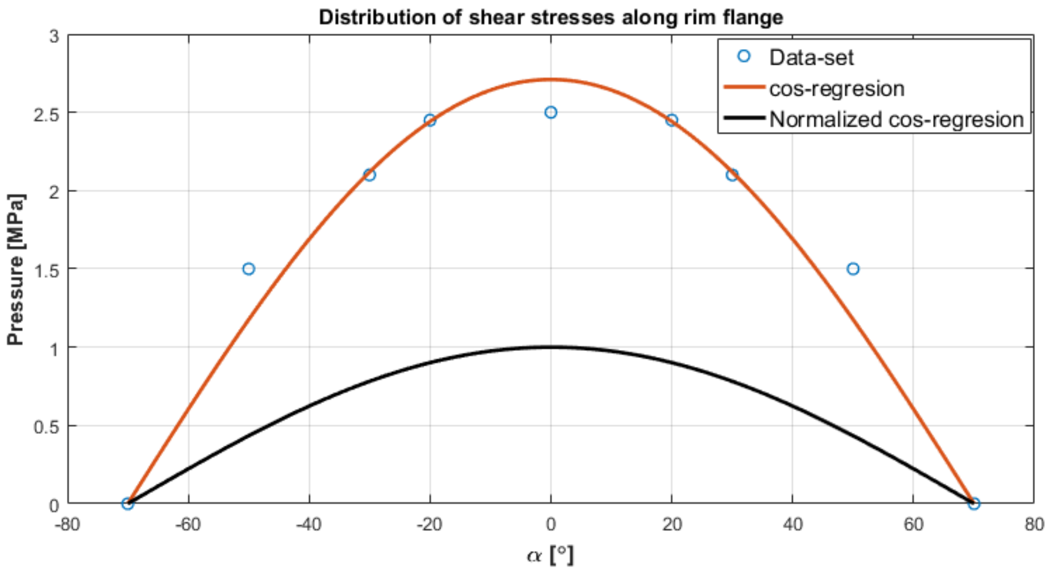

Figure A.1.7: Regression of extracted cornering data from Jesuette & Thive [12]

A.2 FEA - validation Setup

This section will follow all the steps done in Abaqus to setup the FE-model for validation of the wheel. It will be structured as the work tree in Abaqus and go through the following items:

- Part
- Properties
  - Materials
  - Rim shell
  - Rim Center
  - Bolts
  - Hub & center lock
- Assembly
- Step
- Interactions
- Loads
  - Cornering Loads
  - Vertical Loads
  - Brake Loads
  - Pretension in bolts
  - Pretension in Hub & center lock
- Mesh
  - Rim Center
  - Rim Shell
  - Bolts
  - Hub & center lock

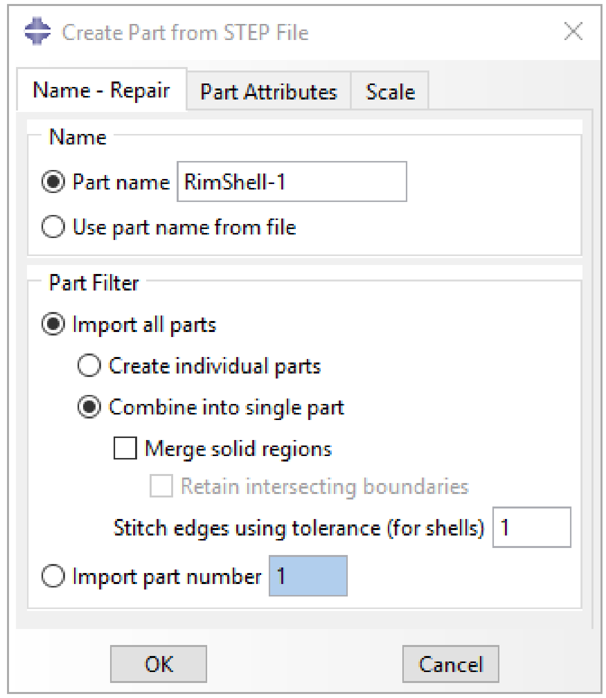

Figure A.2.1

A.2.1 Part

All part geometry was modeled in SolidWorks and imported(Figure A.2.1 to Abaqus with Step file format. Part geometries is found in Figure A.2.2.

A.2.2 Properties

Materials

Four materials was used for the validation: Steel, Al7075 T6 , Hexcel 6376 5HS and Hexcel 6376 UD. All materials was modeled as linear elastic, the metals as isotropic and the composite as lamina. The two lamina was also defined with a failure stress, to calculate Tsai Wu failure criterion. For material data see material data in Appendix D.2 - D.5. All material definitions in Abaqus is found in Figure A.2.3

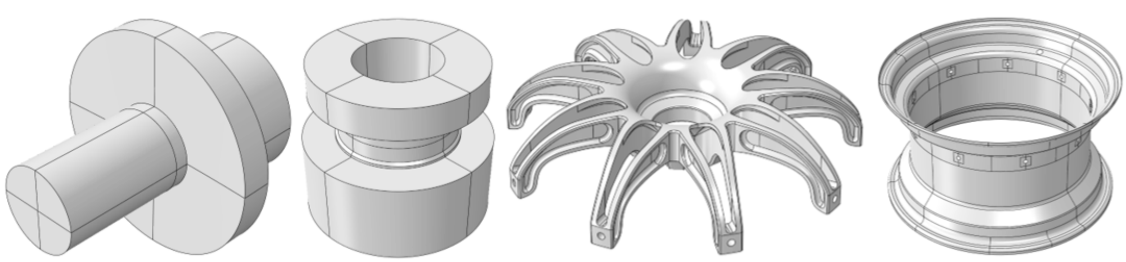

Figure A.2.2

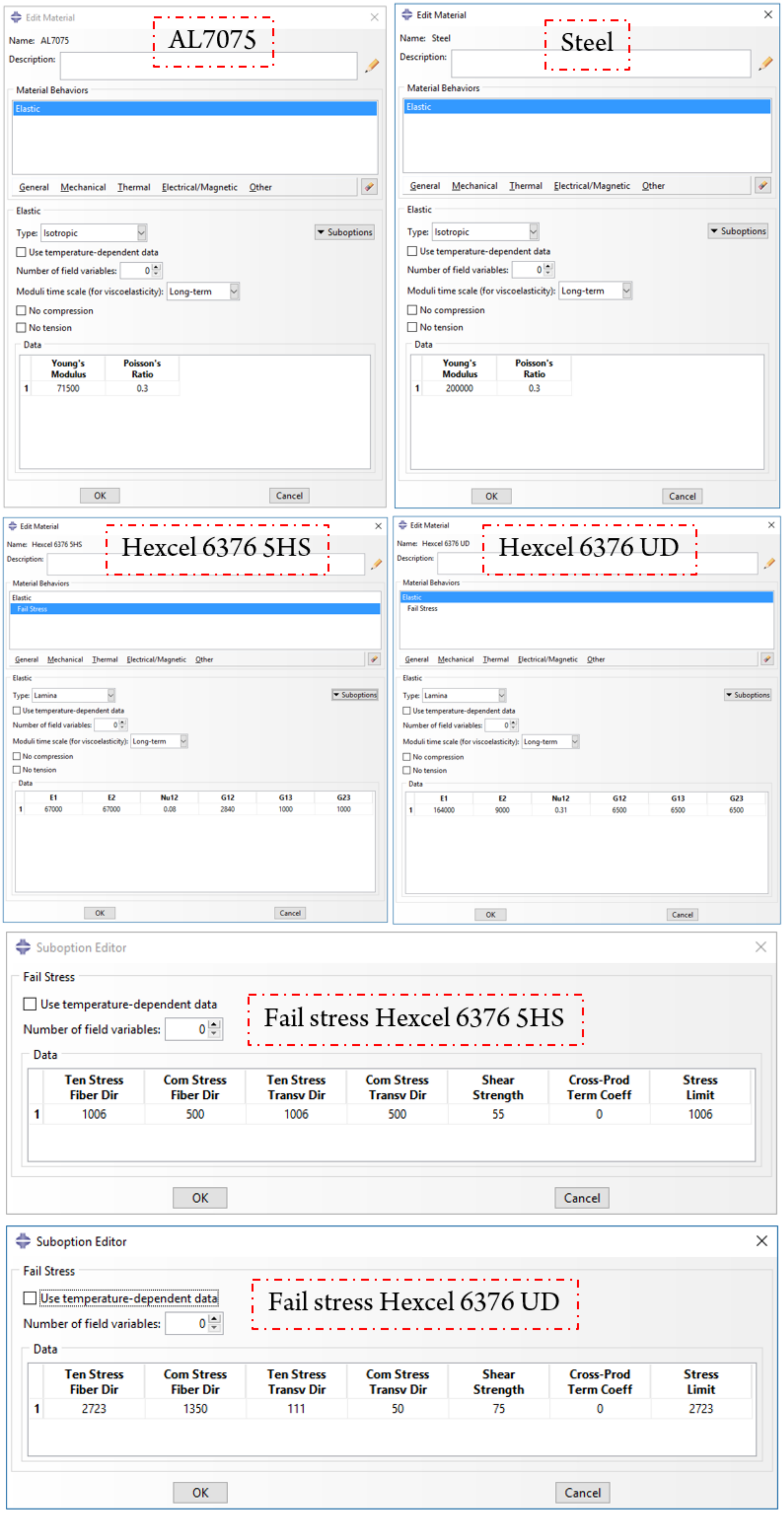
AL7075
Edit Material
Name: AL7075
Material Behaviors
Elastic
Type: Isotropic
Young's Modulus 71500
Poisson's Ratio 0.3
Steel
Name: Steel
Young's Modulus 200000
Poisson's Ratio 0.3
Hexcel 6376 5HS
Name: Hexcel 6376 5HS
Type: Lamina
E1 67000
E2 67000
Nu12 0.08
G12 2840
G13 1000
G23 1000
Hexcel 6376 UD
Name: Hexcel 6376 UD
E1 164000
E2 9000
Nu12 0.31
G12 6500
G13 6500
G23 6500
Suboption Editor
Fail Stress
Fail stress Hexcel 6376 5HS
Ten Stress Fiber Dir 1006
Com Stress Fiber Dir 500
Ten Stress Transv Dir 1006
Com Stress Transv Dir 500
Shear Strength 55
Cross-Prod Term Coeff 0
Stress Limit 1006
Fail stress Hexcel 6376 UD
Ten Stress Fiber Dir 2723
Com Stress Fiber Dir 1350
Ten Stress Transv Dir 111
Com Stress Transv Dir 50
Shear Strength 75
Cross-Prod Term Coeff 0
Stress Limit 2723

Figure A.2.3

Conventional shell was used to model the composite for the rim shell. This was defined with a composite layup for each of the 8 segment. Shell reference surface and offset was set to bottom surface. Layup orientation was defined with a cylindrical (R, θ, Z) coordinate system with R as the normal. The coordinate system was defined in the center of the rim with the Z-axis in the axial direction. Composite layup for the outer flange segment is found in Figure A.2.4.

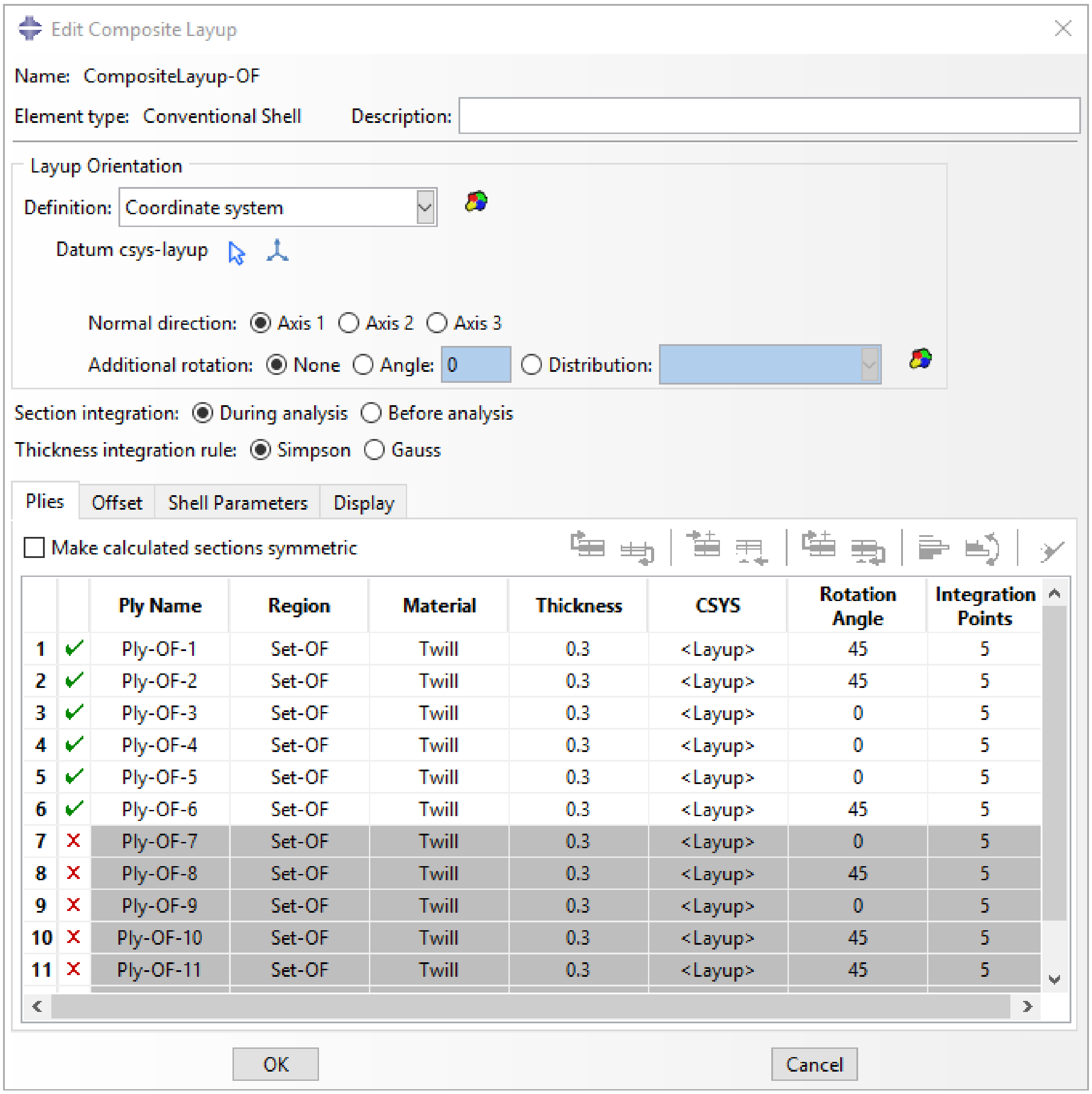

		Ply Name	Region	Material	Thickness	CSYS	Rotation Angle	Integration Points
1	✓	Ply-OF-1	Set-OF	Twill	0.3	<Layup>	45	5
2	✓	Ply-OF-2	Set-OF	Twill	0.3	<Layup>	45	5
3	✓	Ply-OF-3	Set-OF	Twill	0.3	<Layup>	0	5
4	✓	Ply-OF-4	Set-OF	Twill	0.3	<Layup>	0	5
5	✓	Ply-OF-5	Set-OF	Twill	0.3	<Layup>	0	5
6	✓	Ply-OF-6	Set-OF	Twill	0.3	<Layup>	45	5
7	✗	Ply-OF-7	Set-OF	Twill	0.3	<Layup>	0	5
8	✗	Ply-OF-8	Set-OF	Twill	0.3	<Layup>	45	5
9	✗	Ply-OF-9	Set-OF	Twill	0.3	<Layup>	0	5
10	✗	Ply-OF-10	Set-OF	Twill	0.3	<Layup>	45	5
11	✗	Ply-OF-11	Set-OF	Twill	0.3	<Layup>	45	5

Figure A.2.4

Rim Center

Rim Center was modeled with a solid homogeneous section with aluminum as material. This is illustrated in Figure A.2.5.

Bolts

Bolts was modeled with a solid homogeneous section with steel as material.

Hub & center lock

Hub & center lock was modeled with a solid homogeneous section with aluminum as material.

A.2.3 Assembly

All part was imported with coordinate system according to the main assembly in SolidWorks such that assembly constraint was eliminated. All parts was imported with dependent mesh (mesh on part). See Figure A.2.6. Only one bolt was imported from SolidWorks, and radial pattern was used to copy all the bolts in right place. This was done to reduce work as the mesh and partition procedure is only done for one bolt.

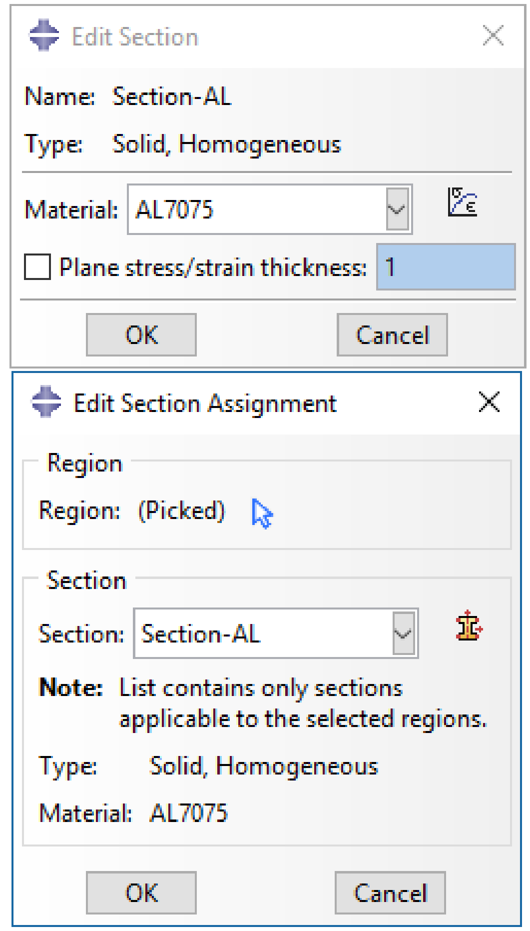

Figure A.2.5

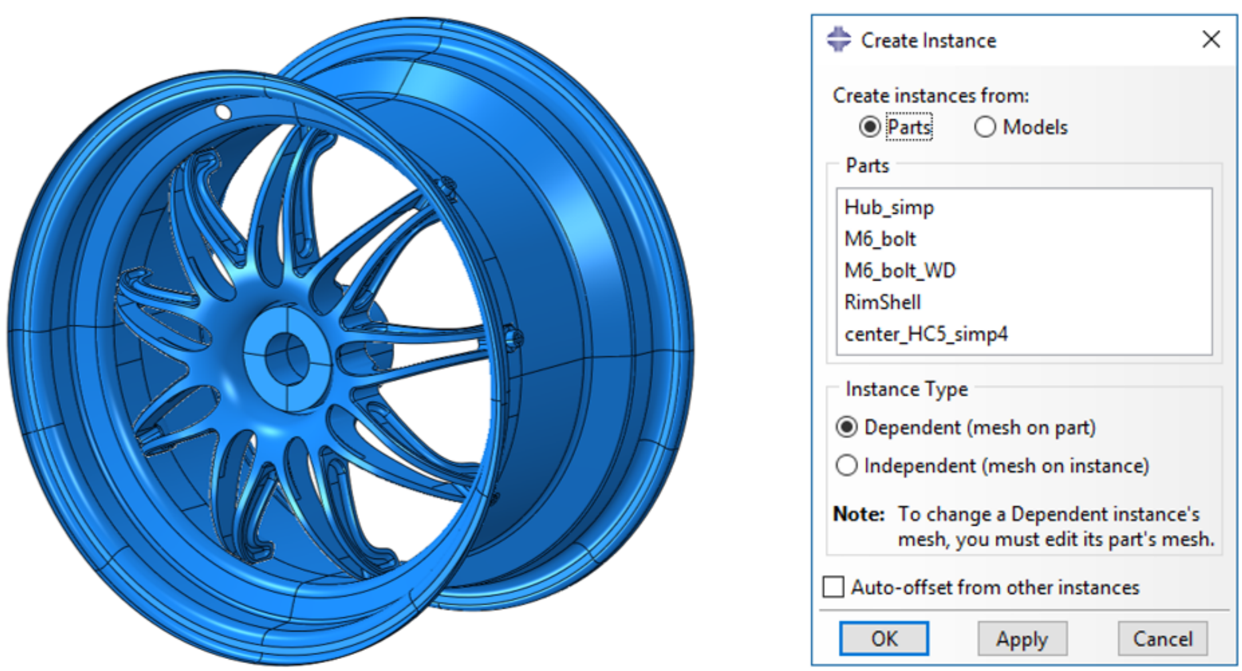

Figure A.2.6

A.2.4 Step

Two static general steps was used. Step one for applying pretension to bolts and center lock, step two for the given load scenario (Cornering, bump etc. see load scenarios in chapter 2 section 2.1.). Due to contact on curved surfaces the unsymmetrical matrix storage was selected, as this storage have bigger chance to success (drawback slower). See Figure A.2.7 for set-up.

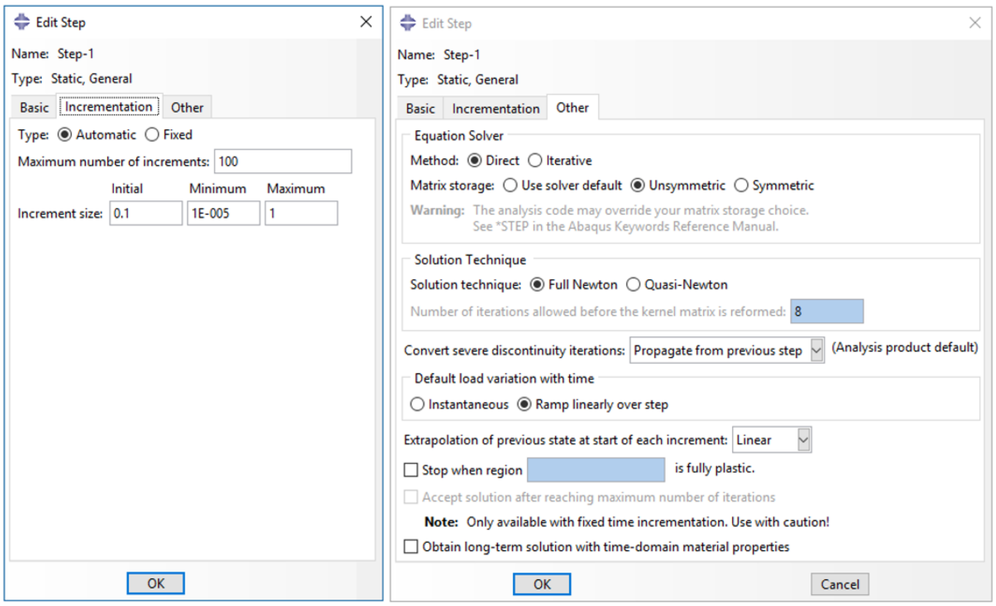

Figure A.2.7

A.2.5 Interactions

General Contact

General contact was used instead of manually specifying each contact set. General contact setup is found in Figure A.2.9. So reduce solving time every unreasonable surfaces was removed from contact definition. This know as excluded surface pair in Abaqus, red surfaces on the rim in the figure show all excluded surfaces. A contact initialization was used to resolve with strain-free adjustments. Contact properties was set with both tangential and normal behavior, all properties is show in the figure. Bolts was modeled with full lengths, so a surface thickness assignment was added to shell geometry to have the right offset for contact definition between rim shell and bolts. Surface thickness assignment is presented in Figure A.2.8.

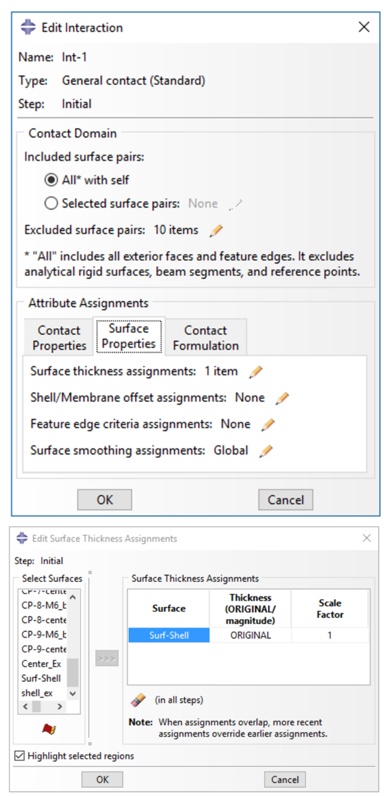

Figure A.2.8

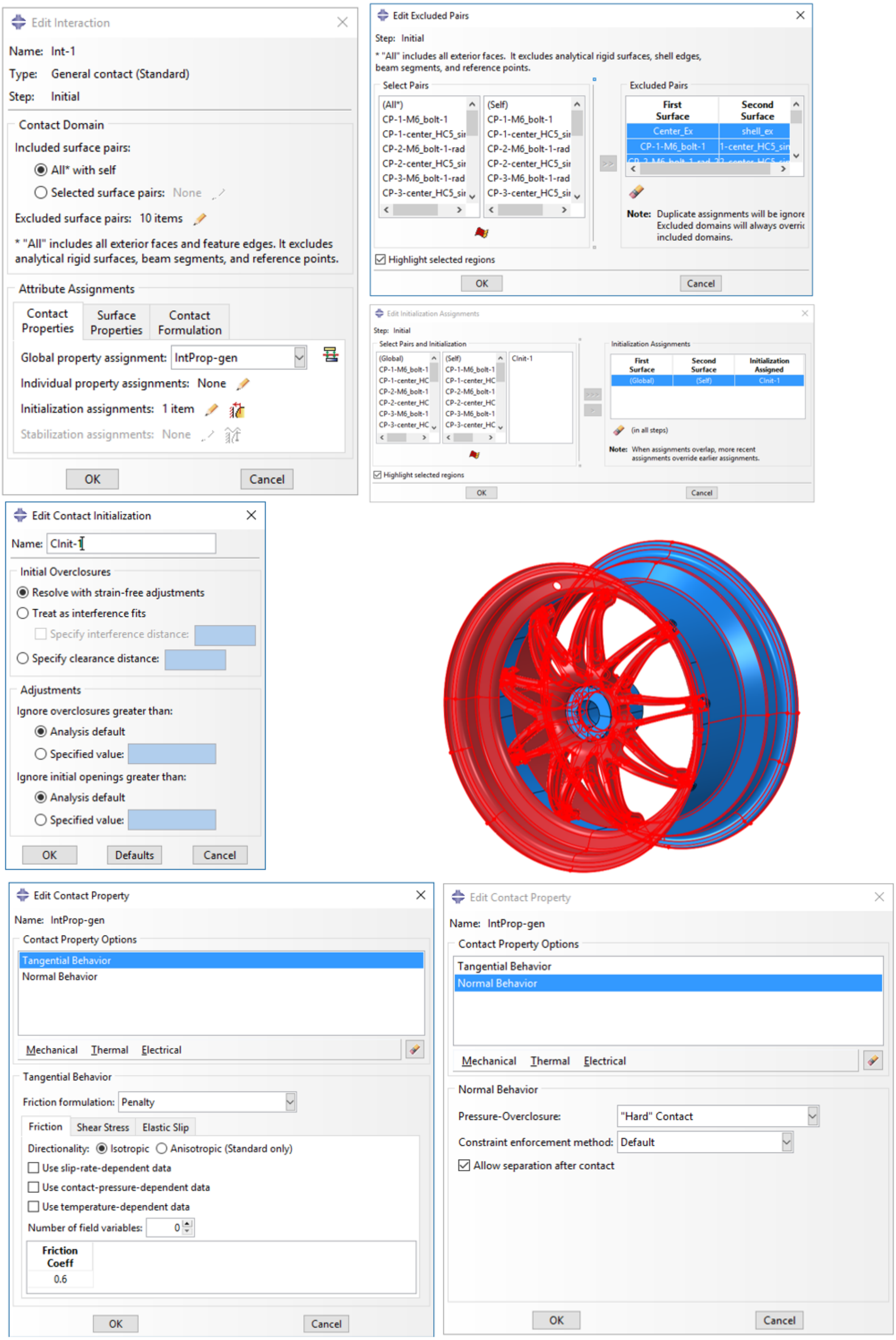
Edit Interaction
Name: Int-1
Type: General contact (Standard)
Step: Initial
Contact Domain
Included surface pairs:
All* with self
Selected surface pairs: None
Excluded surface pairs: 10 items
* "All" includes all exterior faces and feature edges. It excludes analytical rigid surfaces, beam segments, and reference points.
Attribute Assignments
Contact Properties
Surface Properties
Contact Formulation
Global property assignment: IntProp-gen
Individual property assignments: None
Initialization assignments: 1 item
Stabilization assignments: None
OK
Cancel
Edit Excluded Pairs
Step: Initial
* "All" includes all exterior faces. It excludes analytical rigid surfaces, shell edges, beam segments, and reference points.
Select Pairs
(All*)
CP-1-M6_bolt-1
CP-1-center_HC5_sir
CP-2-M6_bolt-1-rad
CP-2-center_HC5_sir
CP-3-M6_bolt-1-rad
CP-3-center_HC5_sir
(Self)
CP-1-M6_bolt-1
CP-1-center_HC5_sir
CP-2-M6_bolt-1-rad
CP-2-center_HC5_sir
CP-3-M6_bolt-1-rad
CP-3-center_HC5_sir
Excluded Pairs
First Surface
Second Surface
Center_Ex
shell_ex
CP-1-M6_bolt-1
1-center_HC5_sir
Note: Duplicate assignments will be ignore
Excluded domains will always overric
included domains.
Highlight selected regions
OK
Cancel
Edit Initialization Assignments
Step: Initial
Select Pairs and Initialization
(Global)
(Self)
CInit-1
Initialization Assignments
First Surface
Second Surface
Initialization Assigned
(Global)
(Self)
CInit-1
(in all steps)
Note: When assignments overlap, more recent assignments override earlier assignments.
Highlight selected regions
OK
Cancel
Edit Contact Initialization
Name: CInit-1
Initial Overclosures
Resolve with strain-free adjustments
Treat as interference fits
Specify interference distance:
Specify clearance distance:
Adjustments
Ignore overclosures greater than:
Analysis default
Specified value:
Ignore initial openings greater than:
Analysis default
Specified value:
OK
Defaults
Cancel
Edit Contact Property
Name: IntProp-gen
Contact Property Options
Tangential Behavior
Normal Behavior
Mechanical
Thermal
Electrical
Tangential Behavior
Friction formulation: Penalty
Friction
Shear Stress
Elastic Slip
Directionality: Isotropic Anisotropic (Standard only)
Use slip-rate-dependent data
Use contact-pressure-dependent data
Use temperature-dependent data
Number of field variables: 0
Friction Coeff
0.6
OK
Cancel
Edit Contact Property
Name: IntProp-gen
Contact Property Options
Tangential Behavior
Normal Behavior
Mechanical
Thermal
Electrical
Normal Behavior
Pressure-Overclosure: "Hard" Contact
Constraint enforcement method: Default
Allow separation after contact
OK
Cancel

Figure A.2.9

A.2.6 Bolts

Jerome Montgomery did a study were he compared three modeling technique's for threaded bolt connections with reload. In Figure A.2.10 the stress distribution of tied, smeared and full modeled threads are compared[19]. A tie constraint was used for representing threads interaction between rim center and bolts. This is not best simplification but gives a all right representation of threads respect to computing time. The effect a bolted connection in term of stiffness was the main interest of modeling of the bolts.

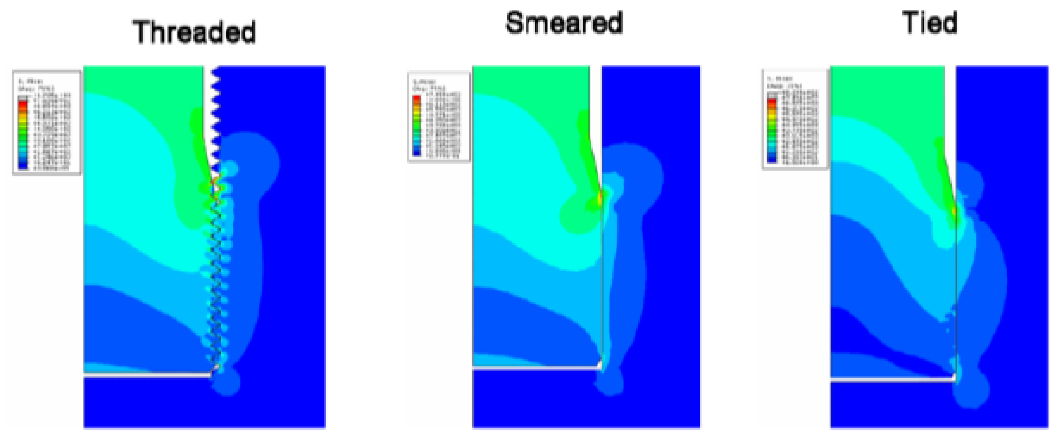

Figure A.2.10: Result from Jerome Montgomery's study [19]

A.2.7 Loads

This subsection will not go into modeling of each combined load, but only each separate load distribution. See chapter: 2 section: 2.1 for load scenarios. Boundary condition was applied as encastre on the dummy hub.

Vertical Loads

The vertical load distribution is defined on the a $+-40^o$ partition of the inner and outer bead. The load was defined as a surface traction working in Z-direction with distributed by analytic field. The analytic field was based on the vertical distribution defined in Appendix A.1. To apply this equation the cylindrical coordinate system used for the layup orientation was used. See FigureA.2.11 for modeling details related to the vertical load.

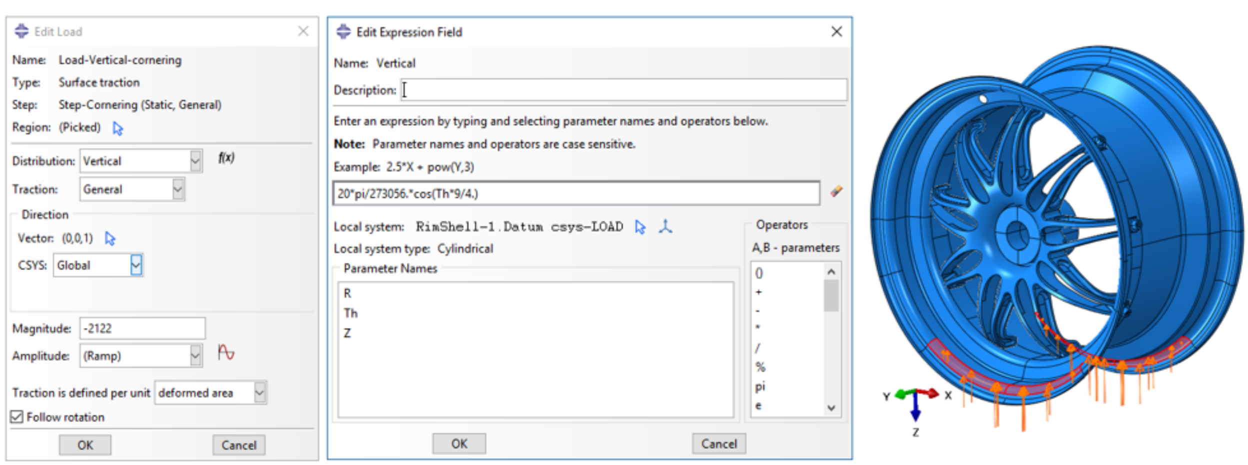

Figure A.2.11

Cornering Loads

The vertical load distribution is defined on the a $+-70^o$ partition of the inner bead. The load was defined as a surface traction working in Y-direction with distributed by analytic field. The analytic field was based on the lateral distribution defined in Appendix A.1. To apply this equation the cylindrical coordinate system used for the layup orientation was used. See Figure A.2.12 for modeling details related to the cornering load.

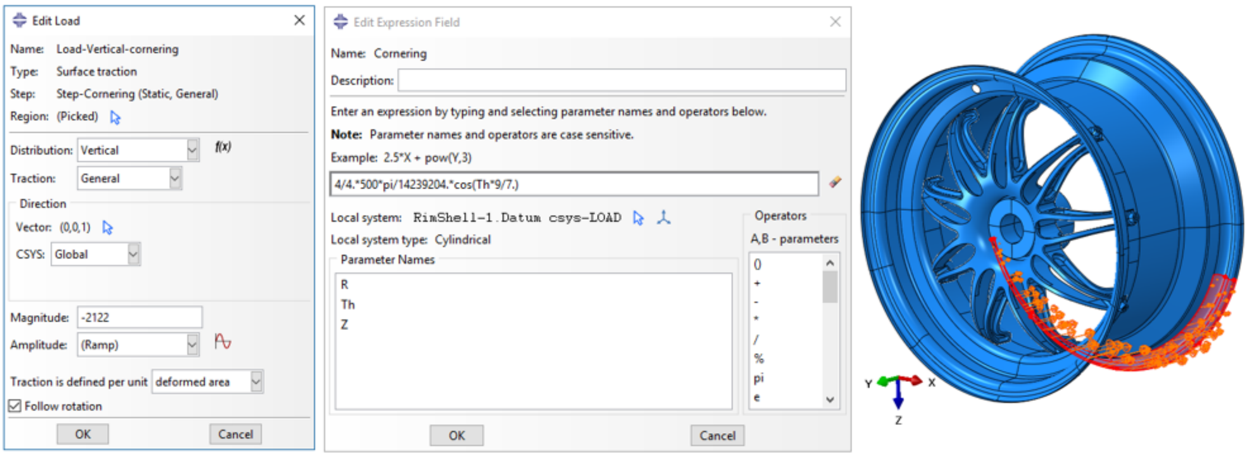

Figure A.2.12

Brake Loads

The brake load distribution is defined on the hole inner and outer bead. The load was defined as a surface traction working as a shear traction distributed by analytic field. The analytic field was based on the brake distribution defined in Appendix A.1. To apply this equation the cylindrical coordinate system used for the layup orientation was used. See Figure A.2.13 for modeling details related to the brake load.

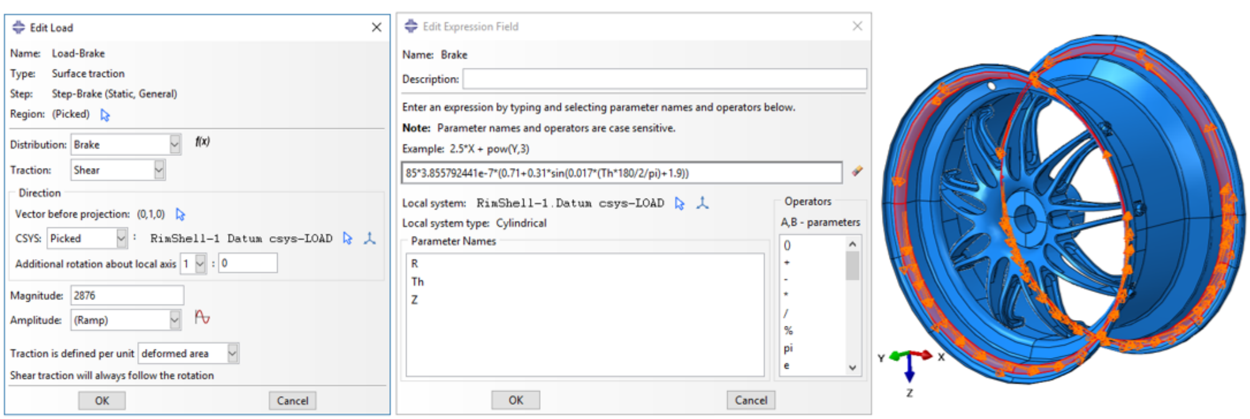

Figure A.2.13

Pretension in bolts

Pretension in the bolts was defined with a bolt load on the middle partition between the threads and the bolt head. For definition of a bolt load a center axis in the axial direction of the bolt is needed. The bolt load is applied in the first step before the main load step, in the main load step the bolt is defined with a fixed length. The bolt load is applied with a ramp where 10% of the load is applied during 0.5 of total step time, and rest during the last of the increment. This is done to easier initialize contact when general contact is used, since Abaqus search for all the contact pairs. See FigureA.2.14 for modeling details related to the bolt load.

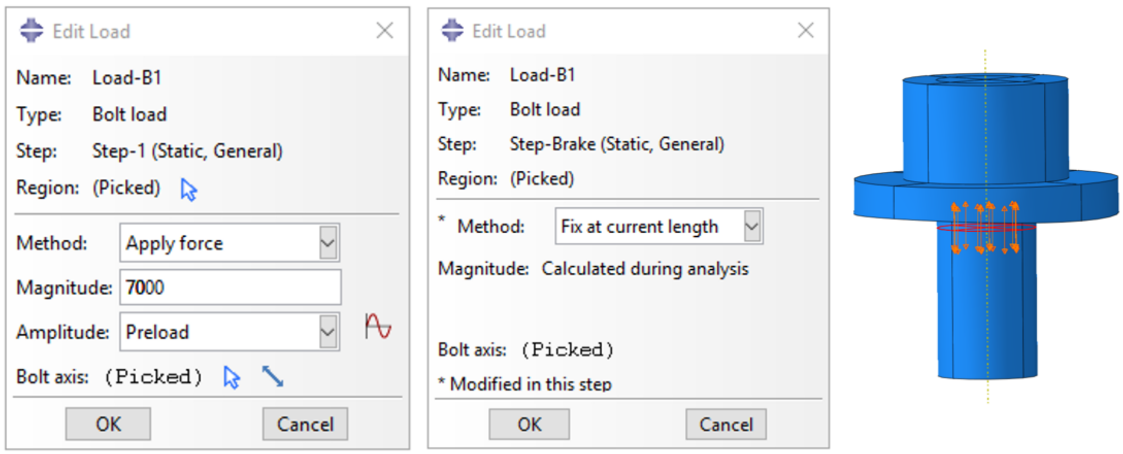

Figure A.2.14

Pretension in Hub & center lock

Pretension in the hub & center lock was defined with a bolt load on the middle partition between the threads and the center lock nut. For definition of a bolt load a center axis in the axial direction of the bolt is needed. The bolt load is applied in the first step before the main load step, in the main load step the bolt is defined with a fixed length. The bolt load is applied with a ramp where 10% of the load is applied during 0.5 of total step time, and rest during the last of the increment. This is done to easier initialize contact when general contact is used, since Abaqus search for all the contact pairs. See Figure A.2.15 for modeling details related to the bolt load.

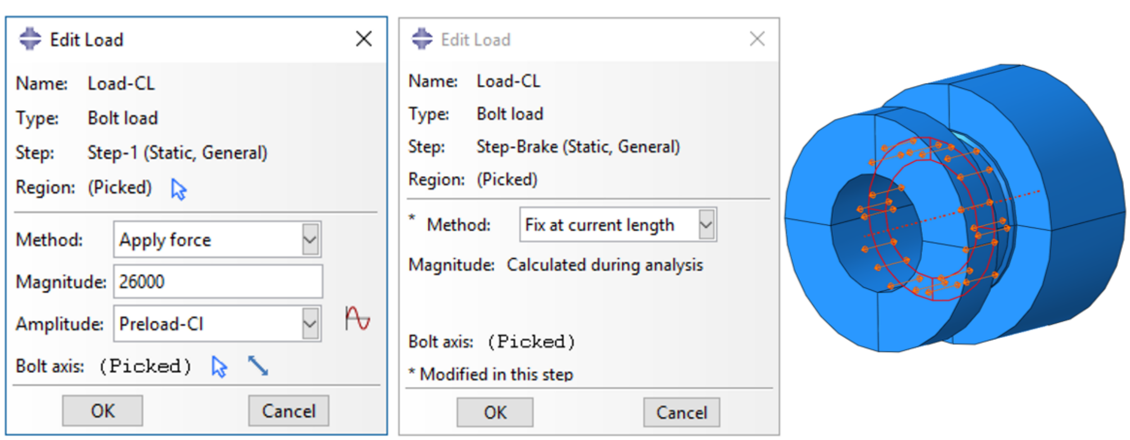

Figure A.2.15

A.2.8 Mesh

Rim Shell

The mesh for the rim shell was made of 4-node doubly curved thin shell elements with reduced integration, hourglass control and finite membrane strains. The element shape is free quad with advancing front as mesh shape algorithm. The global size was set to 5 with a curvature control of 0.05. Mesh refinements was done for all holes in the laminate and to the rim center interaction surfaces. See Figure A.2.16 for details related to mesh.

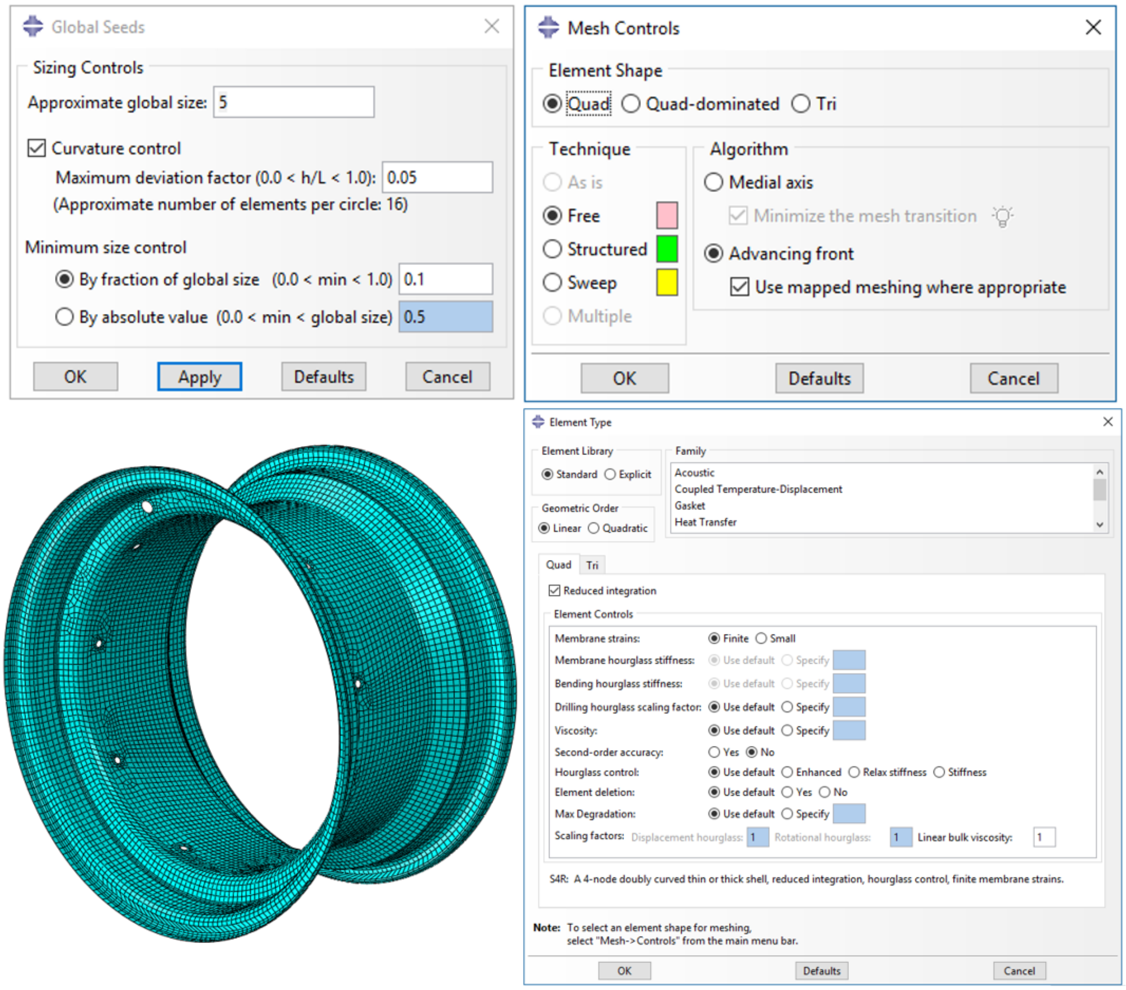

Figure A.2.16

Rim Center

The mesh for the rim center was made of 10-node quadratic tetrahedron elements. The element shape is free tet with default shape algorithm. The global size was set to 4 with a curvature control of 0.1. See Figure A.2.17 for details related to mesh.

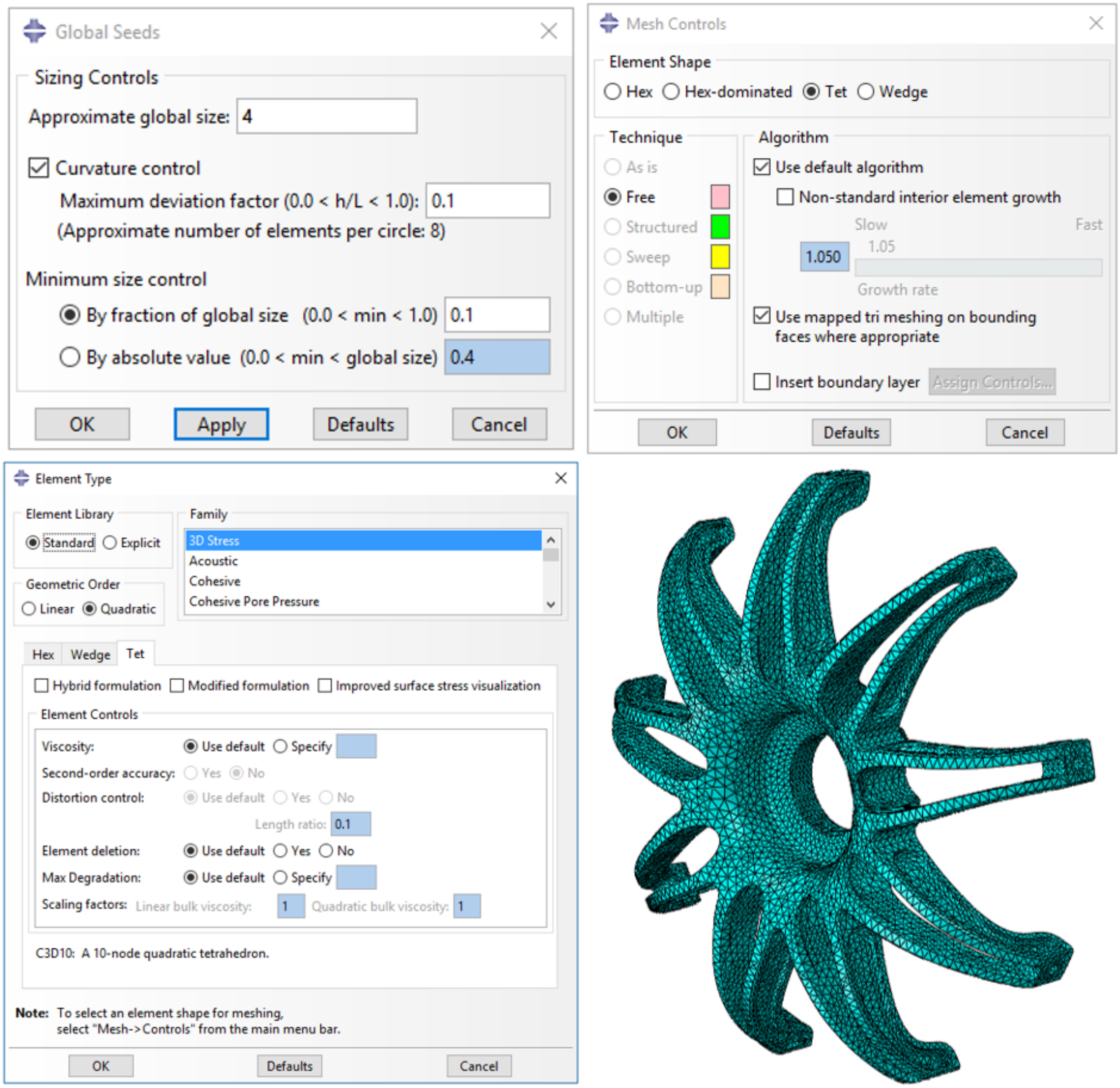

Figure A.2.17

Bolts

The mesh for the bolts was made of 8-node linear brick elements witch reduced integration and hourglass control. The element shape was quad and a combination of structured (green) and sweep (yellow) . The global size was set to 1 with a curvature control of 0.1. See Figure A.2.18 for details related to mesh.

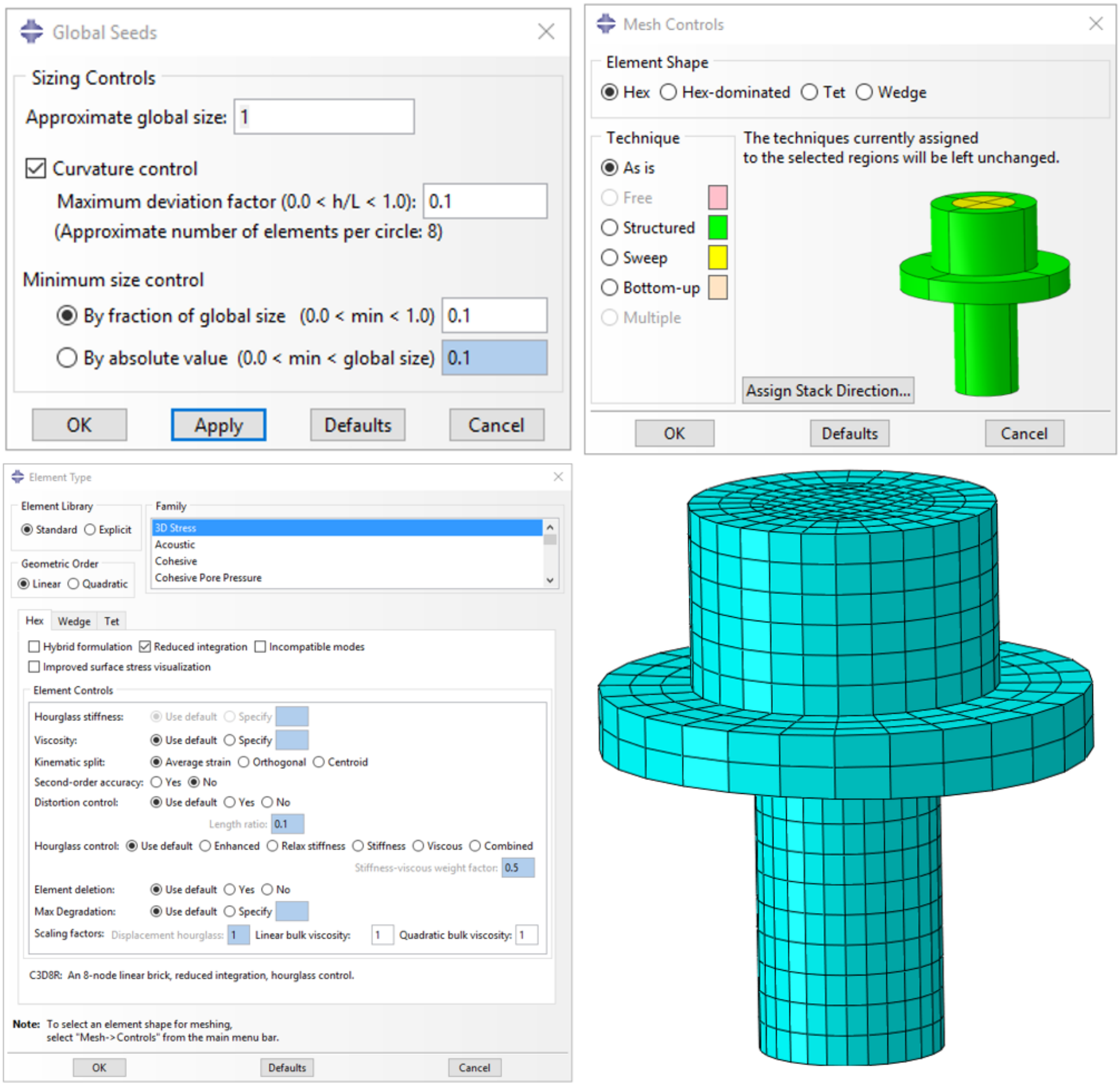

Figure A.2.18

Hub & center lock

The mesh for the Hub & center lock was made of 8-node linear brick elements witch reduced integration and hourglass control. The element shape was quad and with sweep technique. The global size was set to 3 with a curvature control of 0.05. See Figure A.2.19 for details related to mesh.

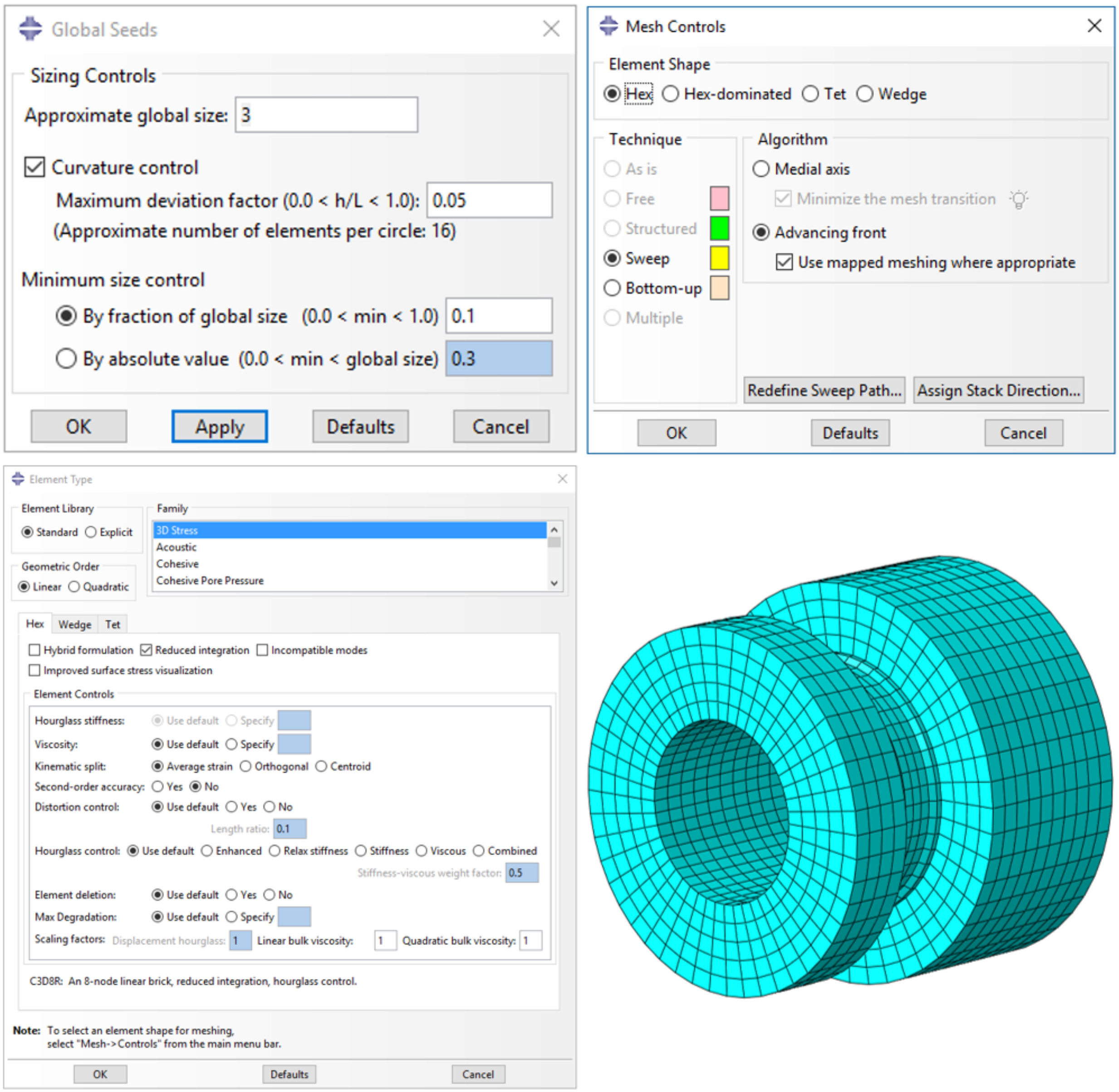

Figure A.2.19

A.3 Material Optimization Setup

This section will follow all steps done in Isight, Matlab and Abaqus to set up the material optimization. It will be divided and structured as the list under:

- Isight
  - Work-flow
  - Optimization
  - Parameters
- Abaqus
  - Part
  - Step
  - Interactions
  - Macro and scripting
- Codes and Script
  - Matlab Code
  - Abaqus Pre-script
  - Abaqus Post-script

A.3.1 Isight

Isight and the SIMULIA Execution Engine (formerly Fiper) are used to combine multiple cross-disciplinary models and applications together in a simulation process flow, automate their execution across distributed compute resources, explore the resulting design space, and identify the optimal design parameters subject to required constraints[20].

Work-flow description

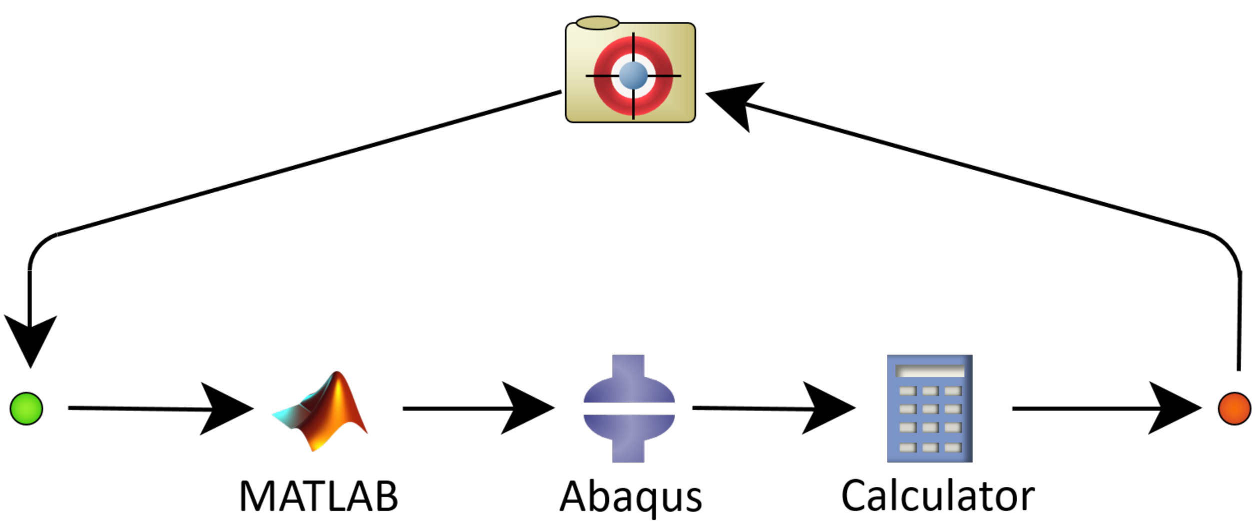

Figure A.3.1

The work-flow used for the material optimization is illustrated in Figure A.3.1. First, the optimizer module (here called Layup optimizer) give Matlab values for each variables consisting; number of plies, orientations and material for all sections. Then Matlab writes 8 text files on the format found in Figure A.3.2 which is on the same format and have all the information needed for the composite layup editor in Abaqus:A.3.2. Then Abaqus is executed with a prescript written in python. This prescript is constructing a FE-model with layup information from Matlab as input. After the FE-analysis is completed a postscript written python is reading the strain energy, and displacement at the rim flange and outputting the values to the Layup optimizer. The layup optimizer then changes the layup parameters based on the response of the design objectives and the design constraint.

```
0, Ply-OF-1,  Set-OF, Twill, 0.3, <Layup>, 45, 5
0, Ply-OF-2,  Set-OF, Twill, 0.3, <Layup>, 45, 5
0, Ply-OF-3,  Set-OF, Twill, 0.3, <Layup>,  0, 5
0, Ply-OF-4,  Set-OF, Twill, 0.3, <Layup>,  0, 5
0, Ply-OF-5,  Set-OF, Twill, 0.3, <Layup>,  0, 5
1, Ply-OF-6,  Set-OF, Twill, 0.3, <Layup>,  0, 5
1, Ply-OF-7,  Set-OF, Twill, 0.3, <Layup>,  0, 5
1, Ply-OF-8,  Set-OF, Twill, 0.3, <Layup>, 45, 5
1, Ply-OF-9,  Set-OF, Twill, 0.3, <Layup>,  0, 5
1, Ply-OF-10, Set-OF, Twill, 0.3, <Layup>, 45, 5
1, Ply-OF-11, Set-OF, Twill, 0.3, <Layup>, 45, 5
1, Ply-OF-12, Set-OF, Twill, 0.3, <Layup>,  0, 5
1, Ply-OF-13, Set-OF, Twill, 0.3, <Layup>,  0, 5
1, Ply-OF-14, Set-OF, Twill, 0.3, <Layup>,  0, 5
```

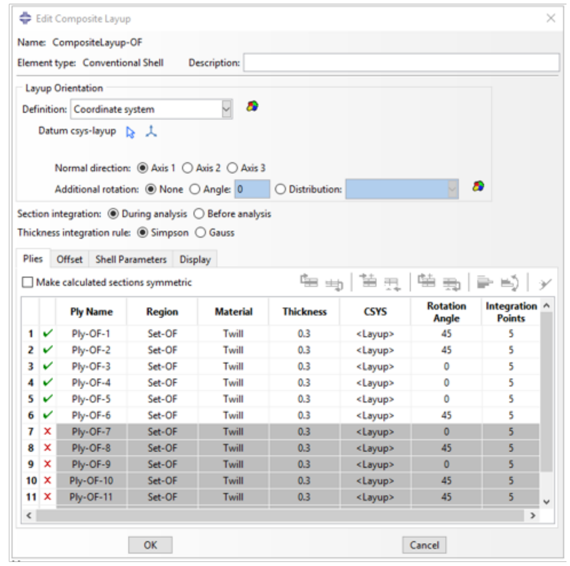

Text file formatting

Composite Layup Editor in Abaqus

Figure A.3.2

Optimization set-up

A evolution based algorithm was used for the optimization, for optimization set-up see Figure A.3.3. The optimization constraints and objectives is found in Table A.3.1. Based on the response of these parameters, Isight updates the variables for each iterations. The variables is updated with goal of fulfilling the design constraint and design objectives. The main goal of the optimization is to hit a weight target of 700 gram and maximize the stiffness by minimizing the strain energy. In addition to this a material-use was set as constraint. This was done as only a limited amount of UD-fibers was available from the sponsors.

Table A.3.1

Design Constraints					
Parameter	**Lower Bound**	**Upper Bound**	**Target**	**Scale Factor**	**Weight Factor**
Square Meter of UD-fiber used per rim	0.3	0.5	0.4	2000.0	0.5
Total mass per Rim Shell	500.0	800.0	700.0	1.42	1.0

Design Objectives				
Parameter	**Direction**	**Target**	**Scale Factor**	**Weight Factor**
Strain Energy	Minimize	-	0.2922	1.2

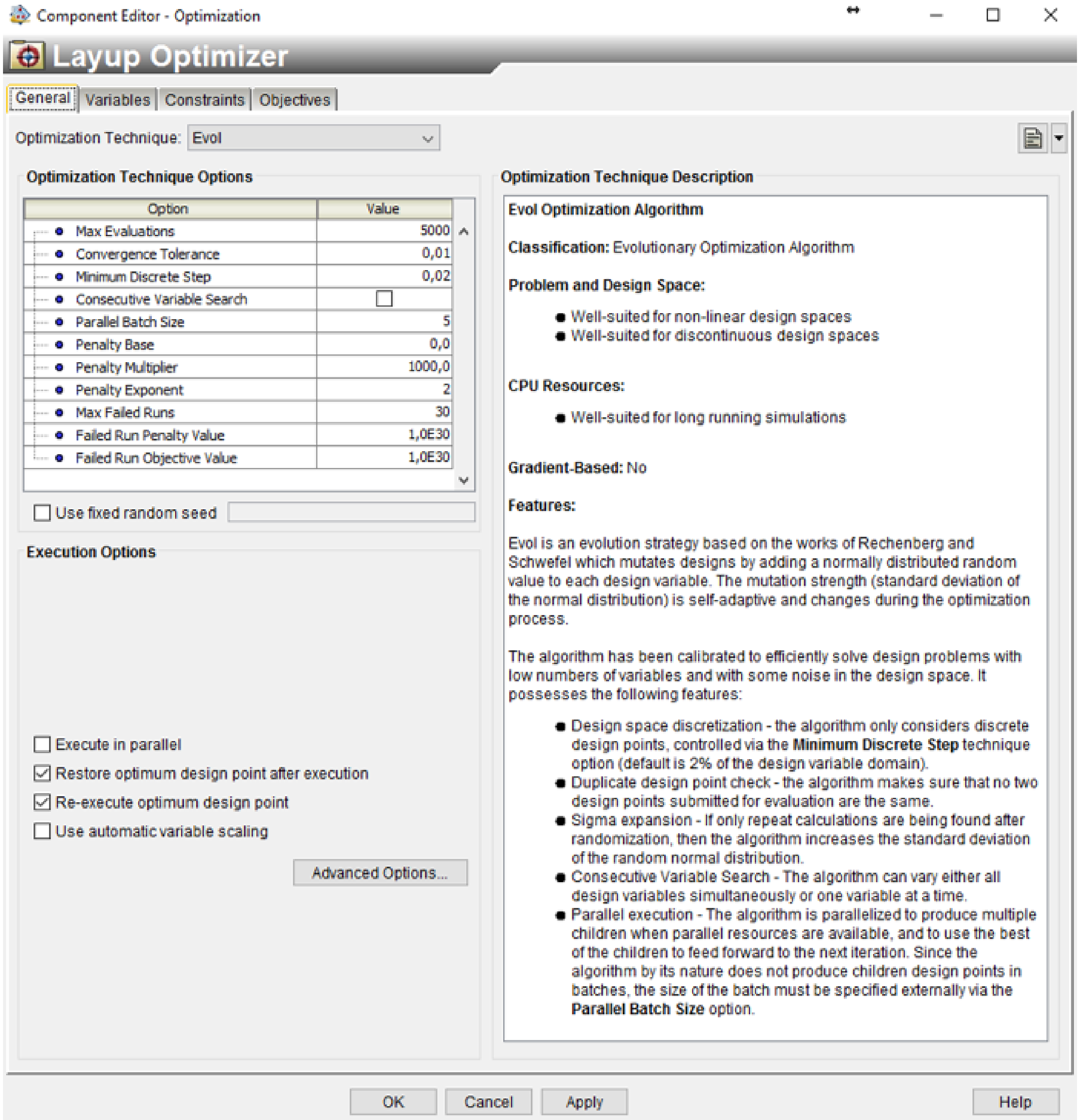

Figure A.3.3

Variables

The variables is based on the segmentation of the rim which is described in chap: 2 section: 2.3.3. Each segment have individual variables which is number of plies, and orientations. In a addition to this variables a material choice (UD & 5HS) was added to segment: OB,CM,CS and IB. Summarized variables is found in Table A.3.2.

Table A.3.2

Segment	Orientations	Number of Layers	Material Choice
OF	0/90 & +-45	5-14	5HS
OB	[-90:15:90]	5-18	UD & 5HS
OD	0/90 & +-45	5-14	5HS
CM	[-90:15:90]	5-18	UD & 5HS
CS	[-90:15:90]	5-18	UD & 5HS
ID	0/90 & +-45	5-14	5HS
IB	[-90:15:90]	5-18	UD & 5HS
IF	0/90 & +-45	5-14	5HS

A.3.2 Abaqus

This section will only go through the modeling which is different from the modeling described in Appendix A.2 which is the following items in underlined in blue bold text:

- **Part**
- Properties
- Assembly
- **Step**
- **Interactions**
- Loads
- Mesh
- **Macro and Scripting**

Part

The part procedure is the same as in FEA-validation Setup, except the model only have two parts, the Rim center and the Rim shell. The rim shell is simplified and does not include any holes for mounting or for the stem valve. The rim center used for the optimization is a early draft, but it have the baseline as the final rim center. Rim center and rim shell is found in Figure A.3.4.

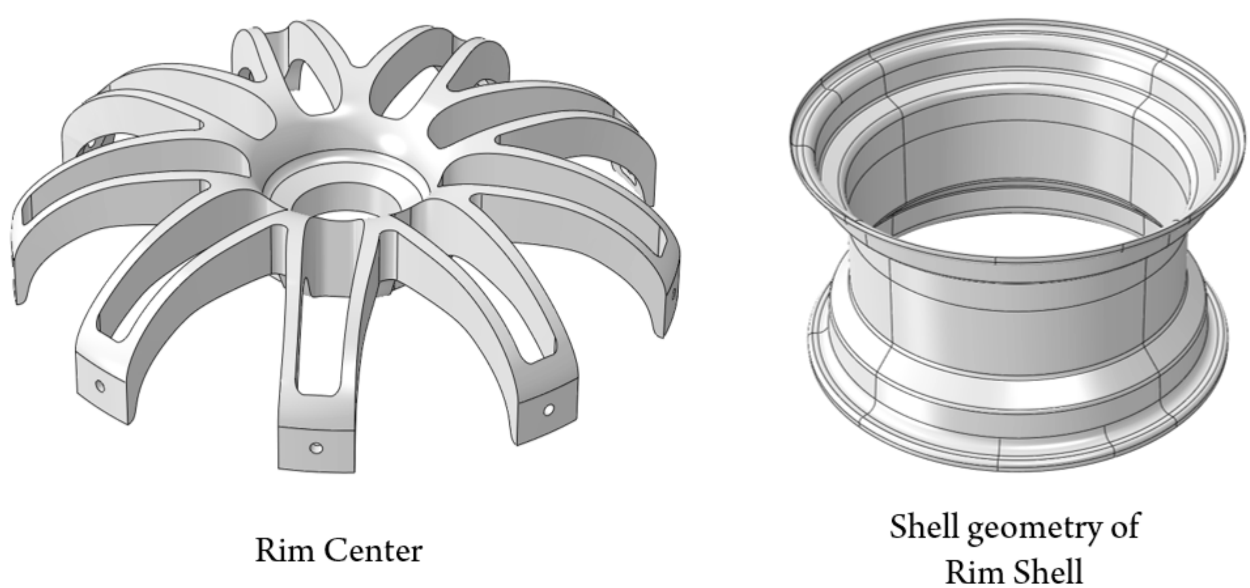

Figure A.3.4

Step

Two quasi-static linear perturbation steps was used. Step one for cornering at 110km/h and step two for braking at 110km/h. See Figure A.3.5 for set-up.

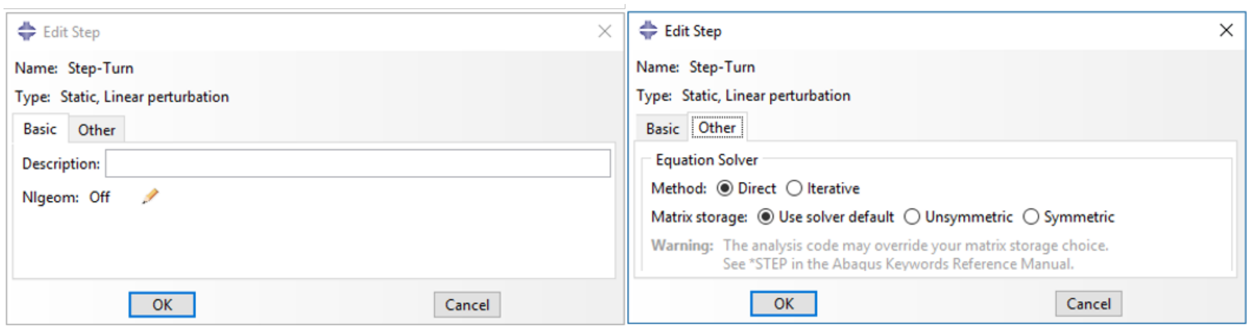

Figure A.3.5

Interactions

The interactions was simplified to reduce computing time as many design iterations was required by the Evolution based optimization algorithm. The interaction of the hub was simplified with a kinematic coupling constrained in all 6 degree of freedom, which was then encastre and used as boundary condition. The bolted connection between the rim center and the rim shell was simplified with a tie constraint discretized with the surface to surface method. See Figure A.3.6 for coupling and tie set-up.

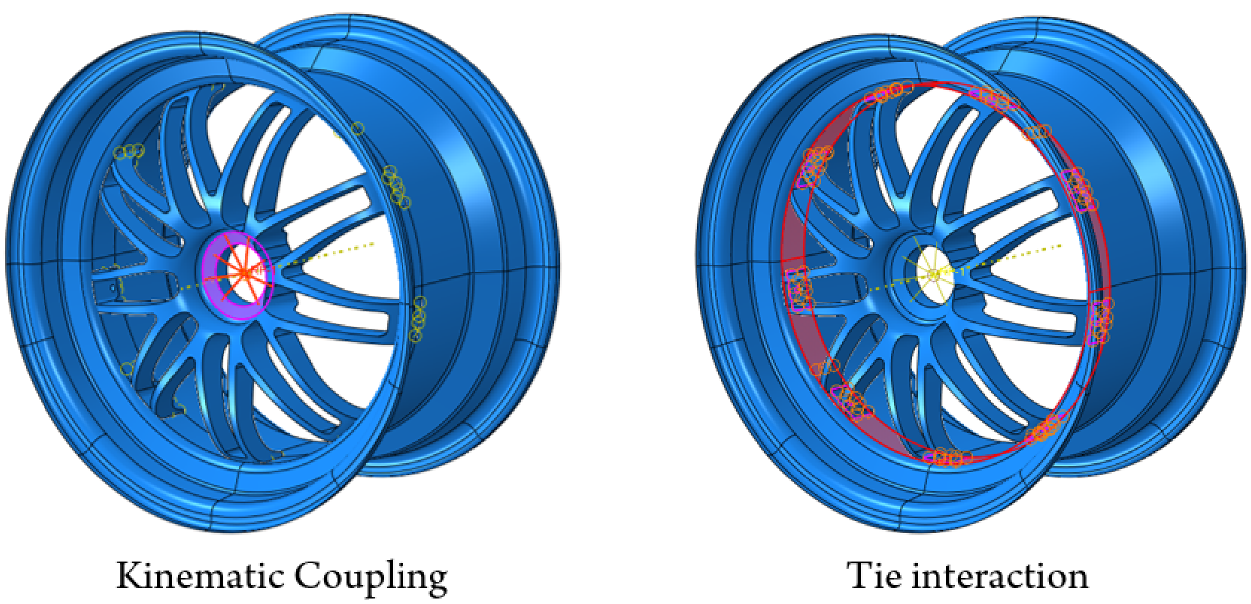

Figure A.3.6

Macro and Scripting

Abaqus/CAE can be automated by running Python scrips. Writing these scripts from scratch is not always intuitive. Abaqus have a built in Macro Recorder which allows the user to work in the GUI-enviorment and record that into scripts [21].

First the complete FE-model was built in Abaqus, all steps in the Abaqus work-three was followed as described in the latter sections. Creating of the composite layup was done last with the Macro Recorder on to generate a python code used for the optimization task. This script was then modified to update the layup based on the text file generated by Matlab. This python script is found in Appendix A.3.3.

Another script was created for reading and saving the output values from ODB-result file. This script created without the Macro Recorder and is found in Appendix A.3.3

A.3.3 Codes and Scripts

Matlab Code

```
%  This script is designed for handling parameters from Isight and writing
%  them into text files suited for the Abaqus composite layup editor. This
%  script is only usable for the spesific task described in the master
%  Thesis.
%%  Parameters for Outer Flange
A_of= 31272*10^-6;  % m^2
double n_of;  % Number of plies
% double O_of1;
O_of1=45;
double O_of2;
double O_of3;
double O_of4;
double O_of5;
double O_of6;
double O_of7;
double O_of8;
double O_of9;
double O_of10;
double O_of11;
double O_of12;
double O_of13;
double O_of14;
O_of=[O_of1,O_of2,O_of3,O_of4,O_of5,O_of6,O_of7,O_of8,O_of9,O_of10,O_of11,...
    O_of12,O_of13,O_of14];  % Orientations
M_of=[1,1,1,1,1,1,1,1,1,1,1,1,1,1]; % Materials % 1=5HS, UD=0;
%%  Parameters for OuterBead
A_ob= 19247.07 *10^-6;  % m^2
double n_ob;  % Number ob plies
O_ob1=45;
double O_ob2;
double O_ob3;
double O_ob4;
double O_ob5;
double O_ob6;
double O_ob7;
double O_ob8;
double O_ob9;
double O_ob10;
double O_ob11;
double O_ob12;
double O_ob13;
double O_ob14;
double O_ob15;
double O_ob16;
double O_ob17;
double O_ob18;
O_ob=[O_ob1,O_ob2,O_ob3,O_ob4,O_ob5,O_ob6,O_ob7,O_ob8,O_ob9,O_ob10,O_ob11,...
    O_ob12,O_ob13,O_ob14,O_ob15,O_ob16,O_ob17,O_ob18];  % Orientation ply1
M_ob1=1;
double M_ob2;
double M_ob3;
double M_ob4;
double M_ob5;
double M_ob6;
```

```
double M_ob7;
double M_ob8;
double M_ob9;
double M_ob10;
double M_ob11;
double M_ob12;
double M_ob13;
double M_ob14;
double M_ob15;
double M_ob16;
double M_ob17;
double M_ob18;
M_ob=[M_ob1,M_ob2,M_ob3,M_ob4,M_ob5,M_ob6,M_ob7,M_ob8,M_ob9,M_ob10,M_ob11,...
      M_ob12,M_ob13,M_ob14,M_ob15,M_ob16,M_ob17,M_ob18];  % 1=5HS, UD=0;
%%  Parameters for Outer Drop
A_od=25819.78*10^-6;  % m^2
double n_od;  % Number of plies
O_od1=45;
double O_od2;
double O_od3;
double O_od4;
double O_od5;
double O_od6;
double O_od7;
double O_od8;
double O_od9;
double O_od10;
double O_od11;
double O_od12;
double O_od13;
double O_od14;
O_od=[O_od1,O_od2,O_od3,O_od4,O_od5,O_od6,O_od7,O_od8,O_od9,O_od10,O_od11,...
      O_od12,O_od13,O_od14];  % Orientations
M_od=[1,1,1,1,1,1,1,1,1,1,1,1,1,1]; %  Materials % 1=5HS, UD=0;
%%  Parameters for Center Flange
A_cf= 23046.38*10^-6;  % m^2
double n_cf;  % Number cf plies
O_cf1=45;
double O_cf2;
double O_cf3;
double O_cf4;
double O_cf5;
double O_cf6;
double O_cf7;
double O_cf8;
double O_cf9;
double O_cf10;
double O_cf11;
double O_cf12;
double O_cf13;
double O_cf14;
double O_cf15;
double O_cf16;
double O_cf17;
double O_cf18;
O_cf=[O_cf1,O_cf2,O_cf3,O_cf4,O_cf5,O_cf6,O_cf7,O_cf8,O_cf9,O_cf10,O_cf11,...
      O_cf12,O_cf13,O_cf14,O_cf15,O_cf16,O_cf17,O_cf18];  % Orientations
M_cf1=1;
double M_cf2;
double M_cf3;
double M_cf4;
double M_cf5;
double M_cf6;
double M_cf7;
double M_cf8;
double M_cf9;
double M_cf10;
double M_cf11;
double M_cf12;
double M_cf13;
double M_cf14;
```

```
double M_cf15;
double M_cf16;
double M_cf17;
double M_cf18;
M_cf=[M_cf1,M_cf2,M_cf3,M_cf4,M_cf5,M_cf6,M_cf7,M_cf8,M_cf9,M_cf10,M_cf11,...
    M_cf12,M_cf13,M_cf14,M_cf15,M_cf16,M_cf17,M_cf18];  % 1=5HS, UD=0;
%% Parameters for Center Shell
A_cs=52808.87*10^-6;  % m^2
double n_cs;  % Number of plies
O_cs1=45;
double O_cs2;
double O_cs3;
double O_cs4;
double O_cs5;
double O_cs6;
double O_cs7;
double O_cs8;
double O_cs9;
double O_cs10;
double O_cs11;
double O_cs12;
double O_cs13;
double O_cs14;
double O_cs15;
double O_cs16;
double O_cs17;
double O_cs18;
O_cs=[O_cs1,O_cs2,O_cs3,O_cs4,O_cs5,O_cs6,O_cs7,O_cs8,O_cs9,O_cs10,O_cs11,...
    O_cs12,O_cs13,O_cs14,O_cs15,O_cs16,O_cs17,O_cs18];  % Orientations
% double M_cs1;
M_cs1=1;
double M_cs2;
double M_cs3;
double M_cs4;
double M_cs5;
double M_cs6;
double M_cs7;
double M_cs8;
double M_cs9;
double M_cs10;
double M_cs11;
double M_cs12;
double M_cs13;
double M_cs14;
double M_cs15;
double M_cs16;
double M_cs17;
double M_cs18;
M_cs=[M_cs1,M_cs2,M_cs3,M_cs4,M_cs5,M_cs6,M_cs7,M_cs8,M_cs9,M_cs10,M_cs11,...
    M_cs12,M_cs13,M_cs14,M_cs15,M_cs16,M_cs17,M_cs18];  % 1=5HS, UD=0;
%% Parameter for Inner Drop
A_id=28377.53*10^-6;  % m^2
double n_id;  % Number of plies
% double O_id1;
O_id1=45;
double O_id2;
double O_id3;
double O_id4;
double O_id5;
double O_id6;
double O_id7;
double O_id8;
double O_id9;
double O_id10;
double O_id11;
double O_id12;
double O_id13;
double O_id14;
O_id=[O_id1,O_id2,O_id3,O_id4,O_id5,O_id6,O_id7,O_id8,O_id9,O_id10,O_id11,...
    O_id12,O_id13,O_id14];  % Orientation
M_id=[1,1,1,1,1,1,1,1,1,1,1,1,1,1]; % Material % 1=5HS, UD=0;
```

```
%% Paramters for Inner Bead
A_ib= 23897.81*10^-6; % m^2
double n_ib; % Number of plies
O_ib1=45;
double O_ib2;
double O_ib3;
double O_ib4;
double O_ib5;
double O_ib6;
double O_ib7;
double O_ib8;
double O_ib9;
double O_ib10;
double O_ib11;
double O_ib12;
double O_ib13;
double O_ib14;
double O_ib15;
double O_ib16;
double O_ib17;
double O_ib18;
O_ib=[O_ib1,O_ib2,O_ib3,O_ib4,O_ib5,O_ib6,O_ib7,O_ib8,O_ib9,O_ib10,O_ib11,...
    O_ib12,O_ib13,O_ib14,O_ib15,O_ib16,O_ib17,O_ib18]; % Orientations
M_ib1=1;
double M_ib2;
double M_ib3;
double M_ib4;
double M_ib5;
double M_ib6;
double M_ib7;
double M_ib8;
double M_ib9;
double M_ib10;
double M_ib11;
double M_ib12;
double M_ib13;
double M_ib14;
double M_ib15;
double M_ib16;
double M_ib17;
double M_ib18;
M_ib=[M_ib1,M_ib2,M_ib3,M_ib4,M_ib5,M_ib6,M_ib7,M_ib8,M_ib9,M_ib10,M_ib11,...
    M_ib12,M_ib13,M_ib14,M_ib15,M_ib16,M_ib17,M_ib18]; % 1=5HS, UD=0;
%% Paramters for InnerFlange
A_if=31110.57*10^-6; % m^2
double n_if; % Number of plies
O_if1=45;
double O_if2;
double O_if3;
double O_if4;
double O_if5;
double O_if6;
double O_if7;
double O_if8;
double O_if9;
double O_if10;
double O_if11;
double O_if12;
double O_if13;
double O_if14;
O_if=[O_if1,O_if2,O_if3,O_if4,O_if5,O_if6,O_if7,O_if8,O_if9,O_if10,O_if11,...
    O_if12,O_if13,O_if14]; % Orientations
M_if=[1,1,1,1,1,1,1,1,1,1,1,1,1,1];% Material % 1=5HS, UD=0;
%% Material properties
m_5HS=471; % GSM 5HS
m_UD=162; % GSM UD
t_5HS=('0.3'); % Thickness 5HS
t_UD=('0.1'); % Thickness UD
%% Abaqus data
int_p=5; % intergration point
```

```
ccys=('<Layup>');
%% OuterFlange
filename='OF.txt';
reg_set='Set-OF';
ply_name='Ply-OF-';
fid=fopen(filename,'w');
mass_of=0;
for i=1:14
    if i<=n_of
    stat=('0');
    ms=1;
    else
    stat=('1');
    ms=0;
    end
    if M_of(i)==1
            mat=('5HS');
            t=t_5HS;
            mass_of=mass_of+m_5HS*A_of*ms;
    else
            mat=('UD');
            t=t_UD;
            mass_of=mass_of+m_UD*A_of*ms;
    end
     fprintf(fid,'%s,%s%d,%s,%s,%s,%s,%d,%d\n',stat,ply_name,i,...
         reg_set,mat,t,ccys,O_of(i),int_p);
end
fclose(fid);
%% OuterBead
filename='OB.txt';
reg_set='Set-OB';
ply_name='Ply-OB-';
fid=fopen(filename,'w');
mass_ob=0;
for i=1:18
    if i<=n_ob
    stat=('0');
    ms=1;
    else
    stat=('1');
    ms=0;
    end
    if M_ob(i)==1
            mat=('5HS');
            t=t_5HS;
            mass_ob=mass_ob+m_5HS*A_ob*ms;
    else
            mat=('UD');
            t=t_UD;
            mass_ob=mass_ob+m_UD*A_ob*ms;
    end
     fprintf(fid,'%s,%s%d,%s,%s,%s,%s,%d,%d\n',stat,ply_name,i,...
         reg_set,mat,t,ccys,O_ob(i),int_p);
end
fclose(fid);
%% OuterDrop
filename='OD.txt';
reg_set='Set-OD';
ply_name='Ply-OD-';
fid=fopen(filename,'w');
mass_od=0;
for i=1:14
    if i<=n_od
    stat=('0');
    ms=1;
    else
    stat=('1');
    ms=0;
```

```
    end

    if M_of(i)==1
            mat=('5HS');
            t=t_5HS;
            mass_od=mass_od+m_5HS*A_od*ms;
    else
            mat=('UD');
            t=t_UD;
            mass_od=mass_od+m_UD*A_od*ms;
    end
     fprintf(fid,'%s, %s%d, %s, %s, %s, %s, %d, %d\n',stat,ply_name,i,...
        reg_set,mat,t,ccys,O_od(i),int_p);
end
fclose(fid);
%% CenterFlange
filename='CF.txt';
reg_set='Set-CF';
ply_name='Ply-CF-';
fid=fopen(filename,'w');
mass_cf=0;
for i=1:18

    if i<=n_cf
    stat=('0');
    ms=1;
    else
    stat=('1');
    ms=0;
    end

    if M_cf(i)==1
            mat=('5HS');
            t=t_5HS;
            mass_cf=mass_cf+m_5HS*A_cf*ms;
    else
            mat=('UD');
            t=t_UD;
            mass_cf=mass_cf+m_UD*A_cf*ms;
    end

     fprintf(fid,'%s, %s%d, %s, %s, %s, %s, %d, %d\n',stat,ply_name,i,...
        reg_set,mat,t,ccys,O_cf(i),int_p);
end
fclose(fid);
%% CenterShell
filename='CS.txt';
reg_set='Set-CS';
ply_name='Ply-CS-';
fid=fopen(filename,'w');
mass_cs=0;
for i=1:18
    if i<=n_cs
    stat=('0');
    ms=1;
    else
    stat=('1');
    ms=0;
    end
    if M_cs(i)==1
            mat=('5HS');
            t=t_5HS;
            mass_cs=mass_cs+m_5HS*A_cs*ms;
        else
            mat=('UD');
            t=t_UD;
            mass_cs=mass_cs+m_UD*A_cs*ms;
    end
     fprintf(fid,'%s, %s%d, %s, %s, %s, %s, %d, %d\n',stat,ply_name,i,...
```

```
            reg_set,mat,t,ccys,O_cs(i),int_p);
end
fclose(fid);
%% InnerDrop
filename='ID.txt';
reg_set='Set-ID';
ply_name='Ply-ID-';
fid=fopen(filename,'w');
mass_id=0;
for i=1:14
    if i<=n_id
    stat=('0');
    ms=1;
    else
    stat=('1');
    ms=0;
    end
    if M_id(i)==1
            mat=('5HS');
            t=t_5HS;
            mass_id=mass_id+m_5HS*A_id*ms;
    else
            mat=('UD');
            t=t_UD;
            mass_id=mass_id+m_UD*A_id*ms;
    end
     fprintf(fid,'%s, %s%d, %s, %s, %s, %s, %d, %d\n',stat,ply_name,i
        ,...
            reg_set,mat,t,ccys,O_id(i),int_p);
end
fclose(fid);
%% InnerBead
filename='IB.txt';
reg_set='Set-IB';
ply_name='Ply-IB-';
fid=fopen(filename,'w');
mass_ib=0;
for i=1:18
    if i<=n_ib
    stat=('0');
    ms=1;
    else
    stat=('1');
    ms=0;
    end
    if M_ib(i)==1
            mat=('5HS');
            t=t_5HS;
            mass_ib=mass_ib+m_5HS*A_ib*ms;
    else
            mat=('UD');
            t=t_UD;
            mass_ib=mass_ib+m_UD*A_ib*ms;
    end
     fprintf(fid,'%s, %s%d, %s, %s, %s, %s, %d, %d\n',stat,ply_name,i
        ,...
            reg_set,mat,t,ccys,O_ib(i),int_p);
end
fclose(fid);
%% InnerFLange
filename='IF.txt';
reg_set='Set-IF';
ply_name='Ply-IF-';
fid=fopen(filename,'w');
mass_if=0;
for i=1:14
    if i<=n_if
    stat=('0');
    ms=1;
    else
```

```
      stat=('1');
      ms=0;
      end
      if M_if(i)==1
              mat=('5HS');
              t=t_5HS;
              mass_if=mass_if+m_5HS*A_if*ms;
      else
              mat=('UD');
              t=t_UD;
              mass_if=mass_if+m_UD*A_if*ms;
      end
       fprintf(fid,'%s,%s%d,%s,%s,%s,%s,%d,%d\n',stat,ply_name,i,...
          reg_set,mat,t,ccys,O_if(i),int_p);
end
mass_tot=mass_of+mass_od+mass_cs+mass_id+mass_if+mass_ob+mass_cf+mass_ib;
% total mass of rim
AUD=(n_ob-sum(M_ob(1:n_ob)))*A_ob + (n_cf-sum(M_cf(1:n_cf)))*A_cf + ...
    (n_cs-sum(M_cs(1:n_cs)))*A_cs + (n_ib-sum(M_ib(1:n_ib)))*A_ib;% Total
% surface area of UD
fclose(fid);
```

Abaqus Pre-script

```
# -*- coding: mbcs -*-
# Do not delete the following import lines
from abaqus import *
from abaqusConstants import *
import __main__


import section
import regionToolset
import displayGroupMdbToolset as dgm
import part
import material
import assembly
import step
import interaction
import load
import mesh
import optimization
import job
import sketch
import visualization
import xyPlot
import displayGroupOdbToolset as dgo
import connectorBehavior

session.viewports['Viewport: 1'].view.setValues(nearPlane=1076.81,
farPlane=1637.08, width=766.687, height=438.824, cameraPosition=(
276.033, -1241.47, 482.228), cameraTarget=(96.8227, -26.6858,
-0.0612259))

# REGION OuterFlange
layupOrientation = mdb.models['Model-1'].parts['Shell'].datums[23]
p = mdb.models['Model-1'].parts['Shell']
region1=p.sets['Set-OF']
p = mdb.models['Model-1'].parts['Shell']
region2=p.sets['Set-OF']
p = mdb.models['Model-1'].parts['Shell']
region3=p.sets['Set-OF']
```

```
p = mdb.models['Model-1'].parts['Shell']
region4=p.sets['Set-OF']
p = mdb.models['Model-1'].parts['Shell']
region5=p.sets['Set-OF']
p = mdb.models['Model-1'].parts['Shell']
region6=p.sets['Set-OF']
p = mdb.models['Model-1'].parts['Shell']
region7=p.sets['Set-OF']
p = mdb.models['Model-1'].parts['Shell']
region8=p.sets['Set-OF']
p = mdb.models['Model-1'].parts['Shell']
region9=p.sets['Set-OF']
p = mdb.models['Model-1'].parts['Shell']
region10=p.sets['Set-OF']
p = mdb.models['Model-1'].parts['Shell']
region11=p.sets['Set-OF']
p = mdb.models['Model-1'].parts['Shell']
region12=p.sets['Set-OF']
p = mdb.models['Model-1'].parts['Shell']
region13=p.sets['Set-OF']
p = mdb.models['Model-1'].parts['Shell']
region14=p.sets['Set-OF']
compositeLayup = mdb.models['Model-1'].parts['Shell'].CompositeLayup(
name='CompositeLayup-OF', description='', elementType=SHELL,
offsetType=BOTTOM_SURFACE, symmetric=False,
thicknessAssignment=FROM_SECTION)
compositeLayup.Section(preIntegrate=OFF, integrationRule=SIMPSON,
thicknessType=UNIFORM, poissonDefinition=DEFAULT, temperature=GRADIENT,
useDensity=OFF)
compositeLayup.ReferenceOrientation(orientationType=SYSTEM,
localCsys=layupOrientation, fieldName='',
additionalRotationType=ROTATION_NONE, angle=0.0,
additionalRotationField='', axis=AXIS_1)



fp  = open('D:/temp/13inch/Layup6376/SIM/OF.txt')
words= [word.strip() for line in fp.readlines() for word in line.split(',') if word.strip()]
#print(", ".join(words)) # or `print(words)` if you want to print out `words` as a list


for i in range(0, 13):
        s=int(words[i+(i*7)])
        pn=words[i+1+(i*7)]
        mat=words[i+3+(i*7)]
        th=float(words[i+4+(i*7)])
        om=float(words[i+6+(i*7)])
        compositeLayup.CompositePly(suppressed=s, plyName=pn,
        region=region1, material=mat, thicknessType=SPECIFY_THICKNESS,
        thickness=th, orientationType=SPECIFY_ORIENT, orientationValue=om,
        additionalRotationType=ROTATION_NONE, additionalRotationField='',
        axis=AXIS_3, angle=0.0, numIntPoints=5)

#---------------------------------------------End OuterFlange---------------------------------------------

# REGION OuterBead
layupOrientation = mdb.models['Model-1'].parts['Shell'].datums[23]
```

```
p = mdb.models['Model-1'].parts['Shell']
region1=p.sets['Set-OB']
p = mdb.models['Model-1'].parts['Shell']
region2=p.sets['Set-OB']
p = mdb.models['Model-1'].parts['Shell']
region3=p.sets['Set-OB']
p = mdb.models['Model-1'].parts['Shell']
region4=p.sets['Set-OB']
p = mdb.models['Model-1'].parts['Shell']
region5=p.sets['Set-OB']
p = mdb.models['Model-1'].parts['Shell']
region6=p.sets['Set-OB']
p = mdb.models['Model-1'].parts['Shell']
region7=p.sets['Set-OB']
p = mdb.models['Model-1'].parts['Shell']
region8=p.sets['Set-OB']
p = mdb.models['Model-1'].parts['Shell']
region9=p.sets['Set-OB']
p = mdb.models['Model-1'].parts['Shell']
region10=p.sets['Set-OB']
p = mdb.models['Model-1'].parts['Shell']
region11=p.sets['Set-OB']
p = mdb.models['Model-1'].parts['Shell']
region12=p.sets['Set-OB']
p = mdb.models['Model-1'].parts['Shell']
region13=p.sets['Set-OB']
p = mdb.models['Model-1'].parts['Shell']
region14=p.sets['Set-OB']
compositeLayup = mdb.models['Model-1'].parts['Shell'].CompositeLayup(
name='CompositeLayup-OB', description='', elementType=SHELL,
offsetType=BOTTOM_SURFACE, symmetric=False,
thicknessAssignment=FROM_SECTION)
compositeLayup.Section(preIntegrate=OFF, integrationRule=SIMPSON,
thicknessType=UNIFORM, poissonDefinition=DEFAULT, temperature=GRADIENT,
useDensity=OFF)
compositeLayup.ReferenceOrientation(orientationType=SYSTEM,
localCsys=layupOrientation, fieldName='',
additionalRotationType=ROTATION_NONE, angle=0.0,
additionalRotationField='', axis=AXIS_1)



fp = open('D:/temp/13inch/Layup6376/SIM/OB.txt')
words= [word.strip() for line in fp.readlines() for word in line.split(',') if
    word.strip()]
#print(", ".join(words)) # or `print(words)` if you want to print out `words`
    as a list


for i in range(0, 13):
        s=int(words[i+(i*7)])
        pn=words[i+1+(i*7)]
        mat=words[i+3+(i*7)]
        th=float(words[i+4+(i*7)])
        om=float(words[i+6+(i*7)])
        compositeLayup.CompositePly(suppressed=s, plyName=pn,
        region=region1, material=mat, thicknessType=SPECIFY_THICKNESS,
        thickness=th, orientationType=SPECIFY_ORIENT, orientationValue=om,
        additionalRotationType=ROTATION_NONE, additionalRotationField='',
        axis=AXIS_3, angle=0.0, numIntPoints=5)
```

```
#-----------------------------------------------End OuterBead
    -----------------------------------------------


#Outer Drop

p = mdb.models['Model-1'].parts['Shell']
session.viewports['Viewport: 1'].setValues(displayedObject=p)
layupOrientation = mdb.models['Model-1'].parts['Shell'].datums[23]
p = mdb.models['Model-1'].parts['Shell']
region1=p.sets['Set-OD']
p = mdb.models['Model-1'].parts['Shell']
region2=p.sets['Set-OD']
p = mdb.models['Model-1'].parts['Shell']
region3=p.sets['Set-OD']
p = mdb.models['Model-1'].parts['Shell']
region4=p.sets['Set-OD']
p = mdb.models['Model-1'].parts['Shell']
region5=p.sets['Set-OD']
p = mdb.models['Model-1'].parts['Shell']
region6=p.sets['Set-OD']
p = mdb.models['Model-1'].parts['Shell']
region7=p.sets['Set-OD']
p = mdb.models['Model-1'].parts['Shell']
region8=p.sets['Set-OD']
p = mdb.models['Model-1'].parts['Shell']
region9=p.sets['Set-OD']
p = mdb.models['Model-1'].parts['Shell']
region10=p.sets['Set-OD']
p = mdb.models['Model-1'].parts['Shell']
region11=p.sets['Set-OD']
p = mdb.models['Model-1'].parts['Shell']
region12=p.sets['Set-OD']
p = mdb.models['Model-1'].parts['Shell']
region13=p.sets['Set-OD']
p = mdb.models['Model-1'].parts['Shell']
region14=p.sets['Set-OD']
compositeLayup = mdb.models['Model-1'].parts['Shell'].CompositeLayup(
name='CompositeLayup-OD', description='', elementType=SHELL,
offsetType=BOTTOM_SURFACE, symmetric=False,
thicknessAssignment=FROM_SECTION)
compositeLayup.Section(preIntegrate=OFF, integrationRule=SIMPSON,
thicknessType=UNIFORM, poissonDefinition=DEFAULT, temperature=GRADIENT,
useDensity=OFF)
compositeLayup.ReferenceOrientation(orientationType=SYSTEM,
localCsys=layupOrientation, fieldName='',
additionalRotationType=ROTATION_NONE, angle=0.0,
additionalRotationField='', axis=AXIS_1)

fp  = open('D:/temp/13inch/Layup6376/SIM/OD.txt')
words= [word.strip() for line in fp.readlines() for word in line.split(',') if
    word.strip()]
#print(", ".join(words)) # or `print(words)` if you want to print out `words`
    as a list


for i in range(0, 13):
        s=int(words[i+(i*7)])
        pn=words[i+1+(i*7)]
```

```
        mat=words[i+3+(i*7)]
        th=float(words[i+4+(i*7)])
        om=float(words[i+6+(i*7)])
        compositeLayup.CompositePly(suppressed=s, plyName=pn,
        region=region1, material=mat, thicknessType=SPECIFY_THICKNESS,
        thickness=th, orientationType=SPECIFY_ORIENT, orientationValue=om,
        additionalRotationType=ROTATION_NONE, additionalRotationField='',
        axis=AXIS_3, angle=0.0, numIntPoints=5)

#---------------------------------------------End OuterDrop ----------------------------------------------

# REGION CenterFlange
layupOrientation = mdb.models['Model-1'].parts['Shell'].datums[23]
p = mdb.models['Model-1'].parts['Shell']
region1=p.sets['Set-CF']
p = mdb.models['Model-1'].parts['Shell']
region2=p.sets['Set-CF']
p = mdb.models['Model-1'].parts['Shell']
region3=p.sets['Set-CF']
p = mdb.models['Model-1'].parts['Shell']
region4=p.sets['Set-CF']
p = mdb.models['Model-1'].parts['Shell']
region5=p.sets['Set-CF']
p = mdb.models['Model-1'].parts['Shell']
region6=p.sets['Set-CF']
p = mdb.models['Model-1'].parts['Shell']
region7=p.sets['Set-CF']
p = mdb.models['Model-1'].parts['Shell']
region8=p.sets['Set-CF']
p = mdb.models['Model-1'].parts['Shell']
region9=p.sets['Set-CF']
p = mdb.models['Model-1'].parts['Shell']
region10=p.sets['Set-CF']
p = mdb.models['Model-1'].parts['Shell']
region11=p.sets['Set-CF']
p = mdb.models['Model-1'].parts['Shell']
region12=p.sets['Set-CF']
p = mdb.models['Model-1'].parts['Shell']
region13=p.sets['Set-CF']
p = mdb.models['Model-1'].parts['Shell']
region14=p.sets['Set-CF']
compositeLayup = mdb.models['Model-1'].parts['Shell'].CompositeLayup(
name='CompositeLayup-CF', description='', elementType=SHELL,
offsetType=BOTTOM_SURFACE, symmetric=False,
thicknessAssignment=FROM_SECTION)
compositeLayup.Section(preIntegrate=OFF, integrationRule=SIMPSON,
thicknessType=UNIFORM, poissonDefinition=DEFAULT, temperature=GRADIENT,
useDensity=OFF)
compositeLayup.ReferenceOrientation(orientationType=SYSTEM,
localCsys=layupOrientation, fieldName='',
additionalRotationType=ROTATION_NONE, angle=0.0,
additionalRotationField='', axis=AXIS_1)



fp = open('D:/temp/13inch/Layup6376/SIM/CF.txt')
words= [word.strip() for line in fp.readlines() for word in line.split(',') if word.strip()]
#print(", ".join(words)) # or `print(words)` if you want to print out `words`
```

```
as a list


for i in range(0, 13):
        s=int(words[i+(i*7)])
        pn=words[i+1+(i*7)]
        mat=words[i+3+(i*7)]
        th=float(words[i+4+(i*7)])
        om=float(words[i+6+(i*7)])
        compositeLayup.CompositePly(suppressed=s, plyName=pn,
        region=region1, material=mat, thicknessType=SPECIFY_THICKNESS,
        thickness=th, orientationType=SPECIFY_ORIENT, orientationValue=om,
        additionalRotationType=ROTATION_NONE, additionalRotationField='',
        axis=AXIS_3, angle=0.0, numIntPoints=5)

#----------------------------------------------End CenterFlange----------------------------------------------

#Center Shell

p = mdb.models['Model-1'].parts['Shell']
session.viewports['Viewport: 1'].setValues(displayedObject=p)
layupOrientation = mdb.models['Model-1'].parts['Shell'].datums[23]
p = mdb.models['Model-1'].parts['Shell']
region1=p.sets['Set-CS']
p = mdb.models['Model-1'].parts['Shell']
region2=p.sets['Set-CS']
p = mdb.models['Model-1'].parts['Shell']
region3=p.sets['Set-CS']
p = mdb.models['Model-1'].parts['Shell']
region4=p.sets['Set-CS']
p = mdb.models['Model-1'].parts['Shell']
region5=p.sets['Set-CS']
p = mdb.models['Model-1'].parts['Shell']
region6=p.sets['Set-CS']
p = mdb.models['Model-1'].parts['Shell']
region7=p.sets['Set-CS']
p = mdb.models['Model-1'].parts['Shell']
region8=p.sets['Set-CS']
p = mdb.models['Model-1'].parts['Shell']
region9=p.sets['Set-CS']
p = mdb.models['Model-1'].parts['Shell']
region10=p.sets['Set-CS']
p = mdb.models['Model-1'].parts['Shell']
region11=p.sets['Set-CS']
p = mdb.models['Model-1'].parts['Shell']
region12=p.sets['Set-CS']
p = mdb.models['Model-1'].parts['Shell']
region13=p.sets['Set-CS']
p = mdb.models['Model-1'].parts['Shell']
region14=p.sets['Set-CS']
compositeLayup = mdb.models['Model-1'].parts['Shell'].CompositeLayup(
name='CompositeLayup-CS', description='', elementType=SHELL,
offsetType=BOTTOM_SURFACE, symmetric=False,
thicknessAssignment=FROM_SECTION)
compositeLayup.Section(preIntegrate=OFF, integrationRule=SIMPSON,
thicknessType=UNIFORM, poissonDefinition=DEFAULT, temperature=GRADIENT,
useDensity=OFF)
compositeLayup.ReferenceOrientation(orientationType=SYSTEM,
localCsys=layupOrientation, fieldName='',
```

```
additionalRotationType=ROTATION_NONE, angle=0.0,
additionalRotationField='', axis=AXIS_1)

fp  = open('D:/temp/13inch/Layup6376/SIM/CS.txt')
words= [word.strip() for line in fp.readlines() for word in line.split(',') if
    word.strip()]
#print(", ".join(words)) # or `print(words)` if you want to print out `words`
   as a list


for i in range(0, 13):
        s=int(words[i+(i*7)])
        pn=words[i+1+(i*7)]
        mat=words[i+3+(i*7)]
        th=float(words[i+4+(i*7)])
        om=float(words[i+6+(i*7)])
        compositeLayup.CompositePly(suppressed=s, plyName=pn,
        region=region1, material=mat, thicknessType=SPECIFY_THICKNESS,
        thickness=th, orientationType=SPECIFY_ORIENT, orientationValue=om,
        additionalRotationType=ROTATION_NONE, additionalRotationField='',
        axis=AXIS_3, angle=0.0, numIntPoints=5)

#--------------------------------------------End CenterShell
   ---------------------------------------------



#Inner drop

p = mdb.models['Model-1'].parts['Shell']
session.viewports['Viewport: 1'].setValues(displayedObject=p)
layupOrientation = mdb.models['Model-1'].parts['Shell'].datums[23]
p = mdb.models['Model-1'].parts['Shell']
region1=p.sets['Set-ID']
p = mdb.models['Model-1'].parts['Shell']
region2=p.sets['Set-ID']
p = mdb.models['Model-1'].parts['Shell']
region3=p.sets['Set-ID']
p = mdb.models['Model-1'].parts['Shell']
region4=p.sets['Set-ID']
p = mdb.models['Model-1'].parts['Shell']
region5=p.sets['Set-ID']
p = mdb.models['Model-1'].parts['Shell']
region6=p.sets['Set-ID']
p = mdb.models['Model-1'].parts['Shell']
region7=p.sets['Set-ID']
p = mdb.models['Model-1'].parts['Shell']
region8=p.sets['Set-ID']
p = mdb.models['Model-1'].parts['Shell']
region9=p.sets['Set-ID']
p = mdb.models['Model-1'].parts['Shell']
region10=p.sets['Set-ID']
p = mdb.models['Model-1'].parts['Shell']
region11=p.sets['Set-ID']
p = mdb.models['Model-1'].parts['Shell']
region12=p.sets['Set-ID']
p = mdb.models['Model-1'].parts['Shell']
region13=p.sets['Set-ID']
p = mdb.models['Model-1'].parts['Shell']
region14=p.sets['Set-ID']
```

```
compositeLayup = mdb.models['Model-1'].parts['Shell'].CompositeLayup(
name='CompositeLayup-ID', description='', elementType=SHELL,
offsetType=BOTTOM_SURFACE, symmetric=False,
thicknessAssignment=FROM_SECTION)
compositeLayup.Section(preIntegrate=OFF, integrationRule=SIMPSON,
thicknessType=UNIFORM, poissonDefinition=DEFAULT, temperature=GRADIENT,
useDensity=OFF)
compositeLayup.ReferenceOrientation(orientationType=SYSTEM,
localCsys=layupOrientation, fieldName='',
additionalRotationType=ROTATION_NONE, angle=0.0,
additionalRotationField='', axis=AXIS_1)



fp  = open('D:/temp/13inch/Layup6376/SIM/ID.txt')
words= [word.strip() for line in fp.readlines() for word in line.split(',') if word.strip()]
#print(", ".join(words)) # or `print(words)` if you want to print out `words` as a list


for i in range(0, 13):
        s=int(words[i+(i*7)])
        pn=words[i+1+(i*7)]
        mat=words[i+3+(i*7)]
        th=float(words[i+4+(i*7)])
        om=float(words[i+6+(i*7)])
        compositeLayup.CompositePly(suppressed=s, plyName=pn,
        region=region1, material=mat, thicknessType=SPECIFY_THICKNESS,
        thickness=th, orientationType=SPECIFY_ORIENT, orientationValue=om,
        additionalRotationType=ROTATION_NONE, additionalRotationField='',
        axis=AXIS_3, angle=0.0, numIntPoints=5)

#------------------------------------End InnerDrop--------------------------------------


# REGION InnerBead
layupOrientation = mdb.models['Model-1'].parts['Shell'].datums[23]
p = mdb.models['Model-1'].parts['Shell']
region1=p.sets['Set-IB']
p = mdb.models['Model-1'].parts['Shell']
region2=p.sets['Set-IB']
p = mdb.models['Model-1'].parts['Shell']
region3=p.sets['Set-IB']
p = mdb.models['Model-1'].parts['Shell']
region4=p.sets['Set-IB']
p = mdb.models['Model-1'].parts['Shell']
region5=p.sets['Set-IB']
p = mdb.models['Model-1'].parts['Shell']
region6=p.sets['Set-IB']
p = mdb.models['Model-1'].parts['Shell']
region7=p.sets['Set-IB']
p = mdb.models['Model-1'].parts['Shell']
region8=p.sets['Set-IB']
p = mdb.models['Model-1'].parts['Shell']
region9=p.sets['Set-IB']
p = mdb.models['Model-1'].parts['Shell']
region10=p.sets['Set-IB']
p = mdb.models['Model-1'].parts['Shell']
```

```
region11=p.sets['Set-IB']
p = mdb.models['Model-1'].parts['Shell']
region12=p.sets['Set-IB']
p = mdb.models['Model-1'].parts['Shell']
region13=p.sets['Set-IB']
p = mdb.models['Model-1'].parts['Shell']
region14=p.sets['Set-IB']
compositeLayup = mdb.models['Model-1'].parts['Shell'].CompositeLayup(
name='CompositeLayup-IB', description='', elementType=SHELL,
offsetType=BOTTOM_SURFACE, symmetric=False,
thicknessAssignment=FROM_SECTION)
compositeLayup.Section(preIntegrate=OFF, integrationRule=SIMPSON,
thicknessType=UNIFORM, poissonDefinition=DEFAULT, temperature=GRADIENT,
useDensity=OFF)
compositeLayup.ReferenceOrientation(orientationType=SYSTEM,
localCsys=layupOrientation, fieldName='',
additionalRotationType=ROTATION_NONE, angle=0.0,
additionalRotationField='', axis=AXIS_1)



fp = open('D:/temp/13inch/Layup6376/SIM/IB.txt')
words= [word.strip() for line in fp.readlines() for word in line.split(',') if
    word.strip()]
#print(", ".join(words)) # or `print(words)` if you want to print out `words`
    as a list


for i in range(0, 13):
        s=int(words[i+(i*7)])
        pn=words[i+1+(i*7)]
        mat=words[i+3+(i*7)]
        th=float(words[i+4+(i*7)])
        om=float(words[i+6+(i*7)])
        compositeLayup.CompositePly(suppressed=s, plyName=pn,
        region=region1, material=mat, thicknessType=SPECIFY_THICKNESS,
        thickness=th, orientationType=SPECIFY_ORIENT, orientationValue=om,
        additionalRotationType=ROTATION_NONE, additionalRotationField='',
        axis=AXIS_3, angle=0.0, numIntPoints=5)
#---------------------------------------------End InnerBead
    ---------------------------------------------


#InneFlange

p = mdb.models['Model-1'].parts['Shell']
session.viewports['Viewport: 1'].setValues(displayedObject=p)
layupOrientation = mdb.models['Model-1'].parts['Shell'].datums[23]
p = mdb.models['Model-1'].parts['Shell']
region1=p.sets['Set-IF']
p = mdb.models['Model-1'].parts['Shell']
region2=p.sets['Set-IF']
p = mdb.models['Model-1'].parts['Shell']
region3=p.sets['Set-IF']
p = mdb.models['Model-1'].parts['Shell']
region4=p.sets['Set-IF']
p = mdb.models['Model-1'].parts['Shell']
region5=p.sets['Set-IF']
p = mdb.models['Model-1'].parts['Shell']
region6=p.sets['Set-IF']
```

```
p = mdb.models['Model-1'].parts['Shell']
region7=p.sets['Set-IF']
p = mdb.models['Model-1'].parts['Shell']
region8=p.sets['Set-IF']
p = mdb.models['Model-1'].parts['Shell']
region9=p.sets['Set-IF']
p = mdb.models['Model-1'].parts['Shell']
region10=p.sets['Set-IF']
p = mdb.models['Model-1'].parts['Shell']
region11=p.sets['Set-IF']
p = mdb.models['Model-1'].parts['Shell']
region12=p.sets['Set-IF']
p = mdb.models['Model-1'].parts['Shell']
region13=p.sets['Set-IF']
p = mdb.models['Model-1'].parts['Shell']
region14=p.sets['Set-IF']
compositeLayup = mdb.models['Model-1'].parts['Shell'].CompositeLayup(
name='CompositeLayup-IF', description='', elementType=SHELL,
offsetType=BOTTOM_SURFACE, symmetric=False,
thicknessAssignment=FROM_SECTION)
compositeLayup.Section(preIntegrate=OFF, integrationRule=SIMPSON,
thicknessType=UNIFORM, poissonDefinition=DEFAULT, temperature=GRADIENT,
useDensity=OFF)
compositeLayup.ReferenceOrientation(orientationType=SYSTEM,
localCsys=layupOrientation, fieldName='',
additionalRotationType=ROTATION_NONE, angle=0.0,
additionalRotationField='', axis=AXIS_1)


fp = open('D:/temp/13inch/Layup6376/SIM/IF.txt')
words= [word.strip() for line in fp.readlines() for word in line.split(',') if word.strip()]
#print(", ".join(words)) # or `print(words)` if you want to print out `words` as a list


for i in range(0, 13):
        s=int(words[i+(i*7)])
        pn=words[i+1+(i*7)]
        mat=words[i+3+(i*7)]
        th=float(words[i+4+(i*7)])
        om=float(words[i+6+(i*7)])
        compositeLayup.CompositePly(suppressed=s, plyName=pn,
        region=region1, material=mat, thicknessType=SPECIFY_THICKNESS,
        thickness=th, orientationType=SPECIFY_ORIENT, orientationValue=om,
        additionalRotationType=ROTATION_NONE, additionalRotationField='',
        axis=AXIS_3, angle=0.0, numIntPoints=5)
#--------------------------------------------End InnerFlange--------------------------------------------

p = mdb.models['Model-1'].parts['Shell']
session.viewports['Viewport: 1'].setValues(displayedObject=p)

a = mdb.models['Model-1'].rootAssembly
a.regenerate()
```

Abaqus Post-script

```
"""
userscript_odb.py
```

```
"""
#
#from abaqus import *
from abaqusConstants import *
import odbAccess
from odbAccess import *
import __main__
import operator
import sys
import math

#
# S T A R T
#


# Open .odb results file
odbName = 'Job-layup.odb'
myOdb = openOdb(odbName,readOnly=True)


#Create a variable that refers to the last frame of the first step.
step = myOdb.steps['Step-Turn']
step_brake=myOdb.steps['Step-Brake']

lastFramebrake = myOdb.steps['Step-Brake'].frames[-1]
lastFrame = myOdb.steps['Step-Turn'].frames[-1]
displacement=lastFrame.fieldOutputs['U']
displacement_brake=lastFramebrake.fieldOutputs['U']
#Create a variable that refers to the displacement 'U' in the last frame of the frist step.

STRAINENERGY=step.historyRegions['Assembly ASSEMBLY'].historyOutputs['ALLSE']
STRAINENERGY_brake=step_brake.historyRegions['Assembly ASSEMBLY'].historyOutputs['ALLSE']

#Create a variable that refers to the node located at the flange of the rim (Nodes= NODEID-1)
NODE443=myOdb.rootAssembly.instances['SHELL-1'].nodes[442]

NODE443Displacement=displacement.getSubset(region=NODE443).values[0]
N443Disp_brake=displacement_brake.getSubset(region=NODE443).values[0]

u_turn=NODE443Displacement.data[2]*NODE443Displacement.data[2]+NODE443Displacement.data[1]*NODE443Displacement.data[1]+NODE443Displacement.data[0]*NODE443Displacement.data[0]
u_turn=sqrt(u_turn)
u_brake=N443Disp_brake.data[2]*N443Disp_brake.data[2]+N443Disp_brake.data[1]*N443Disp_brake.data[1]+N443Disp_brake.data[0]*N443Disp_brake.data[0]
u_brake=sqrt(u_brake)

step1=STRAINENERGY.data[0]
step2=STRAINENERGY_brake.data[0]
st_turn=step1[1]
st_brake=step2[1]
```

```
# Write the angle in the output parameters file
paramsFile = open ('user_params.txt','w')
paramsFile.write('Tot_strain_turn'+'\t'+ str(st_turn)+'\n'+'Tot_strain_brake'+
    '\t'+ str(st_brake)+'\n'+'U3_flange_turn'+'\t'+ str(u_turn)+'\n'+'
    U3_flange_brake'+'\t'+str(u_brake))
paramsFile.close()
```

A.4 Topology Optimization Setup

This section will follow all the steps done in Abaqus to setup the FE-model used for the TO in Tosca Structures, together with all steps needed to set up the TO in Tosca Structures. The set-up description will be structured and go through the following items outlined in bold blue text:

- **Part**
- Properties
- Assembly
- **Step**
- **Interactions**
- Loads
- **Mesh**
  - Rim Shell
  - Design space for Rim Center
- **Optimization Task**
  - Design Response
  - Objective Functions
  - Constraints
  - Geometric Restrictions

A.4.1 Part

The part procedure is the same as in FEA-validation Setup, except the model only have two parts, the design space for the rim center and the shell geometry for the rim shell. The design space and the rim shell is modeled as 9th part to reduce computing time. Rim center and rim shell is found in Figure A.4.1.

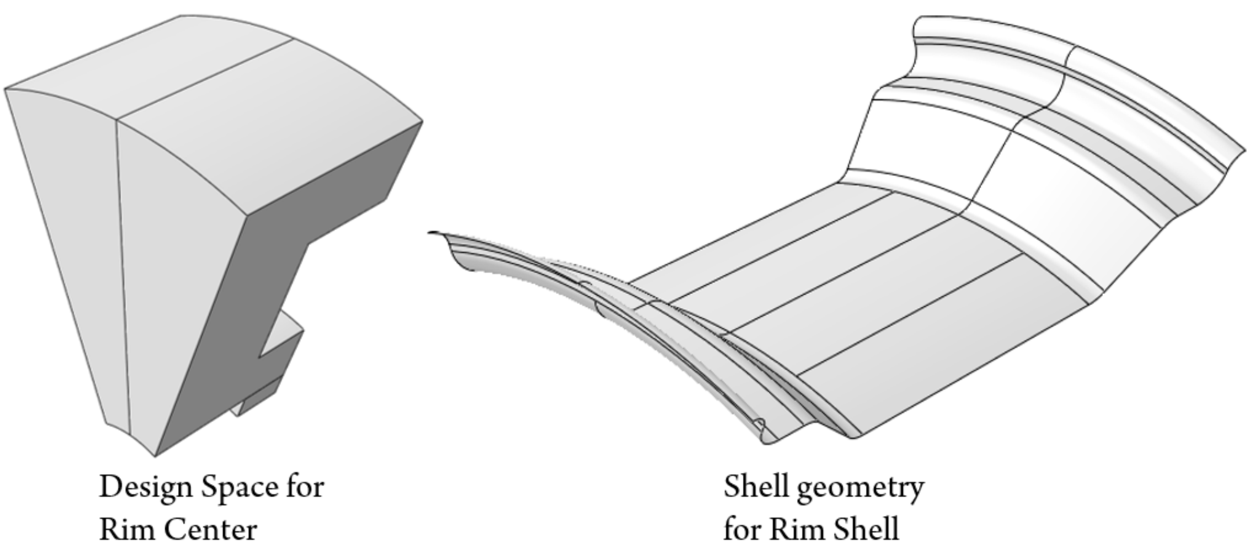

Figure A.4.1

A.4.2 Step

The step procedure is same as described for the material optimization, Appendix A.3.2

A.4.3 Interactions

The interactions are similar to the interactions for the material optimization, see Appendix A.3.2. In Figure A.4.2 the interaction set-up is presented.

Figure A.4.2

A.4.4 Mesh

Rim Shell

The mesh for the rim shell was made of 4-node doubly curved thin shell elements with reduced integration, hourglass control and finite membrane strains. The element shape is combination of free quad and structured quad.See Figure A.4.3 for details related to mesh.

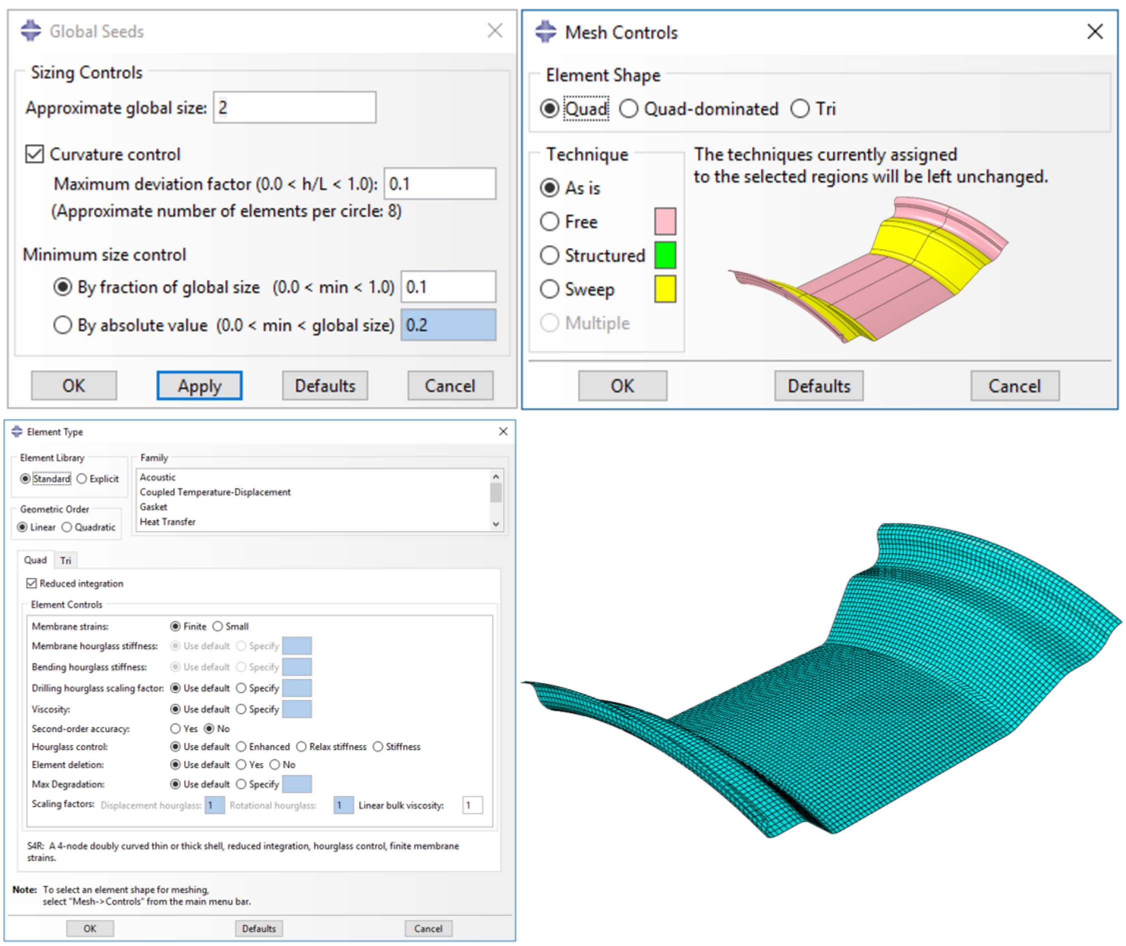

Figure A.4.3

The mesh for the design space was made of 8-node linear brick elements witch reduced integration and hourglass control. Linear brick element was used instead of tet elements which save computing time as fever elements is needed for same mesh size. The element shape was quad and a combination of structured (green) and sweep (yellow) . The global size was set to 2 with a curvature control of 0.1. See Figure A.4.4 for details related to mesh.

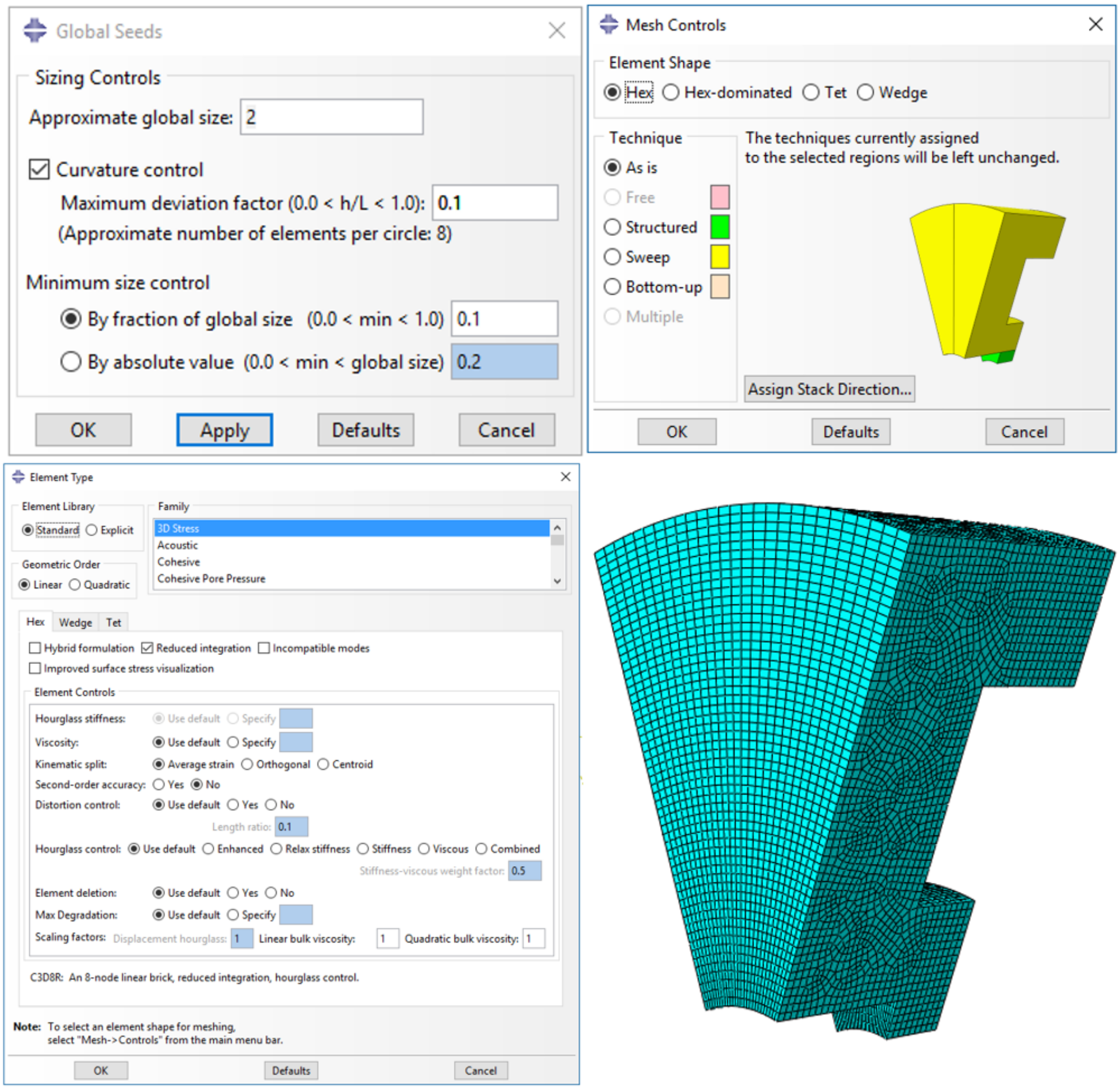

Figure A.4.4

A.4.5 Optimization Task

For the optimization task the whole model was set as region with sensitive-based algorithm. No loads or boundary conditions was set as frozen.

Design Response

Two different design response was created. Strain Energy for the whole model and weight for the design space. See Figure A.4.5 for design response set-up.

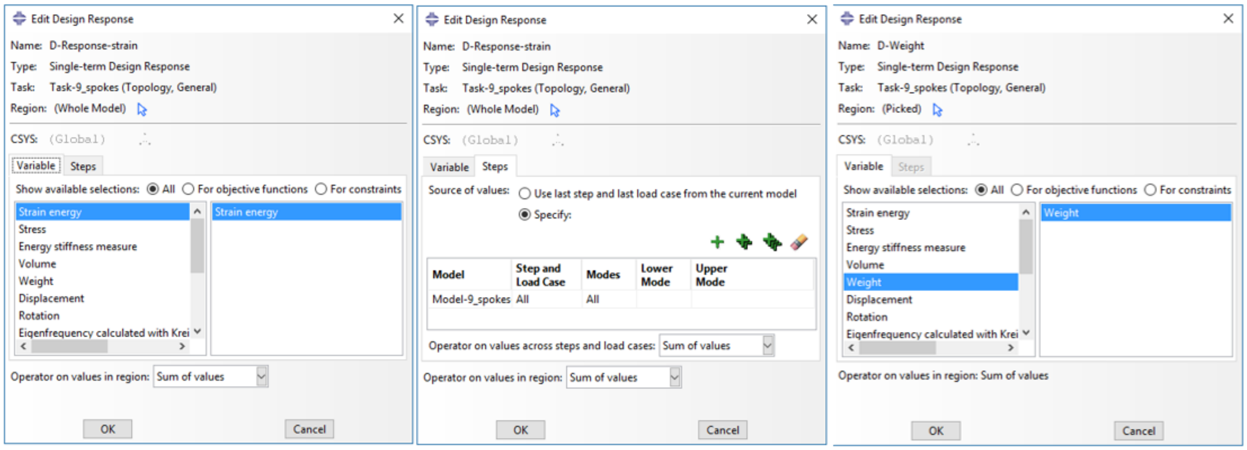

Figure A.4.5

Objective Functions

The design response strain energy is set as objective function and was set to be minimized.The design response strain energy was set to be the sum of both load case. This means that Tosca would treat both load case equally, and will prioritize stiffness equally for both load case. See Figure A.4.6 for design objective set-up.

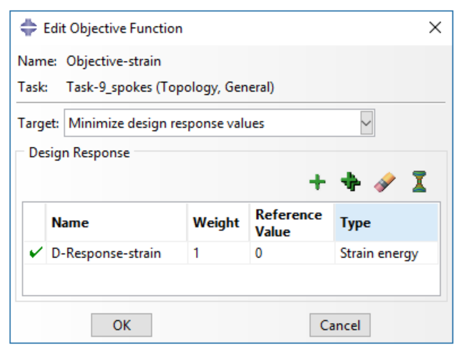

Figure A.4.6

Constraints

The weight design response was set as constraint. It was set as a weight target where the weight should less or equal to 150 gram. See Figure A.4.7 for constraint set-up. The design weight target of rim center was less than 1.0 kilogram, which means 111 gram for a 9Th part of the rim. The final target was set to 150 gram, as this gave a more machinable design. The design was then tweaked during regenerating to be less than 1 kilogram.

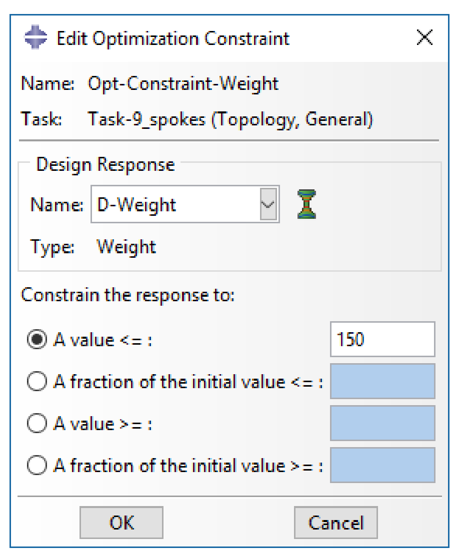

Figure A.4.7

Five geometric restrictions was added to the TO model. The center lock region and the rim shell was frozen. A planar symmetry was added to the design space to ensure that the design is performing the same for both brake and acceleration loads. The planar symmetry set-up is found in Figure A.4.8 To have a 3-axis kind of production constraint, forging constraint was added in both axial directions. Forging set-up is found in Figure A.4.9

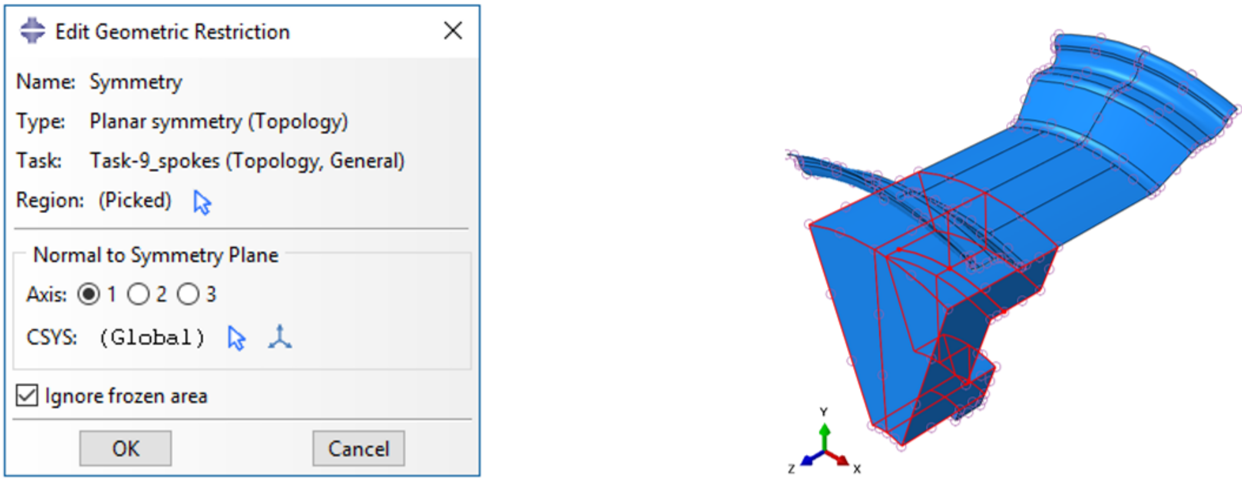

Figure A.4.8

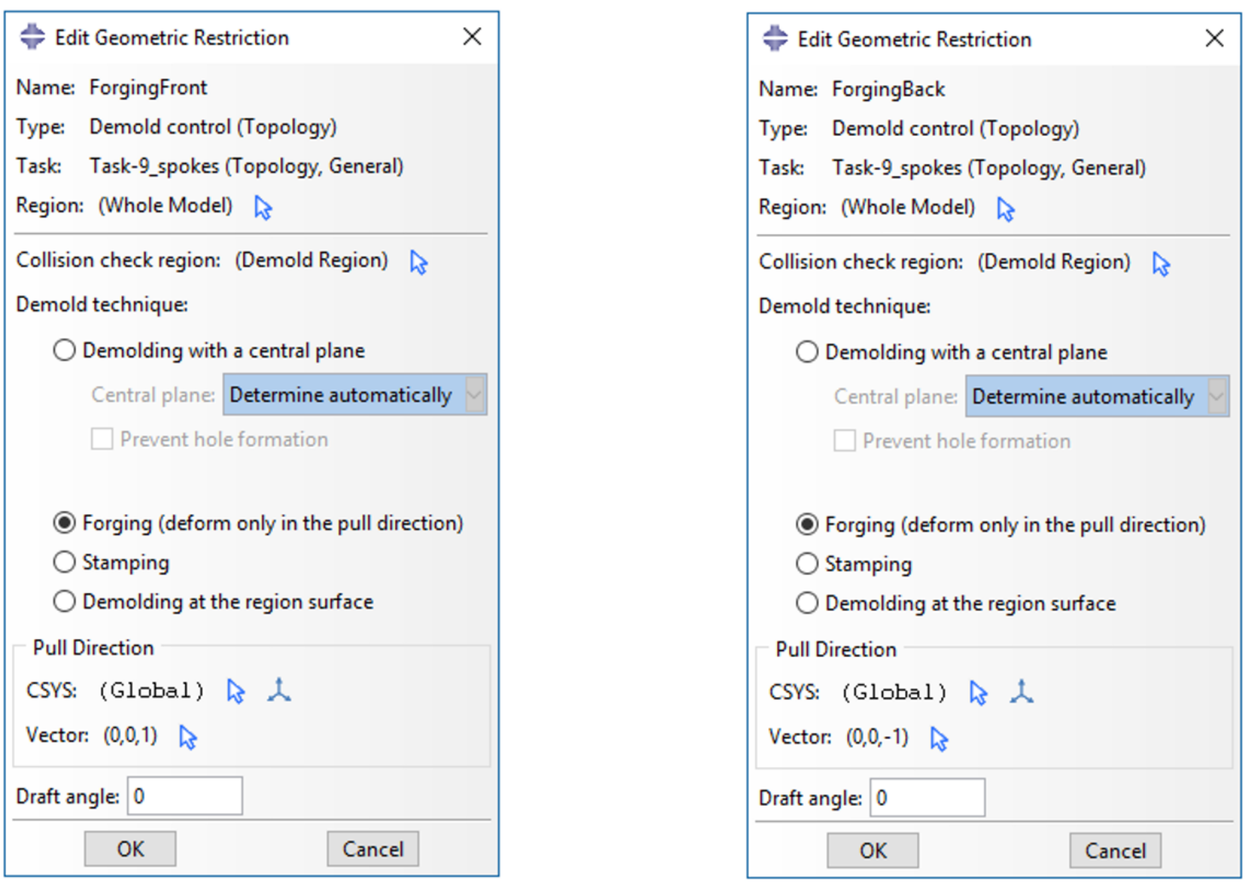

Figure A.4.9

A.5 FEM validation Results

A.5.1 Cornering @ 110km/h

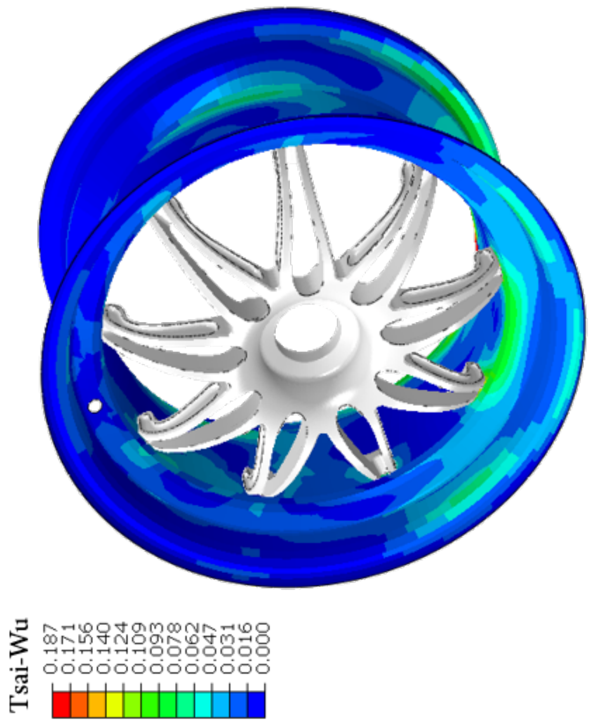

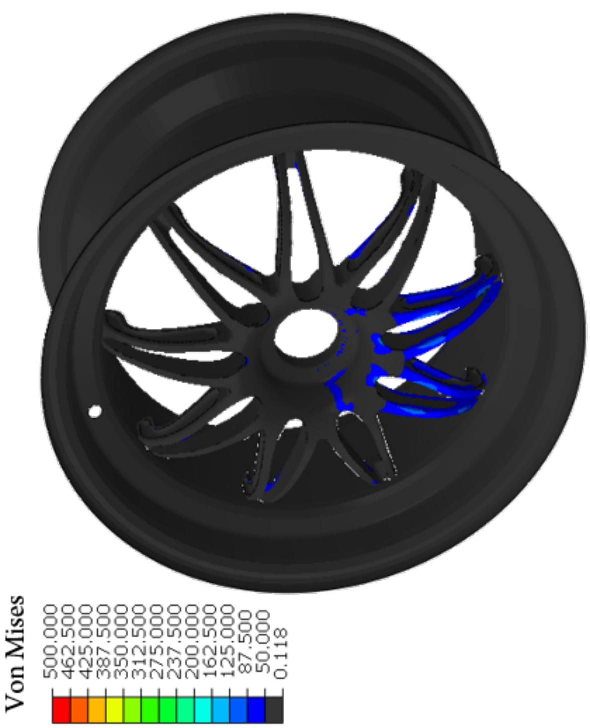

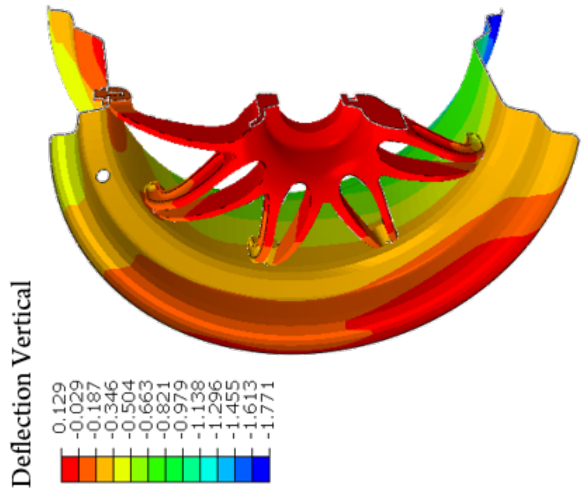

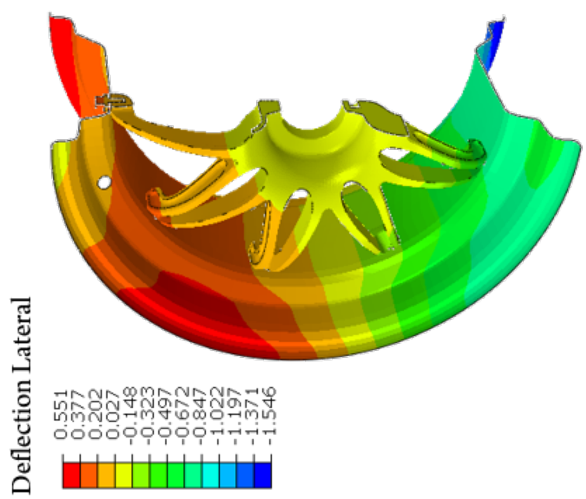

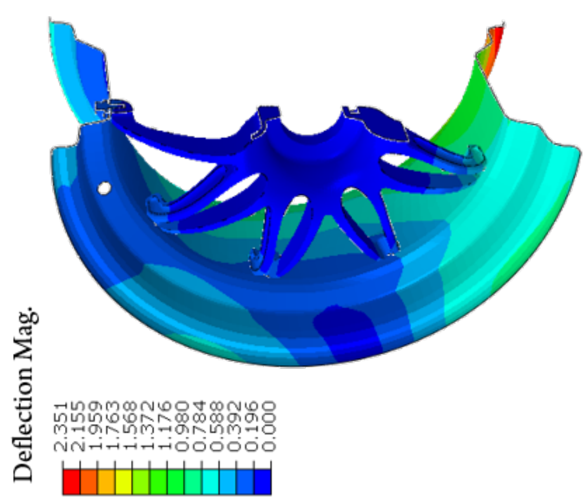

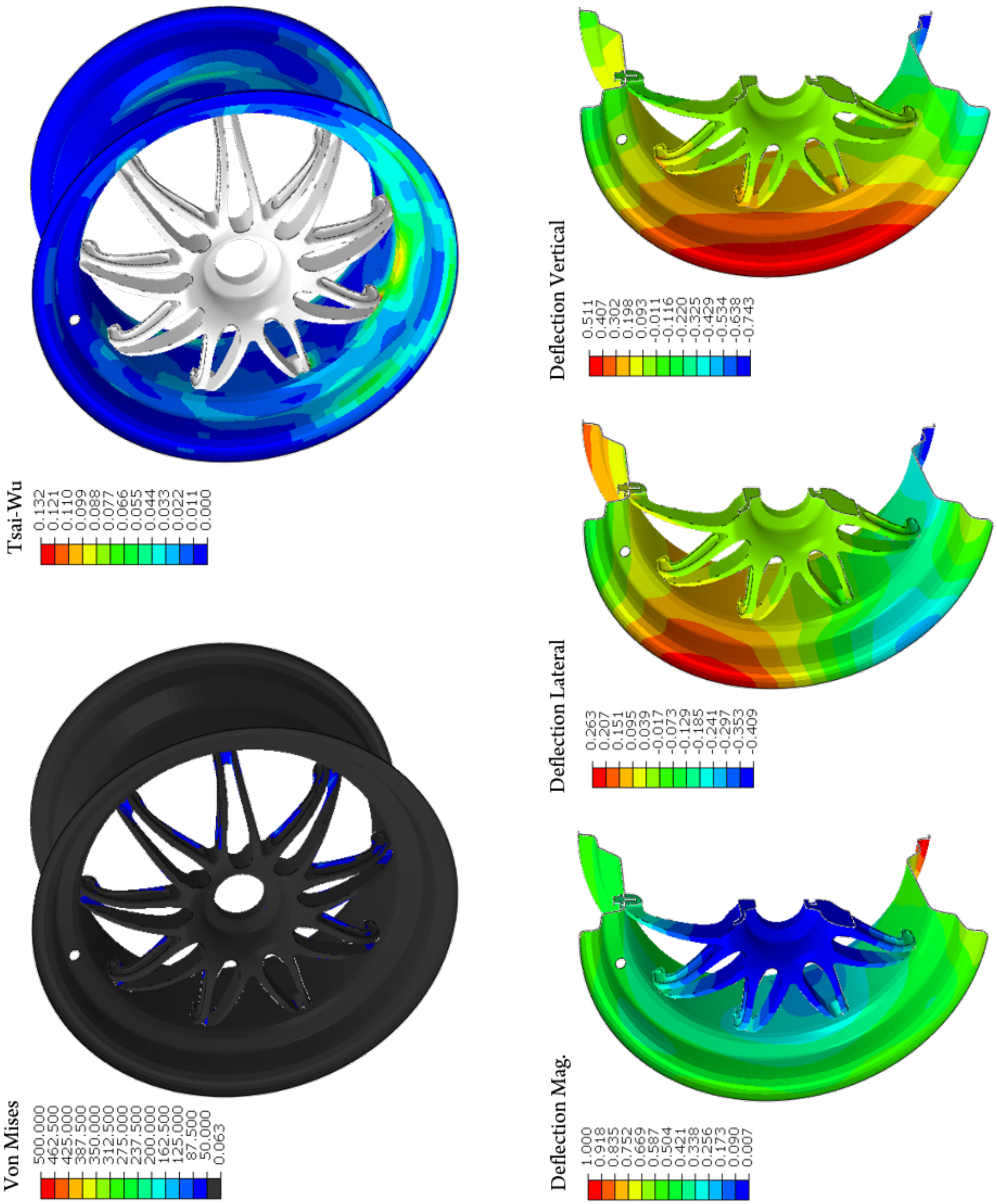
Von Mises
500.000
462.500
425.000
387.500
350.000
312.500
275.000
237.500
200.000
162.500
125.000
87.500
50.000
0.063
Tsai-Wu
0.132
0.121
0.110
0.099
0.088
0.077
0.066
0.055
0.044
0.033
0.022
0.011
0.000
Deflection Mag.
1.000
0.918
0.835
0.752
0.669
0.587
0.504
0.421
0.338
0.256
0.173
0.090
0.007
Deflection Lateral
0.263
0.207
0.151
0.095
0.039
-0.017
-0.073
-0.129
-0.185
-0.241
-0.297
-0.353
-0.409
Deflection Vertical
0.511
0.407
0.302
0.198
0.093
-0.011
-0.116
-0.220
-0.325
-0.429
-0.534
-0.638
-0.743

A.5.3 3G BUMP

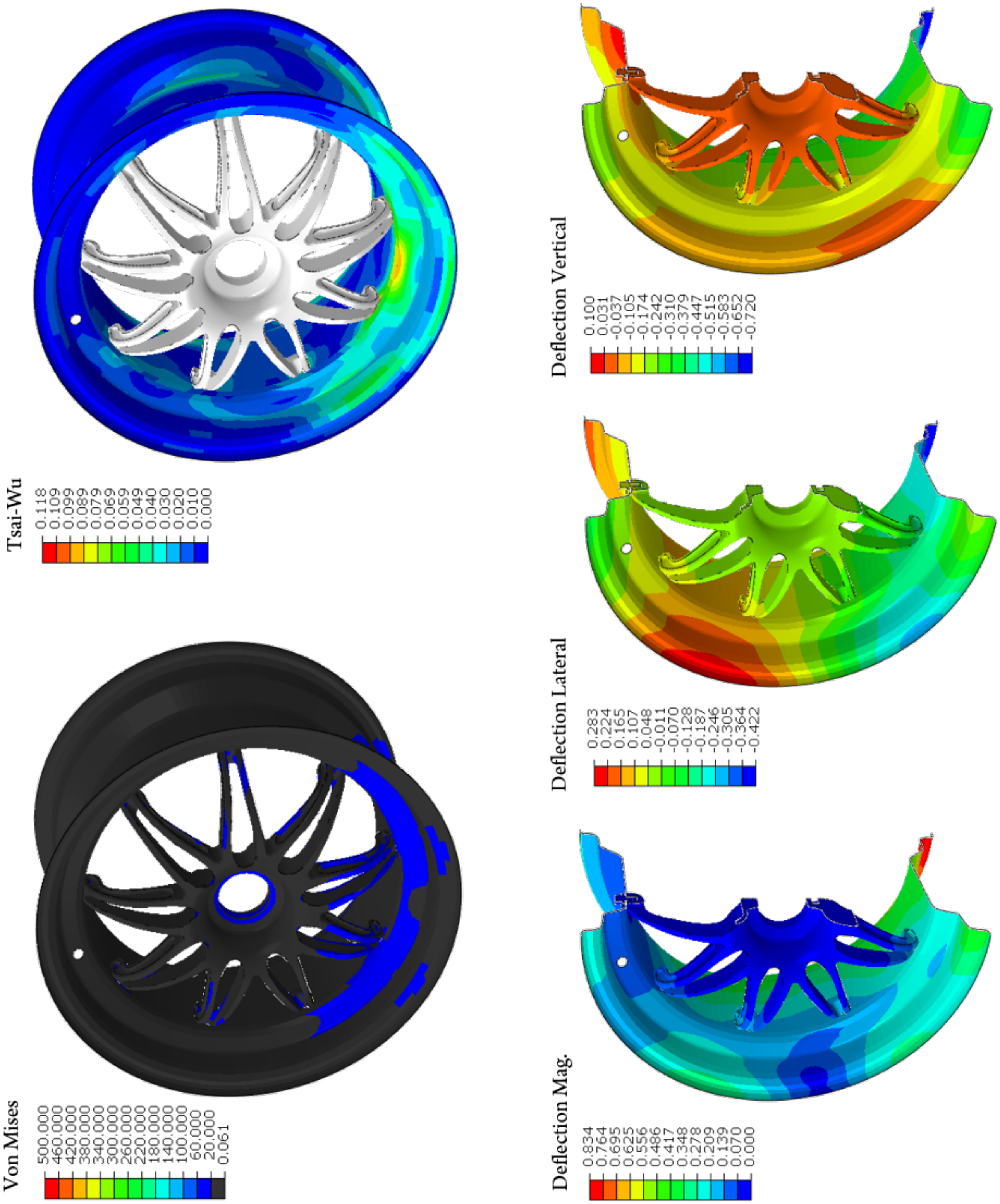

Tsai-Wu
0.118
0.109
0.099
0.089
0.079
0.069
0.059
0.049
0.040
0.030
0.020
0.010
0.000
Von Mises
500.000
460.000
420.000
380.000
340.000
300.000
260.000
220.000
180.000
140.000
100.000
60.000
20.000
0.061
Deflection Vertical
0.100
0.031
-0.037
-0.105
-0.174
-0.242
-0.310
-0.379
-0.447
-0.515
-0.583
-0.652
-0.720
Deflection Lateral
0.283
0.224
0.165
0.107
0.048
-0.011
-0.070
-0.128
-0.187
-0.246
-0.305
-0.364
-0.422
Deflection Mag.
0.834
0.764
0.695
0.625
0.556
0.486
0.417
0.348
0.278
0.209
0.139
0.070
0.000

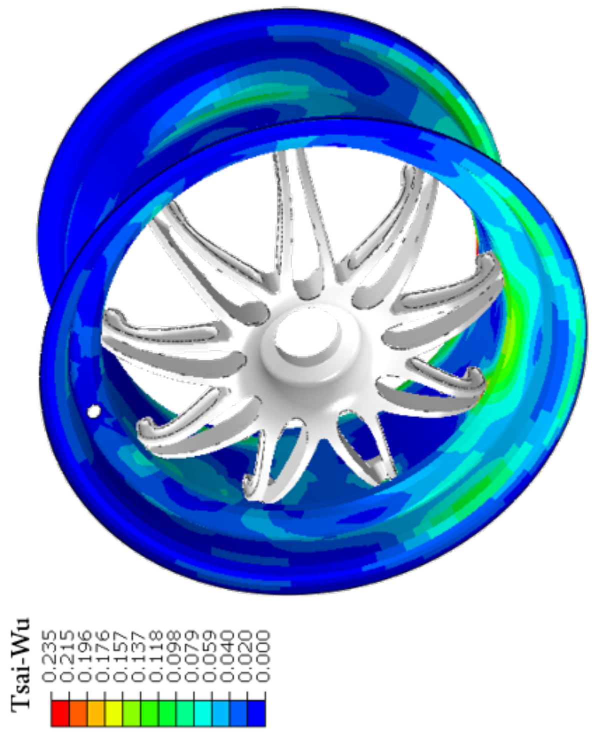
Tsai-Wu
0.235
0.215
0.196
0.176
0.157
0.137
0.118
0.098
0.079
0.059
0.040
0.020
0.000

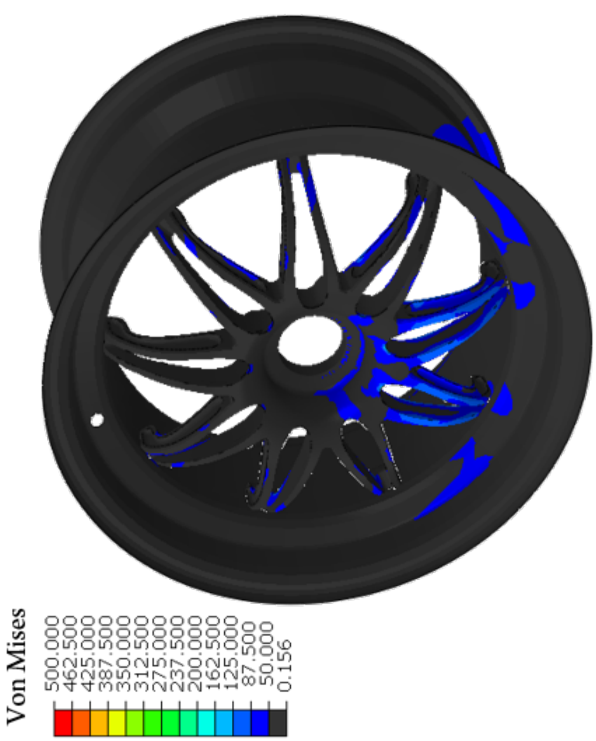
Von Mises
500.000
462.500
425.000
387.500
350.000
312.500
275.000
237.500
200.000
162.500
125.000
87.500
50.000
0.156

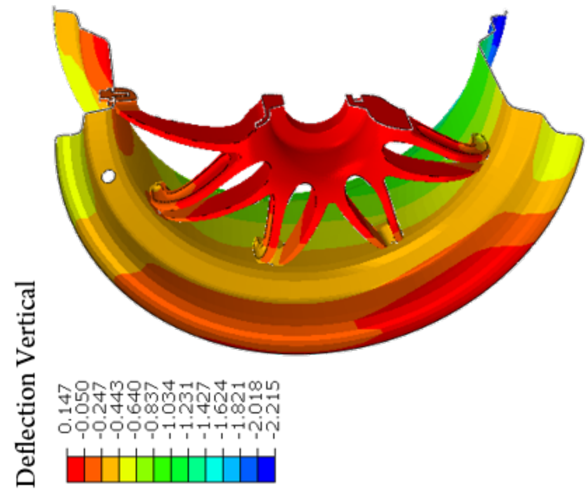
Deflection Vertical
0.147
-0.050
-0.247
-0.443
-0.640
-0.837
-1.034
-1.231
-1.427
-1.624
-1.821
-2.018
-2.215

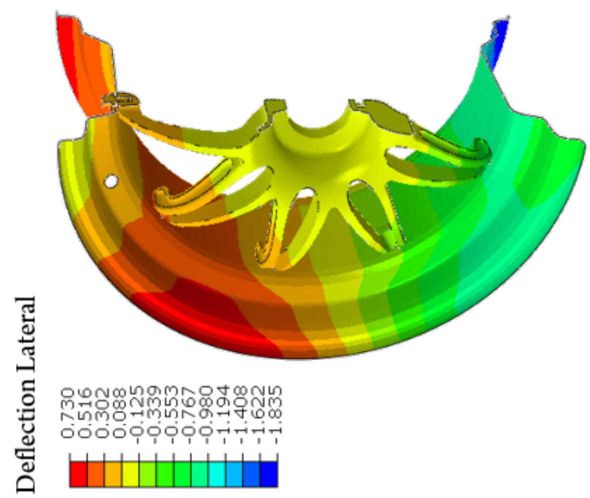
Deflection Lateral
0.730
0.516
0.302
0.088
-0.125
-0.339
-0.553
-0.767
-0.980
-1.194
-1.408
-1.622
-1.835

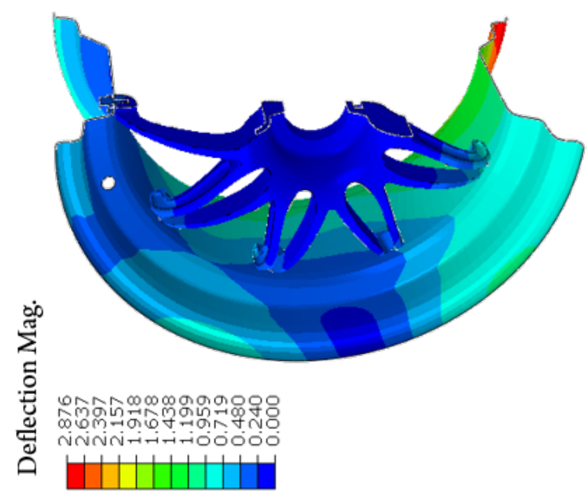
Deflection Mag.
2.876
2.637
2.397
2.157
1.918
1.678
1.438
1.199
0.959
0.719
0.480
0.240
0.000

A.5.5 2G bump + brake @ 110km/h

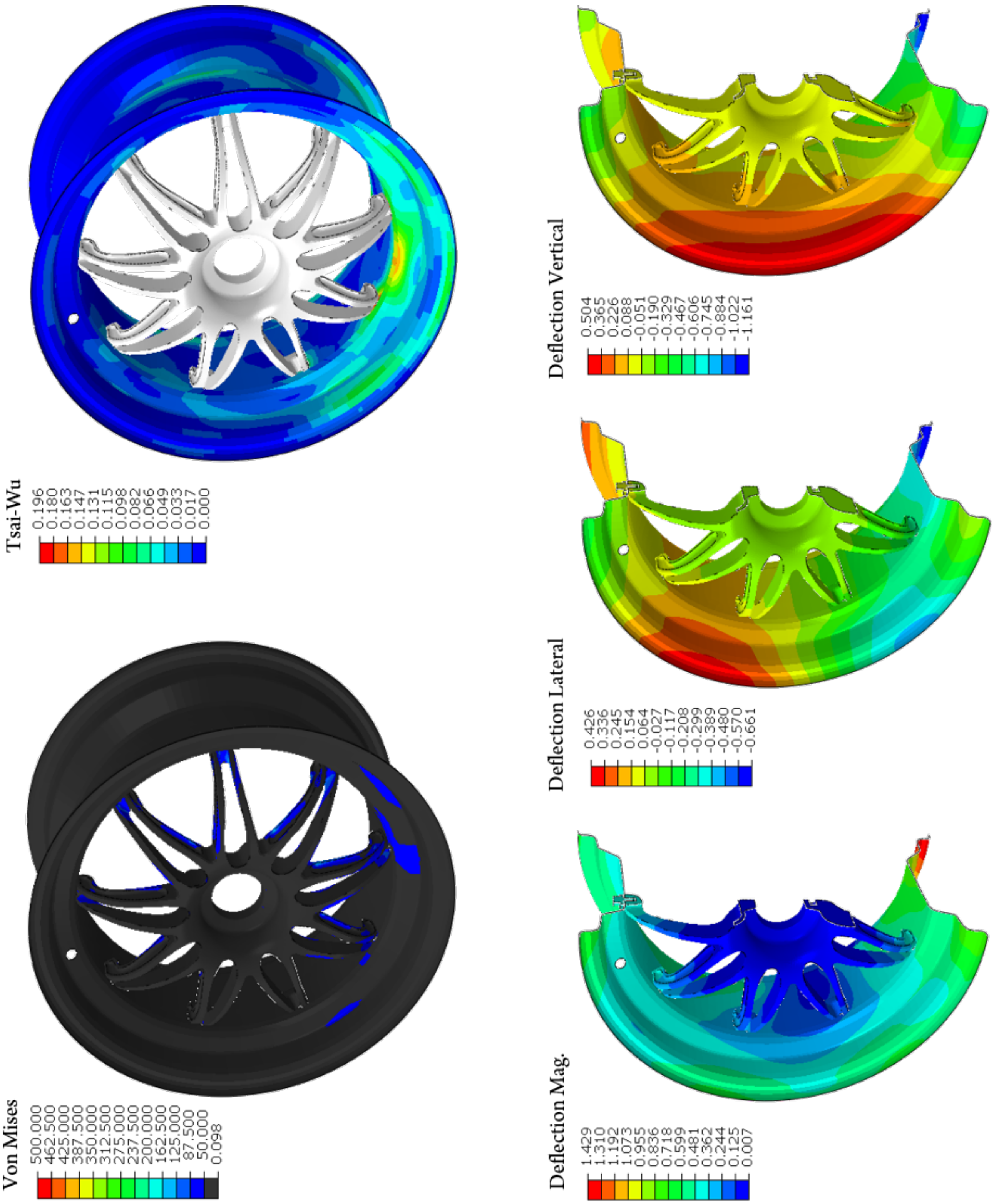

A.5.6 Inflation Pressure 1 bar

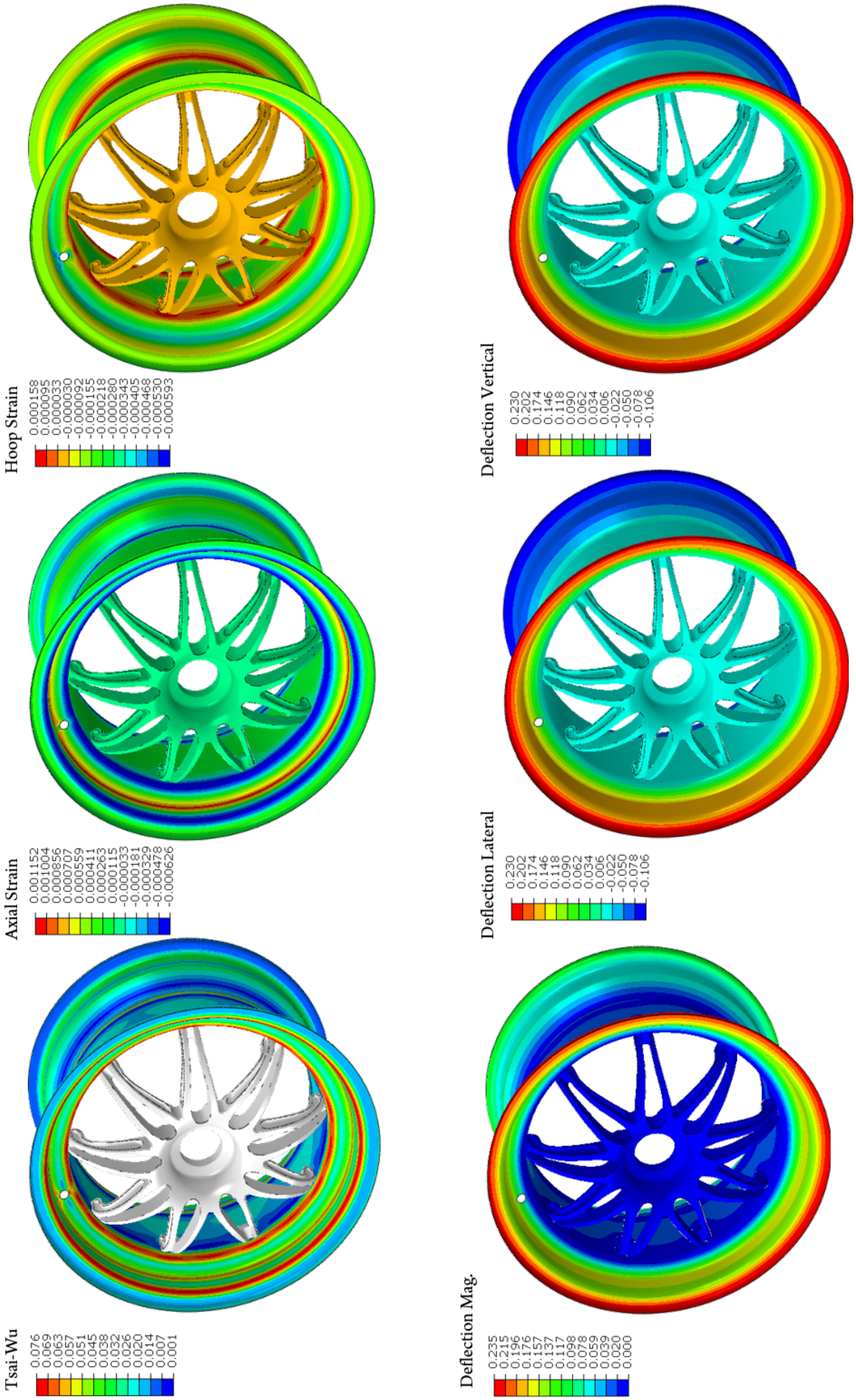

A.5.7 Pretension effects

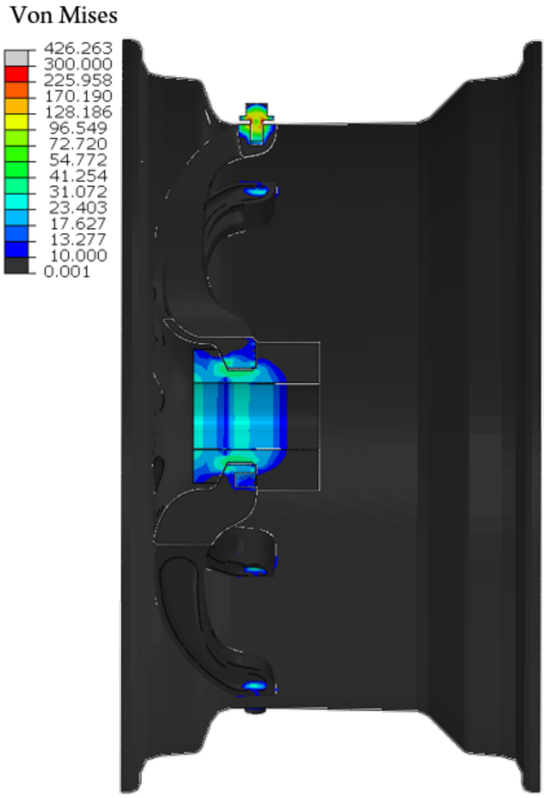

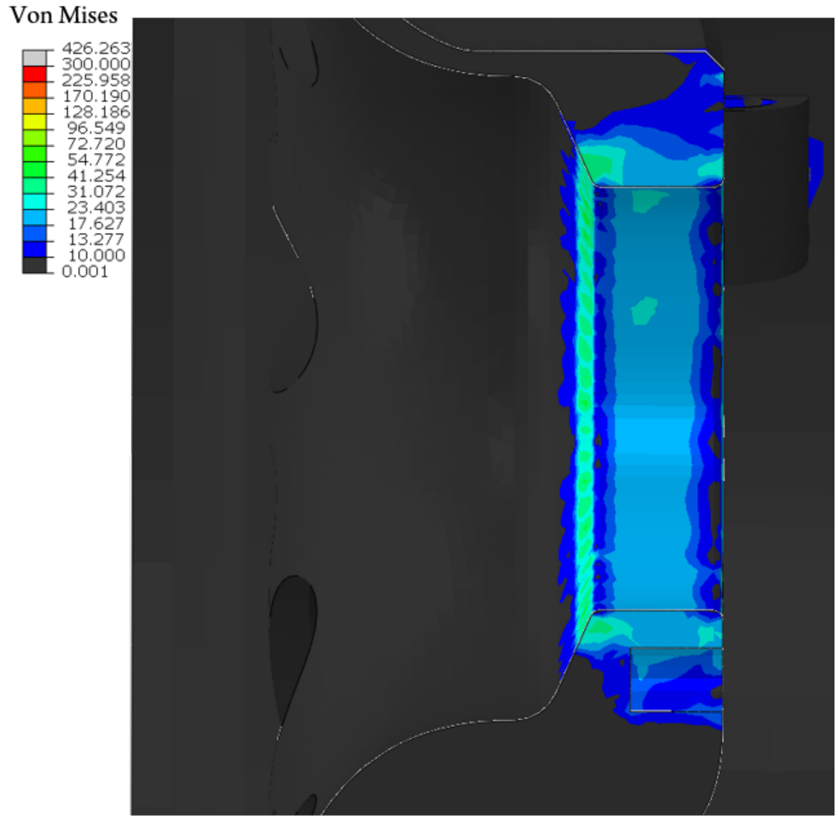

Close up of pretension effect of center -lock on Rim Center

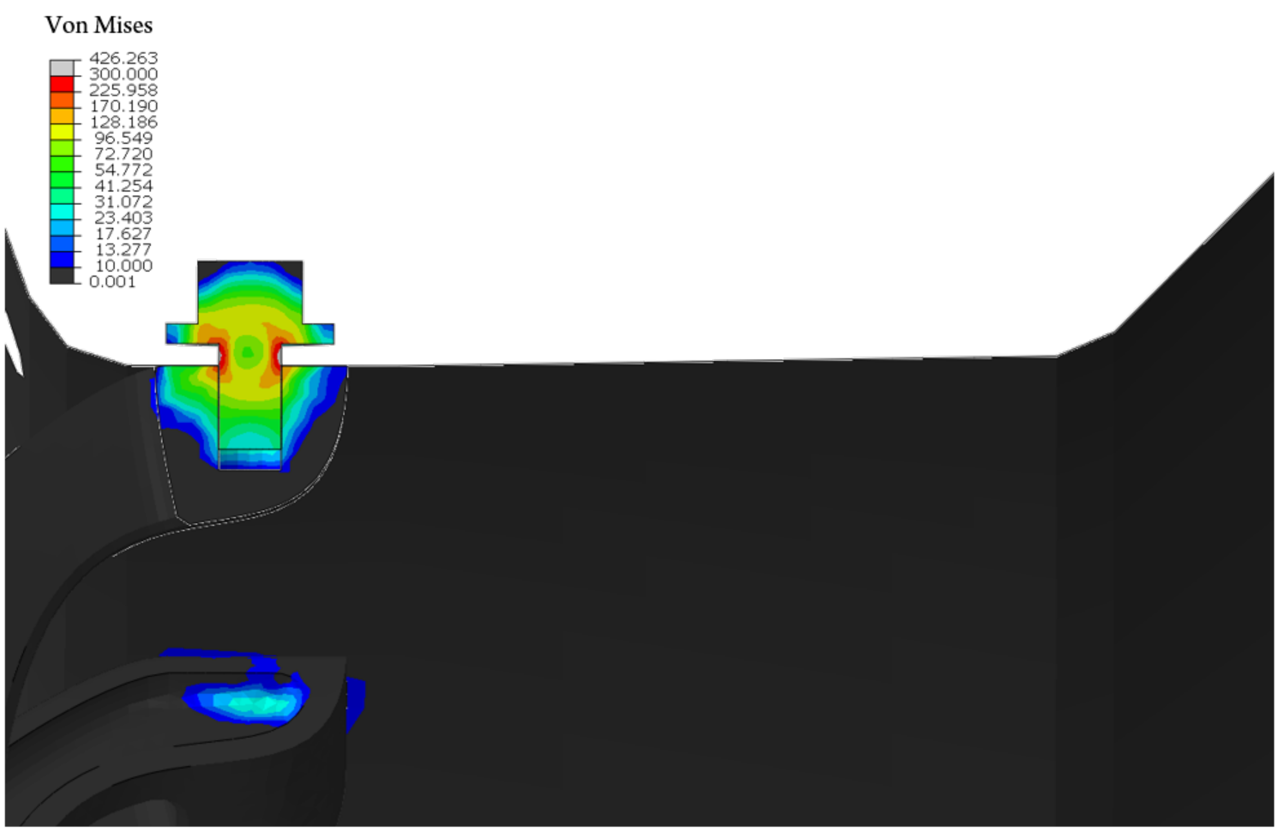

Close up of pretension effect of bolts on Rim Center

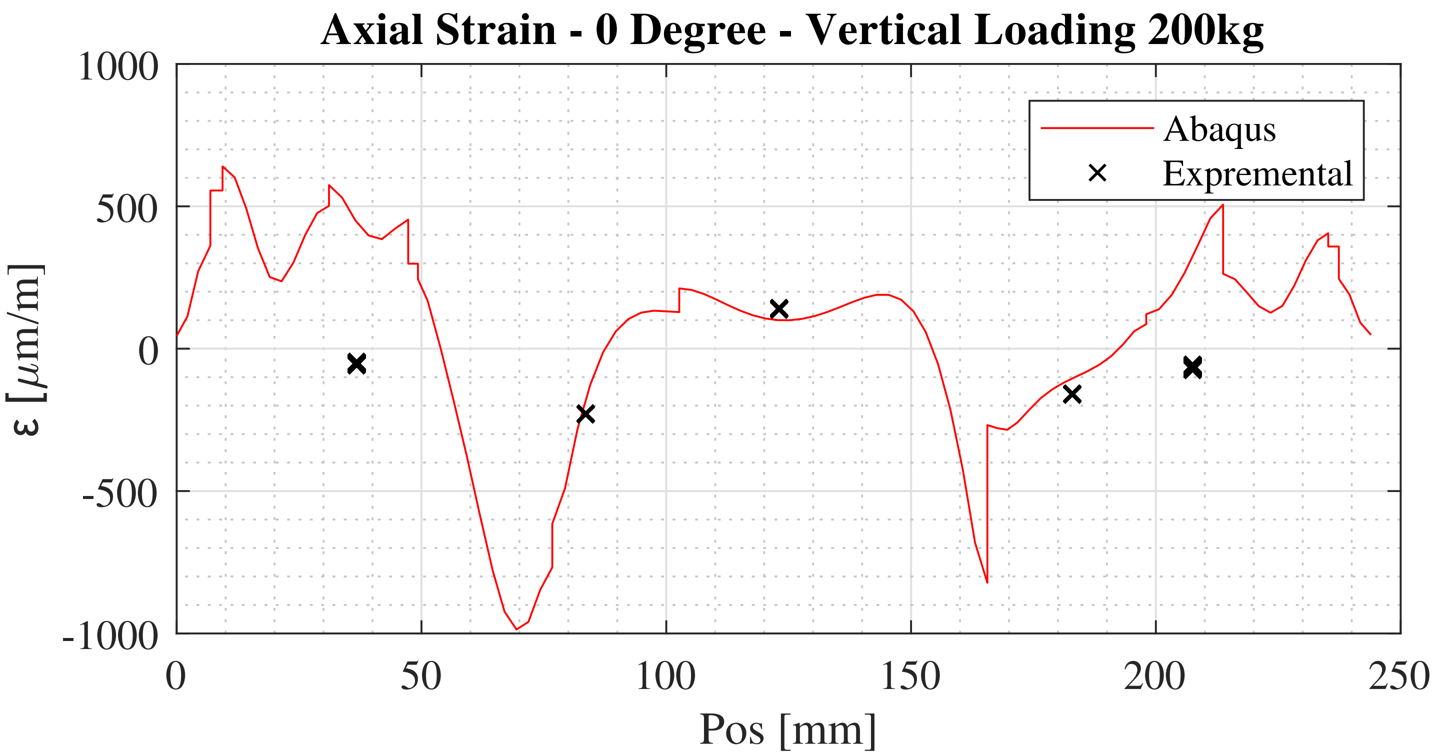
Axial Strain - 0 Degree - Vertical Loading 200kg
Abaqus
Exprementally
1000
500
0
-500
-1000
0
50
100
150
200
250
Pos [mm]
ε [μm/m]

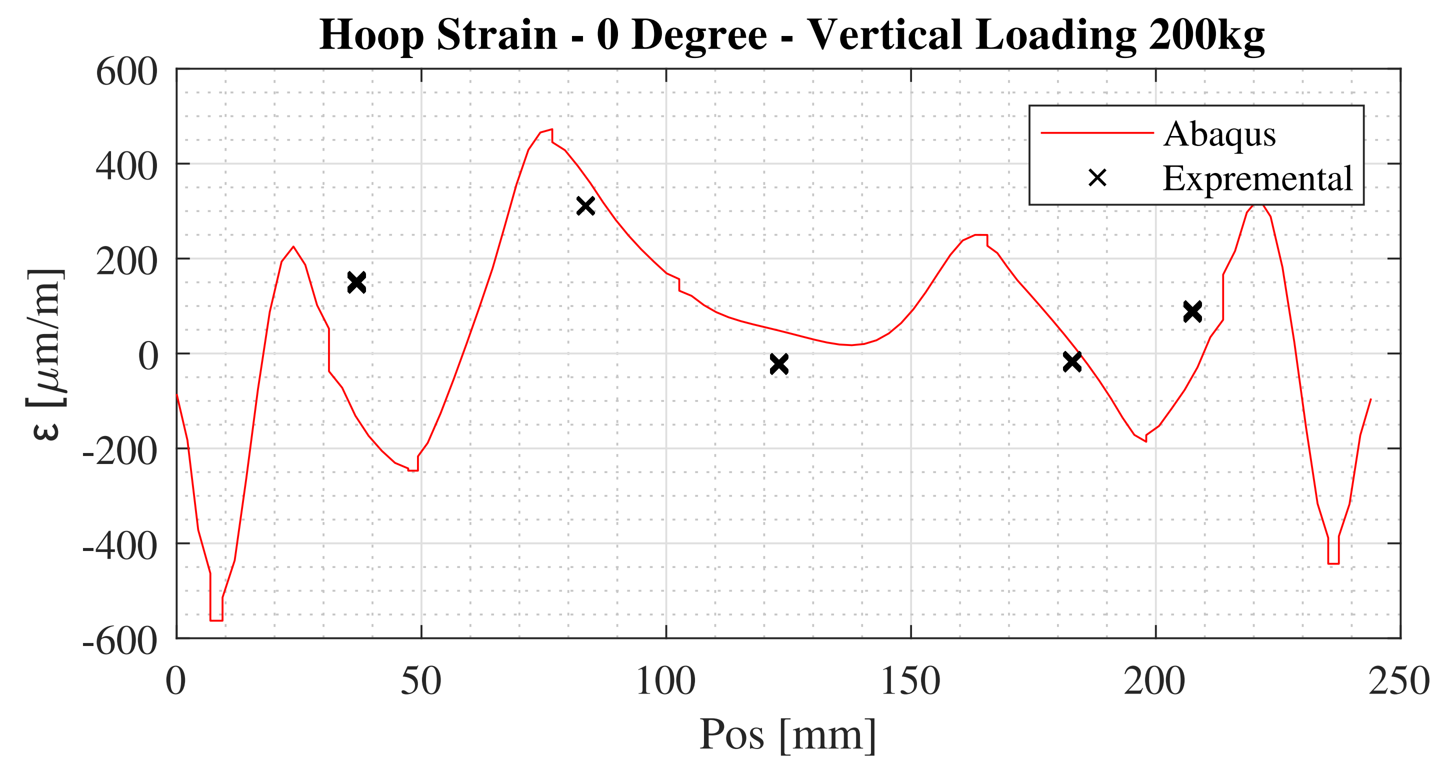
Hoop Strain - 0 Degree - Vertical Loading 200kg
Abaqus
Exprementally
600
400
200
0
-200
-400
-600
0
50
100
150
200
250
Pos [mm]
ε [μm/m]

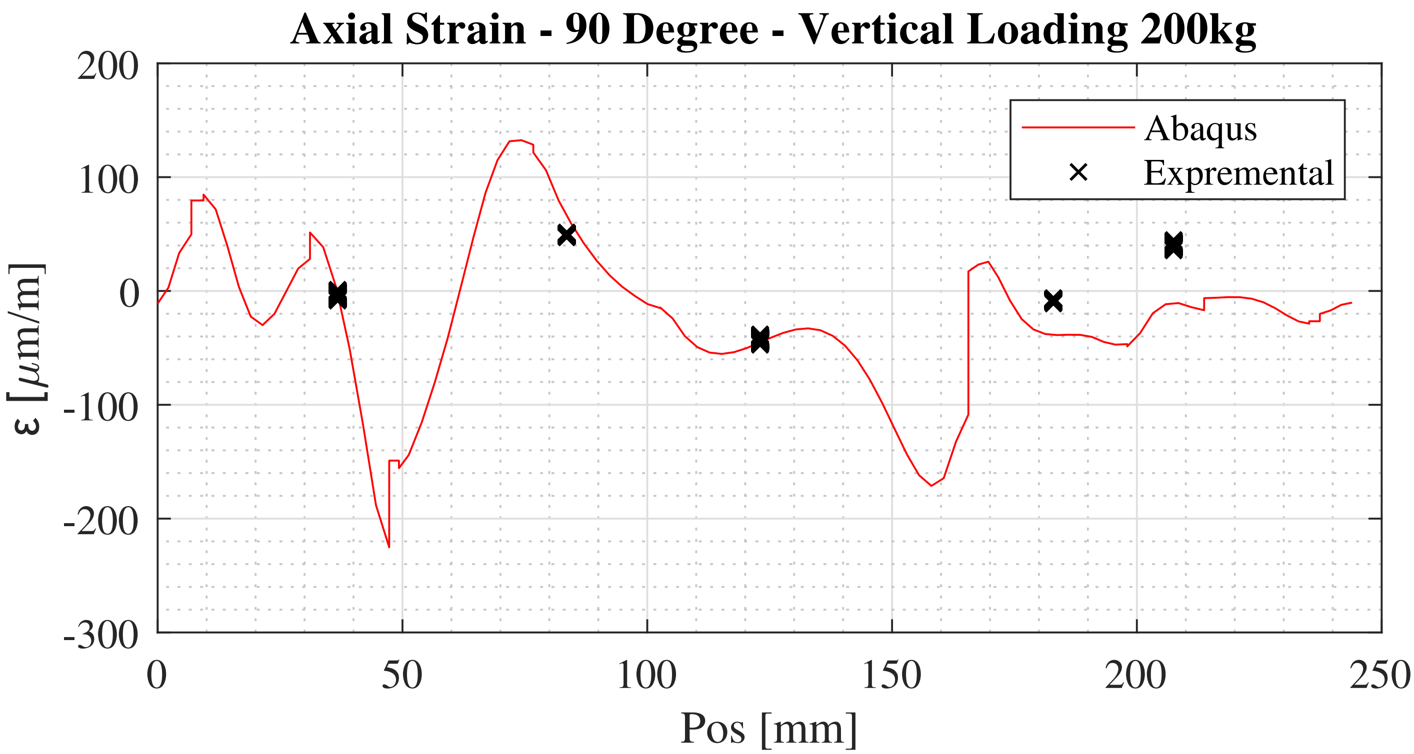

Axial Strain - 90 Degree - Vertical Loading 200kg
200
100
0
-100
-200
-300
ε [μm/m]
0
50
100
150
200
250
Pos [mm]
Abaqus
Exprementa l

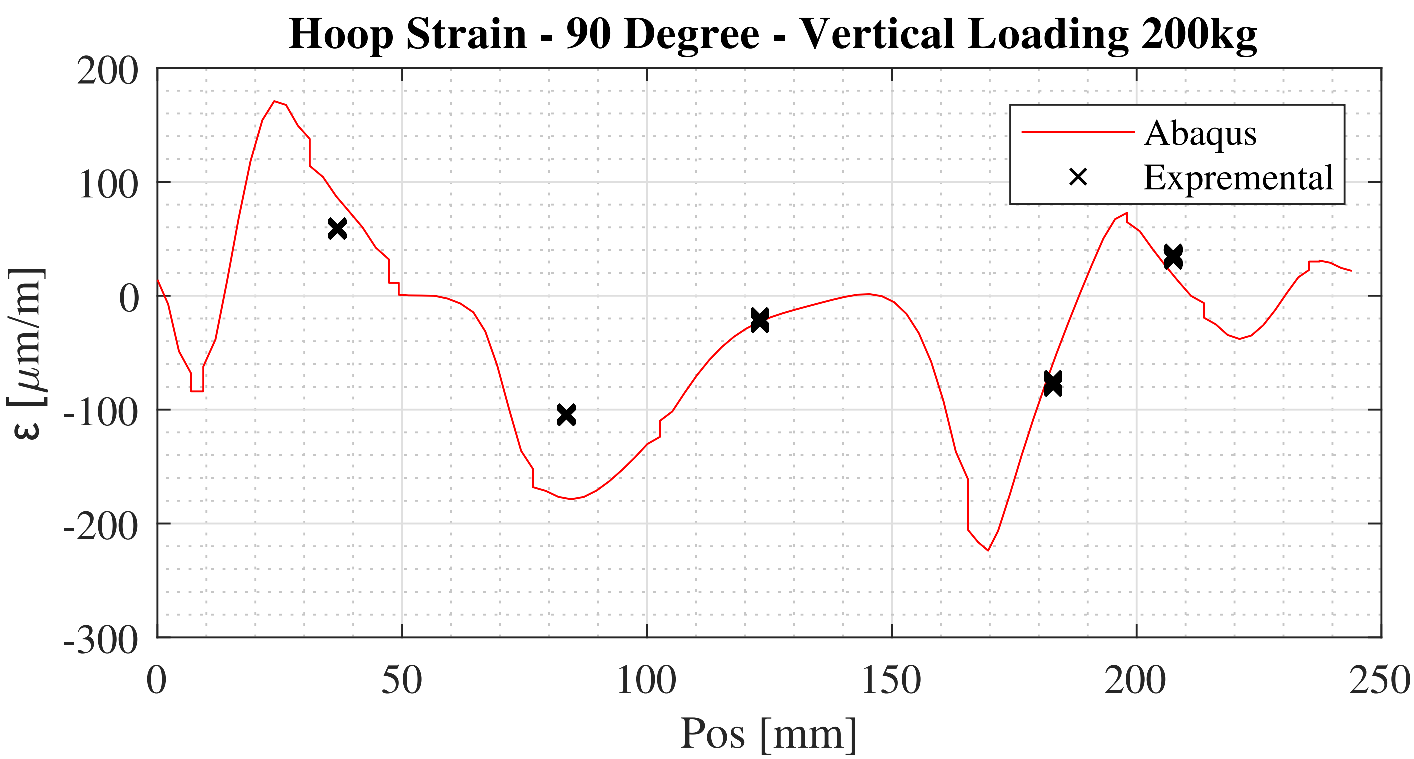

Hoop Strain - 90 Degree - Vertical Loading 200kg
200
100
0
-100
-200
-300
ε [μm/m]
0
50
100
150
200
250
Pos [mm]
Abaqus
Exprementa l

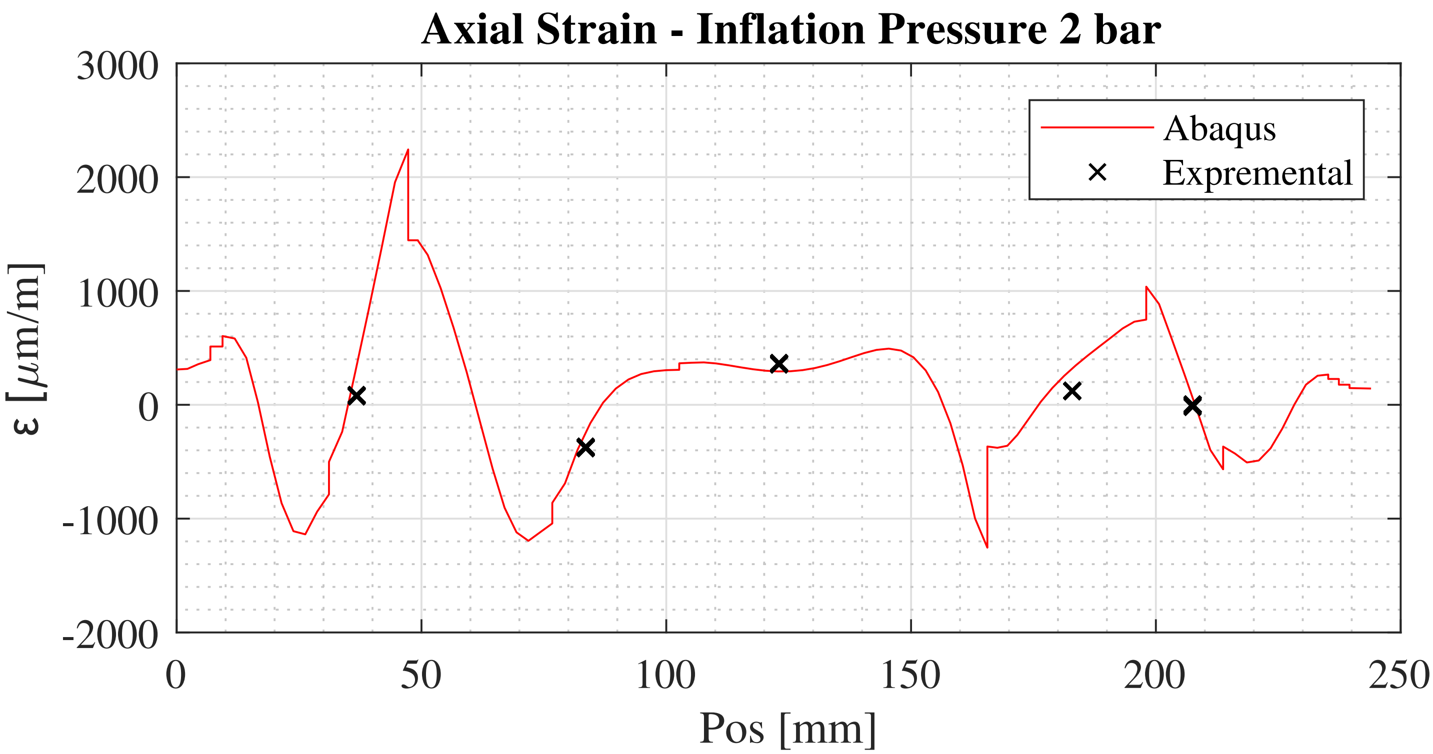
Axial Strain - Inflation Pressure 2 bar
Abaqus
Exprememental
ε [μm/m]
3000
2000
1000
0
-1000
-2000
0
50
100
150
200
250
Pos [mm]

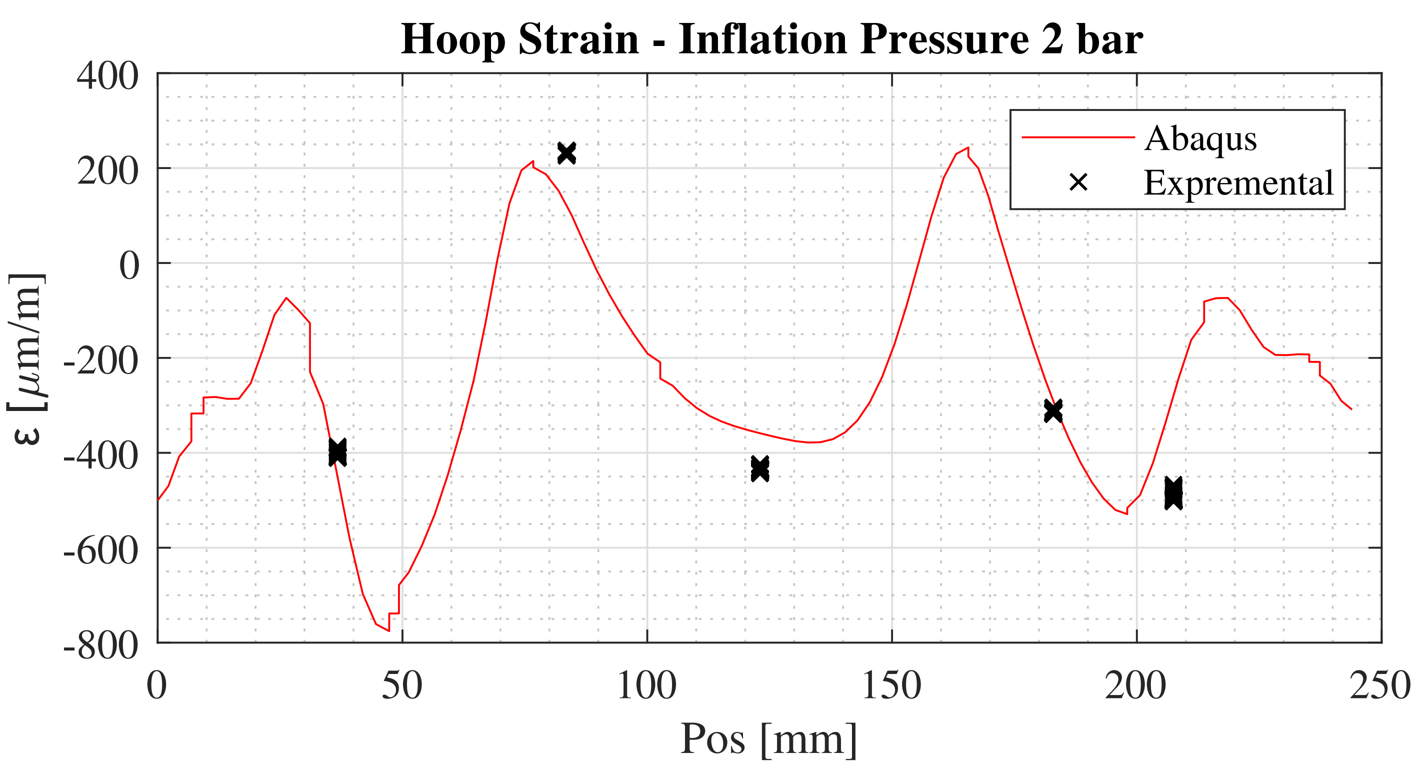
Hoop Strain - Inflation Pressure 2 bar
Abaqus
Exprememental
ε [μm/m]
400
200
0
-200
-400
-600
-800
0
50
100
150
200
250
Pos [mm]

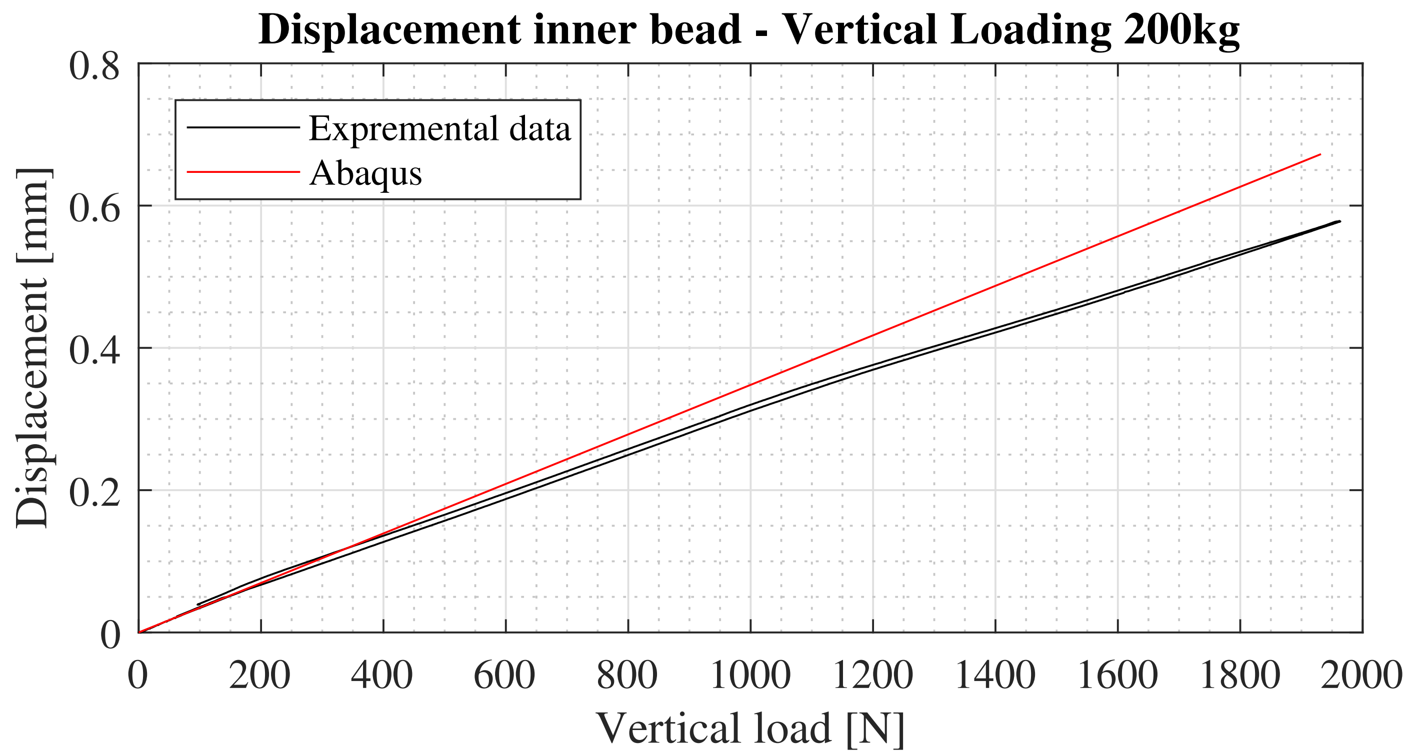
Displacement inner bead - Vertical Loading 200kg
Expremental data
Abaqus
Displacement [mm]
0.8
0.6
0.4
0.2
0
0
200
400
600
800
1000
1200
1400
1600
1800
2000
Vertical load [N]

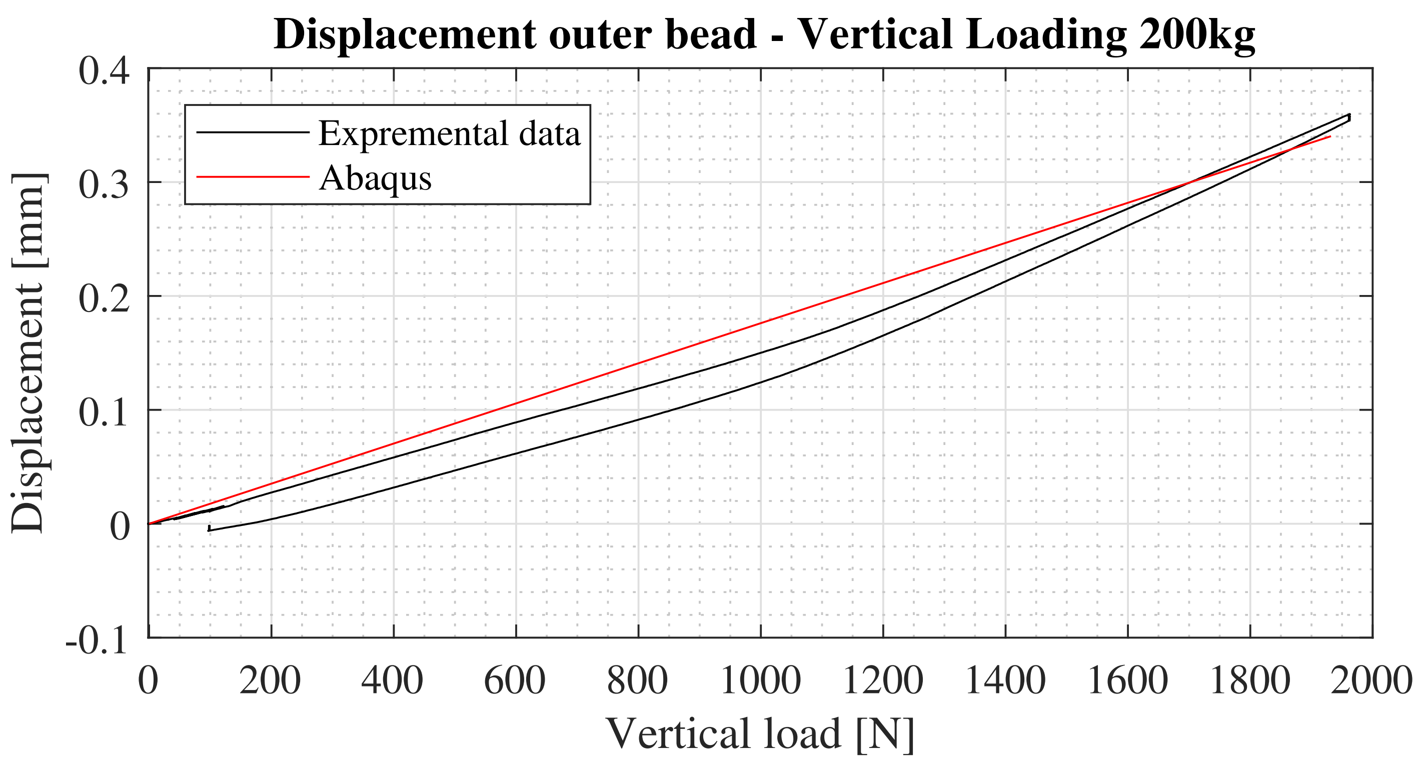
Displacement outer bead - Vertical Loading 200kg
Expremental data
Abaqus
Displacement [mm]
0.4
0.3
0.2
0.1
0
-0.1
0
200
400
600
800
1000
1200
1400
1600
1800
2000
Vertical load [N]

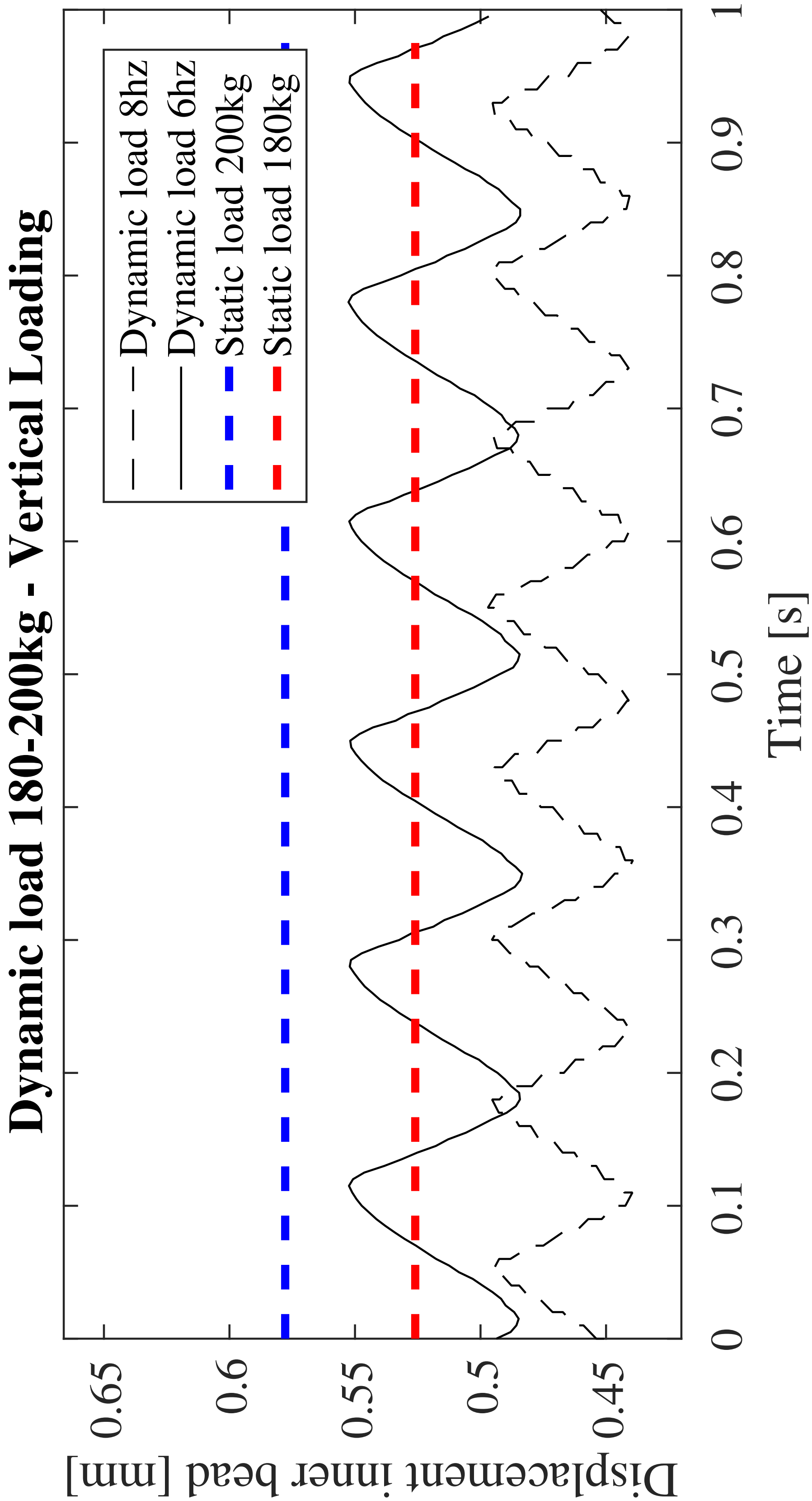

Dynamic load 180-200kg - Vertical Loading
Dynamic load 8hz
Dynamic load 6hz
Static load 200kg
Static load 180kg
Displacement inner bead [mm]
Time [s]
0.65
0.6
0.55
0.5
0.45
0
0.1
0.2
0.3
0.4
0.5
0.6
0.7
0.8
0.9
1

A.7 Reaction Forces on tire - estimated from log data - Half Endurance

The reaction forces on the tire was estimated from damper-position data, accelerometer-data and total mass of car with driver. Lateral and longitudinal forces was balanced by the normal forces working on each tire. The log-data was from testing at Værnes of the 2016 car Gnist.

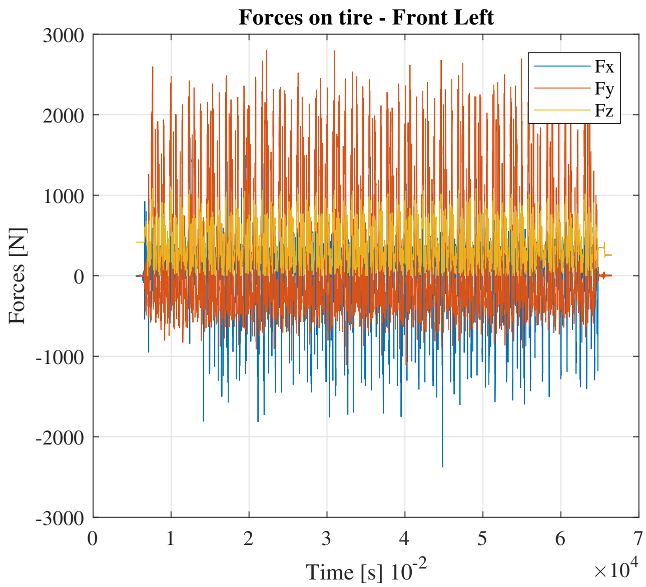

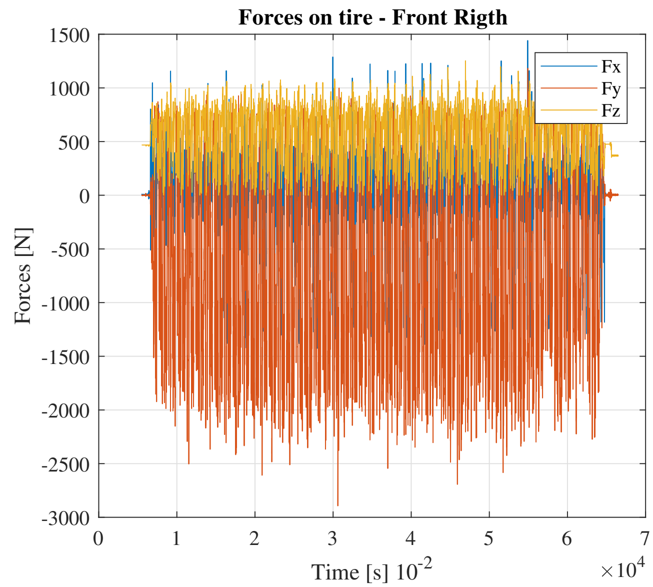

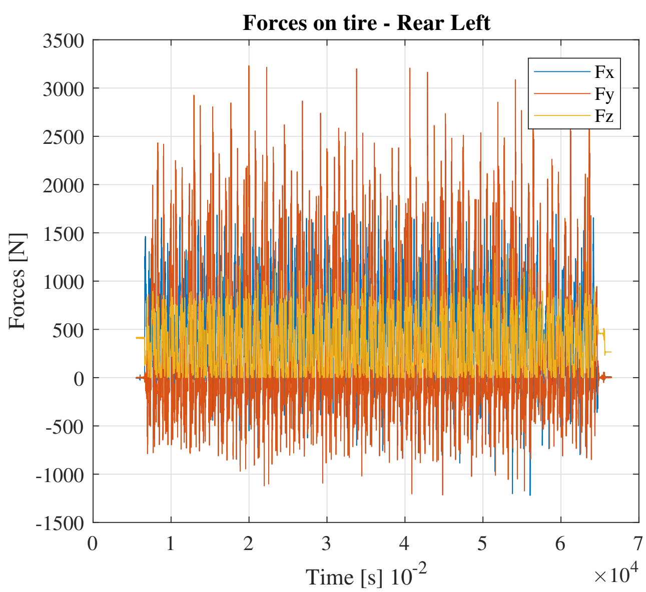

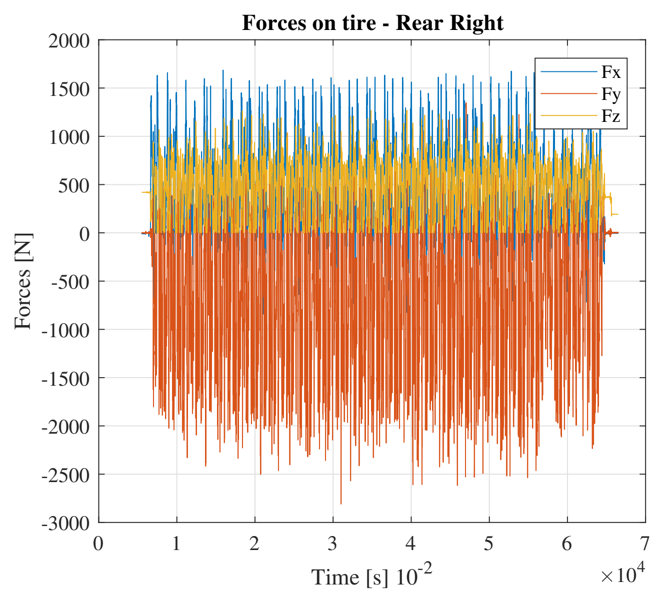

A.8 Rim Shell Production - Pictures

Figure A.8.1: Molds after polishing, application of sealer and release agent.

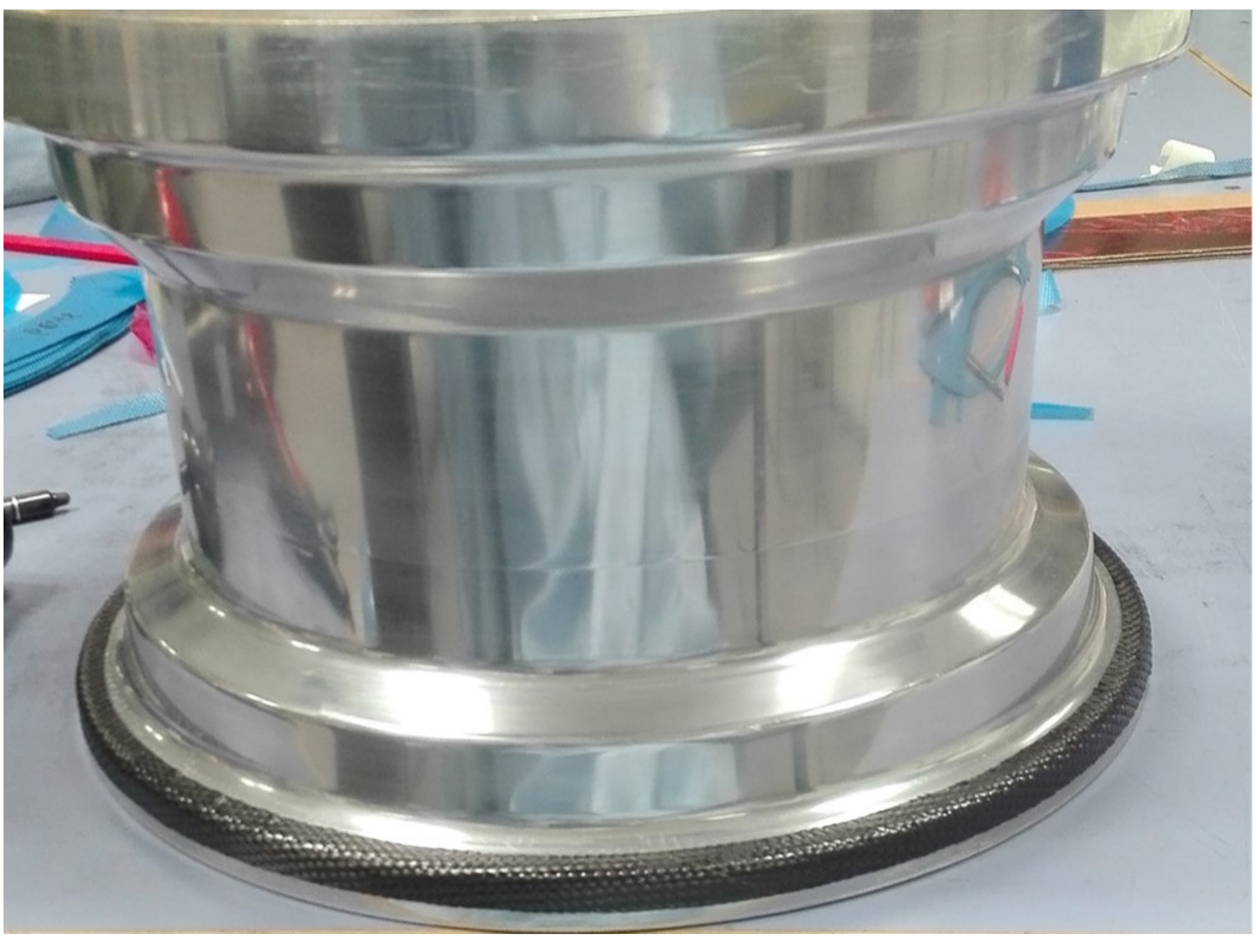

Figure A.8.2: Initial ply added on outer flange

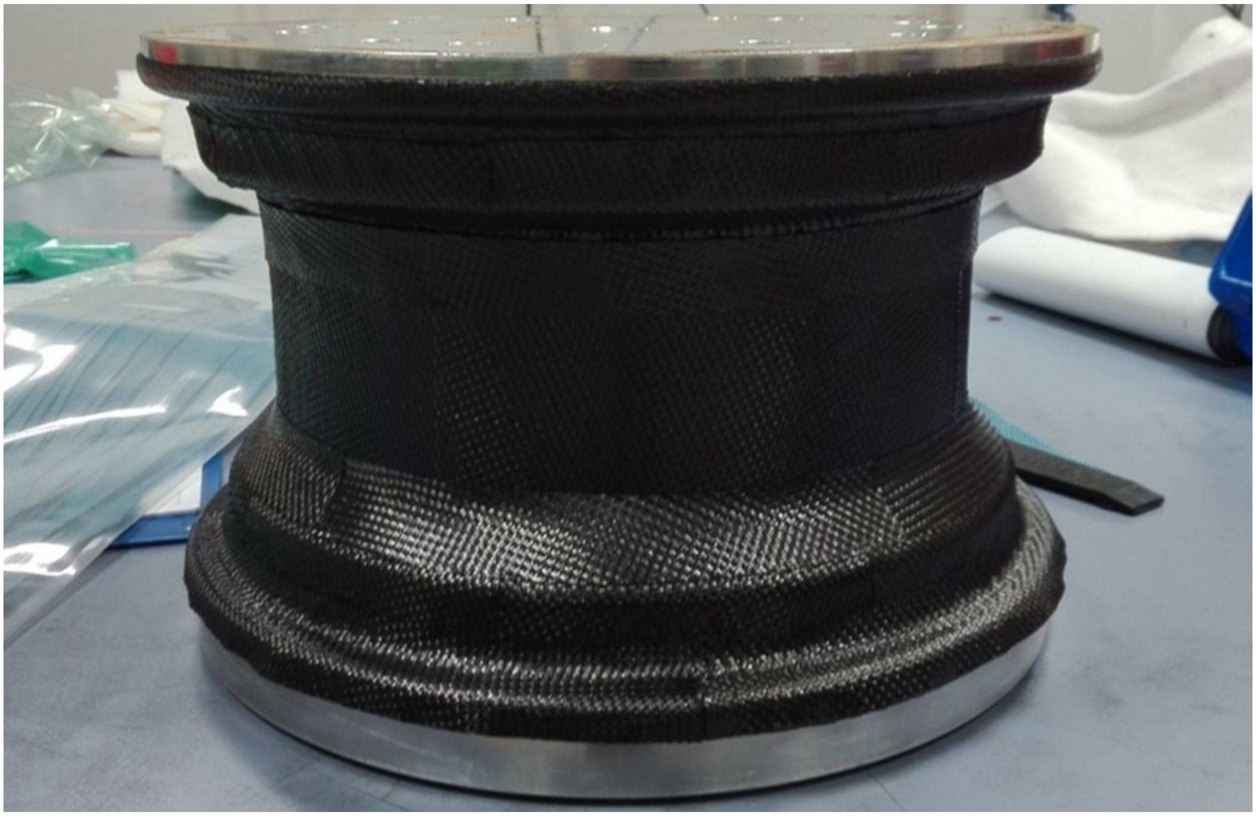

Figure A.8.3: Initial layer before debulking

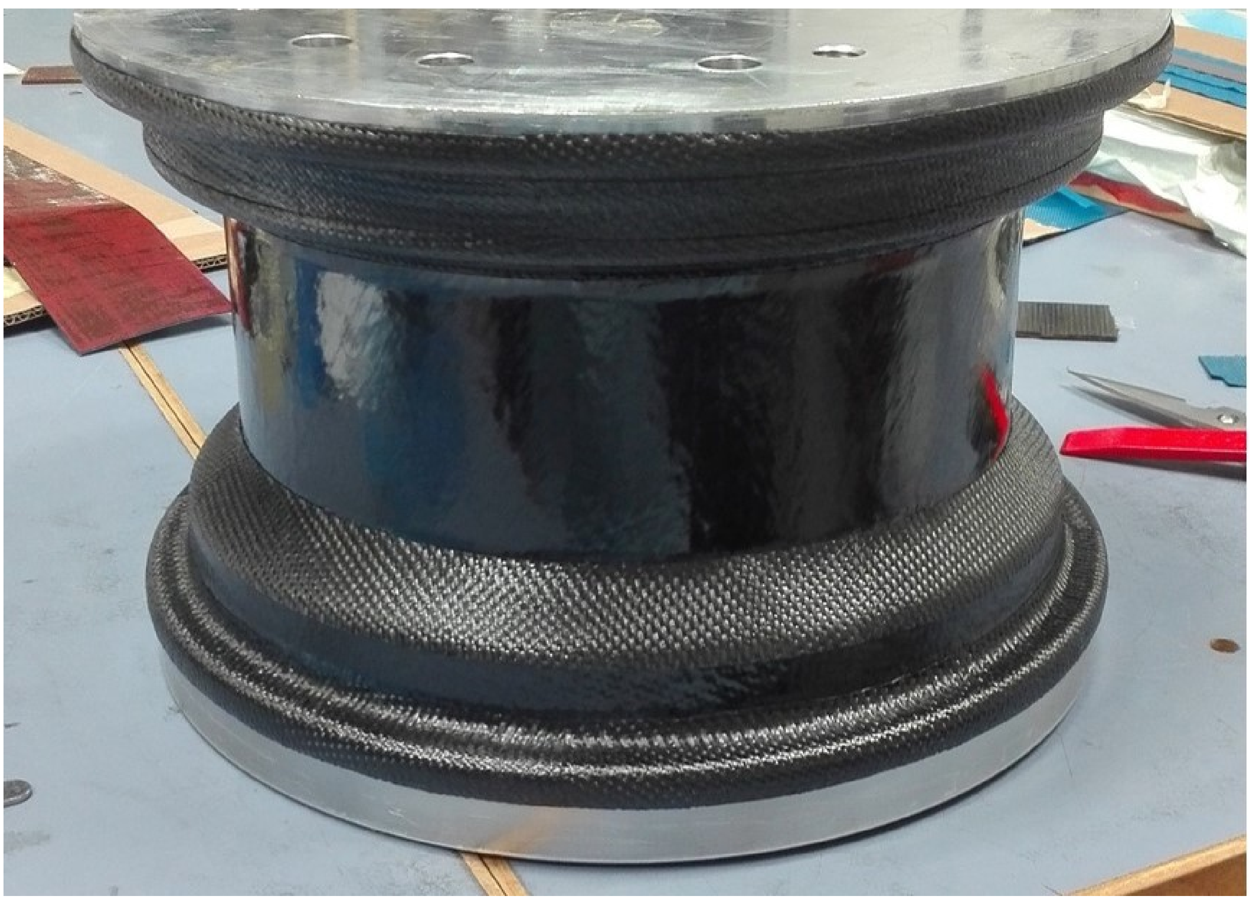

Figure A.8.4: 4 Th layer after debulking

Figure A.8.5: Rim shell under debulking

Figure A.8.6: The hump was created by stacking small stripes of CFRP

Figure A.8.7: Application of peel ply

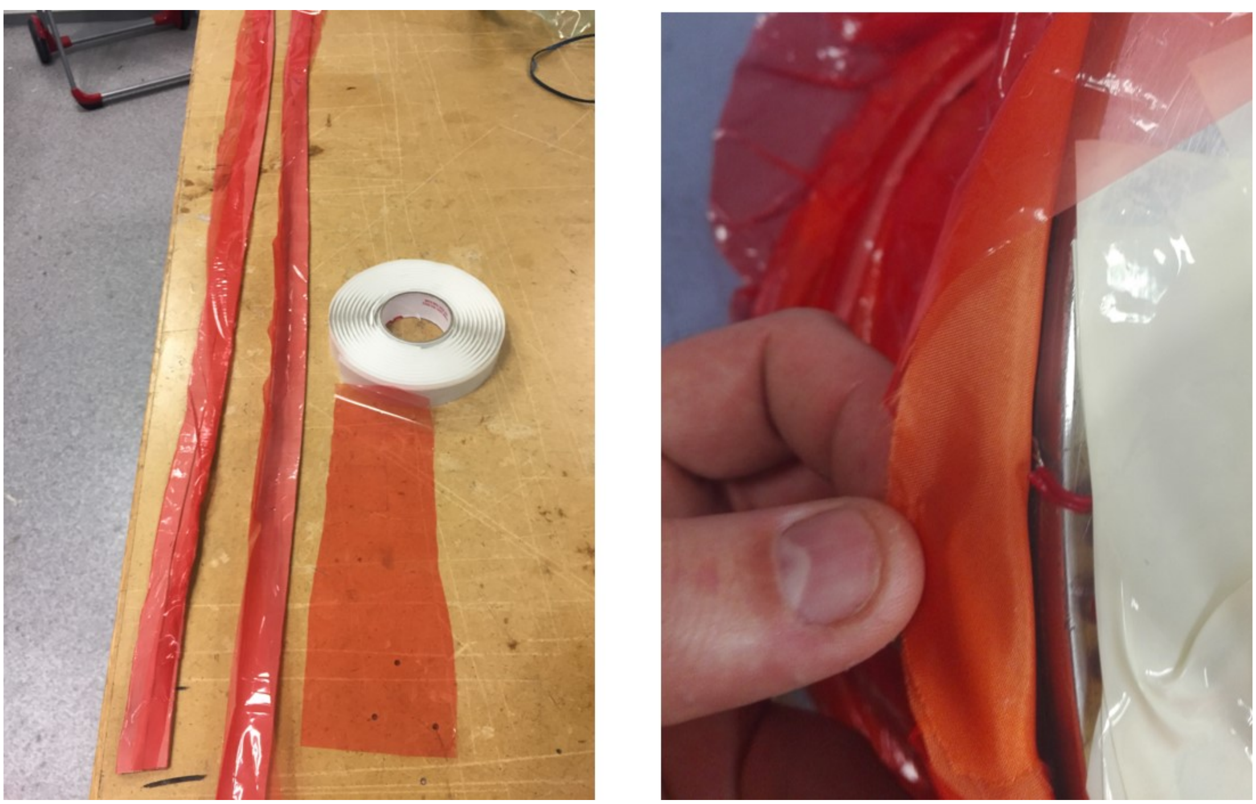

Figure A.8.8: Left: Bagtape rolled in release film, used to reduce bridging around bead. Right: Temperature sensor, mounted between mold and laminate

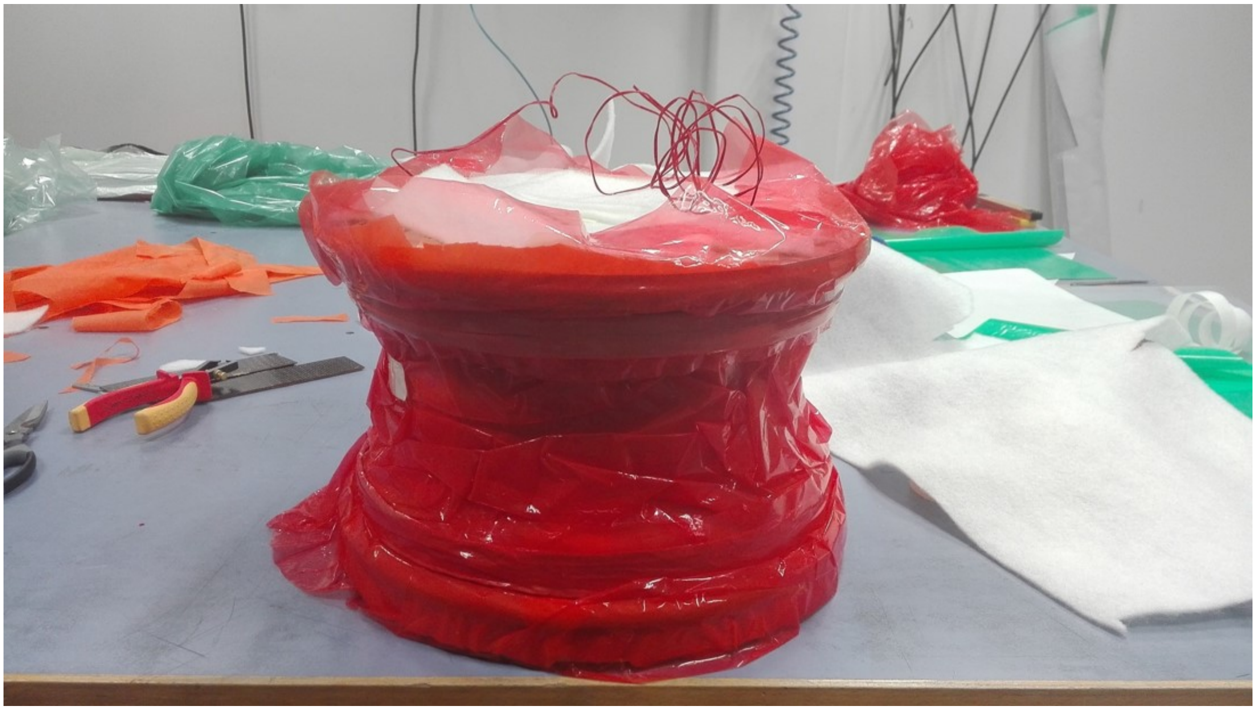

Figure A.8.9: Finished application of release film

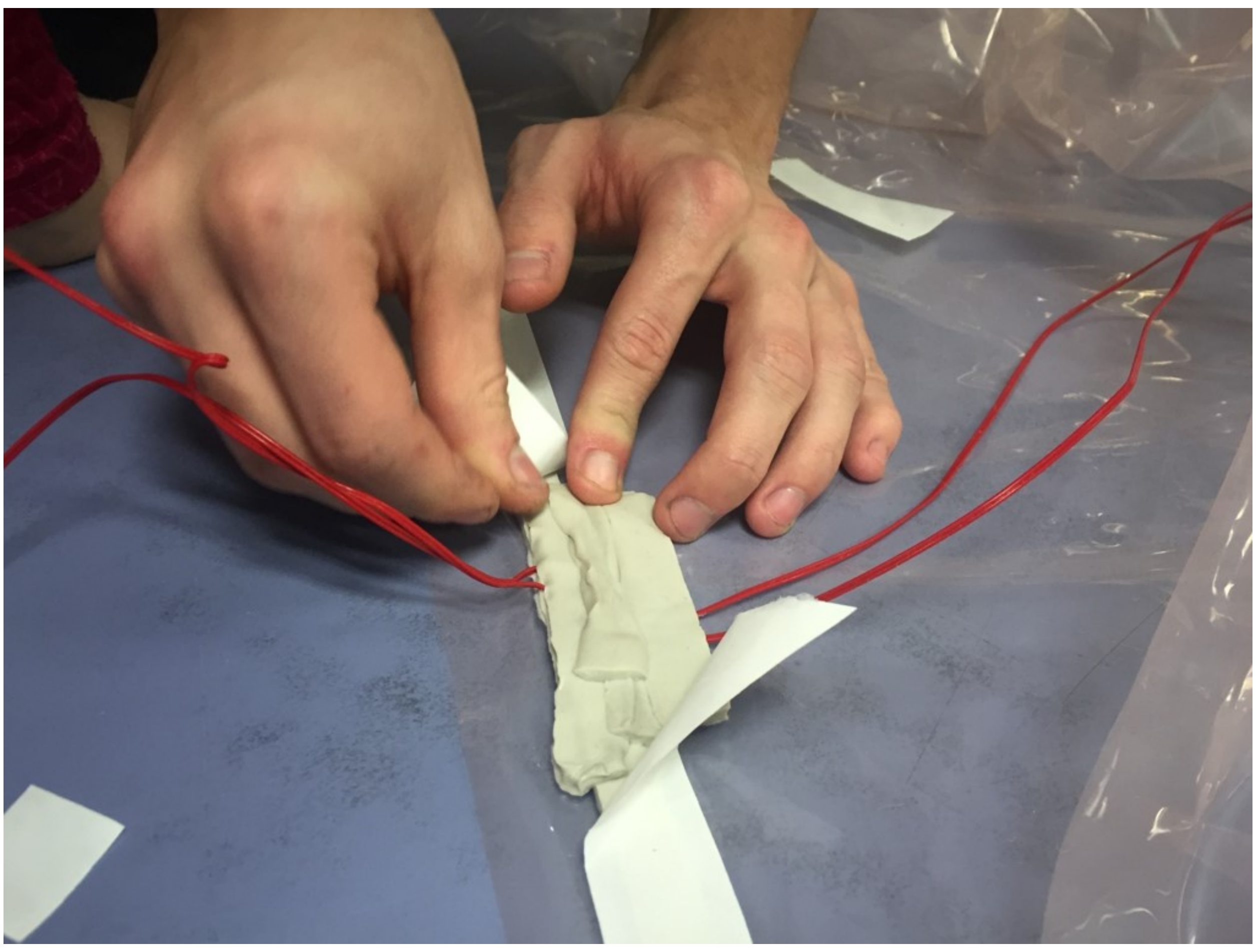

Figure A.8.10: Sealing of temp sensor though tha bag

Figure A.8.11: Vacuum bag ready for sealing

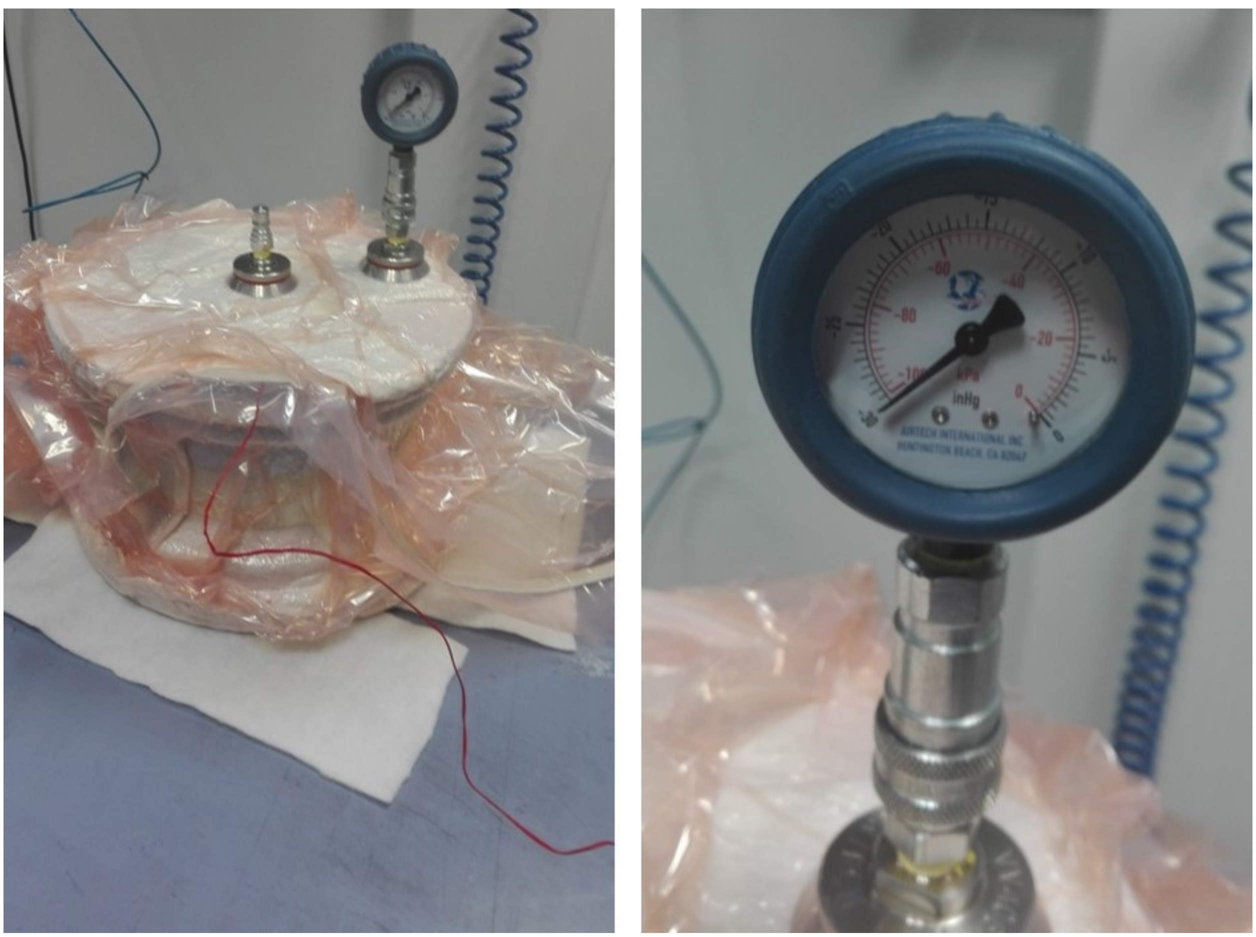

Figure A.8.12: Vacuum leak test

Figure A.8.13: Rim shell ready for autoclave curing

Figure A.8.14: Set-point for autoclave during curing

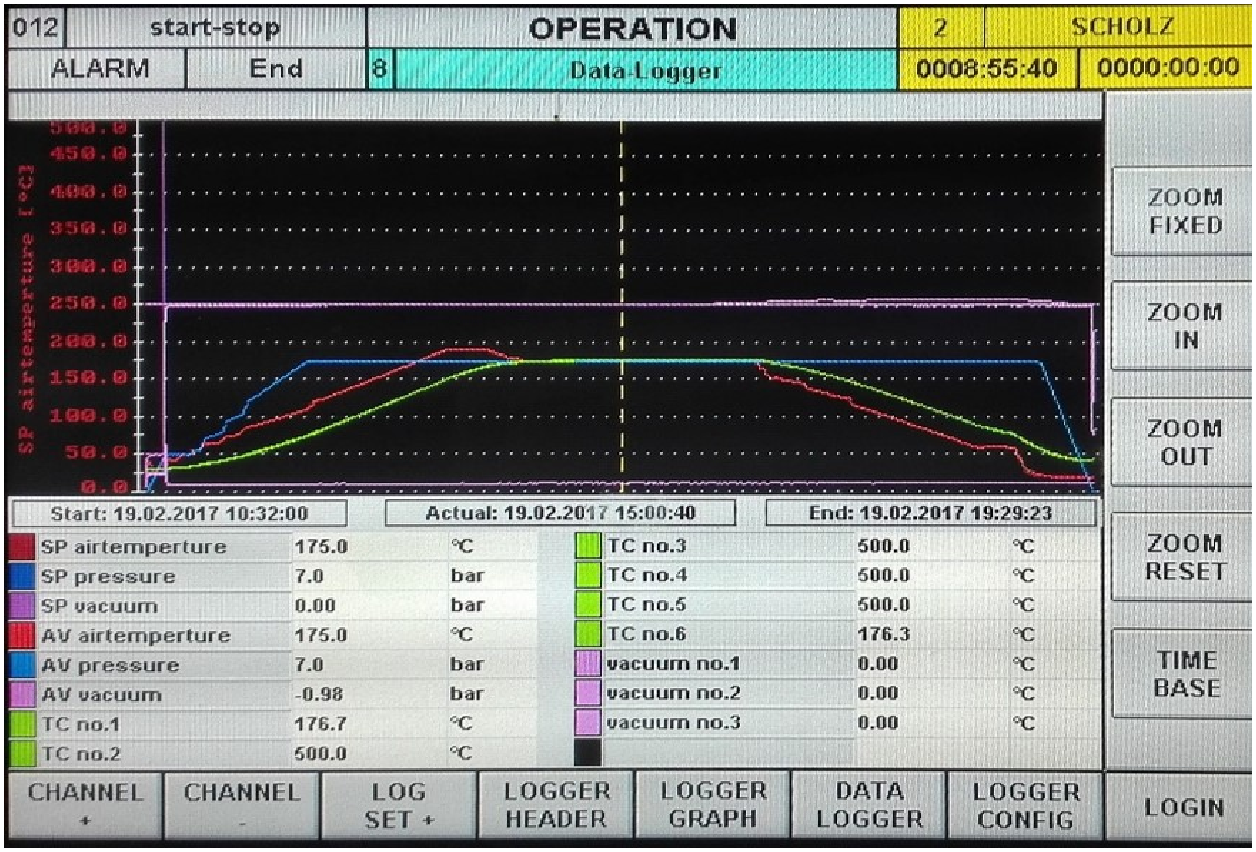

Figure A.8.15: Curing log-data

Figure A.8.16: Rim shell under demoulding

Figure A.8.17: Removement of release film

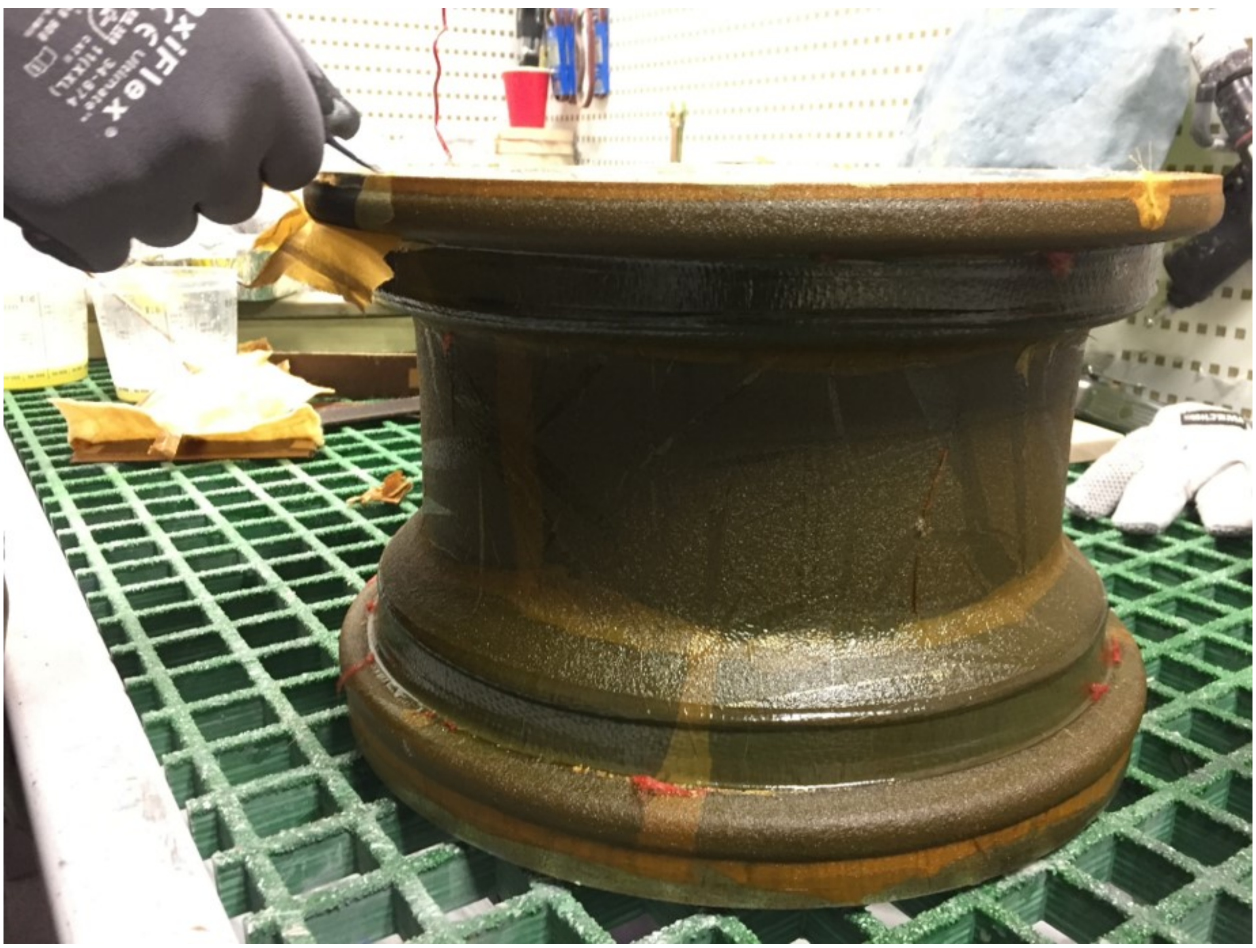

Figure A.8.18: Removement of peel ply before demoulding

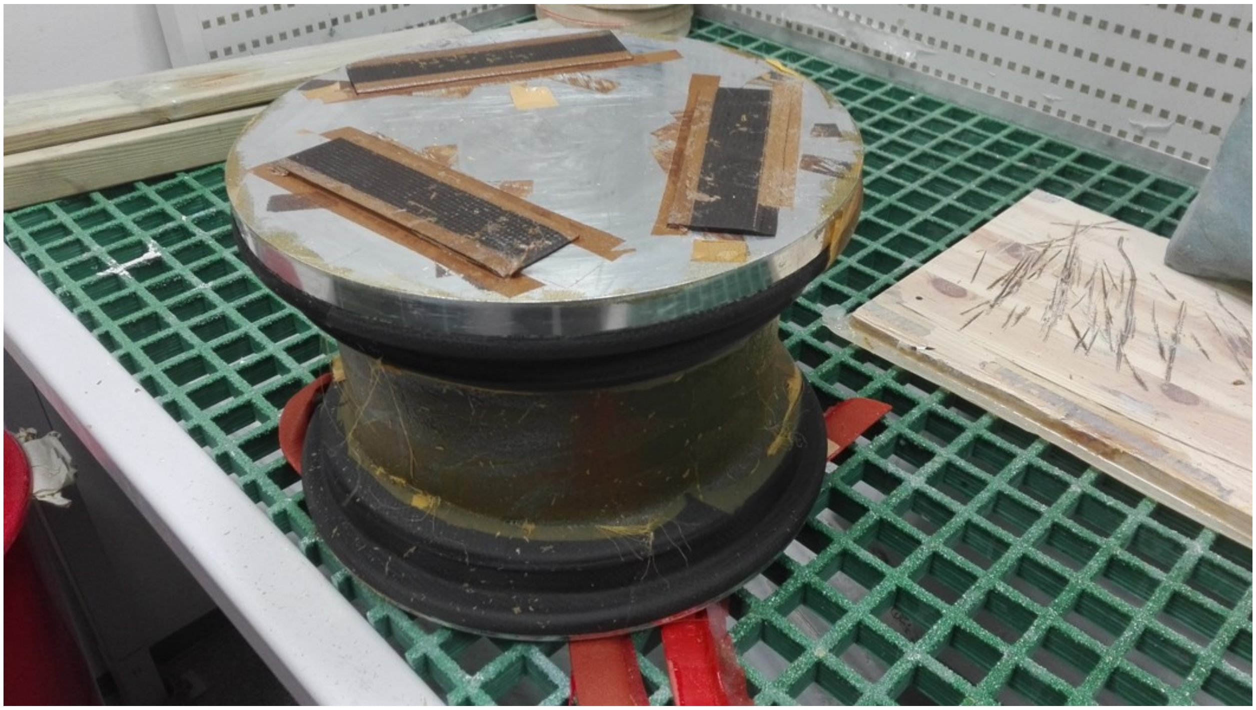

Figure A.8.19

Figure A.8.20: Finished cured and demulded rim shell, here on a scale for controlling the weight

Ply.	OF	OB	OD	CM	CS	ID	IB	IF
1	S 0	S 0	S 0	S 0	S 0	S 0	S 0	S 0
2	S 0	S 0	S 0	U 0	U 0	S 45	U 0	S 45
3	S 45	U 90	S 45	U 90	U 90	S 0	U 90	S 45
4	S 45	U 90	S 45	U 0	U 0	S 0	U 0	S 45
5	S 0	U 90	S 0	U 90	U 90	S 45	U 90	S 45
6	S 0	U 90	S 0	U 0	U 0	S 0	U 0	S 0
7	-	S 0	-	S 45	S 45	-	S 45	-
8	-	S 0	-	S 0	S 0	-	S 0	-

S - Satin weave U - Unidirecitonal

B
Machine Drawings

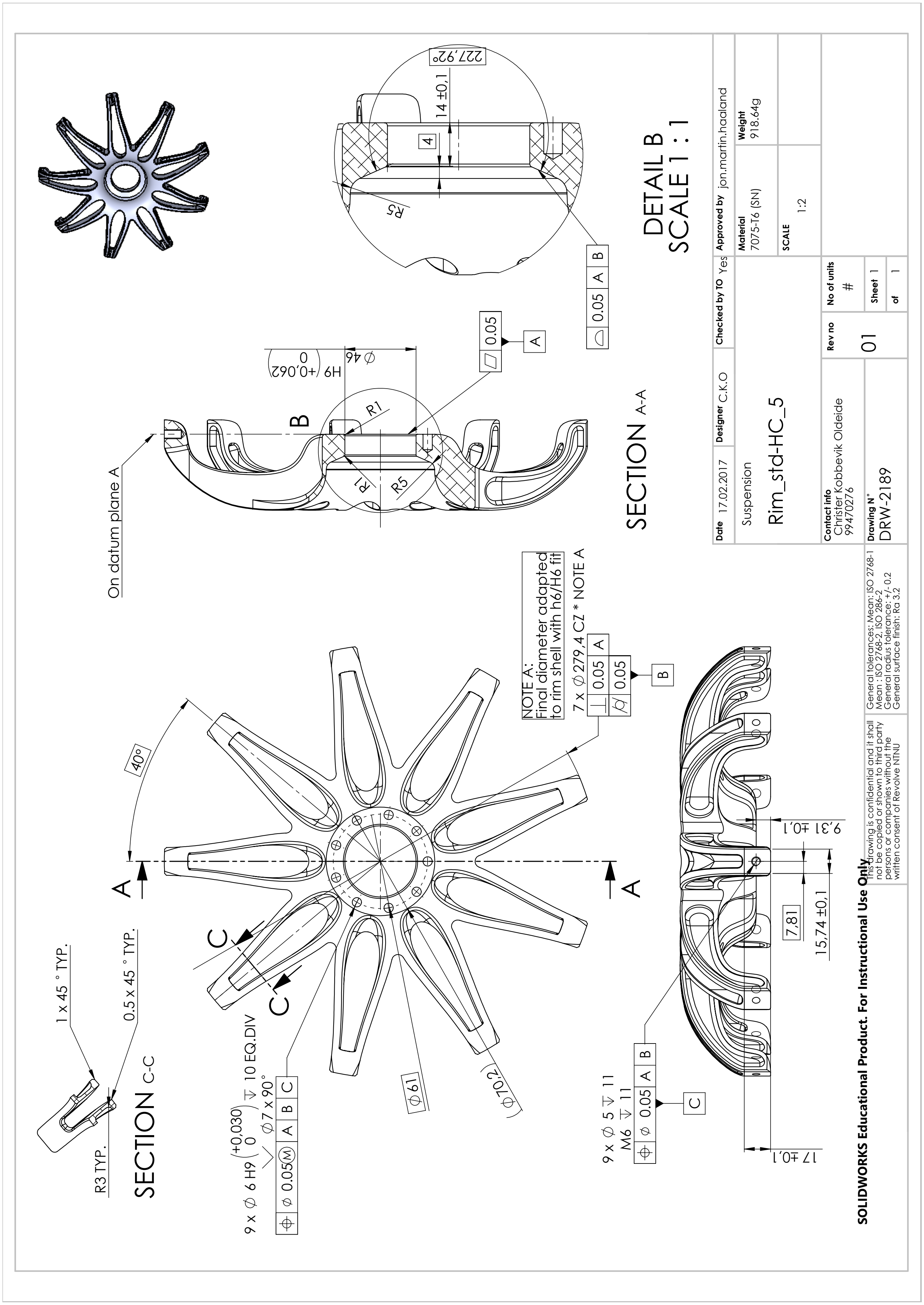
DETAIL B
SCALE 1 : 1
SECTION A-A
SECTION C-C
On datum plane A
NOTE A:
Final diameter adapted to rim shell with h6/H6 fit
7 x ⌀279,4 CZ * NOTE A
1 x 45 ° TYP.
0.5 x 45 ° TYP.
R3 TYP.
40°
⌀61
⌀70,2
9 x ⌀ 6 H9 (+0,030 0) ↧ 10 EQ.DIV
⌀7 x 90°
9 x ⌀ 5 ↧ 11
M6 ↧ 11
⌀46 H9 (+0,062 0)
227,92°
14 ±0,1
9,31 ±0,1
7,81
15,74 ±0,1
17 ±0,1
R1
R5
Date 17.02.2017
Designer C.K.O
Checked by TO Yes
Approved by jon.martin.haaland
Suspension
Rim_std-HC_5
Material 7075-T6 (SN)
Weight 918.64g
SCALE 1:2
Contact info
Christer Kobbevik Oldeide
99470276
Rev no 01
No of units #
Sheet 1 of 1
Drawing N° DRW-2189
General tolerances: Mean: ISO 2768-1
Mean : ISO 2768-2, ISO 286-2
General radius tolerance: +/- 0.2
General surface finish: Ra 3.2
This drawing is confidential and it shall not be copied or shown to third party persons or companies without the written consent of Revolve NTNU
SOLIDWORKS Educational Product. For Instructional Use Only

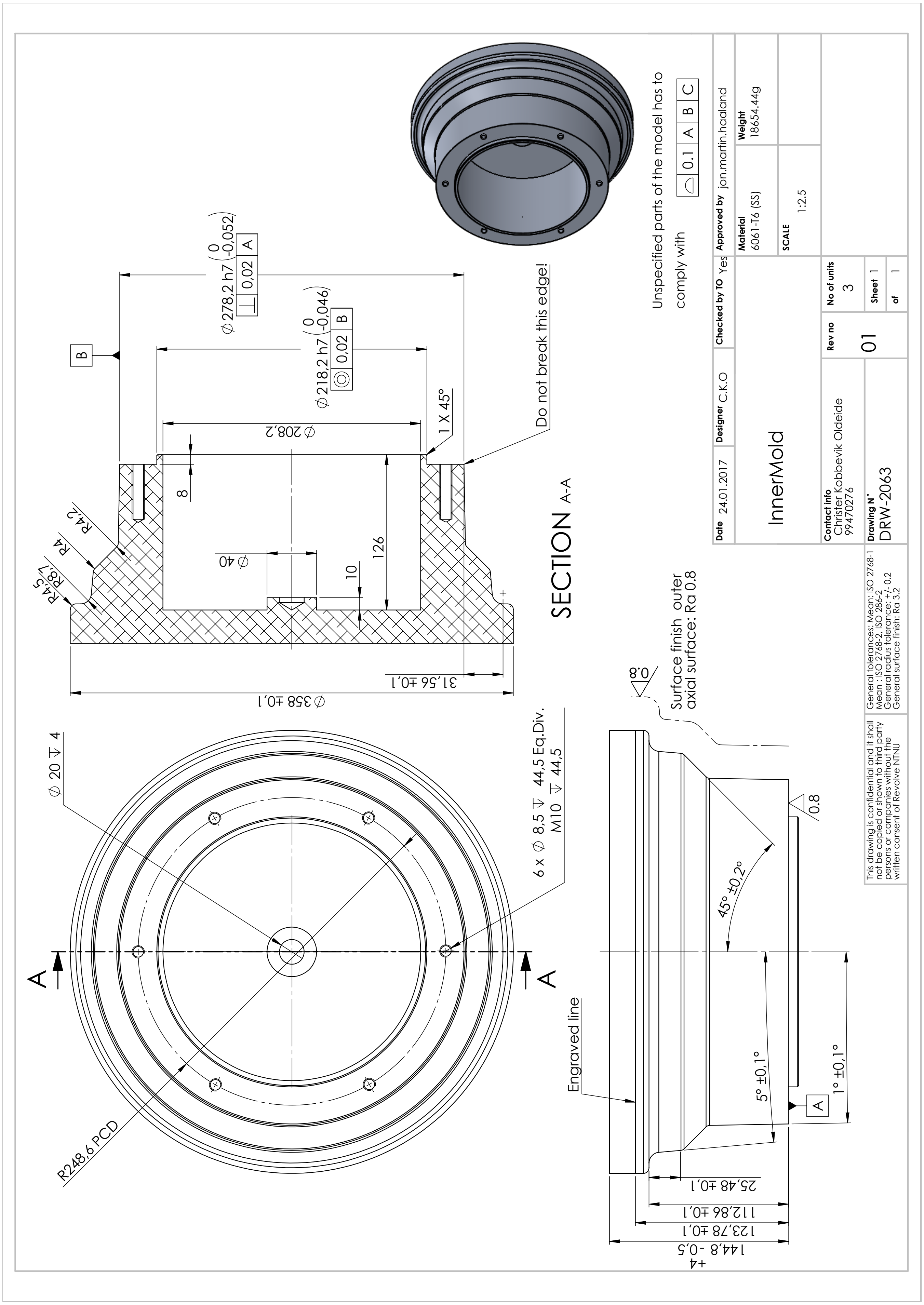

Ø 20 ↧ 4
6 x Ø 8,5 ↧ 44,5 Eq.Div.
M10 ↧ 44,5
A
A
Engraved line
R248,6 PCD
Ø 358 ±0,1
31,56 ±0,1
R4,5
R8,1
R4
R4,2
Ø 40
10
126
8
Ø 208,2
1 X 45°
Ø 218,2 h7 (0 -0,046)
0,02 B
Ø 278,2 h7 (0 -0,052)
0,02 A
B
SECTION A-A
Do not break this edge!
Surface finish outer axial surface: Ra 0.8
0.8
45° ±0,2°
5° ±0,1°
1° ±0,1°
A
25,48 ±0,1
112,86 ±0,1
123,78 ±0,1
144,8 +4 -0,5
Unspecified parts of the model has to comply with
0.1 A B C
Date 24.01.2017
Designer C.K.O
Checked by TO Yes
Approved by jon.martin.haaland
Material 6061-T6 (SS)
Weight 18654.44g
SCALE 1:2.5
InnerMold
Contact info
Christer Kobbevik Oldeide
99470276
Drawing N°
DRW-2063
Rev no 01
No of units 3
Sheet 1
of 1
General tolerances: Mean: ISO 2768-1
Mean : ISO 2768-2, ISO 286-2
General radius tolerance: +/- 0.2
General surface finish: Ra 3.2
This drawing is confidential and it shall not be copied or shown to third party persons or companies without the written consent of Revolve NTNU

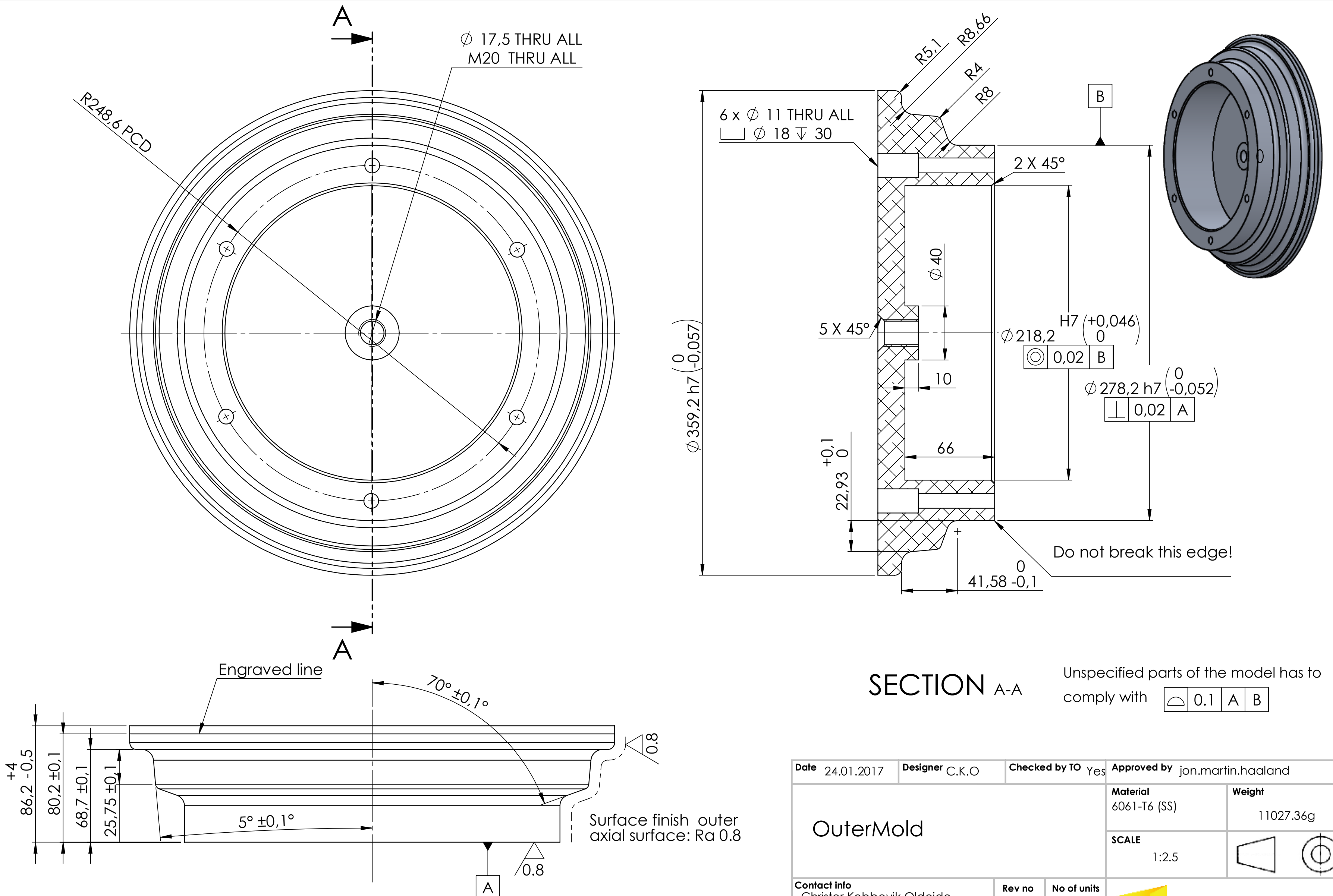

Unspecified parts of the model has to comply with ⌓ 0.1 A B

Date 24.01.2017	Designer C.K.O	Checked by TO Yes	Approved by jon.martin.haaland
OuterMold		Material 6061-T6 (SS)	Weight 11027.36g
		SCALE 1:2.5	
Contact info Christer Kobbevik Oldeide 99470276	Rev no 01	No of units 3	
Drawing N° DRW-2058		Sheet 1 of 1	

General tolerances: Mean: ISO 2768-1
Mean : ISO 2768-2, ISO 286-2
General radius tolerance: +/- 0.2
General surface finish: Ra 3.2

B.3 Machine Drawings Rim Shell

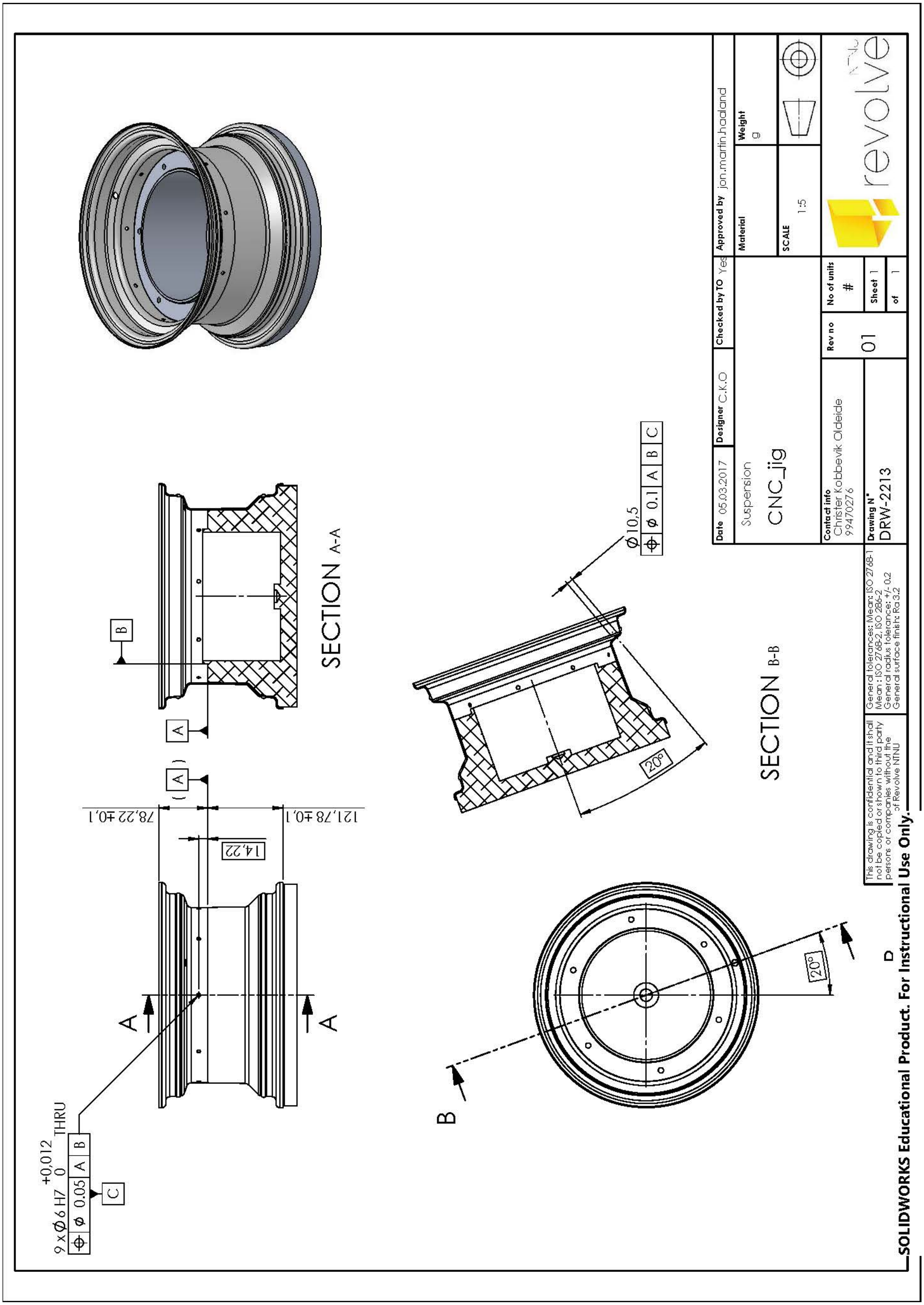

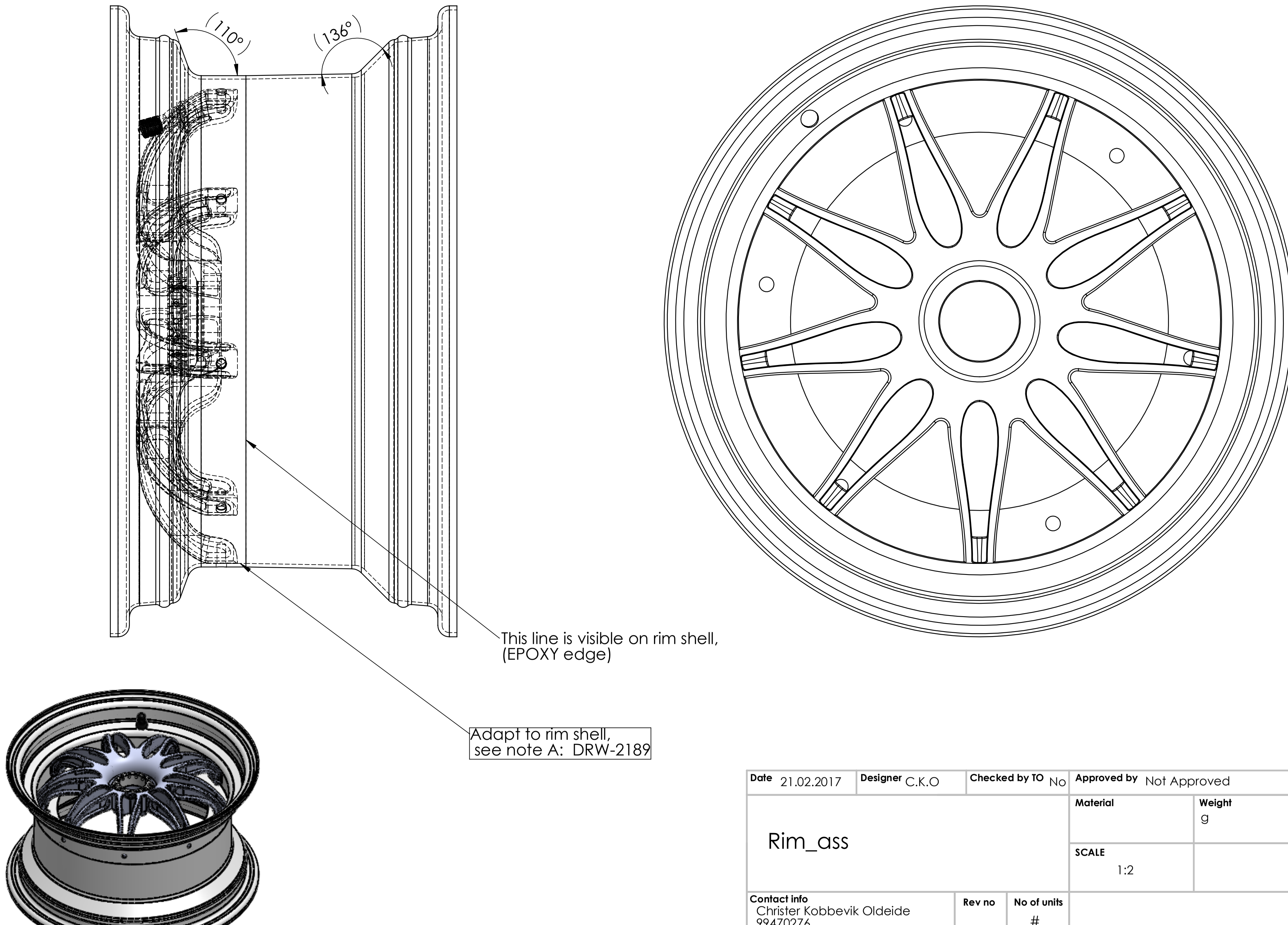

Date 21.02.2017	Designer C.K.O	Checked by TO No	Approved by Not Approved
Rim_ass		Material	Weight g
		SCALE 1:2	
Contact info Christer Kobbevik Oldeide 99470276	Rev no 01	No of units #	
Drawing N° DRW-2193		Sheet 1 of 1	

This drawing is confidential and it shall not be copied or shown to third party persons or companies without the written consent of Revolve NTNU

General tolerances: Mean: ISO 2768-1
Mean : ISO 2768-2, ISO 286-2
General radius tolerance: +/- 0.2
General surface finish: Ra 3.2

B.4 Base dimensions of Test jig

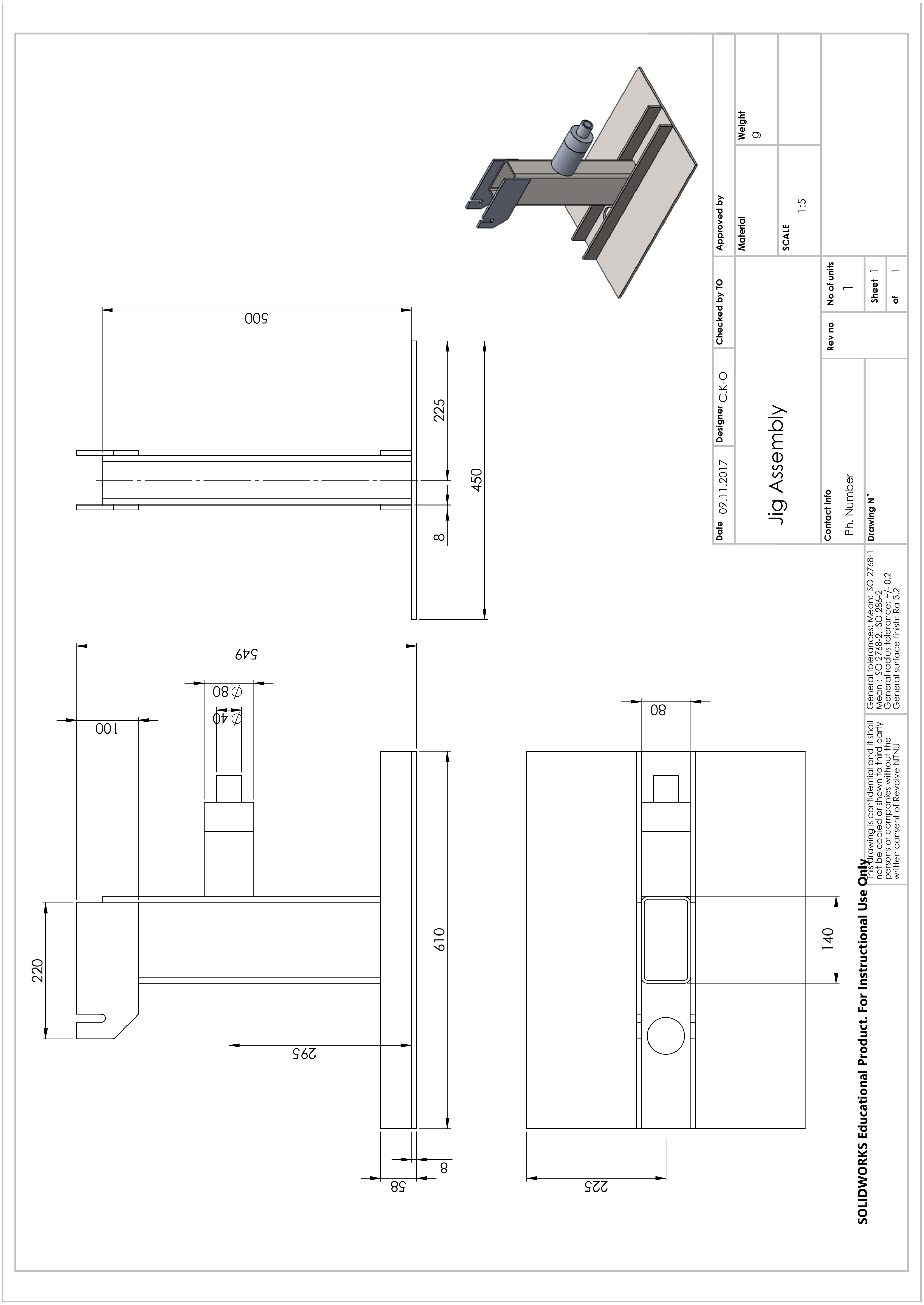

C
Measuring Reports & Standards

C.1 Measuring Raport Rim Center

ZEISS Calypso

MJØS METALLVAREFABRIKK AS — ZEISS

Measurement Plan NTNU DRW2189	Date March 1, 2017	Operation no 40
Drawing No. DRW2189	Time 9:39:56 am	Order 33112
Inspector Øystein Nordås	Customer name Øystein	Incremental Part Number 1

	Actual	Nominal	Upper Tol.	Lower Tol.		Deviation
Overall Result						
All Characteristics:	6					
...in Tolerance:	6					
...Out of tolerance:	0					
...Over Warning Limit:	0					
...Not Calculated:	0					
Total Coord. systems:	0					
...Not Calculated:	0					
Total Text elements:	0					
Flatness Ref A 0.05	0.001	0.000	0.050		|	0.001
Diameter 46H9	46.027	46.000	0.062	0.000	-|	0.027
Diameter_Cylinder2	278.722	278.720	0.020	-0.020	|-	0.002
Perpendicularity 0.05 to A	0.001	0.000	0.050		|	0.001
Cylindricity 0.05	0.016	0.000	0.050		|--	0.016
Curve Form1 Shape Of Zone: Standard	0.088	0.000	0.100	-0.100	|--	0.088

1

ZEISS Calypso

Measurement Plan NTNU DRW2189 Opr-50	Date March 1, 2017	Operation no 1
Drawing No. * drawingno *	Time 9:41:47 am	Order
Inspector Øystein Nordås	Customer name Mjøs Metallvarefabrikk AS	Incremental Part Number 2

	Actual	Nominal	Upper Tol.	Lower Tol.		Deviation
Overall Result						
All Characteristics:	4					
...in Tolerance:	4					
...Out of tolerance:	0					
...Over Warning Limit:	0					
...Not Calculated:	0					
Total Coord. systems:	0					
...Not Calculated:	0					
Total Text elements:	0					
Y Value_Intersection1	14.002	14.000	0.100	-0.100	|-	0.002
Profile2	0.027	0.000	0.050		|---	0.027
Curve Form2 Shape Of Zone: Standard	0.032	0.000	0.100	-0.100	|-	0.032

C.2 Measuring Raport Rim Shell - inner contour

Calypso 6.0.1202	Carl Zeiss		Date	February 28, 2017
			Order	33112
Part Number 7	CMM Type ACCURA_2	Drawing No. DRW2189	Department:	
			Operator	Master
			Signature:	
Meas. Plan Name NTNU DRW2189				

1: Curve Form1

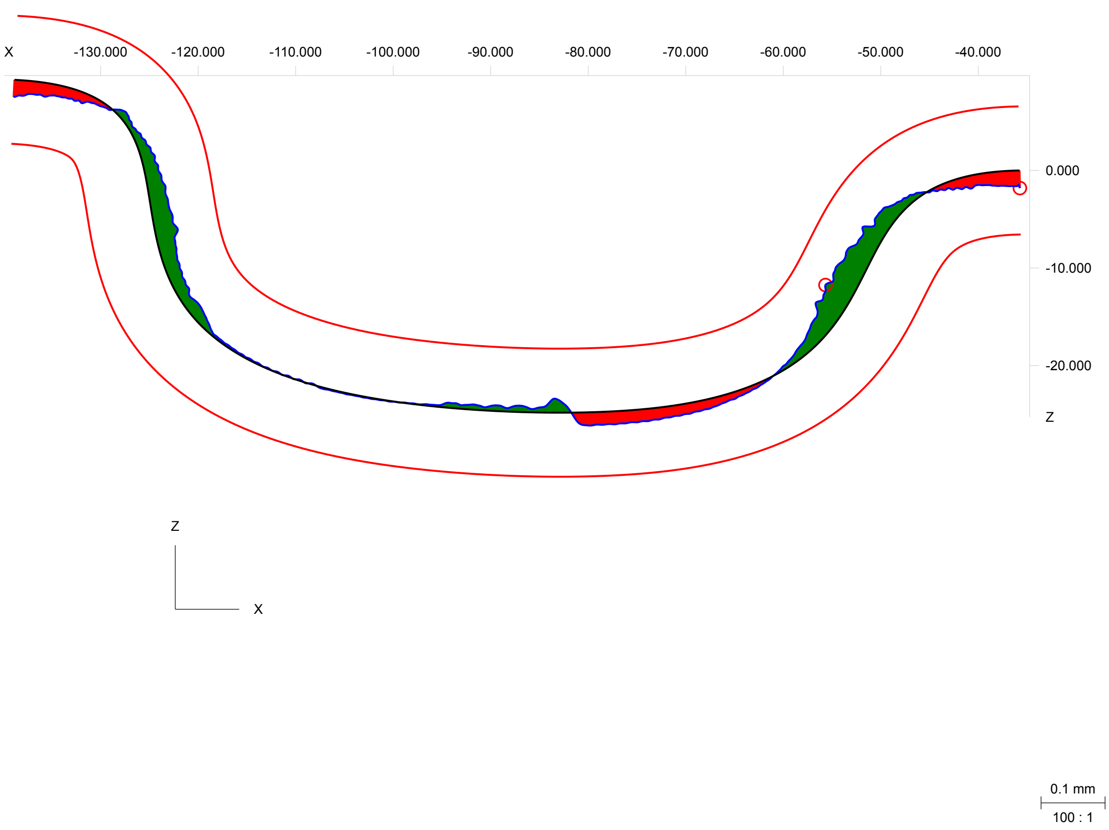

No	Identifier		Sigma [mm]	Form [mm]	Number of Points	Lower Tol. [mm]	Upper Tol. [mm]	MinInd	Min Dev. [mm]	MaxInd	Max Dev. [mm]
1	Curve Form1		0.019	0.088	1000	-0.100	0.100	998	-0.043	817	0.045
	Best Fit	Translation	X [mm]-0.011	Y [mm]0.000	Z [mm]0.012	Rotation		X 0.000	Y 0.015	Z 0.000	

C.3 Measuring Raport Rim Shell - outer contour

ZEISS	Calypso 6.0.1202	Carl Zeiss	Date	March 1, 2017
			Order	
Part Number 2	CMM Type ACCURA_2	Drawing No.	Department: Operator Master Signature:	
Meas. Plan Name NTNU DRW2189 Opr-50				

1: Curve Form2

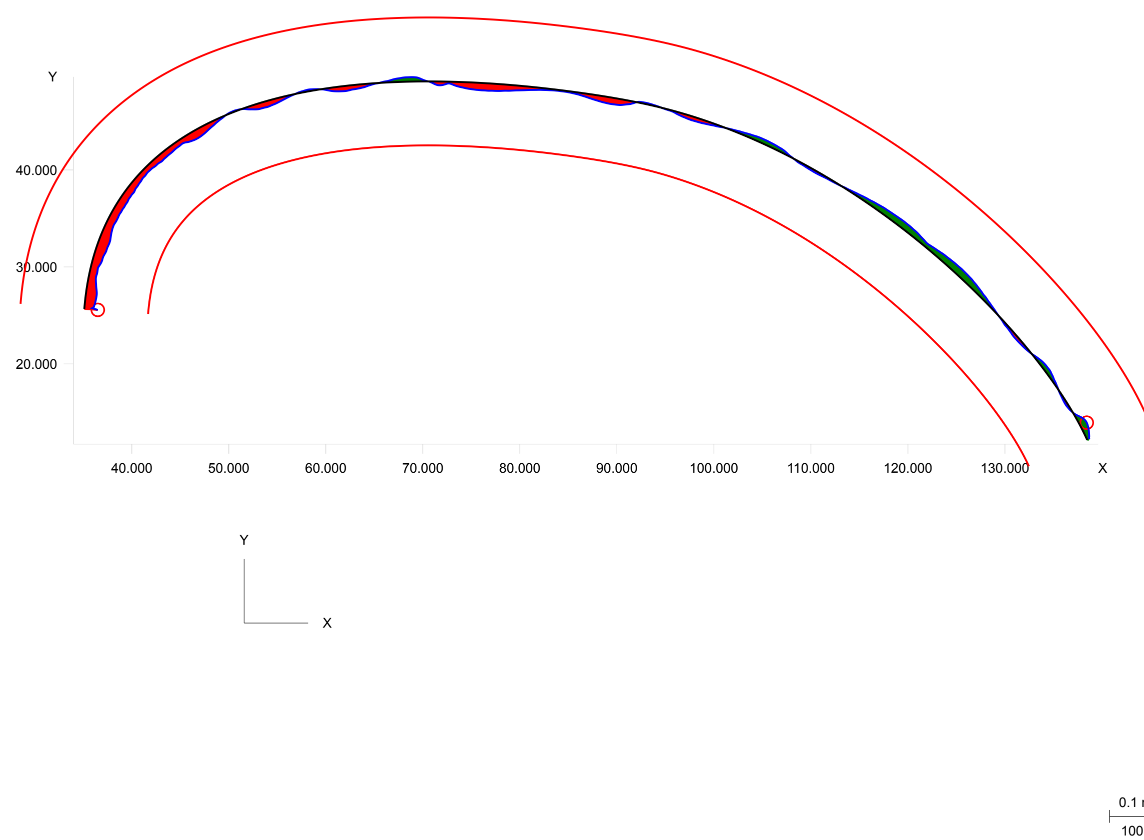

No	Identifier	Sigma [mm]	Form [mm]	Number of Points	Lower Tol. [mm]	Upper Tol. [mm]	MinInd	Min Dev. [mm]	MaxInd	Max Dev. [mm]
1	Curve Form2	0.007	0.032	993	-0.100	0.100	977	-0.021	29	0.011
	Best Fit	Translation	X [mm]0.000	Y [mm]0.000	Z [mm]0.000	Rotation	X 0.000	Y 0.000	Z 0.000	

all tyre brands of Continental 95

R_4 and R_5: between
4 and 10 mm
R_5: not larger than 10 mm

Valve Hole-Ø:
11.5 mm (11.3$_{-0}^{+0,4}$) centrally in the side of the rim well.
16.0 mm (15.7 mm$_{-0}^{+0,4}$) only with Ø-Code 15.

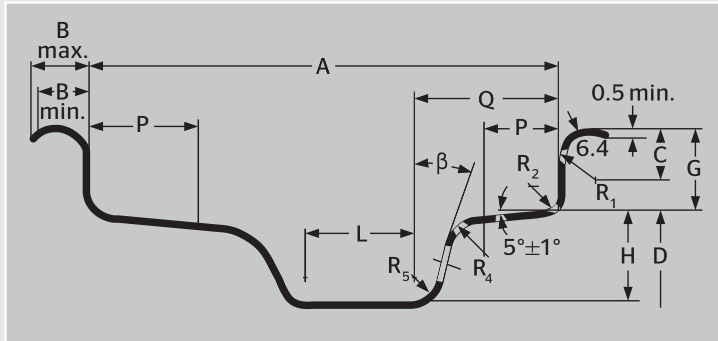

Rim Contour	Dimensions (mm)											
	A		B Min.	B Max. [1]	G ± 0,6	P Min.	H Min. [2]	L Min.	Q Max.	R_1 Min.	R_2 Max.	β Min.
3.00 B	76	± 1	10	13	14.1	13	15	16	28	7.5	4.5	10°
3.50 B	89					15		19	34			13°
4.00 B	101.5								45			
4.50 B	114.5					19.5		22				
5.00 B	127											
5.50 B	139.5											
6.00 B	152.5											
3 J	76		11	15	17.3	13	17.3	16	28	9.5	6.5	10°
3 ½ J	89					15		19	34			20°
4 J	101.5											
4 ½ J	114.5					19.5		22	45			
5 J	127											
5 ½ J	139.5											
6 J	152.5											
6 ½ J	165	± 1.5										
7 J	178											
7 ½ J	190.5											
8 J	203											
8 ½ J	216											
9 J	228.5											
9 ½ J	241.5											
10 J	254											
10 ½ J	266.5											
11 J	279.5											
11 ½ J	292											
12 J	305											
12 ½ J	317.5											

[1] B max. values may be exceeded on rims for light commercial vehicles

[2] Minimum dimensions for well depth (H) and well angle are required for tyre mounting

Rim diameter

Code (ins)	12	13	14	15	16	17	18	19	20	21	22	23	24
D (mm)	304.0	329.4	354.8	380.2	405.6	436.6	462.0	487.4	512.8	538.2	563.6	589.0	614.4

Special rim executions for passenger cars

In many countries safety rims must be used for tubeless radial tyres.

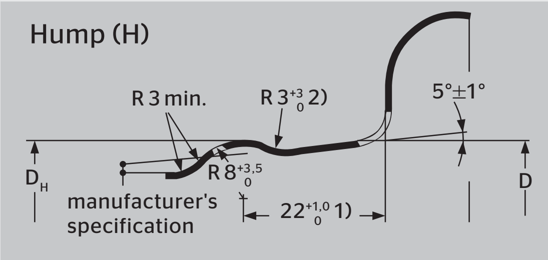

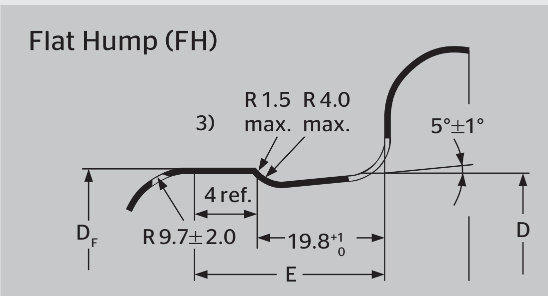

[1] In most car rims 19.8 mm.
[2] For B-Rims R = 8.5 mm max. resp. R = 4 ±1 mm.
[3] Deburred.

These **full-drop centre rims with safety shoulders** for cars, estate cars and light trucks are marked with the following-codes shown after rim size designation:

H = one-sided round hump on outer shoulder (formerly: H 1)
H2 = double round hump
FH = flat hump on outer shoulder (formerly: FHA 1)
FH2 = double flat hump (formerly: FHA 2)
CH = combination hump = flat hump on outer shoulder, round hump on inner shoulder (formerly: FHA-H)
SL = special ledge
EH2 / 2+ = Extended Hump (with extended hump on both sides)
(see following page)

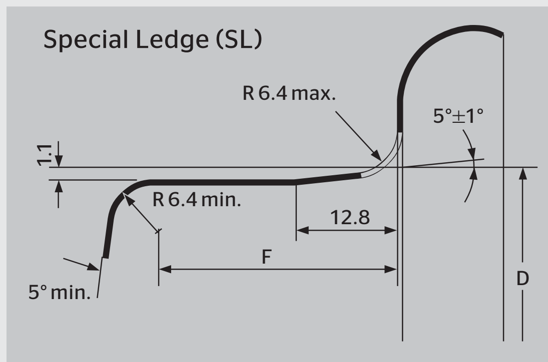

Ledge	Rim diameter Code (ins)	Dimensions (mm)		
		H	FH	
		Circumference $\pi \cdot D_H$ (+ 0/-3)	Circumference $\pi \cdot D_F$ (+ 0/-3)	E Max.
B	12	957.6	-	-
	13	1037.0	1034.8	24.5
	14	1116.8	1114.6	
J	13	1037.0	1034.8	28.5
	14	1116.8	1114.6	
	15	1196.6	1194.4	
	16	1276.4	1274.2	
	17	1373.8	1371.6	
	18	1453.6	1451.4	
	19	1533.4	1531.2	
	20	1613.2	1611.0	
	21	1693.0	1690.8	
	22	1772.8	1770.6	
	23	1852.6	1850.4	
	24	1932.4	1930.2	

D
Datasheets

D.1 Strain gauge FRA-5-11-3L

–196°C Operating temperature range +150°C

Temperature compensation range +10°C +100°C

Suffix code for temperature compensation materials
-11: Mild steel -17: Stainless steel -23: Aluminium

For ordering, the above suffix code should be added to the basic gauge type.

FOIL STRAIN GAUGES series **F**

Applicable adhesives

CN	–196 ~ +120°C
P-2	–30 ~ +150°C
EB-2	–60 ~ +150°C

GENERAL USE

Gauge pattern	Basic type	Gauge size L	Gauge size W	Backing L	Backing W	Resistance Ω

M metal G general

0°/90° 2-element Rosette Stacked: FCA

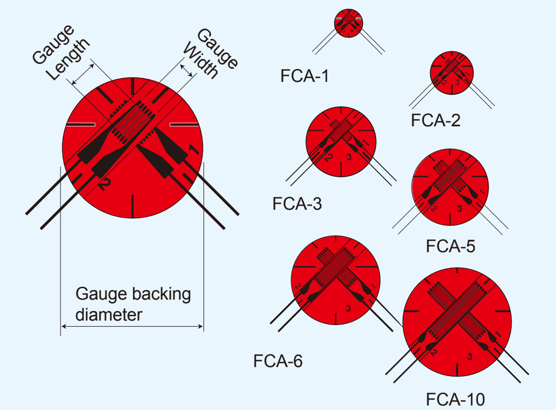

Each package contains 10 gauges.

Basic type	Gauge size L	Gauge size W	Backing	Resistance Ω
FCA-1	1	0.7	ϕ 4.5	120
FCA-2	2	0.9	ϕ 7	120
FCA-3	3	1.7	ϕ 11	120
FCA-5	5	1.9	ϕ 12	120
FCA-6	6	2.4	ϕ 14	120
FCA-10	10	2.5	ϕ 17	120

350Ω 0°/90° 2-element Rosette Stacked: FCA

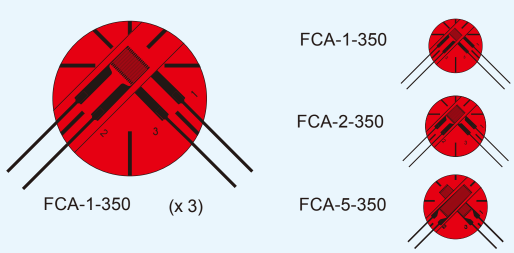

Each package contains 10 gauges.

Basic type	Gauge size L	Gauge size W	Backing	Resistance Ω
FCA-1-350	1	1.6	ϕ 8	350
FCA-2-350	2	1.9	ϕ 9.5	350
FCA-3-350	3	2	ϕ 10	350
FCA-5-350	5	1.8	ϕ 10	350

0°/45°/90° 3-element Rosette Stacked: FRA

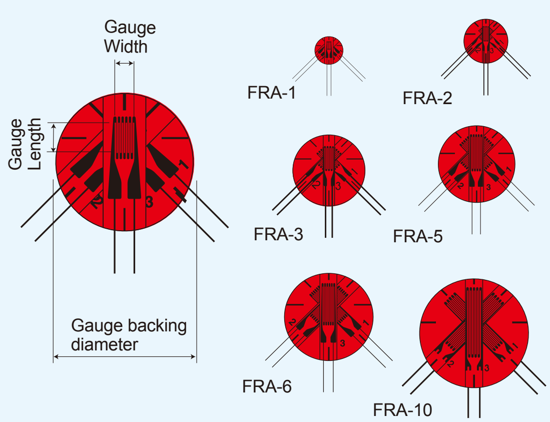

Each package contains 10 gauges.

Basic type	Gauge size L	Gauge size W	Backing	Resistance Ω
FRA-1	1	0.7	ϕ 4.5	120
FRA-2	2	0.9	ϕ 7	120
FRA-3	3	1.7	ϕ 11	120
FRA-5	5	1.9	ϕ 12	120
FRA-6	6	2.4	ϕ 14	120
FRA-10	10	2.5	ϕ 17	120

FOIL STRAIN GAUGES series F

–196°C Operating temperature range +150°C

Temperature compensation range +10°C +100°C

Suffix code for temperature compensation materials
-11: Mild steel -17: Stainless steel -23: Aluminium

For ordering, the above suffix code should be added to the basic gauge type.

Applicable adhesives		
	CN	–196 ~ +120°C
	P-2	–30 ~ +150°C
	EB-2	–60 ~ +150°C

GENERAL USE

M metal G general

Example of type number designation

FLA-5 -350 -11 -3LJB/-3LJBT (2-wire/3-wire)

- Length in meter and type of integral leadwire(*1)
- Self-temperatrure-compensation number(*2)
- Gauge resistance in ohm (Blank for 120Ω)
- Basic strain gauge type and gauge length

*1 : Not mentioned for gauges without leadwire
*2 : The following numbers are available for F series gauges
-11: Mild steel (11ppm/°C)
-17: Stainless steel, Copper alloy (17ppm/°C)
-23: Aluminium (23ppm/°C)

350Ω 0°/45°/90° 3-element Rosette Stacked: FRA

Each package contains 10 gauges.

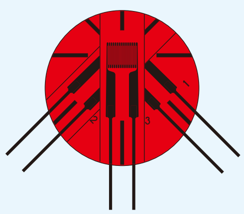

FRA-1-350 (x 3)

FRA-1-350
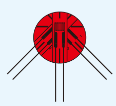

FRA-2-350
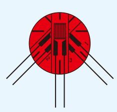

FRA-5-350
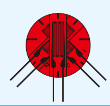

Basic type	Gauge size L	Gauge size W	Backing L	Backing W	Resistance Ω
FRA-1-350	1	1.6	ϕ 8		350
FRA-2-350	2	1.9	ϕ 9.5		350
FRA-3-350	3	2	ϕ 10		350
FRA-5-350	5	1.8	ϕ 10		350

SPECIAL USE

M metal G general

Option F
This code is appended to the basic type for strain gauges with lead-free solder in place of leaded solder. Fatigue life of the strain gauge may become shorter by the lead-free solder.

Example of type number designation

FLT-05A -11 -350 -F -3LJC -F

- Option F : LEAD-free soldering of leadwire
- Length in meter and type of integration leadwire
- Option F: LEAD-free soldering of strain gauge
- Gauge resistance (Blank for 120Ω)
- Self-temperature-compensation number
- Basic strain gauge type

Shearing strain measurement : FLT

Each package contains 10 gauges.

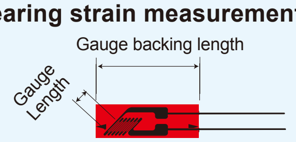

Left 45°

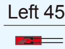
Right 45°

Basic type	Gauge size L	Gauge size W	Backing L	Backing W	Resistance Ω
FLT-05A	0.5	0.66	4	1.3	120
FLT-05B	0.5	0.66	4	1.3	120

Torque measurement : FCT

Each package contains 10 gauges.

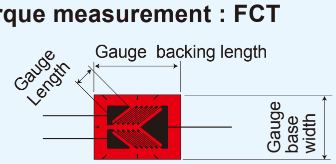

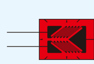

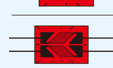

Basic type	Gauge size L	Gauge size W	Backing L	Backing W	Resistance Ω
FCT-2	2	1.5	8.7	6.5	120
FCT-2-350	2	1.5	7.6	5.3	350

Aluminum 7075-T6; 7075-T651

Subcategory: 7000 Series Aluminum Alloy; Aluminum Alloy; Metal; Nonferrous Metal

Close Analogs: none

Composition Notes: A Zr + Ti limit of 0.25 percent maximum may be used with this alloy designation for extruded and forged products only, but only when the supplier or producer and the purchaser have mutually so agreed. Agreement may be indicated, for example, by reference to a standard, by letter, by order note, or other means which allow the Zr + Ti limit.

Aluminum content reported is calculated as remainder.

Composition information provided by the Aluminum Association and is not for design.

Key Words: Aluminium 7075-T6; Aluminium 7075-T651, UNS A97075; ISO AlZn5.5MgCu; Aluminium 7075-T6; Aluminium 7075-T651; AA7075-T6

Component	Wt. %	Component	Wt. %	Component	Wt. %
Al	87.1 - 91.4	Mg	2.1 - 2.9	Si	Max 0.4
Cr	0.18 - 0.28	Mn	Max 0.3	Ti	Max 0.2
Cu	1.2 - 2	Other, each	Max 0.05	Zn	5.1 - 6.1
Fe	Max 0.5	Other, total	Max 0.15		

Material Notes: General 7075 characteristics and uses (from Alcoa): Very high strength material used for highly stressed structural parts. The T7351 temper offers improved stress-corrosion cracking resistance.

Applications: Aircraft fittings, gears and shafts, fuse parts, meter shafts and gears, missile parts, regulating valve parts, worm gears, keys, aircraft, aerospace and defense applications; bike frames, all terrain vehicle (ATV) sprockets.

Data points with the AA note have been provided by the Aluminum Association, Inc. and are NOT FOR DESIGN.

Physical Properties	Metric	English	Comments
Density	2.81 g/cc	0.102 lb/in³	AA; Typical
Mechanical Properties	**Metric**	**English**	**Comments**
	150	150	AA; Typical; 500

CRP MECCANICA S.r.l.

Sede Legale e Amministrativa/Headquarters and Administration Office
Via Cesare Della Chiesa 21 - 41126 Modena
Tel./Phone +39-059-330544/821135/826025
Fax +39-059-822071/381148
C.F./ P.IVA/Registro Imprese Modena IT00782680367 (VAT number)
Capitale sociale Euro 564.000 i. v.

Hardness, Brinell			g load; 10 mm ball
Hardness, Knoop	191	191	Converted from Brinell Hardness Value
Hardness, Rockwell A	53,50	53,50	Converted from Brinell Hardness Value
Hardness, Rockwell B	87	87	Converted from Brinell Hardness Value
Hardness, Vickers	175	175	Converted from Brinell Hardness Value
Ultimate Tensile Strength	572 MPa	83000 psi	AA; Typical
Tensile Yield Strength	503 MPa	73000 psi	AA; Typical
Elongation at Break	11 %	11 %	AA; Typical; 1/16 in. (1.6 mm) Thickness
Elongation at Break	11 %	11 %	AA; Typical; 1/2 in. (12.7 mm) Diameter
Modulus of Elasticity	71.7 GPa	10400 ksi	AA; Typical; Average of tension and compression. Compression modulus is about 2% greater than tensile modulus.
Poisson's Ratio	0.33	0.33	
Fatigue Strength	159 MPa	23000 psi	AA; 500,000,000 cycles completely reversed stress; RR Moore machine/specimen
Fracture Toughness	20 MPa-m½	18.2 ksi-in½	K(IC) in S-L Direction
Fracture Toughness	25 MPa-m½	22.8 ksi-in½	K(IC) in T-L Direction
Fracture Toughness	29 MPa-m½	26.4 ksi-in½	K(IC) in L-T Direction
Machinability	70 %	70 %	0-100 Scale of Aluminum Alloys
Shear Modulus	26.9 GPa	3900 ksi	
Shear Strength	331 MPa	48000 psi	AA; Typical
Electrical Properties	**Metric**	**English**	**Comments**
Electrical Resistivity	5.15e-006 ohm-cm	5.15e-006 ohm-cm	AA; Typical at 68°F
Thermal Properties	**Metric**	**English**	**Comments**

CRP MECCANICA S.r.l.

Sede Legale e Amministrativa/Headquarters and Administration Office
Via Cesare Della Chiesa 21 - 41126 Modena
Tel./Phone +39-059-330544/821135/826025
Fax +39-059-822071/381148
C.F./ P.IVA/Registro Imprese Modena IT00782680367 (VAT number)
Capitale sociale Euro 564.000 i. v.

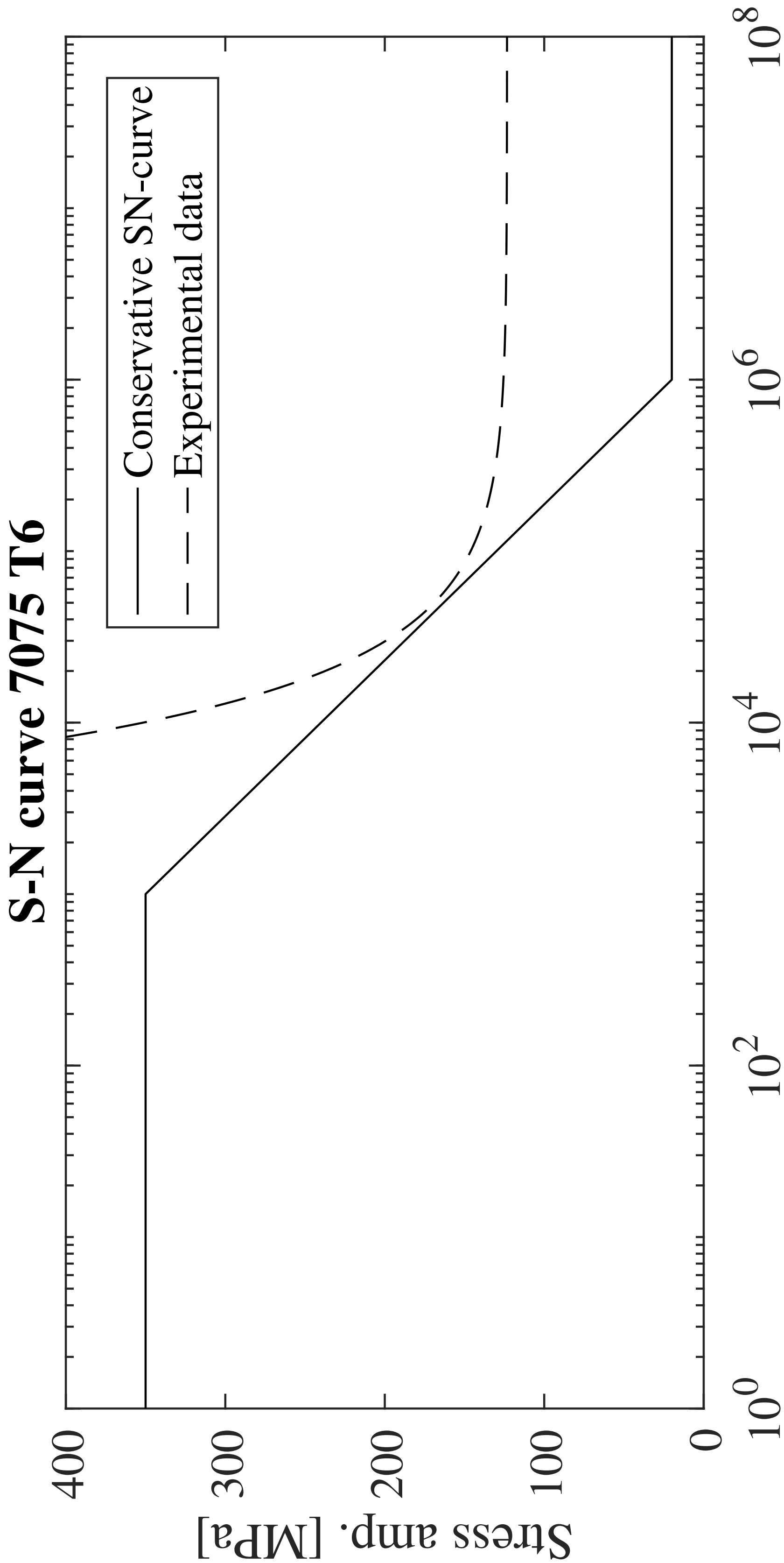
S-N curve 7075 T6
Conservative SN-curve
Experimental data
Stress amp. [MPa]
N [cycles]
400
300
200
100
0
10^0
10^2
10^4
10^6
10^8

HexPly® 6376

175°C curing epoxy matrix

Product Data

Description

HexPly 6376 is a high performance tough matrix formulated for the fabrication of primary aircraft structures. It offers high impact resistance and damage tolerance for a wide range of high temperature applications.

Benefits and Features

- Excellent toughness and damage tolerance
- Simple straight-up cure cycle
- Controlled matrix flow for ease of processing
- Effective translation of fibre properties
- Good hot/wet properties up to 150°C

Resin Matrix Properties

Rheology

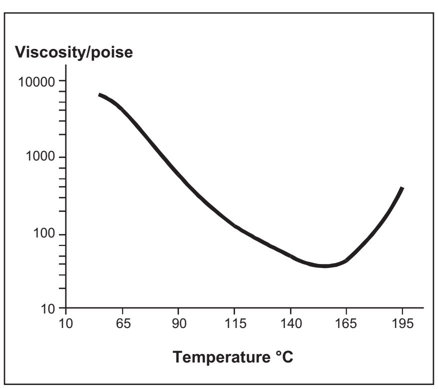

Gel Time

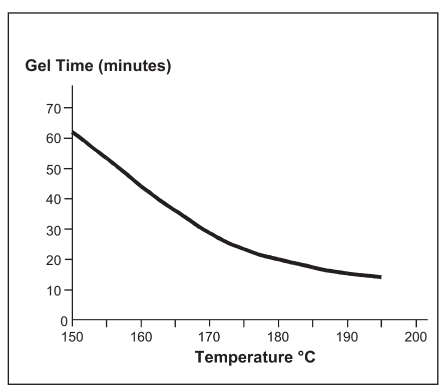

HexPly® 6376 *Product Data*

Cured Matrix Properties (cured at 175°C)

		Method
Tensile strength	105 MPa	ISO R527 type 1
Tensile modulus	3.60 GPa	ISO R527 type 1
Tensile strain	3.1%	ISO R527 type 1
Flexural strength	144 MPa	ISO 178
Flexural modulus	4.4 GPa	ISO 178
Toughness G_{1C}	432 J/m^2	Tested in accordance with EGF Task Group on Polymers and Composites protocol.
Cured density	1.31 g/cm^3	

Prepreg Curing Conditions

2 hours at 175°C and 700kN/m^2 (7 bar) pressure.

Heat up rate 2°C to 5°C.

Components up to 30 mm thick can be cured without a dwell in the schedule provided that the heat-up rate is not more than 3°C/minute. There is no deterioration in performance after 3 times the recommended cure schedule (verified by interlaminar shear strength tests).

Prepreg Storage Life

- Tack Life @ 23°C 10 days (still processable for up to 21 days).
- Guaranteed Shelf Life @ -18°C 6 months (minimum)
- Storage conditions.

HexPly 6376 prepregs should be stored as received in a cool dry place or in a refrigerator. After removal from refrigerator storage, prepreg should be allowed to reach room temperature before opening the polythene bag, thus preventing condensation. (A full reel in its packaging can take up to 48 hours).

Precautions for Use

The usual precautions when handling uncured synthetic resins and fine fibrous materials should be observed, and a Safety Data Sheet is available for this product. The use of clean disposable inert gloves provides protection for the operator and avoids contamination of material and components.

Important

All information is believed to be accurate but is given without acceptance of liability. Users should make their own assessment of the suitability of any product for the purposes required. All sales are made subject to our standard terms of sale which include limitations on liability and other important terms.

Publication FTA051b (March 2007)

For More Information

Hexcel is a leading worldwide supplier of composite materials to aerospace and other demanding industries. Our comprehensive product range includes:

- Carbon Fibre
- RTM Materials
- Honeycomb Cores
- Continuous Fibre Reinforced Thermoplastics
- Carbon, glass, aramid and hybrid prepregs
- Reinforcement Fabrics
- Structural Film Adhesives
- Honeycomb Sandwich Panels
- Special Process Honeycombs

For US quotes, orders and product information call toll-free 1-800-688-7734

For other worldwide sales office telephone numbers and a full address list please go to:

http://www.hexcel.com/contact/salesoffices

HexPly® 6376C-905-36%

Epoxy Matrix

Product Data Sheet

Description

HexPly® 6376C-905-36% is a Epoxy High Strength Carbon Woven prepreg, whereby 6376 is the resin type; 36% is the resin content by weight; 905 is the reinforcement reference and C represents High Strength Carbon fibre. This data sheet is complementary to the 6376 resin data sheet, which should be consulted for additional information.

Reinforcement Data

			0°	90°
Nominal Area Weight	g/m²	280	140	140
Composition		5H satin		
Fibre Type		High Strength Carbon 3K		
Nominal Fibre Density	g/cm³	1,77		

Matrix Properties

Glass transition temperature of laminate (Cure cycle: 120min @ 175°C)	°C	196 (DMA onset, 5°C/min, 1Hz, 30µm),
Nominal Resin Density	g/cm³	1,31

Prepreg Data

Nominal Area Weight	g/m²	438
Nominal Resin Content	weight %	36
Tack Level		Medium

Processing

Cure Cycle	@ 175 °C	120 min
Recommended heat up rate	ºC/min	2 - 5°C/min
Pressure gauge	bar	7

The optimum cure cycle, heat up rate and dwell period depend on part size, laminate construction, oven capacity and thermal mass of tool. (See prepreg technology brochure on our website for more information),

Cured Laminate Properties

(nominal composite density 1,57 g/cm³)

RESIN CONTENT % vs CURED PLY THICKNESS

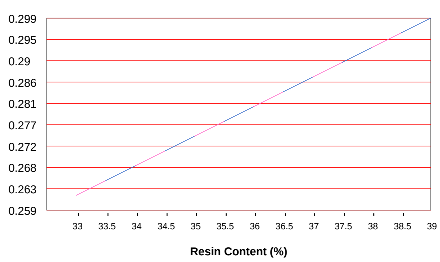

RESIN CONTENT % vs FIBRE VOLUME %

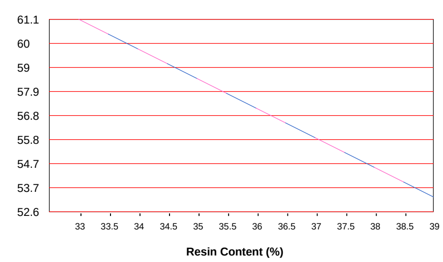

The above graphs enable the fibre volume content of a laminate to be estimated using the measured cured ply thickness. The calculation assumes no resin loss.

HEXCEL

For other worldwide sales office telephone numbers and a full address list please go to : http://www.hexcel.com/contact/salesoffices

HexPly® 6376C-905-36%

Mechanical Properties

(Normalised to 60% fibre volume, except for ILSS)

Mechanical Properties are based on 175 °C cure for 120 min, at 7 bar pressure and 0,9 bar vacuum.

Data is the result from several tests on Autoclave cured laminates. Some of the values achieved will have been higher, and some lower, than the figure quoted. These are nominal values.

Warp (RT / Dry)	Tensile	Flexural	ILSS	Compression
Strength (MPa)	1006	-	83	920
Modulus (GPa)	67	-	.	-
Test Method	EN 2561		EN 2563	EN 2850

Prepreg Storage Life

Shelf Life[1]: 6 months at -18°C/0°F (from date of manufacture).

[1] Shelf Life: the maximum storage life for HexPly® prepreg, when stored continuously, in a sealed moisture-proof bag, at -18°C/0°F or 5°C/41°F. To accurately establish the exact expiry date, consult the box label.

Out Life[2]: 21 days at Room Temperature.

[2] Out Life: the maximum accumulated time allowed at room temperature between removal from the freezer and cure.

Tack Life[3]: 10 days at Room Temperature.

[3] Tack Life: the time, at room temperature, during which prepreg retains enough tack for easy component lay-up.

Prepreg should be stored as received in a cool dry place or in a refrigerator. After removal from refrigerator storage, prepreg should be allowed to reach room temperature before opening the polyethylene bag, thus preventing condensation. (A full reel in its packing can take up to 48 hours).

Precautions for Use

The usual precautions when handling uncured synthetic resins and fine fibrous materials should be observed, and a Safety Data Sheet is available for this product. The use of clean disposable inert gloves provides protection for the operator and avoids contamination of material and components.

Important

All information is believed to be accurate but is given without acceptance of liability. All users should make their own assessment of the suitability of any product for the purposes required. All sales are made subject to our standard terms of sale which include limitations on liability and other terms

HexPly® | 6376C-905-36% | 12/2005 | version : a

HexTow® IM7
Carbon Fiber

Product Data Sheet

HexTow® IM7 carbon fiber is a continuous, high performance, intermediate modulus, PAN based fiber available in 12,000 (12K) filament count tows. This fiber has been surface treated and can be sized to improve its interlaminar shear properties, handling characteristics, and structural properties. It is suggested for use in weaving, prepregging, filament winding, braiding, and pultrusion.

The unique properties of HexTow® IM7 fiber, such as higher tensile strength and modulus, as well as good shear strength, allow structural designers to achieve both higher safety margins for both stiffness and strength critical applications.

IM7-G 12K (0.25%) carbon fiber has been qualified to NMS 818 Carbon Fiber Specification (NCAMP). This allows customers to call out an industry standard, aerospace grade carbon fiber without the need to write and maintain their own specification.

Typical Fiber Properties	U.S. Units	SI Units
Tensile Strength		
6K	800 ksi	5,516 MPa
12K	820 ksi	5,654 MPa
Tensile Modulus (Chord 6000-1000)	40.0 Msi	276 GPa
Ultimate Elongation at Failure		
6K	1.9%	1.9%
12K	1.9%	1.9%
Density	0.0643 lb/in^3	1.78 g/cm^3
Weight/Length		
6K	12.5 x 10^{-6} lb/in	0.223 g/m
12K	25.0 x 10^{-6} lb/in	0.446 g/m
Approximate Yield		
6K	6,674 ft/lb	4.48 m/g
12K	3,337 ft/lb	2.24 m/g
Tow Cross-Sectional Area		
6K	1.94 x 10^{-4} in^2	0.13 mm^2
12K	3.89 x 10^{-4} in^2	0.25 mm^2
Filament Diameter	0.203 mil	5.2 microns
Carbon Content	95.0%	95.0%
Twist	Never Twisted	Never Twisted

Typical HexPly 8552 Composite Properties (at Room Temperature)	U.S. Units	SI Units	Test Method
0º Tensile Strength	395 ksi	2,723 MPa	ASTM D3039
0º Tensile Modulus	23.8 Msi	164 GPa	
0º Tensile Strain	1.6%	1.6%	
0º Flexural Strength	270 ksi	1,862 MPa	ASTM D790
0º Flexural Modulus	22.0 Msi	152 GPa	
0º Short Beam Shear Strength	18.5 ks	128 MPa	ASTM D2344
0º Compressive Strength	245 ksi	1,689 MPa	ASTM Mod. D695
0º Compressive Modulus	21.2 Msi	146 GPa	
0˚ Open Hole Tensile Strength	62 ksi	427 MPa	ASTM D5766
0˚ Open Hole Compressive Strength	48.8 ksi	336 MPa	ASTM D6484
90º Tensile Strength	16.1 ksi	111 MPa	ASTM D3039
Fiber Volume	60%	60%	

HexTow® IM7 carbon fiber

HEXCEL®

Product Data Sheet

Yarn/Tow Characteristics	U.S. Units	SI Units
Specific Heat	0.21 Btu/lb-°F	0.21 cal/g-°C
Electrical Resistivity	4.9 x 10^{-5} ohm-ft	1.5 x 10^{-3} ohm-cm
Coefficient of Thermal Expansion	-0.36 ppm/ºF	-0.64 ppm/ºC
Thermal Conductivity	3.12 Btu/hr-ft-ºF	5.40 W/m-ºK

Carbon Fiber Certification
This carbon fiber is manufactured to Hexcel aerospace grade specification HS-CP-5000. A copy of this specification is available upon request. A Certification of Analysis will be provided with each shipment.

Available Sizing
Sizing compatible with various resin systems, based on application are available to improve handling characteristics and structural properties. Please see additional information on available Sizes on our website or contact our technical team for additional information.

Packaging
Standard packaging of HexTow® IM7 is as follows:

Filament Count	Nominal Weight		Nominal Length	
	(lb)	(kg)	(ft)	(m)
6K	4.0	1.8	26,400	8,050
12K	4.0	1.8	13,350	4,070

Other package sizes may be available on request. The fiber is wound on a 3-inch ID by 11-inch long cardboard tube and overwrapped with plastic film.

Safety Information
Obtain, read, and understand the Material Safety Data Sheet (MSDS) before use of this product.

For more information

Hexcel is a leading worldwide supplier of composite materials to aerospace and industrial markets. Our comprehensive range includes:

- HexTow® carbon fibers
- HexForce® reinforcements
- HiMax™ non-crimp fabrics
- HexPly® prepregs
- HexMC® molding compounds
- HexFlow® RTM resins
- Redux® adhesives
- HexTOOL® tooling materials
- HexWeb® honeycombs
- Acousti-Cap® sound attenuating honeycomb
- Engineered core
- Engineered products

For US quotes, orders and product information call toll-free 1-866-556-2662. For other worldwide sales office telephone numbers and a full address list, please go to:

http://www.hexcel.com/contact/salesoffice

CTA 351 JY16

LOCTITE®

Technical Data Sheet

Loctite® Frekote® B-15™

Known as Frekote B-15
December 2013

PRODUCT DESCRIPTION

Loctite® Frekote® B-15™ provides the following product characteristics:

Technology	Mold Sealer
Appearance	Clear, colorless[LMS]
Chemical Type	Solvent Based Polymer
Odor	Solvent
Cure	Room temperature cure
Cured Thermal Stability	≤400 °C
Application	Mold Sealer
Application Temperature	20 to 60 °C
Specific Benefit	• No contaminating transfer • High thermal stability • Seals mold porosity, scratches or imperfections

Loctite® Frekote® B-15™ is formulated specifically as a sealer for composite and metal molds with micro porosity problems, small surface scratches or imperfections. Used in conjunction with other Frekote® products, Loctite® Frekote® B-15™ provides an excellent base coat enhancing the release advantages offered.

TYPICAL PROPERTIES OF UNCURED MATERIAL

Specific Gravity @ 25 °C	0.745 to 0.775[LMS]
Flash Point - See SDS	
Release Agent Transfer	≥4[LMS]

GENERAL INFORMATION

This product is not recommended for use in pure oxygen and/or oxygen rich systems and should not be selected as a sealant for chlorine or other strong oxidizing materials.

For safe handling information on this product, consult the Safety Data Sheet (SDS).

Mold Preparation
Cleaning:

Mold surfaces must be thoroughly cleaned and dried. All traces of prior release must be removed. This may be accomplished by using Loctite® Frekote® PMC or other suitable cleaner. Loctite® Frekote® 915WB™ or light abrasives can be used for heavy build-up.

Directions for use:

1. Loctite® Frekote® B-15™ can be applied to mold surfaces by spraying, brushing, dipping or wiping with a clean, lint free, cotton wiping cloth. When spraying, ensure a dry air source is used or use an airless spray system making sure the nozzles is 20 to 25 cm from the mold surface.
2. Brushing and dipping are effective methods of application, but care should be taken to avoid excessive pooling and to ensure that the part is well drained. Wiping on is the best method of application.
3. Only a thin wet film is required. It is suggested that small areas be coated, working progressively from one mold to the other.
4. Apply a minimum of two coats, allowing 30 minutes between coats.
5. The final coat will cure within 24 hours at 23°C or the cure process can be shortened by baking the mold for 60 minutes at 95°C after ensuring that the mold is dry and all sovents have flashed off.
6. The mold is now ready to be coated with Frekote mold release products. Please refer to individual product data sheets for the proper application of the release agent.

Mold Touch up

Touch up coats with a sealer should only be applied to areas where the mold was repaired. On repaired areas apply the same number of sealer and release agent coats like for the base coating onto new or refurbished molds.

Loctite Material Specification[LMS]

LMS dated December 18, 2002. Test reports for each batch are available for the indicated properties. LMS test reports include selected QC test parameters considered appropriate to specifications for customer use. Additionally, comprehensive controls are in place to assure product quality and consistency. Special customer specification requirements may be coordinated through Henkel Quality.

Henkel

Storage

The product is classified as flammable and must be stored in an appropriate manner in compliance with relevant regulations. Do not store near oxidizing agents or combustible materials. Store product in the unopened container in a dry location. Storage information may also be indicated on the product container labelling.
Optimal Storage: 8 °C to 21 °C. Storage below 8 °C or greater than 28 °C can adversely affect product properties. Material removed from containers may be contaminated during use. Do not return product to the original container. Henkel cannot assume responsibility for product which has been contaminated or stored under conditions other than those previously indicated. If additional information is required, please contact your local Technical Service Center or Customer Service Represenitive.

Reference 0.1

Technical Data Sheet

LOCTITE® FREKOTE 700-NC™

Known as 700-NC™
January 2015

PRODUCT DESCRIPTION

LOCTITE® FREKOTE 700-NC™ provides the following product characteristics:

Technology	Mold Release
Appearance	Clear, colorless[LMS]
Chemical Type	Solvent Based Polymer
Odor	Solvent
Cure	Room temperature cure
Cured Thermal Stability	≤400 °C
Application	Release Coatings
Application Temperature	13 to 135 °C
Specific Benefit	• No chlorinated solvents • High gloss finish • High slip • No contaminating transfer • No mold build-up

LOCTITE® FREKOTE 700-NC™ offers excellent release properties for the most demanding applications and is a great all-purpose release agent. LOCTITE® FREKOTE 700-NC™ releases epoxies, polyester resins, thermoplastics, rubber compounds and most other molded polymers.

TYPICAL PROPERTIES OF UNCURED MATERIAL

Specific Gravity @ 25 °C 0.755 to 0.764[LMS]

Flash Point - See SDS

GENERAL INFORMATION

This product is not recommended for use in pure oxygen and/or oxygen rich systems and should not be selected as a sealant for chlorine or other strong oxidizing materials.

For safe handling information on this product, consult the Safety Data Sheet (SDS).

Mold Preparation
Cleaning:
Mold surfaces must be thoroughly cleaned and dried. All traces of prior release must be removed. This may be accomplished by using Frekote® PMC or other suitable cleaner. Frekote® 915WB™ or light abrasives can be used for heavy build-up.

Sealing New/Repaired Molds:
Occasionally, green or freshly repaired molds are rushed into service prior to complete cure causing an increased amount of free styrene on the mold surface. Fresh or "production line" repairs, new fiberglass and epoxy molds should be cured per manufacturer's instructions, usually a minimum of 2 -3 weeks at 22°C before starting full-scale production. Fully cured previously unused molds should be sealed before use. This can be accomplished by applying one to two coats of an appropriate Frekote® mold sealer, following the directions for use instructions. Allow full cure of the appropriate Frekote® mold sealer before you apply the first coat of LOCTITE® FREKOTE 700-NC™ as outlined in the directions of use.

Directions for use:

1. LOCTITE® FREKOTE 700-NC™ can be applied to mold surfaces at room temperature up to 135°C by spraying, brushing or wiping with a clean lint-free, cloth. When spraying ensure a dry air source is used or use an airless spray system. Always use in a well ventilated area.
2. Wipe or spray on a smooth, thin, continuous, wet film. Avoid wiping or spraying over the same area that was just coated until the solvent has evaporated. If spraying, hold nozzle 20 to 30cm from mold surface. It is suggested that small areas be coated, working progressively from one side of the mold to the other.
3. Initially, apply 2 to 3 base coats allowing 5 to 10 minutes between coats for solvent evaporation .
4. Allow the final coat to cure for 15 to 20 minutes at 22°C.
5. Maximum releases will be obtained as the mold surface becomes conditioned to LOCTITE® FREKOTE 700-NC™ . Performance can be enhanced by re-coating once, after the first few initial pulls.
6. When any release difficulty is experienced, the area in question can be "touched-up" by re-coating the entire mold surface or just those areas where release difficulty is occurring.
7. **NOTE**: LOCTITE® FREKOTE 700-NC™ is moisture sensitive, keep container tightly closed when not in use. The product should always be used in a well ventilated area.
8. **Precaution:** Users of closed mold systems (rotomolding) must be certain that solvent evaporation is complete and that all solvent vapors have been ventilated from the mold cavity prior to closing the mold. An oil-free compressed air source can be used to assist in evaporation of solvents and ventilation of the mold cavity.

Mold Touch up

Touch up coats should only be applied to areas where poor release is noticed and should be applied using the same method as base coats. This will reduce the possibility of release agent or polymer build-up. The frequency of touch ups will depend on the polymer type, mold configuration, and abrasion parameters.

Loctite Material Specification[LMS]

LMS dated May 10, 2006. Test reports for each batch are available for the indicated properties. LMS test reports include selected QC test parameters considered appropriate to specifications for customer use. Additionally, comprehensive controls are in place to assure product quality and consistency. Special customer specification requirements may be coordinated through Henkel Quality.

Storage

The product is classified as flammable and must be stored in an appropriate manner in compliance with relevant regulations. Do not store near oxidizing agents or combustible materials. Store product in the unopened container in a dry location. Storage information may also be indicated on the product container labelling.

Optimal Storage: 8 °C to 21 °C. Storage below 8 °C or greater than 28 °C can adversely affect product properties. Material removed from containers may be contaminated during use. Do not return product to the original container. Henkel cannot assume responsibility for product which has been contaminated or stored under conditions other than those previously indicated. If additional information is required, please contact your local Technical Service Center or Customer Service Representive.

Conversions

(°C x 1.8) + 32 = °F
kV/mm x 25.4 = V/mil
mm / 25.4 = inches
µm / 25.4 = mil
N x 0.225 = lb
N/mm x 5.71 = lb/in
N/mm² x 145 = psi
MPa x 145 = psi
N·m x 8.851 = lb·in
N·m x 0.738 = lb·ft
N·mm x 0.142 = oz·in
mPa·s = cP

Reference 0.1

E

Science in the Age of Experience Conference

3DEXPERIENCE®

DASSAULT SYSTEMES | The 3DEXPERIENCE® Company

CERTIFICATE

PARTICIPANT

This certifies that Christer Oldeide,Norwegian University of Science and Technology

participated in the

2017 SCIENCE IN THE AGE OF EXPERIENCE

Academic Poster Showcase

and received Favorite of the Conference for

their submission

Charles WILCOX
Director, SIMULIA Global Academia

Development of Hybrid Aluminum Carbon Fiber Composite Wheels for a Formula Style Race Car

Christer Kobbevik Oldeide*[1-2], Jørgen Elliasen*[1-2], Jan Torgersen*[2]

christer.oldeide@revolve.no

[1] *Revolve NTNU, S. P. Andersens veg 5, 7031 NORWAY*
[2] *NTNU, MTP, Richard Birkelands vei 2B, NORWAY*

NTNU
Norwegian University of Science and Technology

Race car applications pose stringent requirements to machine design. Today's requirements necessitate optimizing weight while maximizing stiffness, providing best possible traction while considering all dynamic and static loads during the competition. Working on this year's NTNU race car has introduced Evolution Based Optimization (EBO) and Topology Optimization (TO) into the design process. A hybrid design with a Carbon Fibre Reinforced Plastics (CFRP) shell and an aluminium center was chosen for the wheels. Layup and material choice was optimized in an EBO approach integrating various considerations in a holistic virtual design environment. The aluminium wheel center was TO considering manufacturing constraints and the complete assembled wheel was validated in Abaqus. The entire wheel weighs 1.68 kg while keeping stiffness to the twice of a aluminium racing wheel. The weight exactly matches the optimized design. Simulation based design continues to progress modern product development. Student race cars are a perfect showcase of what is possible and will be an integral part of future engineering.

Rim Shell - Evolutionbased material and layup optimalization

- Loads from tire tests and estimated reaction forces through log data
- Design responses: strain energy (all steps)
- Constraint: Weight target 700 g, material use <=0.4 m2 UD
- Design varialbles: 8 independent zones on shell: numbers of plies, orientations (90:15:90), materials(UD, weave)

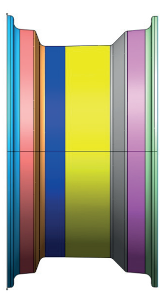

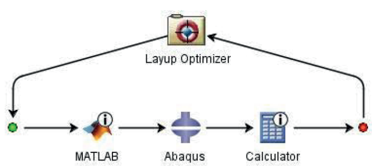

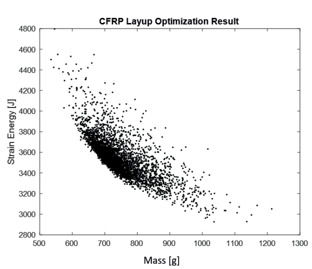

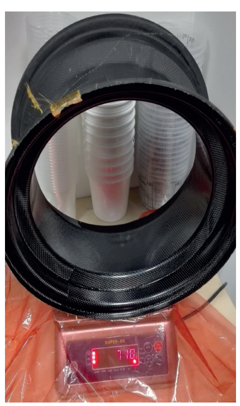

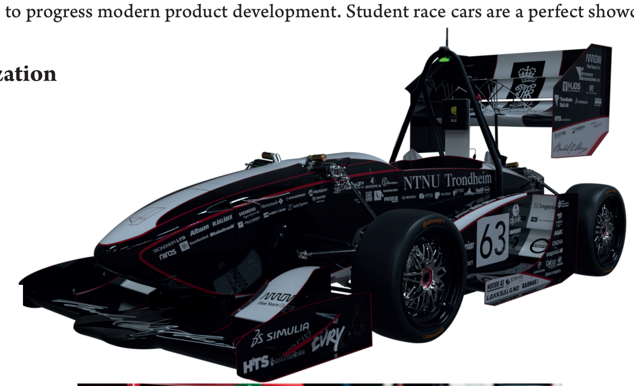

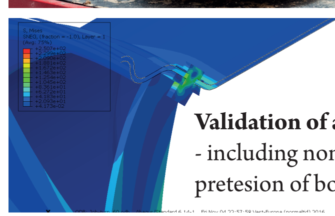

Validation of assumption made:
- including non-linear effect from pretesion of bolts and center lock

Rim Center - Design process

- Optimized with Tosca and Isight (minimizing strain energy and maximizing stiffness)
- Manually optimized for CNC machining
- Weight 920 g

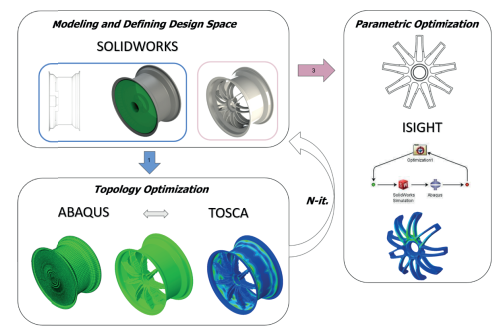


38
Development of Hybrid Aluminum Carbon Fiber
Composite Wheels for a Formula Style Race Car
DASSAULT SYSTEMES
revolve

Colophon

THIS THESIS WAS TYPESET using LaTeX, originally developed by Leslie Lamport and based on Donald Knuth's TeX. The body text is set in 11 point Arno Pro, designed by Robert Slimbach in the style of book types from the Aldine Press in Venice, and issued by Adobe in 2007. A template, which can be used to format a PhD thesis with this look and feel, has been released under the permissive MIT (X11) license, and can be found online at github.com/suchow/ or from the author at suchow@post.harvard.edu.